

Improvement of Strength and Reduction of Surface Erosion Soil Slopes by Treated Natural Fibers and Plant Roots

THESIS

Submitted in partial fulfilment
of the requirements for the degree of

DOCTOR OF PHILOSOPHY

by

GUNDE SACHINCHAKRAVARTHY

ID. No. 2018PHXF0015H

Under the Supervision of

Prof. Anasua GuhaRay

&

Prof. Arkamitra Kar



BITS Pilani
Pilani | Dubai | Goa | Hyderabad

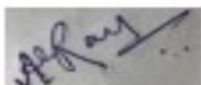
BIRLA INSTITUTE OF TECHNOLOGY AND SCIENCE, PILANI

2024

BIRLA INSTITUTE OF TECHNOLOGY AND SCIENCE, PILANI

CERTIFICATE

This is to certify that the thesis titled **Improvement of Strength and Reduction of Surface Erosion of Soil Slopes by Treated Natural Fibers and Plant Roots** submitted by **Gunde SachinChakravarthy** ID No **2018PHXF0015H** for award of Ph.D. of the Institute embodies original work done by him/her under my supervision.

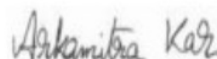


Signature of the Supervisor

Name: Prof. Anasua GuhaRay

Designation: Associate Professor

Date:



Signature of the Supervisor

Name: Prof. Arkamitra Kar

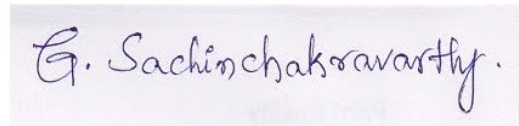
Designation: Associate Professor

Date:

DECLARATION

I certify that

- a) The work contained in the thesis is original and has been done by myself under the general supervision of my supervisor and co-supervisor.
- b) The work has not been submitted to any other Institute for any degree or diploma.
- c) I have followed the guidelines provided by the Institute in writing the thesis.
- d) I have conformed to the norms and guidelines given in the Ethical Code of Conduct of the Institute.
- e) Whenever I have used materials (data, theoretical analysis, and text) from other sources, I have given due credit to them by citing them in the text of the thesis and giving their details in the references.
- f) Whenever I have quoted written materials from other sources, I have put them under quotation marks and given due credit to the sources by citing them and giving the required details in the references.



G. Sachin Chakravarty.

Signature of the Student

Dedicated to my parents and my wife (N. Pavani)
for their love, endless support
and blessing

Acknowledgement

This research could not have been possible without the support of several individuals, and I would like to take this opportunity to extend my sincere thanks to them. First and foremost, I would like to express my immense gratitude to my supervisor, Prof. Anasua GuhaRay, for her guidance, inspiration, encouragement and affection. Her supervisions and discussions were extremely helpful while developing various ideas presented in this thesis. Also, I would like to thank my co-supervisor Prof. Arkamitra Kar, for his unconditional support and encouragement. His guidance helped me in all the time of research. Both of my supervisors helped me in writing this thesis. Without their assistance, I could not have imagined having greater advisors and mentors for my PhD studies.

I thank my Doctoral Advisory Committee (DAC) members, Prof. Sridhar Raju and Prof. V. Vinayaka Ram, who gave thought-provoking ideas and constantly monitored my progress. Their ideas were very helpful in analyses of results and experimental works. I would also like to thank all faculty members of the Department of Civil Engineering, BITS – Pilani Hyderabad Campus, for helping me to progress in my research work. I would also like to express my deep gratitude to the Head of the Department, Prof. Murari RR Varma and DRC conveners, Prof. Anasua GuhaRay, Dr Prasanta Sahu, Dr K Rajitha and Dr Mohan S.C. I thank lab technicians Mr P. Hemanth Kumar, Mr Manish Kumar Yadav, Bhuvaneshwaran S and all other lab technicians, and my fellow research scholars Syed Mazhar, Ch. Sai Kiran, S. Ashok Kumar, T. Venkateshwarlu, Mallikarjun Patil, Sheik Sk Rahaman, N. Sathish, R. Kruti Kiran, Mohammad Zoheb Nawaz, Ankur and Meenu Krishan of our department.

I thankfully acknowledge the support rendered by the DST India- WTZ-OEAD Austria project-based personnel exchange programme for funding the research project through the Department of Science and Technology (DST), Government of India. I thank Prof. Anasua GuhaRay (BITS Pilani Hyderabad) and Prof. Wei Wu (BOKU Austria) for choosing me for this project.

I would also like to thank my friends K. Srinivas, G. Sainath, Abdul Rasheed, J. Nipun Kumar, S. Kalyan Pradeep, D. Navaneth, M. Sai Kumar, S. Dasharath and my school senior Birru Bhaskar for pushing me into this research field.

Finally, I express my gratitude to my father, Mr Gunde Laxmaiah and mother, Mrs Saraswathi, wife Neelapu Pavani, mother in law Eeshwaramma Dhannana and father in law Neelapu Ramu, my brothers G. Gopala Krishna, G. Radha Krishna, brothers in law N. Chakravarthy and N. Gnanendra for their continual love, inspiration, support and encouragement to see me scaling greater heights of life.

Place: Hyderabad

Date:

(Gunde Sachin Chakravarthy)

Abstract

Soil slopes are susceptible to surface erosion, particularly in regions with significant rainfall and steep topography, resulting in slope failures. Failures of slopes, such as landslides and rockfalls, can cause severe damage to infrastructure, property, and human life. In India, landslides have resulted in significant loss of life and damage to communication networks, human settlements, agricultural areas, and forest regions. Rainfall-induced slope failures are widespread in many regions of the world. According to the Disaster Management Authority of India, Ministry of Home Affairs (MHA), Govt. of India, roughly 100 to 150 crores of monetary loss occurred in the last decade. According to the Geological Survey of India, around 0.42 million km² (12.6% of landmass) of the area in India is prone to landslides. Hence it is necessary to stabilise the slopes prone to excessive rainfall. Several traditional methods of soil stabilisation involve the use of synthetic materials that have negative environmental impacts. Geosynthetic materials are popular for slope stabilisation and erosion control due to their high efficiency and reliable performance. However, they can be costly, difficult to install, and have negative environmental impacts. Synthetic geosynthetics, such as geomembranes, geotextiles, and geogrids, may remain in the environment for hundreds of years, leading to landfill accumulation and long-term pollution. Toxic additives or chemicals in certain geosynthetics may leach into the environment and pollute soil and water. PVC geosynthetics release dioxins and microplastics, which can enter the food chain and harm animals.

Thus, searching for natural materials to stabilise soil slopes has gained significant attention recently. Implementing natural fibres and plants to stabilise slopes and decrease surface erosion has recently gained popularity. Natural geotextiles such as coir, jute, and sisal provide immediate protection when installed in the ground, but these are biodegradable in less than one year (Sanyal, 2017). Issues like soil erosion due to frequent rainfalls can wash away germinating seeds and tiny plants in the initial stages, preventing plants from properly growing on such a slope. Treatment of natural fibres with antimicrobial chemicals, plant-derived oils, acetylation, and bitumen coating improves the durability of natural fibres, but these methods are costly and may cause leaching (Gupta et al., 2018). The treatment of natural fibres with antimicrobial agents, plant-derived oils, acetylation, and bituminous coating increases the durability of natural fibres; however, these methods are expensive and may cause leachate (Gupta et al., 2018). Thus, the primary goal of the present study is to

develop a new method for treating natural geotextiles that is environmentally friendly, economically advantageous, and adaptable to increase their durability. Natural geotextiles made of jute are utilised in the research.

To increase the durability and strength of natural jute geotextiles, the present study recommends a novel method that includes treating them with an alkali-activated binder (AAB). Fly ash, an aluminosilicate-rich industrial waste, reacts with an activator solution of sodium silicate and sodium hydroxide to produce AAB. To treat the fibres, AAB's different water-to-solids ratios (w/s) are kept at 0.35, 0.4, and 0.45. The untreated and treated natural geotextiles are subjected to different durability tests, including soil burial, compost burial, exposure to acids and alkalis, and water hydrolysis for 180 days. The durability performance is assessed by analysing the surface texture, surface morphology, change in chemical bonds, weight loss, tensile strength, and elongation at failure (fibre breaking). It is observed from the durability studies that the AAB treatment makes the jute geotextile harder and more resistant to exposure to different chemicals. It is also determined that jute coated with an AAB of 0.35 w/s ratio degrades the least.

The primary factors affecting soil erosion are rainfall intensity, duration, and slope angles. To study the effect of these parameters on the stability of the slope, artificial rainfall and laboratory-scale slope model arrangements were made. The slope model reinforced with untreated and jute geotextiles is exposed to low and high rainfall intensities. Bermuda grass is transplanted in conjunction with reinforcements to find the effect of plants on the slope model under the rain. This study compares the effect of rain on the respective stabilities of the slope with reinforcement and the slope without reinforcement. Slope failure due to the effect of rainfall can be identified by finding soil erosion in the form of sediment yield when exposed to rainfall and validating with the Modified Universal Soil Loss Equation model. The results show that soil erosion was reduced by 68.6% when slopes were reinforced with jute. Erosion was effectively reduced by reinforcing the slope with vegetation and AAB-treated jute geotextiles. Vegetation with 0.35 w/s AAB-treated jute geotextiles significantly reduced erosion by 84% for a 30° slope under heavy rainfall. The MUSLE model-based observations showed that the MUSLE-calculated sediment yield values were close to those in experiments. Between 79.9% and 95.8% of the MUSLE results and experimental data match each other.

An attempt was made to numerically simulate the behaviour of soil slopes reinforced with untreated and treated jute geotextiles under rainfall conditions. A software called Plaxis 2D

which is based on the Finite Element Method (FEM), is used to simulate the slope model. The soil is described using the Mohr-Coulomb model with plane strain 15-noded triangular elements. In this research, the effects of low (10.2 mm/hr) and high (23.4 mm/hr) rainfall intensities on unreinforced and reinforced soil slopes of different slope angles (30°, 45°, 60°) are investigated. Numerical studies show that the maximum deformation of the slope under rainfall mainly depends on rainfall intensity, slope steepness, and reinforcement. The 0.35 AAB treated jute reinforcement application improved the slope's stability by increasing the soil's shear strength and providing additional tensile strength to increase the slope failure time. Under lower rainfall conditions, a 30° slope with a reinforcement resulted in a maximum slope failure time of 6.37 hours. This model can be utilized in future research to evaluate the stability of various slope angles during rainfall events. Current research is a step toward a sustainable and environmentally friendly solution for applying treated natural geotextiles and plants to improve slope stability, reduce surface erosion, and have a significant practical impact on slope construction at a low cost.

Keywords: Alkali Activated Binder; Durability; Slope Model; Plants; MUSLE Model; Plaxis 2D

TABLE OF CONTENTS

Acknowledgement	v
Abstract	vii
Contents	x
List of Tables	xvii
List of Figures	xix
List of Abbreviations	xxiv
List of Symbols	xxvi
CHAPTER 1 Introduction	
1.1 General	1
1.2 Background	1
1.3 Importance of proposed research	5
1.4 Goals and Objectives	6
1.5 Thesis Organization	6
CHAPTER 2 A Review of Literature	8
2.1 General	8
2.2 Improvement of Strength of Soil Using Natural Geotextiles	8
2.2.1 Natural Geotextiles	8
2.2.2 Strengthening of Soil using Natural Geotextiles	10
2.3 Reduction of Surface Erosion Using Natural Geotextiles	14
2.3.1 Soil Erosion Mechanism	16
2.3.2 Soil Erosion Agents	16
2.3.3 Soil Erosion Control Methods	19
2.3.4 Erosion Control by Natural Geotextile	20
2.4 Slope Stabilization using Natural Geotextiles	25

2.4.1 Slope Failure	25
2.4.2 Slope Stability Analysis	26
2.4.3 Improvement of Slope stability by Natural Geotextiles	28
2.5 Improving Soil Strength and Decreasing Surface Erosion by Bioengineering Methods	29
2.5.1 Effect of Vegetation on Surface Erosion	30
2.5.2 Vegetation influence on Mass Loss	31
2.5.3 Role of Vegetation in Slope Stability	32
2.5.4 Root Morphology and Strength	34
2.5.4.1 Root Architecture	34
2.5.4.2 Root Strength	35
2.5.5 Bioengineering	36
2.6 Durability and Treatment Methods for Natural Geotextiles	39
2.6.1 Treatment Methods	39
2.6.1.1 Scouring and Bleaching	40
2.6.1.2 Rot Resistant Solution	41
2.6.1.3 Acetylation	41
2.6.1.4 Transesterification	43
2.6.2 Durability Studies of Natural Geotextiles	44
2.7 Numerical Studies of Reinforced Soil Slopes	48
2.7.1 Numerical Simulation Methodology	51
2.7.2 Calculation of Van Genuchten Parameters	52
2.8 Summary of Literature Review and Limitations of Existing Research	54
2.9 Research Significance	55
CHAPTER 3 Materials and Experimental Methodology	56
3.1 General	56
3.2 Materials Used	56
3.2.1 Red Soil	56

3.2.2 Natural Jute Geotextile	58
3.2.3 Alkali Activated Binder (AAB)	60
3.2.4 Bermuda Grass	62
3.3 Mineralogical, Chemical, and Microstructural Characterizations	63
3.3.1 Stereomicroscopy	64
3.3.2 X-ray Diffraction (XRD)	64
3.3.2 Fourier Transform Infra-Red (FTIR) Spectroscopy	64
3.3.4 Scanning Electron Microscope (SEM)	64
3.3.5 Thermogravimetric Analysis (TGA)	65
3.4 Geomechanical Characterisation	65
3.4.1 Natural Jute Geotextile	65
3.4.1.1 Aperture Opening Size	65
3.4.1.2 Thickness	66
3.4.1.3 Mass per unit area	67
3.4.1.4 Tensile Strength Test (Grab Test)	68
3.4.2 Permeability of jute-reinforced soil	69
3.4.3 CBR of jute-reinforced soil	70
3.4.4 UCS of jute-reinforced soil	71
3.4.5 Interface Friction Angle between soil and untreated / treated jute	73
3.5 Mechanical Properties of Bermuda Grass	74
3.5.1 Bermuda Grass Growth Mechanism	74
3.5.2 Root Matrix of Bermuda Grass	76
3.5.3 Tensile strength of roots	77
3.5.4 Shear strength of soil infused with roots	78
3.6 Soil Erosion Model Setup	79
3.6.1 Artificial Rainfall Simulating Assembly	79
3.7 Summary	81

CHAPTER 4 Durability Studies of Jute	82
4.1 General	82
4.2 Methodology of Durability Tests	82
4.2.1 Soil Burial Test	82
4.2.2 Resistance to Acid and Alkali Test	84
4.2.3 Resistance to Hydrolysis	85
4.2.4 Compost Burial method	86
4.3 Determination of Mechanical Properties	87
4.3.1 Weight Loss Test	87
4.3.2 Tensile Strength	87
4.3.3 Elongation at Break	88
4.4 Determination of Chemical Characteristics	88
4.4.1 Surface Texture	88
4.4.2 Crystallinity	88
4.4.3 Molecular Bonds	88
4.4.4 Morphology	89
4.4.5 Thermogravimetric Analysis	89
4.5 Results and Discussions on Durability Tests	89
4.5.1 Soil Burial Test	89
4.5.1.1 Weight Loss for Soil Burial	89
4.5.1.2 Tensile Strength for Soil Burial	90
4.5.1.3 Elongation at Break for Soil Burial	91
4.5.2 Resistance to Acid and Alkali Test	92
4.5.2.1 Weight Loss for Acid and Alkali Test	92
4.5.2.2 Tensile Strength for Acid and Alkali Test	92
4.5.2.3 Elongation at Break for Acid and Alkali Test	93
4.5.3 Resistance to Hydrolysis Test	94

4.5.3.1 Weight Loss for Hydrolysis Test	94
4.5.3.2 Tensile Strength for Hydrolysis Test	95
4.5.3.3 Elongation at Break for Hydrolysis Test	96
4.5.4 Compost Burial Test	96
4.5.4.1 Weight Loss for Compost Burial Test	97
4.5.4.2 Tensile Strength for Compost Burial Test	97
4.5.4.3 Elongation at Break for Compost Burial Test	98
4.5.5 Reasons for Strength Reduction in Jute Geotextile	99
4.6 Results and Discussions on Chemical Characteristics	100
4.6.1 Surface Texture	100
4.6.2 Crystallinity	105
4.6.3 Molecular Bonds	107
4.6.4 Morphology	109
4.6.5 Thermogravimetric Analysis	113
4.7 Conclusions	114
CHAPTER 5 Bioengineering Methods for Soil Erosion Control and Stability	115
5.1. General	115
5.2 Laboratory Scale Soil Erosion Model setup	115
5.2.1 Laboratory Scale Slope Model	115
5.2.2 Sediment Yield Calculation from Experimental Investigation	117
5.3 Soil Loss Prediction Models	119
5.3.1 Empirical Models	119
5.3.1.1 The Universal Soil Loss Equation (USLE)	119
5.3.1.2 The Revised Universal Soil Loss Equation (RUSLE)	120
5.3.1.3 The Modified Universal Soil Loss Equation (MUSLE)	121
5.3.2 Sediment Yield Calculation Using MUSLE Model	126
5.4 Effect of Vegetation on Slope Stability	127

5.4.1 Laboratory Scale Vegetated Slope Model	128
5.4.2 Sediment Yield Calculation for Vegetation Applied Slope	129
5.4.3 Sediment Yield Calculation for Vegetation Applied Slope Using MUSLE Model	129
5.5 Results and Validation of Models with Experimental Data	131
5.6 Summary	135
CHAPTER 6 Numerical Modelling Slope Using Finite Element Method	136
6.1. General	136
6.2 Formulation of PLAXIS 2D model	136
6.2.1 Geometric Configuration of Model	137
6.2.2 Geogrid Element	138
6.2.3 Soil Properties and Constitutive Model	138
6.2.4 Ground Water Parameters	139
6.2.5 Interface Elements	140
6.2.6 Boundary Conditions and Mesh Convergence Study	141
6.2.7 Ground Water Flow Boundary Condition	143
6.2.8 Staged Construction	143
6.2.9 Factor of Safety Analysis	144
6.3 Validation of Plaxis 2D Results with Past Research Work	144
6.4 Results and Discussions	145
6.5 Parametric Analysis	149
6.4.1 Effect of Variation of Rainfall Intensities	154
6.4.2 Effect of Variation of Geometry of Slope	155
6.6 Summary	145
CHAPTER 7 Conclusions	157
7.1. General	157
7.2 Summary and Conclusions	157
7.2.1 Microstructural Characterization of Untreated and Treated Jute	158

7.2.2 Durability Studies of Untreated and Treated Jute	159
7.2.3 Experimental Assessment of Erosion Control of Treated Soil Slopes	160
7.2.4 Numerical Modelling of Strength of Treated Soil Slopes	161
7.3 Contribution made by the scholar	163
7.4 Recommendations for Future Research	164
7.4 Design Procedure and Practical Application of Vegetation along with AAB Treated Jute	164

List of Tables

Table 2.1 Effects and applications of various natural geotextiles	22
Table 2.2 Causes of Slope Failure	25
Table 2.3 Nominal tensile strengths of different Tree Species	36
Table 3.1 Properties of Red Soil	58
Table 3.2 Fundamental characteristics of untreated jute	59
Table 3.3 FTIR peaks and corresponding for Jute	59
Table 3.4 Amount of AAB required treating per sq. meter jute geotextile	61
Table 3.5 Basic Properties of Bermuda Grass	63
Table 3.6 Thickness values of Untreated and Treated jute at various times	67
Table 3.7 Tensile strength of untreated and treated jute	68
Table 3.8 Permeability of jute-reinforced soil	70
Table 3.9 CBR of jute-reinforced soil (Unsoaked)	71
Table 3.10 CBR of jute-reinforced soil (Soaked)	71
Table 3.11 UCS values red soil reinforced with different jute fibres	72
Table 3.12 Tensile Strength of different Root Matrix Systems	78
Table 3.13 Shear strength of Soil Infused with Roots	79
Table 5.1 Soil Yield Values Obtained from Experimental Procedures	118
Table 5.2 Soil Erodibility factor values	123
Table 5.3 Topographic Factor Values	123
Table 5.4 Cover Management factors for different conditions	124
Table 5.5 Cover Management Factors for reinforcement	124
Table 5.6 Support Practice Factor (P) Values	125
Table 5.7 Sediment Yield Values Calculated from the MUSLE Model	126
Table 5.8 Experimental Values of Soil Yield	129
Table 5.9 Sediment Yield Values calculated from MUSLE model	130

Table 6.1 Axial stiffness of untreated and AAB treated jute used in PLAXIS 2D	138
Table 6.2 Soil and Ground Water Parameters used in Plaxis 2D	140
Table 6.3 R_{inter} values for different interfaces	141
Table 6.4 Number of elements and nodes generated with the variation of mesh fineness	142
Table 6.5 (a) Sediment yield at the time of slope failure for reinforced slopes under rainfall	147
Table 6.5 (b) Slope failure times for both experimental and numerical simulation	148
Table 6.6 Factor of Safety Values of Slopes	153

List of Figures

Figure 1.1 Failure of the railway embankment due to rainfall in Belgavi, Karnataka, India	2
Figure 2.1 Schematic representation of forces acting on particles	16
Figure 2.2 Different types of Soil Erosion	17
Figure 2.3 Water Erosion Process due to rain fall	18
Figure 2.4 Slope failure models or mechanisms for mass stability analysis a) transitional failure infinite slope model; b) rotational failure, circular arc model	28
Figure 2.5 Factors involved in the infinite slope method	33
Figure 2.6 Main influences of vegetation on slope stability	33
Figure 2.7 Soil Water Characteristic Curve image	51
Figure 3.1 Grain size distribution curve of red soil	57
Figure 3.2 (a) FTIR Spectral Image (b) XRD image of untreated Jute	60
Figure 3.3 Jute Geotextile before and after AAB treatment	62
Figure 3.4 Bermuda grass grew in laboratory condition	63
Figure 3.5 AOS obtained from the stereomicroscopic image	66
Figure 3.6 Mass per unit area values of Untreated and Treated jute at various times	67
Figure 3.7 Tensile strength test of untreated and AAB treated jute geotextile	69
Figure 3.8 Permeability of jute reinforced soil	70
Figure 3.9 Images of jute reinforced CBR sample at H/3, H/2, and 2H/3 positions from top	71
Figure 3.10 Untreated and jute-reinforced UCS samples at 38mm position from the top	72
Figure 3.11 Schematic Diagram of Large Shear Box Test	73

Figure 3.12 Friction angle between red soil and different reinforcements	74
Figure 3.13 Seed sowing process for healthy germination of Bermuda grass	75
Figure 3.14 Germinated plant from Bermuda grass after 25 days from the sowing date	75
Figure 3.15 Length of Bermuda Grass Plant and Root System	75
Figure 3.16 Bermuda Grass Regrowing mechanism	76
Figure 3.17 Root Matrix for Bermuda Grass	76
Figure 3.18 Root Matrix and Root System Diameter for Bermuda Grass	76
Figure 3.19 Tensile Strength Test of Bermuda Grass	77
Figure 3.20 Sample collection from root-penetrated soil	78
Figure 3.21 Schematic Diagram of Experimental Setup for Surface Erosion	80
Figure 3.22 Non-recording type rain guage	80
Figure 3.23 Rotameter	81
Figure 4.1 Image of jute geotextiles in (a) Lab burial; (b) field burial condition	83
Figure 4.2 Images of (a) Untreated (b) AAB-treated jute geotextiles subjected to soil burial under lab conditions at 30, 90 & 180 days duration	83
Figure 4.3 Images of (a) AAB-treated jute immersed in acidic and alkaline solution (b) Raw Jute(c) AAB-treated jute after 30 days of HCl and NaOH treatment	84
Figure 4.4 Images of (a) Raw Jute after 90 days of HCl and NaOH treatment; (b) AAB treated jute after 90 days of NaOH	85
Figure 4.5 (a) Hydrolysis tests (b) Raw jute (c) AAB jute after 90 days of hydrolysis test	86
Figure 4.6 (a) Fresh Compost (b) AAB-treated jute at 0 days (c) Compost after 180 days (d) AAB Treated Jute after 180 days	87

Figure 4.7 (a) Weight loss of untreated and treated jute with time in soil burial test	90
Figure 4.7 (b) Reduction in Tensile Strength of untreated and treated jute with time in soil burial test	91
Figure 4.7 (c) Reduction in Elongation at Breaking of untreated and treated jute with time in soil burial test	91
Figure 4.8 (a-b) Weight loss of untreated and treated jute with time in acid test (left) and alkali test (right)	92
Figure 4.8 (c-d) Reduction in Tensile Strength of untreated and treated jute with time in acid test (left) and alkali test (right)	93
Figure 4.8 (e-f) Reduction in Elongation at Breaking of untreated and treated jute with time in acid test (left) and alkali test (right)	94
Figure 4.9 (a) Weight loss of untreated and treated jute with time in hydrolysis test	95
Figure 4.9 (b) Reduction in Tensile Strength of untreated and treated jute with time in hydrolysis test	95
Figure 4.9 (c) Reduction in Elongation at Breaking of untreated and treated jute with time in hydrolysis test	96
Figure 4.10 (a) Weight loss of untreated and treated jute with time in hydrolysis test	96
Figure 4.10 (b) Reduction in Tensile Strength of untreated and treated jute with time in compost burial test	98
Figure 4.10 (c) Reduction in Elongation at Break of untreated and treated jute with time in Compost burial test	98
Figure 4.11 Stereomicroscopic images of (a) untreated jute (b) 0.35 AAB jute (c) 0.40 AAB jute (d) 0.45 AAB jute at magnification 1.5 x	101
Figure 4.12 Stereomicroscopic Images of Untreated and Treated Jute (a) before durability tests and in (b) Soil Burial (c) Compost Burial (d) Acid (e) Alkali (f) Hydrolysis Tests after	

90 days of exposure	103
Figure 4.13 Stereomicroscopic Images of Untreated and Treated Jute (a) before durability tests (b) Soil Burial (c) Compost Burial (d) Acid (e) Alkali (f) Hydrolysis Tests after 180 days of exposure	104
Figure 4.14 XRD images of Untreated and Treated Jute (a) before durability tests and in (b) Soil Burial (c) Compost Burial (d) Acid (e) Alkali (f) Hydrolysis Tests after 180 days of exposure	106
Figure 4.15 FTIR spectral image profile of Untreated and Treated Jute (a) before durability tests (b) Soil Burial (c) Compost Burial (d) Acid; (e) Alkali; (f) Hydrolysis Tests after 180 days of exposure	108
Figure 4.16 SEM images of a) untreated jute b) 0.35 AAB Jute c) 0.40 AAB Jute d) 0.45 AAB Jute	109
Figure 4.17 SEM Images of Untreated and Treated Jute (a) before durability tests (b) Soil Burial (c) Compost Burial (d) Acid (e) Alkali (f) Hydrolysis Tests after 90 days of exposure	111
Figure 4.18 SEM Images of Untreated and Treated Jute (a) before durability tests (b) Soil Burial (c) Compost Burial (d) Acid (e) Alkali (f) Hydrolysis Tests after 180 days of exposure	112
Figure 4.19 TGA images of a) Untreated and Treated Jute (b) 0.35 AAB Treated Jute (c) 0.40 AAB Treated Jute (d) 0.45 AAB Treated	114
Figure 5.1 (a) Bare soil slope (b) Unreinforced Slope exposed to rainfall (c) Slope reinforced with jute d) Slope reinforced with 0.35 AAB jute reinforcement e) Slope reinforced with untreated jute after one month of rainfall exposure f) Slope reinforced with 0.35 AAB jute after one month of rainfall exposure	116
Figure 5.2 Flow chart showing different types of soil erosion models	119
Figure 5.3 Soil erosion test for Vegetated Slope with Jute reinforcement (Left) and 0.35 AAB treated Jute Reinforcement (Right)	128

Figure 5.4 Sediment yield data of (a) 30° slope - low rainfall condition (b) 30 ° slope - High rainfall condition (c) 45 ° slope - Low rainfall condition (d) 45 ° slope - High rainfall condition (e) 60 ° slope - Low rainfall condition (f) 60 ° slope - High rainfall condition	133
Figure 6.1 Images of (a) plane strain (b) axisymmetric models	137
Figure 6.2 Images of (a) 15- Node (b) 6-Node triangular elements	138
Figure 6.3 Mesh convergence study of 30° soil slope model	142
Figure 6.4 Meshing and boundary condition of 30° soil slope	142
Figure 6.5 Ground Water flow boundary condition applied for 30° slope	143
Figure 6.6 Validation of Plaxis 2D Results	144
Figure 6.7 Images of a) 45° slope before rainfall; b) 45° slope exposed to 23.4 mm/hr rainfall; c) slope reinforced 0.35 AAB jute; d) slope reinforced with untreated jute	146
Figure 6.8 Images of a) 45° unreinforced slope; b) 45° jute reinforced slope after exposure to high rainfall for a period of 1 hr	146
Figure 6.9 Deformed images of a) 30° slope without any reinforcement; b) 30° with jute reinforcement; c) 45° slope without any reinforcement; d) 45° slope with jute reinforcement; e) 60° slope without any reinforcement; f) 60° slope with jute reinforcement under low rainfall condition	150
Figure 6.10 Slope failure time images of a) 30° unreinforced slope, b) 45° jute reinforced slope, c) 60° jute reinforced slope	152
Figure 6.11 Factor of safety values of 8m height 30° slope reinforced with 0.35AAB jute	155
Figure 6.12 Factor of safety values of 8m high slopes with varying slope angles	156

List of Abbreviations

AAB	:	Alkali Activate Binder
AlO ₂ SiO ₃	:	Aluminium Silicate
AOS	:	Aperture Opening Size
ASTM	:	American Society for Testing and Materials
BFREC	:	Bbamboo Fibre-Reinforced Eepoxy Composite
CBR	:	California Bearing Ratio
CEA	:	Central Electric Authority
CF	:	Coir Fibre
CH ₄	:	Methane
CO	:	Carbon Monoxide
CO ₂	:	Carbon Dixoide
CSNL	:	Cashew Nut Shell Liquid
ECB	:	Erosion Control Blankets
ECRM	:	Erosion Control Revegetation Blankets
FA	:	Fly ash
FDM	:	Finite Difference Method
FEM	:	Finite Element Method
FTIR	:	Fourier Transform Infrared Spectroscopy
FOS	:	Factor of Safety
HCL	:	Hydrochloric Acid
HDPE	:	High Density Polyethylene
IRC	:	Indian Road Congress
JGT	:	Jute Geotextile
JU	:	Unprocessed jute geotextiles
KFRUPC	:	Kenaf Fibre Reinforced Unsaturated Polyester Composites
LA	:	Limit Analysis

L/D	:	Length to Diameter Ratio/ Aspect Ratio
LEA	:	Limit Equilibrium Analysis
LEM	:	Limit Equilibrium Method
LVDT	:	Linearly Variable Differential Transformers
MDD	:	Maximum Dry Density
MUSLE	:	Modified Universal Soil Loss Equation
NaCl	:	Sodium Chloride
NaOH	:	Sodium Hydroxide
N ₂ O	:	Nitrous Oxide
Na ₂ SiO ₃	:	Sodium Silicate
O	:	Oxygen
OH	:	Hydroxyl Compressed Natural Gas
OMC	:	Optimum Moisture Content
PALF	:	Pineapple Leaf Fibres
PBS	:	Poly Butylene Succinate
pH	:	Potential of Hydrogen
PLA	:	Poly Lactic Acid
PTF	:	Pedo Transfer Functions
PVC	:	polyvinyl chloride
RUSLE	:	Revised Universal Soil Loss Equation
SEM	:	Scanning Electron Microscope
Si	:	Silicon
SM	:	Silty Sand
SWCC	:	Soil Water Characteristic Curve
T1	:	Woven Geotextile with treated fiber
T2	:	Treated geotextile at fabric level

TPU	:	Thermoplastic Polyurethane
UCS	:	Unconfined Compressive Strength
UTM	:	Universal Testing Machine
USA	:	United States of America
USCS	:	Unified Soil Classification System
USDA	:	United States Department of Agriculture
USLE	:	Universal Soil Loss Equation
UV	:	Ultraviolet
WHO	:	World Health Organization
W/S	:	Water to Solid Ratio
XRD	:	X-Ray Diffraction

List of Symbols

An	:	Analcine
Al	:	Aluminium
C	:	Carbon
C	:	Crop management factor
C _u	:	Coefficient of Uniformity
c'	:	Effective Cohesion
d ₆₀	:	Particle Size
E	:	Young's Modulus
g _a	:	air entry value
g _n	:	rate of water extraction
H	:	Hydrogen
J	:	Jute
K	:	Soil erodibility factor

k_{sat}	:	Saturated Permeability of Soil
LS	:	Topographic Factor
M	:	Mullite
N_{α}	:	Normalised values of α with the same empirical formula for wetting and drying
N_{nw} & N_{nd}	:	Normalised n values for wetting and drying conditions
O	:	Oxygen
P	:	Erosion control-practice factor
Q	:	Quartz
q_p	:	peak runoff rate in m^3/ sec
R_{inter}	:	strength reduction factor
S	:	Hydroxy sodalite
Si	:	Silicon
S_{res}	:	residual volumetric water content
S_{sat}	:	saturated volumetric water content
Y	:	Sediment yield in metric tons
τ	:	Shear strength of unsaturated soil
σ_n	:	Total normal stress
u_a	:	Pore Air Pressure
u_w	:	Pore Water Pressure
ϕ'	:	Internal Friction Angle
χ	:	Scalar Multiplier
θ_w	:	Volumetric Water Content
θ_{res}	:	Residual Volumetric Water Content
θ_{sat}	:	Saturated Volumetric Water Content
α, n	:	Van Genuchten Parameters
α_{1w}, n_{1w}	:	Vangenuchten α, n values corresponding to wetting

- α_{1d}, n_{1d} : Vangenuchten α, n values corresponding to drying
- λ : Slope Length (m)
- γ_{unsat} : Unsaturated unit weight of soil (KN/m³)
- γ_{sat} : Saturated unit weight of soil (KN/m³)
- ν : Poisson's ratio

CHAPTER 1

Introduction

1.1 General

The necessity of using eco-friendly materials in the construction sector to reduce environmental pollution justifies the use of natural materials in slope stabilization. Biodegradability issues with natural geotextiles hinder their popularity of usage in geotechnical structures such as retaining walls, slopes, and river bank protection. Controlling the environmentally hazardous effects of geosynthetic materials and, at the same time, reusing waste materials in the construction industry, such as fly ash (FA), is of the highest priority in modern times, particularly in developing countries. The present research seeks to develop a method for the sustainable and environmentally favourable use of natural materials in slope stabilization. The background and motivation of the research are presented in this chapter. The organizational structure of the thesis is discussed in detail in this chapter.

1.2 Background of the Proposed Study

Stabilizing slopes and reducing surface erosion are important goals in many civil and environmental engineering projects. Slope failures, such as landslides and rockfalls, may devastate human life, property, and infrastructure. At the same time, surface erosion can lead to soil loss, sedimentation, and water quality degradation. Slope failures in soil due to intense rainfall are major global geotechnical disasters. In India, landslides have resulted in major mortality rate and destruction of communication systems, human settlements, agricultural areas, and forest regions. The occurrence of intense rainfall in various regions worldwide has the potential to induce slope failures, resulting in severe consequences for human lives and infrastructure. There are several cases of large-scale devastating landslides produced by rainfall in nations such as China, Chile, India, Japan, and Venezuela (Brown *et al.*, 1982; Lagmay *et al.*, 2006; Sengupta *et al.*, 2010; Schuster *et al.*, 2002; Van Sint Jan & Talloni, 1993). According to the Disaster Management Authority of India, Ministry of Home Affairs (MHA), Govt. of India, roughly 100 to 150 crores of monetary loss occurred in the last decade and, as per the Geological Survey of India, around 0.42 million km² (12.6% of landmass) of the area in India is prone to landslides. In 2003, 2007 and 2008, the proportion of landslides in India was in the top ten worldwide (Kirschbaum *et al.*, 2010). During the monsoon season, which typically lasts from June to September and October to December,

landslides occur more frequently (NDMG, 2009). Weak geological patterns, extremely intense rainfall, naturally critical slopes and the absence of permeable granular soil are the most identified causes of landslides. Figure 1.1 shows a railway embankment failure because of excessive rainfall at Shivatan railway station in Belagavi district, Karnataka, India.



Figure 1.1 Railway embankment failure due to rainfall in Belgavi, Karnataka, India (Deccan Herald, August 17, 2020)

Traditional methods for prevention of erosion and stabilization of slope have relied on geosynthetics and hard armor solutions, such as retaining walls and concrete structures. Geosynthetics, including geomembranes, geotextiles, and geogrids, are designed to have desirable physical characteristics for various engineering applications. Their high efficiency and reliable performance make them popular for various civil engineering projects, including erosion control, soil stabilization, and drainage systems. However, these methods can be costly, difficult to install, and have negative environmental impacts. Artificial geosynthetics that do not biodegrade, such as polyethylene, polyester, or polypropylene, may persist in the environment for centuries, leading to landfill accumulation and long-term pollution. Toxic additives or chemicals in certain geosynthetics potentially leach into the environment and pollute soil and water. During manufacturing and disposal, certain polyvinyl chloride (PVC) geosynthetics release dioxins, a hazardous toxin. Artificial geosynthetics degrade into microplastics, which may enter the food chain and harm animals. Manufacturing geosynthetics in a plant requires the use of energy-intensive equipment and the extraction and processing of fossil fuels. Thus it contributes to global warming by emitting greenhouse gases (CO_2 , CH_4 , N_2O) (Dixon *et al.*, 2016).

The use of materials like natural fibres and plant roots has gained popularity recently to stabilize slopes and reduce surface erosion. Natural geotextiles such as coir, jute, and sisal provide immediate protection when installed in the ground. They have no negative effects on

the environment, and their slow biodegradation benefits plant life by providing organic matter and essential minerals which can improve soil fertility, water retention, vegetation process and establishment of roots (Daria *et al.*, 2020; Shavandi and Ali, 2019; Sarasini and Fiore, 2018; Broda *et al.*, 2016). As the vegetation grows, it helps to anchor the soil and prevent erosion. Plant roots, particularly those of certain grasses and shrubs, can stabilize slopes effectively and reduce erosion. These plants have deep, fibrous root systems that can help to anchor the soil and absorb water, preventing it from flowing across the surface and causing erosion. The plant roots can also improve soil strength and nutrient availability.

Traditional techniques for controlling soil erosion on steep slopes include bench terracing and dry rubble-packed bunds. However, these usual approaches cannot support plant development on steep slopes. Natural vegetation is an effective way of erosion management and slope protection on sloping terrain. Issues like soil erosion due to frequent rainfalls can wash away germinating seeds and tiny plants in the initial stages, preventing plants from properly growing on such a slope. Under such circumstances, geotextiles protect the soil and seeds during the earliest phase of plant development.

Natural fibres, such as coir, jute, etc., are preferable over synthetic fibres due to the environmental friendliness of the material and ecological compatibility as it degrades with the soil. In contrast to synthetic fibres, natural geotextiles are more efficient in preventing soil erosion due to their enhanced drapability (Bhattacharyya *et al.*, 2010). Unlike synthetic geotextiles, natural fibres may absorb water and degrade over time, making them unsuitable for slope stability applications (Lekha, 2004). Based on mechanical performance, natural geotextiles are equivalent to synthetic geotextiles. Natural fibres have similar specific tensile strength and Young's modulus as compared to synthetic fibres (Nam *et al.*, 2006). Natural geotextile costs less than synthetic geotextiles and leaves no carbon dioxide (CO₂) footprint (Wambua *et al.*, 2003). Moreover, natural geotextiles may be substituted for synthetic ones in various construction applications. For example, river banks and hill slopes need protection against erosion until the vegetation is mature enough to hold the soil. Many uses have been found for raw jute geotextile (JGT) and treated JGT in India. Datta (2007) has provided several examples of the successful use of JGT to halt soil erosion, enhance road subgrade, and safeguard river and canal banks.

Nevertheless, the global use of natural geotextiles is considerably low, such as less than 6% of total geotextile use (Sanyal, 2017). Several potential factors may contribute to the limited utilisation of natural geotextiles, such as (i) paucity of academic research on the

properties of natural geotextiles along with the behaviour and performance of soil reinforced with them, (ii) the differences in properties among geotextiles of the same kind can be attributed to disparities in their origin and manufacturing procedures, and (iii) low resistance to microbial, physical, and environmental deterioration.

Slope parameters determine the applicability of the natural geotextile material as reinforcement. Natural geotextiles are efficient on low-volume roads, river banks and mild to moderate steeper slopes. Natural geotextiles on mild slopes may stabilize the soil and prevent erosion. Natural geotextiles act effectively on slopes with vegetation. In the process of stabilizing slopes over time geotextiles protect vegetation and promote plant growth. On slopes with mild to moderate erosion, natural geotextiles are effective. They work particularly well in areas with a significant erosion risk from water runoff. Natural geotextiles may be used on construction sites and embankment slopes. During construction, they stabilize disturbed soil and prevent erosion while vegetation develops.

However, the life span of JGT is of a maximum period of 6 to 12 months (Shukla, 2021; Sanyal, 2017). In regions with varying precipitation, the durability of natural geotextiles can differ due to several factors, such as material type, installation technique, and local conditions. Therefore, certain procedures are necessary to prolong the practical lifespan of these fibres. Bitumen coating, acetylation, and treatments with sodium hydroxide and hydrogen peroxide are all effective, but they are expensive and may lead to leachate (Gupta *et al.*, 2018). Therefore, an innovative treatment for extending the durability of JGTs has to be developed. At the same time, the treatment method, which is environmentally and economically friendly treatment can be adaptable, like an alkali activated binder (AAB) treatment that uses the industrial by-product fly ash for production. In vitreous phases, AAB is produced by disrupting the covalent bonds of Al-O-Si, Si-O-Si, and Al-O-Al, yielding a long-chain polymerized sodium aluminosilicate structure (Davidovits, 1994). By dissolving NaOH in an alkaline medium, the covalent bonds between Si-O-Si, Al-O-Al, and Al-O-Si in the vitreous phase of the raw material are broken, allowing the SiO_2 and Al_2O_3 ions to be transformed into colloids and released into the solution. This concentration of $\text{Al}_2\text{O}_2\text{SiO}_3$ polymerizes into a highly reactive material, producing a well-structured alumino-silicate matrix. The degree to which covalent bonds are destroyed depends on volume, pH, and alumina-silica origin variables. Utilizing AAB for the treatment of natural geotextile has dual advantages. It reduces the need for conventional treatment methods (e.g. acetylation, bitumen coating) and landfill disposal expenses for fly ash. In addition, AAB has a low carbon

footprint (80% less CO₂ and 70% less potential for global warming) and excellent mechanical performance, workability, and durability (Gartner 2004; Taylor *et al.*, 2006). The treatment technique proposed for natural geotextiles in this study involves the utilisation of fly ash as the primary constituent. India is the third most prominent producer of coal-based electricity globally, following China and the United States. According to research by the central electrical authority India, power plants of the country generate between 106.37 and 133.9 million tons of fly ash annually, of which % is very fine (CEA 2022). Every year, between 20 and 25 % of fly ash is wasted. In India, the land area occupied by fly ash and other ash ponds amounts to approximately 65,000 acres. It is projected that the annual production of ash in the country will exceed 230 million tonnes by the year 2022(IRC: SP:20-2002). Since most of the factories generate fly ash as a leftover product, the manufacturing costs for AAB are less than those of conventional treatment processes such as acetylation. However, a significant amount of research encompassing extensive laboratory investigations is needed before recommending AAB for treating natural geotextiles. Alternative stabilisers for slope stabilisation are becoming a viable option as the use of eco-friendly materials gains popularity in civil engineering.

1.3 Importance of Proposed Research

The research results (optimal design of natural fiber and plant root stabilization soil slope) can be innovative solutions to protect soil erosion on road and railway embankments. This innovation will be very useful for the construction industry. Fly ash is produced in huge quantities in India as an industrial byproduct of coal-based thermal power plants. The methodology adopted in the present study will make use of fly ash as one of its primary components. The use of AAB-treated natural fiber on road/railway embankments, river dykes, and other embankments will be an economically and environmentally friendly solution to utilize waste products. In addition, a numerical model is simulated to compute the effects of various reinforcements to stabilize slopes when exposed to rainfall will significantly assist the design of embankments and slopes. Using natural fibers for the protection of slopes and erosion control will be a best practice example for all and the results can be used as educational material for spreading awareness on sustainable slope management and erosion control practice.

1.4 Goals and Objectives

An attempt is made in this research to utilize natural geotextiles for slope stabilization and to treat the natural geotextiles with industrial byproducts to increase their durability and performance. This research aimed at finding environmentally friendly alternatives to traditional chemical treatments for JGTs. The main goal of this study is to determine the optimal AAB mix for a wide range of w/s ratios and aluminosilicate precursor concentrations in alkaline mixtures. The main focus of this study is to evaluate the microstructural properties of untreated and treated JGTs to assess the durability of jute. Experimentally, the stability of a slope reinforced with various JGTs together with and without vegetation is evaluated when subjected to varying rainfall intensities. After installing different reinforcements on the slope surface, the stability of the slope under rainfall conditions is simulated using commercially available finite element software Plaxis 2D. Considering the goals mentioned above, the specific objectives of this research are listed as follows:

- Development of a novel treatment method with Alkali Activated Binder (AAB) for natural fibres to improve their strength and durability.
- Geotechnical and material characterization of AAB-treated natural fibres, plant roots and locally available soil.
- Comparison of relative soil reinforcing efficiency of plant roots and AAB-treated natural fibre, both individually and in combination.
- Evaluation of the effectiveness of treated natural fibres and plant roots in reducing surface erosion by the construction of a laboratory scale slope model exposed to rainfall.
- Assessment of stability behaviour of slopes, reinforced with treated JGTs and subjected to varying rainfall patterns using numerical modeling

1.5 Thesis Organization

A brief description of the work carried out in various chapters is presented chronologically.

Chapter 1: This chapter briefly overviews the research topic and emphasizes the significance of the current investigation.

Chapter 2: Extensive literature reviews are conducted to assess the performance of different natural geotextiles in enhancing soil strength, decreasing surface erosion, and stabilizing

slopes. Several methods for improving the durability of natural geotextiles are covered. Bioengineering methodology in preventing slope instability and soil erosion is discussed. Various numerical strategies for dealing with slopes that have been reinforced are also addressed.

Chapter 3: This chapter illustrates the characterization of red soil and locally available natural JGT. Methods for microstructural characterization of natural geotextiles, performing geotechnical tests, study on vegetation, and soil erosion models are discussed in detail.

Chapter 4: This chapter focuses on the extensive durability research on untreated and treated natural JGTs. Studies characterizing the mechanical strength of JGTs are also reported. Analysis of chemical, mineralogical, and morphological changes of natural JGTs after being treated with AAB solution is also discussed.

Chapter 5: The soil erosion experiments carried out in the laboratory on a slope model consisting of different inclinations reinforced with untreated and treated jute reinforcement, along with and without vegetation, are elaborated on in this chapter. The Modified Universal Soil Loss Equation model is also used to analyze the values of soil erosion.

Chapter 6: In this chapter, the stability behaviour of soil slope reinforced with various untreated, treated JGTs and exposed to various rainfall intensities are discussed in detail with the help of Plaxis 2D, a commercial finite element software.

Chapter 7: This chapter provides a summary of the most important results from the current study and discusses the possibilities for future research.

CHAPTER 2

A Review of Literature

2.1 General

This chapter presents an overview of existing research on natural geotextiles and their application in ground improvement, specifically slope stability. It discusses the role of natural geotextiles in protecting the slope against erosion to reduce the risk of erosion caused by raindrops and flood waters, slope stabilization, and their reinforcing performance along with vegetation in their natural, chemically treated form. The uses of natural geotextiles against conventional synthetic geotextiles are also discussed.

The major concern of this chapter is to examine the efficacy of natural geotextiles for slope protection. A comprehensive analysis of how natural geotextiles are used to enhance the strength properties of weak soil is presented. A thorough explanation of the durability of natural geotextiles, as well as their limitations and a variety of treatment approaches to increase their durability, are highlighted. The effectiveness of various chemically treated geotextiles for ground improvement and slope stability is also discussed. The influence of different bioengineering methods on slope stability is reviewed. In addition, the significant research gaps and possibilities for future research are also addressed.

The review is presented chronologically under the following categories:

- ❖ Improvement of the strength of soil using natural geotextiles
- ❖ Reduction of surface erosion using natural geotextiles
- ❖ Slope stabilization using natural geotextiles
- ❖ Strengthening of soil and decreasing surface erosion by bioengineering methods
- ❖ Durability studies and treatment methods for natural geotextiles
- ❖ Numerical studies of reinforced soil slopes

2.2 Improvement of Strength of Soil Using Natural Geotextiles

2.2.1 Natural Geotextiles

Geotextiles have gained significant popularity in engineering applications in recent decades owing to their multifunctional capabilities in soil filtration, reinforcement, drainage, and

separation. The excellent mechanical properties of manmade synthetic geotextiles have led to their widespread recognition in the engineering field (Shtykov *et al.*, 2017; Bouazza *et al.*, 2006). Artificial geosynthetics, also known as geotextiles, geogrids, geonets, etc., are polymeric products used in direct interaction with soil and/or rock in civil and environmental engineering. (Wiewel and Lamoree, 2016). Müller and Saathoff (2015) estimated that the annual worldwide geosynthetics market is around 6,125 million square metres, with a value of \$5.76 billion. Artificial geosynthetics, in general, are made from petroleum-based polymers like polyolefins and polyesters. While polyethylene makes up the remaining 10%, polypropylene dominates (90%) as the geosynthetic material (Wiewel and Lamoree, 2016). Petroleum-derived polymers exhibit commendable mechanical strength and durability, however, prolonged exposure to normal environmental conditions can generate microplastic particles (less than 5 mm) to release and leach eco-toxic chemicals into the surrounding environment (Browne *et al.*, 2007). Micro-plastics have been found in various concentrations in drinking water, including bottled and tap water, marine water, wastewater, fresh water, food, and the air. Micro-plastics may be ingested or inhaled, and once within the body, they may be absorbed by different organs and have a variety of potential negative effects on health, such as causing cell damage or inflammatory and immunological responses (WHO 2019). Consequently, many researchers are currently exploring the efficacy of natural geotextiles, including JGT (JGT), coir, hemp, and flax by studying their mechanical and performance characteristics (Sanyal, 2017; Subaida *et al.*, 2009; Rawal and Anandjiwala, 2007; Lekha, 2004).

Natural geotextiles such as JGT, coir, hemp, sisal, and flax are widely used in civil engineering. The majority of JGT originates from India, Bangladesh, and China. The adaptability of JGT was recognized as early as the fifteenth century. An organised effort to grow JGT probably was initiated around the 16th century (Ghosh *et al.*, 2014; Singhavi, 2003). The premier center for textile processing, research, and training was established in Dundee, Scotland, and the experts suggested using JGT to spin thicker yarns suitable for weaving into sacking, wrapping, and backing materials. The demand for JGT to make sacks increased in the years between the American Civil War (1860–1865) and Crimean War (1854–1856) (Sanyal, 2004; Mitra, 1999). Dundee, Scotland, witnessed the first successful use of JGT as a road reinforcement in 1920, and Strand Road, Kolkata, India, followed in 1934. In the 1950s, a woven synthetic cloth was used to prevent erosion in Florida. However, in 1966, a nonwoven fabric was first used for asphalt overlay in the USA (Ghosh *et al.*,

2014). This is how the utilization of JGT in civil engineering came into implementation. The following chapters will discuss various aspects of JGT.

In the last several years, JGT has emerged as a potentially useful material in many fields of civil engineering (Panigrahi and Pradhan, 2019). Plants of the genus *Corchorus* are used to produce JGT. Manufacturing JGT is commercially popular in countries like Bangladesh, India, and China. Compared to other natural fibres, this material stands out as both cost-effective and extensively manufactured. (Faruk *et al.*, 2010). JGT is a biodegradable lignocellulose fiber. After cotton, it is the most widely produced natural fibre. The composition of this fibre primarily consists of cellulose, hemicellulose, and lignin (Saha *et al.*, 2010). The presence of a high amount of cellulose in JGT provides high tensile strength. The strength ratio of expansive soils improved up to fiber content of 0.6% and the shear strength of the soil increased with an increase in the length of the fiber (Wang *et al.*, 2017). The incorporation of a woven variant of JGT (85%) in the cross-direction geotextile for the construction of unpaved rural roads led to a significant enhancement in modulus, breaking strength, and puncture resistance as measured by the California Bearing Ratio (CBR), in comparison to the strength improvement achieved with a 100% HDPE geotextile (Basu *et al.*, 2010). Natural geotextiles serve multiple functions within civil engineering, such as soil stabilisation and erosion prevention. The following sections discuss in detail some prominent civil engineering applications by natural geotextiles.

2.2.2 Strengthening of Soil using Natural Geotextiles

Due to rising industrialization and urbanization, the construction industry requires improving the engineering properties of existing ground. Ground improvement techniques are employed to enhance the geotechnical characteristics and engineering properties of soils that are weak and soft. Since ancient times, stabilizing these soils has improved their engineering properties. Soil reinforcement is a ground improvement technique that enhances the bearing capacity, ductility, and resistance to soil deformation. Shear strength of sand that has been reinforced with various synthetic, natural, and metallic fibres was studied by Grey and Ohashi (1983). These factors included the orientation, content, area ratios, and stiffness of the fibres. The researchers concluded that the relationship between the area of fibres and the area of the matrix directly influences the shear strength of a material. In their study, Maher and Grey (1990) conducted triaxial compression experiments on sand that had been reinforced with discrete, randomly dispersed fibres. Mechanical characteristics of a kaolinite-fiber soil

composite were examined by Maher and Ho (1994) using splitting tension, unconfined compression, and three-point bending tests. In recent decades, research has demonstrated that the engineering properties of various soil types, including sand, silt, and clay, can be improved through the incorporation of fibre reinforcement (Shaia et al., 2016). The study conducted by Aggarwal and Sharma (2010) examined the utilization of JGT to improve the characteristics of subgrade materials. The findings indicate that applying JGT reinforcement resulted in a reduction in the maximum dry density and an increase in the optimal moisture content of the subgrade soil. According to Singh and Yachang (2012), reinforced soil may have a deviatoric stress at failure that is maximum of 3.5 times higher than that of plain soil. They also found that the increased stiffness modulus of reinforced soil dramatically reduced soil settling. Multiple laboratory CBR experiments on soil reinforced with JGT of varied lengths and diameters were also performed by Singh and Bagra (2013). Soil CBR values were found to rise by a large amount (200%) after being treated with JGT. Experimental research on the usage of JGT for subgrade soil enhancement has been conducted by Al *et al.*, (2016). The research included a series of testing, including rutting, dynamic load, CBR, and durability. With JGT, the subgrade soil's CBR value was increased, the rutting depth was decreased, and the cost of maintenance was lowered. Using JGT reduces the pavement's thickness and the associated construction expense. Choudhary *et al.*, (2011) assessed the utility of JGT and geogrid through CBR tests on both the reinforced and unreinforced soil in wet conditions. It was found that increasing the number of reinforcing layers significantly raised the soil's CBR value. Compared to geogrid, JGT was also proven to be more successful at strengthening.

The study conducted by Kumar (2012) found that the incorporation of woven and nonwoven geotextiles in the interface between a soft subgrade and unbound gravel within an unpaved flexible pavement system resulted in improved penetrating resistance and, consequently, enhanced the CBR strength of the unpaved road, especially when dealing with a soft subgrade. Incorporating geotextiles into the design of an unpaved road increased its performance, and this effect was amplified with deeper penetration. Ghosh *et al.*, (2014) constructed two types of clayey soil, one with JGT and one without, to compare the effects of adding and removing the geotextile on the soil properties. They discovered that the JGT substantially impacted final form of the soil. The JGT geo-shear textile strength, dry density, and permeability values were examined before and after being laid. Hence, it may be

concluded that JGT is a powerful tool for enhancing soil quality by lowering compressibility and raising strength.

Pozzolan materials including fly ash, JGT, lime, and water-resistant compounds were added to black cotton soil by Pandey *et al.*, (2013) for the study. Multiple Proctor compaction tests, CBR and Atterberg limit tests were performed on soil containing JGT of varying diameters (2-8mm) and lengths (0.5-2mm) and percentages (0.2%-1%) of fly ash (10%, 15%, 20%, and 25%) to determine the optimum amount of each. The results showed that combining 1% JGT, 20% fly ash, and 5% lime in soil yielded superior results than adding each ingredient separately for soil improvement, thereby reducing the cost of the road (black cotton soil) by approximately 50-60% and increasing the CBR values by around 80-20 times.

As part of their research, Philip and Charly (2016) examined the effects of geotextile reinforcement on granular soils when applied at the top, middle, and bottom of the model, the CBR values of geotextile-sheet-reinforced granular soils were observed to rise. When compared to unreinforced soil, soil that was strengthened using a geotextile sheet possessed greater shear strength. Naeini (2008) studied geotextiles to understand more about their usage as a tension material in the strengthening of granular soils. The effectiveness of reinforcing on three samples of granular soil of varying sizes was evaluated. Geotextile sheets were stacked in one or two layers at various depths inside the sample. They found that granular soils with reinforced geotextile materials had a greater bearing capacity and CBR after being covered with geotextile sheets. Compaction, deformation, and strength properties of fly ash-stabilized soils were studied by Tapas and Baleshwar (2014). A higher soil dry unit weight was observed after incorporating JGT layers. Two-layer compacted samples made of JGT were subjected to unconfined compression strength (UCS) test. The UCS of soil reinforced with JGT was found to be higher than that of soil that had not been treated. Four layers of JGT, with uniform vertical spacing between each layer, significantly increased strength of the soil. Dasgupta (2014) examined how roads with and without JGTs performed and how much they cost to build. Results showed that geotextile construction was more cost-effective than using natural granular materials for roads. This was because geotextile helped improve road performance and economy via lower road thickness and shortened building times. Using triaxial testing at four distinct locations, Singh (2013) conducted experimental work to measure the soil stiffness and strength after geotextile reinforcement. Each soil sample was dried to a density of 17.46 kN/m^3 and a moisture content of 14.55%. With the JGT sheet

incorporated into the soil, they observed an increase in the shear strength values. Soil cohesion (c) and angle of friction (ϕ) values are maximized by 72% and 46%, respectively when 4 layers of JGT sheets were used. The stiffness modulus of soil is also increased with confined pressures. Adding 4 layers of JGT sheets increased soil stiffness modulus by an average maximum of 112%. Several studies found that after being reinforced with JGTs, soil CBR values increased. The bearing capacity of a foundation resting on weak or poor soils may be increased and settlement can be minimised when geotextile reinforcements are utilised in the construction process. It has a wide range of applications in geotechnical engineering, including foundations, retaining walls, embankments, and more. In combination with soil, geotextiles are permeable materials that serve to separate, filter, reinforce, protect, and drain (Panigrahi and Pradhan, 2019). The bearing capacity of subgrade soil was found to be greatly enhanced by adding a layer of JGT between the sub-base and subgrade (Jadhav *et al.*, 2011). Aggarwal and Sharma (2010) used CBR and compaction experiments to investigate the use of JGT-reinforced clay soil in subgrade construction. By using JGT, the CBR value was able to be raised from 1.8 to 5.5, resulting in a 35% reduction in subgrade thickness. Fiber addition lowered MDD and raised OMC for the subgrade material. Using a series of CBR experiments, Kumar *et al.*, (2015) compared the performance of JGT- and coir-reinforced silty loam soil. It was found that the CBR values of JGT were greater than those of coir fibres for the aspect ratio ($L/D = 20$ to 100). Datta (2007) summarised many case studies demonstrating the effectiveness of JGT in preventing soil erosion, enhancing the quality of the subgrade for new roads, and protecting the river and canal banks from damage.

Constructing low-traffic highways on top of black cotton soil subgrade, blended JGT can be a cost-effective and environmentally safe alternative for 100% synthetic geotextiles (Ghosh *et al.*, 2021). Natural geotextiles, such as coir geotextiles, when used in conjunction with sand interfaces, exhibit significant resistance to bonding, particularly under low normal stresses (Menon *et al.*, 2021). By improving its strength and stiffness, the bearing capacity of soft soil for supporting footing was enhanced by the use of JGT and sisal as geocell reinforcement (Kolathayar *et al.*, 2020). JGTs also have higher tensile stiffness and modulus than synthetic geotextiles (Buragadda and Thyagaraj, 2019). Even though JGTs have many positive attributes, one major drawback is their biodegradability, which reduces their effectiveness as a soil-stabilizing agent.

2.3 Reduction of Surface Erosion of Soil Using Natural Geotextiles

External processes like wind and water flow remove soil from the surface of earth, which is subsequently transported and deposited on other sites as a result of soil erosion. As a general rule, soil erosion is the physical loss of topsoil by different causes, such as rain, river flow, wind, glaciers, or gravitational attraction. Surface erosion is particularly likely to occur on bare or unprotected ground surfaces. Mass movement differs from erosion in that it is generated by the sliding, collapsing, toppling, or spreading of quite large and, in some cases, whole masses. During a slide, shear failure occurs over a defined surface or set of surfaces inside the failure mass, causing a gradual, sloping movement. The factors that control surface erosion, such as slope, soil, rainfall, and so on, also control the movement of mass. Although precipitation plays a significant role in rainfall erosion, precipitation has only a secondary effect on mass movement via its effect on the groundwater regime at a location. On the other hand, geological features like the orientation of joints and bedding planes in a slope may have a significant impact on mass stability while having little effect on erosion at the surface. Land and water are the most important natural resources for human life. About two-thirds people of India depend on farming, which provides half of the employment of country and keeps the environment in balance. Soil erosion affects plants and crops by removing the physical characteristics of soil. About 45 percent total land area of India is affected by severe soil erosion through gorges and gullies, crop rotation, cultivated wastelands, sandy regions, deserts, and water-logged areas.

In India, landslides have resulted in significant loss of life and damage to communication networks, human settlements, agricultural areas, and forest regions. In many parts of the globe, rainfall may cause slopes to collapse, which can have devastating effects on both people and property. Countries like India, Chile, Japan, China, and Venezuela have all seen large-scale landslides caused by rain. (Sengupta *et al.*, 2010; Lagmay *et al.*, 2006; Schuster *et al.*, 2002; Van Sint Jan and Talloni, 1993; Brown *et al.*, 1982;). According to the Disaster Management Authority of India, Ministry of Home Affairs (MHA), Govt. of India, roughly 100 to 150 crores of monetary loss occurred in the last decade and, as per the Geological Survey of India, around 0.42 million km² (12.6% of landmass) of the area in India is prone to landslides. According to Kirschbaum *et al.* (2010), India ranked among the top ten countries in terms of landslip rates in the years 2003, 2007, and 2008. The monsoon season, occurring from June to September and October to December is characterised by a heightened occurrence of landslides (NDMG, 2009). Weak geological patterns, extremely intense

rainfall, naturally critical slopes, and the absence of permeable granular soil are the most identified causes of landslides.

The failure of slopes caused by rainfall is a major problem in India. Several researchers have reported landslides and slope failures due to rainfall occurrences. Embankments cut slopes, and fill slopes along the natural slopes are prone to these storm-based failures (Chen *et al.*, 2004; Day and Axten, 1989). According to the findings of Xu and Zhang (2010), the occurrence of a slope failure above a railway line in China was attributed to the combined effects of rainfall infiltration, inadequate drainage system, and subsequent saturation of clay within the retaining wall. Because of the existence of inefficient soil to disperse surplus water generated inside the soil slope during rainfall penetration, pore water pressure increased, lowering the shear strength (Chatterjee and Krishna, 2019; Bhattacharjee and Viswanadham, 2018). In the context of unsaturated soils, the process of rainfall infiltration results in an increase in groundwater level, the augmentation of pore water pressure, and the reduction of matric suction (Ng and Shi, 1998).

However, the significance of matric suction in ensuring the stability of unsaturated slopes has been highlighted by Fredlund and Rahardjo (1993). Soil shear strength was affected by both increased water pressure and decreased matric suction. Consequently, this could potentially lead to occurrences of landslides and slope failure. Wu *et al.*, (2021) elaborated that rainfall intensity was the main reason for 80% of landslides. As rainfall intensity increased, the displacement of soil sediment also increased, leading to greater soil erosion and lower embankment stability. The amount of soil erosion is directly correlated with slope angles, the higher the gradient, the more erosion occurs. Several research projects have been conducted to comprehend the processes of slope collapse under situations of rainwater infiltration. In the general scenario, there are two types of failure mechanisms: shallow and deep slope failure mechanisms, as explained by Cai and Ugai (2004). According to Zhang *et al.*, (2011), infiltration is a major factor in the instability of slopes during rainy weather. Consequently, soil erosion estimates are necessary for developing floodway soil conservation strategies. Some areas of India have seen significant soil erosion as a result of massive deforestation, substantial road development, mining, and farming on steep slopes (Mahabaleshwara *et al.*, 2014). Hence, it is necessary to understand soil erosion and mass movement mechanism to control them effectively.

2.3.1 Soil Erosion Mechanism

To effectively develop and implement soil management approaches to reduce and manage soil erosion risk, thorough understanding of the processes through which erosion happens is essential (Garca-Daz *et al.*, 2017; Keesstra *et al.*, 2016). Soil erosion, as described by Morgan (2005), is a dual-phase phenomenon characterised by the initial detachment of soil particles followed by their subsequent displacement through the action of erosive agents (such as water or wind). The forces exerted on particles near the boundary or interface of a fluid bed are illustrated in Figure 2.1. Erosion is primarily attributed to the influence of drag or tractive forces, contingent upon velocity, discharge, particle shape, and roughness. The inertial or cohesive forces between the particles balance out the drag forces generated by the fluid. However, the erosion process is impeded by inertia, friction, and cohesion, which arise from inherent soil properties, soil structure, and physicochemical interactions. The primary methods for protecting soil against erosion involve main strategies such as 1) reducing the drag or tractive forces by diminishing the speed of water flowing across the surface or by dissipating the water's energy within a protected region, and 2) enhancing erosion resistance by shielding or protecting the surface with a suitable reinforcement or by augmenting the strength of inter-particle bonds.

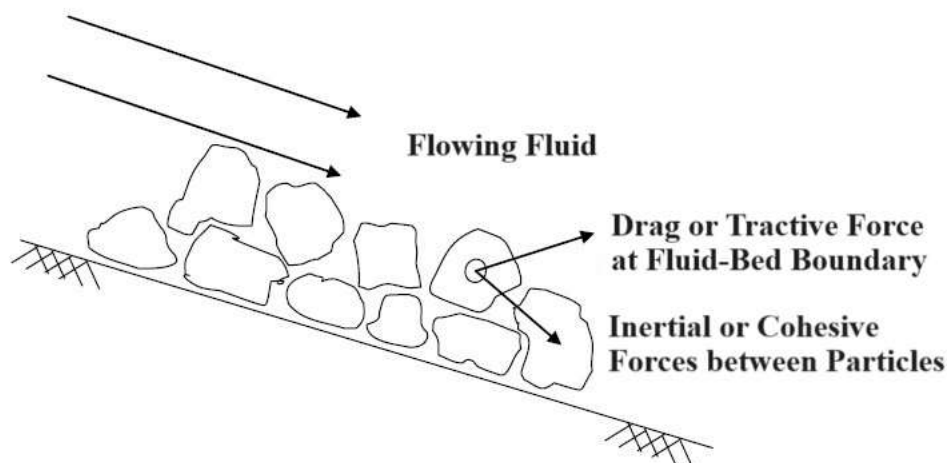


Figure 2.1. Schematic representation of forces acting on particles (Gray and Sotir, 1996)

2.3.2 Soil Erosion Agents

Soil erosion can be categorised into three types, as depicted in Figure 2.2: water erosion, wind erosion, and chemical or geological erosion, in accordance with the causes of erosion.

Soil erosion resulting from the forces of water and wind is a prevalent phenomenon that is readily identifiable. Erosion by a chemical or geological agent can take years or even decades, and it is sometimes difficult to measure that erosion. Water erosion is classified based on the degree of influence it has on the environment. The subsequent sections explain the various forms of erosion. Figure 2.2 shows the image illustrating water erosion.

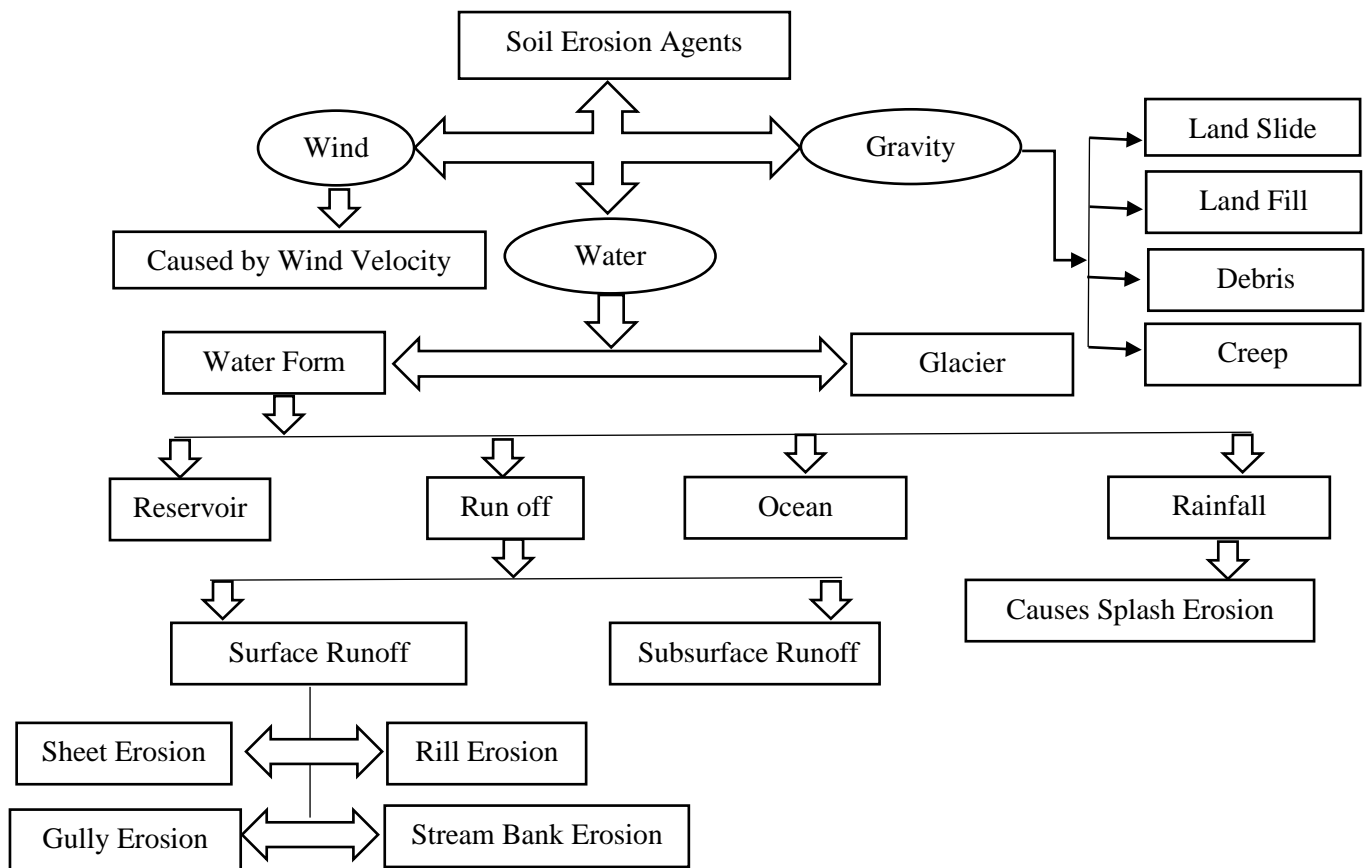


Figure 2.2. Different types of Soil Erosion (Das, 2000)

Water erosion is the term used to describe soil erosion that is caused by water. During water erosion, the water works as a dislodging and transporting agent for the eroded soil particles. The image of water erosion is shown in Figure 2.3. The many forms of erosion include rill erosion, tunnel erosion, stream bank erosion, coastal erosion, and splash erosion.

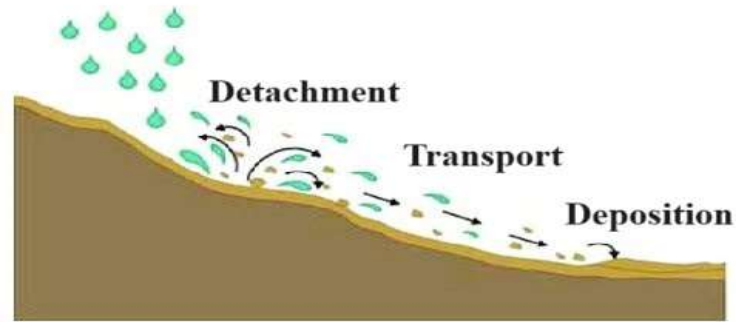


Figure 2.3. Water Erosion Process due to rain fall (Maitra *et al.*, 2020)

Angulo-Martinez *et al.* (2012) define splash erosion as a complex phenomenon in which the impact of a raindrop on a soil surface causes soil particle to detach from the surface and be transported over relatively short distances. Splash erosion, which involves the separation of soil particles, may be seen as the first stage of soil erosion caused by water, and as such, it is important to investigate the causes and processes that regulate this process. Splash erosion, aided by the wind, may carry soil particles more than 5 metres horizontally (Erpul *et al.*, 2009a, 2009b) and up to 1.5 metres vertically (Ryzak *et al.*, 2015).

Sheet erosion occurs when raindrops and shallow surface flow cause the loss of thin layers of soil. In the agricultural industry, skimming is a regular practice to be engaged in. As a result of this type of farming, soil nutrients, and organic matter are severely depleted. The often unnoticed nature of soil loss is a consequence of its sluggishness. This has a severe negative impact on the soil over time. This type of soil erosion is mostly responsible for the decline in soil productivity. Because of the lack of vegetation to act as a soil buffer and stabilizer in overgrazed and cultivated soils, sheet erosion is more likely. Rainfall causes water to pool on the ground, allowing grass and tree roots to be seen, as well as subsoil or stony soils to be seen. When examining soil deposits on the upper sides of fences or other barriers, sheet erosion can be identified.

When water flows downslope in croplands and rangelands, a substantial soil erosion process known as rill erosion takes place (Kimaro *et al.*, 2008; Cai *et al.*, 2004). Rills are formed when erosion leads to gullies. The first step in gully development is the advanced form of rill. In terms of geomorphology, rill erosion is important because it creates erosion features and moves sediment from areas of inter-rill erosion to areas of rill erosion (Bewket and Sterk, 2003). Rill networks might develop at various levels of complexity (Mancilla *et al.*, 2005; Brunton and Bryan, 2000). Developing a rill network improves the concentration of water flow and the connections between runoff areas along the channeling system (Heras *et*

al., 2011). It is common to see rill erosion on newly tilled soil and overgrazed land due to the loosening of the soil structure. Rill erosion is common in the Chambal River basin in India, where alluvial soil is prevalent.

When the rill is more than 50 cm deep and wide, gully development begins. It is impossible to clear gullies with standard tillage. Deforestation, overgrazing, or other methods of clearing vegetation make hillsides more prone to gullying. When heavy rain occurs in rapid, violent storms, the eroded soil is quickly taken away by the rushing water. The phenomenon of gully erosion has been attributed to the rapid depletion of soil moisture and groundwater in arid and semiarid regions, as evidenced by studies conducted by Avni (2005) and Nyssen *et al.*, (2004). According to Poesen *et al.*, (2003), gully erosion has been a major problem, having a devastating impact on agriculture and infrastructures including roads and bridges. Assessment of gully extension and agricultural soil loss in the Jawa Block of the Rewa District in Madhya Pradesh, India, conducted by Savindra and Prakash (1987), reveals a worrying annual average loss of 2.35 million m³ of agricultural soil. In the next half-century, the impacted region is expected to grow by almost 50 percent. Severe soil erosion affects around 27% of the land in India, with yearly soil loss estimated at 1.6 kg/m² (Lekha 2004).

2.3.3 Soil Erosion Control Methods

Erosion of soil occurs when soil particles become detached from their original locations and are carried away by wind, water, or other agents. This is a major environmental concern that may lead to many different ecological and social problems. There are several types of techniques used to prevent soil erosion which are afforestation, crop rotation, mulching, terrace farming, vegetation, etc.

- **Afforestation:** Afforestation is reforesting an area by planting new trees and plants. The survival of plants is directly responsible for human life's existence. Therefore, whenever trees are felled, they must be replaced with new ones. The best conservation results may be achieved by planting trees in mountainous regions.
- **Crop Rotation:** There is a time when farmland has no crops, between when one crop is harvested, and the next is planted. To prevent soil erosion, farmers often plant grass or other cover crops at this time. Soil may replenish some of its mineral content in this way.

- **Terrace Farming:** Steps are dug into the hillside for cultivation in mountainous regions. Water is slowed while the soil is deposited on the next level, and the process repeats. This means that the soil is preserved forever.
- **Shelterbelts:** The vegetative cover encompassing the field serves the purpose of impeding the velocity of powerful winds, thereby safeguarding the soil against erosion caused by wind-induced displacement.
- **Embankments:** Agricultural land may be safeguarded against river floods by building strong embankments along the banks of the river. These barriers keep the river and rains from washing away a lot of the rich, productive soil.
- **Vegetation:** Ground cover is a vegetative layer formed by plants, the plants roots effectively bind the soil, thereby impeding the process of soil erosion.
- **Matting the soil:** Implementing a protective covering, similar to a blanket, over the soil to facilitate the growth of small plants also serves as a preventive measure against soil erosion.
- **Application of mulches:** It is a layer of material applied to the soil surface, which betters the quality and holding capacity of the soil.
- **Constructing windbreakers:** It prevents soil erosion resulting due to speedy wind.
- **Turning the slope area into a flat surface:** At the time of rain, the soil surface can run down with water, however, it can be prevented by flattening the surface.
- **Bio engineering methods:** All types of vegetation techniques come under this category. Sometimes it includes mulching matting methods.
- **Application geotextiles:** Using geotextiles to prevent soil erosion is one of the effective methods.
- **Using rock material:** The utilisation of crushed stone, wood chips, and analogous materials in areas characterised by challenging conditions for plant growth and maintenance.

2.3.4 Erosion Control by Natural Geotextile

Installation of geotextiles on slopes is a popular method of erosion control (Rickson, 1995). Soil erosion on designed slopes may be reduced in several ways, and one of them is by using geotextiles as suggested by Jankauskas *et al.*, (2008b). Using geosynthetics to prevent erosion involves slowing the flow of soil particles away from the bank, diverting runoff to an appropriate disposal area, and keeping silt from washing away (Sanyal, 2011). Mats or nets

made of geotextile materials are used to protect soil from being washed away by precipitation and overland flow (Alvarez-Mozos *et al.*, 2014). Numerous physical characteristics of geotextiles contribute to their efficacy in soil protection. The percentage of open area (or the proportional size of apertures), moisture sorption depth, mat thickness, hydraulic roughness, and tensile strength are important characteristics that determine how well such materials operate in a given situation (Rickson, 2006). Additionally, the length and gradient of a slope, the type of soil, and the local precipitation regime all affect erosion reduction ability of a geotextile (Bhattacharyya *et al.*, 2010). The majority of geotextiles can decompose in landfills and are constructed from sustainable materials. In the last 50 years, geotextiles have made significant contributions to erosion control. When it comes to preventing soil erosion on and off construction sites, geotextiles are often utilised (Mitchell *et al.*, 2003; Dayte and Gore, 1994; Sutherland, 1998a). To prevent soil erosion and support plant growth, establishment, and protection, a wide range of temporary degradable and permanent non-degradable materials have been developed or fabricated into rolls (Allen, 1996). Some of them are erosion control blankets (ECBs), erosion control re-vegetation mats (ECRMs), and turf reinforcement mats (TRMs) (Gray and Sotir, 1996; Theisen, 1992). In most cases, geotextiles come in rolls and are installed in the field with the help of different anchoring mechanisms. Synthetic geotextiles are those made from man-made polymeric materials. Non-degradable synthetic geotextiles have the potential to pollute the soil (Fullen *et al.*, 2007). Furthermore, the manufacturing process may result in environmental damage to the air and water. The cost of synthetic geotextiles may be more than 10 times that of natural geotextiles per unit area (Ingold, 1996). Recent environmental concerns have prompted research into the production of environmentally friendly materials for engineering purposes, such as ground improvement, slope protection, etc. The replacement of artificial geotextiles with natural geotextiles to reduce associated CO₂ emissions is one option for achieving sustainability (Kiffle *et al.*, 2017). Because of easy accessibility, reproducibility, low cost, and good biocompatibility, natural fibres such as JGT, coir, and hemp are commonly used to replace synthetic fibres as reinforcing agents in soil (Muthukumar *et al.*, 2019; Mishra *et al.*, 2017; Rawal and Sayeed, 2013). Despite the extensive use of synthetic geotextiles in the industry, geotextiles produced from natural geotextile materials are particularly successful in preventing erosion and encouraging the vegetation growth (Chakrabarti *et al.*, 2016). The protective function of natural geotextiles is summarised in Table 2.1. Natural geotextiles are superior to synthetic geotextiles in terms of erosion control and soil adherence (Jankuskas *et al.*, 2012). Because of their 100% biodegradability and superior adhesion to the soil, natural

fibres were the chosen option for reducing erosion (Sutherland and Ziegler, 1996; Langford and Coleman, 1996). In addition, biomats may aid in preventing excessive heat from the sun from reaching the soil, keep soil temperatures from swinging wildly, limit water loss from evaporation, and foster healthy plant development (Sprague and Paulson, 1996). JGT was the first material employed as a rolling erosion control geotextile due to its lower cost and wider availability (Ranganathan, 1992). JGT is a natural cellulose-based fabric that is abundantly available, particularly in the Indian subcontinent. Wool geotextile, which is slow to biodegrade and supports plants for full slope protection, can provide immediate protection against soil erosion (Broda *et al.*, 2018). Table 2.1 summarises the effects and applications of natural geotextiles.

Table 2.1. Effects and applications of various natural geotextiles (Wu *et al.*, 2020)

Type of Geotextiles	Application	Effect
Palm-mat geotextiles	Reduce soil erosion on slopes	1) Palm-mat geotextiles have demonstrated significant efficacy in mitigating soil erosion and minimising water runoff.
	Desert fixing sand	2) Repair gullies and take measures to stop erosion. 3) Palm-mat geotextiles are very effective in preventing water loss and erosion.
Coir geotextiles	Reducing the risk of riverbank erosion	1) Coir geotextiles have a great impact as a protective measure for river banks. 2) The tensile strength of untreated fibres maintained just 23% of their original strength after being exposed to the environment over 12 months.
JGTs	Protection against riverbank erosion	1) It can filter and separate freely flowing water, preventing the passage of microscopic particles. 2) 600–700 days is the lifespan of the modified JGT. 3) The tensile strength of treated JGTs for riparian applications is sufficient, and they last for up to four years. 4) JGTs may delay runoff, decrease runoff by 62.1%, and prevent erosion by 99.4%. 5) JGTs provide superior runoff control effectiveness compared to coir geotextiles.
Elephant grass & York grass geotextiles	Prevention of Soil erosion	1) The soil loss of the two geotextiles was reduced by 56.6% and 97.3%, respectively, when compared to the reference case study, indicating effective control over erosion and

sediment management.

Water hyacinth, reed, sisal, Roselle geotextiles	Prevention of Soil erosion	1) Geotextile raw materials like sisal and roselle indicate potential, and reed and water hyacinth fabrics are effective in preventing soil erosion.
--	----------------------------	--

Soil conservation seems to be greatly enhanced by the use of palm mats, according to results collected in the field in the United Kingdom. Rates of erosion were from 0.45 Mg ha⁻¹ for uncovered soil to 0.09 Mg ha⁻¹ for grass plots and 0.17 Mg ha⁻¹ for both covered and buffer zone plots, respectively (Davies *et al.*, 2006). Reduced sediment yield from South African tailing dam slopes by 55% was achieved using biodegradable geotextiles made from the leaves of the Lala palm (*Hyphaene coriacea*) (Buhmann *et al.*, 2010). Producing biogeotextiles is also economic (often between €0.34 and €4.40 per square metre) according to Fullen *et al.*, (2011). Geotextiles fabricated from palm leaves were shown to be effective in reducing soil erosion. These materials are abundant and renewable when they are gathered properly. They are permeable, making them useful even on cohesive soils, and biodegradable, giving organic matter to soil stabilization (Booth *et al.*, 2007; Fullen *et al.*, 2006). Geotextiles are used to improve soil quality in a variety of engineering applications. On steep erodible slopes, geotextiles may be utilised as a substitute for vegetative cover when erosive pressures of precipitation and runoff constrain plant development (Smets *et al.*, 2007).

Open weave JGT is applied to the slope surface at the beginning to prevent soil erosion and promote plant growth because of its coarse fibre nature, thick threads, and 3-D qualities. With their open weave, JGTs operate like a series of mini-check dams to divert water away from a specific area. JGT may be stretched and arranged to imitate the topography of wherever it is planted (Thomson, 1988). To prevent further soil erosion along the eroding banks of Indian rivers, a fabric made from JGT treated with resistant chemicals was utilised. Additionally, JGT was proposed as an innovative material for soil erosion control (Ingold, 1994). The erosion rates on sandy soils were significantly reduced when JGTs were used. The JGT net provided 35% and the JGT mat 247% of the control runoff compared with the bare control as stated by Mitchel *et al.*, (2003). Additionally, Tauro *et al.*, (2018) demonstrated that JGT was an excellent choice for hillslope protection because of its high hygroscopic characteristic. They evaluated the efficiency of two biodegradable geotextiles made from JGT in preventing soil erosion on a steep slope. Water storage was made possible by unique ability of JGT to absorb water at a rate of 4.5 to 6 times its dry

weight (Rickson, 1988). Overland storage and preventing soil from detaching from slopes are effective ways to manage soil erosion during times of high precipitation and impermeable soil. JGTs are naturally hygroscopic due to their inherent characteristic, which also contributes to the adaptability of the material. JGT is used for erosion management for several reasons, including its advantages, biodegradability, and ability to contribute rich organic nutrients to the soil and promote plant growth. Because of its low cost and wide variety of available manufacturers, JGT has become a popular erosion control method (Ghosh *et al.*, 1994). The eco-friendliness of the material is important to the widespread use of JGT in erosion control, which makes it a natural, risk-free alternative (Manivannan *et al.*, 2018).

Henderson (1982) proposed using strips of biodegradable paper knitted together to protect vulnerable soils while construction sites are stabilized with vegetation. Balan and Rao (1996) demonstrated that using a geotextile from natural fibres stabilises soil surfaces and reduces erosion. Banerjee (1996) introduced a highly versatile material, blended natural fibre geotextiles made of coir and JGT. Rao and Balan (2000) conducted a comprehensive data collection effort pertaining to the sustainability of the coir geotextiles market. In a study conducted by Lekha (2004), the focus was on the stabilisation of slopes through the utilisation of coir geotextiles. The findings of the study indicated that the implementation of coir nettings effectively prevented the displacement of seeds caused by erosion, while also serving as a protective barrier against the erosive forces of rain and wind. Soil erosion was greatly reduced when lemongrass turf was installed over coir netting. One such protected plot was found to have a yearly soil loss of 94.9% less than a neighbouring non-protected plot. Soil erosion decreased by 99.6% ,95.7%, and 78.1% before, during and after the monsoon in the protected plot, compared to the unprotected plot. This proves that the method is very effective in preventing soil erosion in damaged mountainous areas. Cotton palm may reduce soil erosion in Mediterranean climates, according to research by Gimenez-Morera *et al.*, (2010), and palm geotextiles reduce runoff coefficients and reduce soil erosion on hillslopes, according to research by Smets *et al.*, (2007). Laboratory tests showed that soil loss might be drastically decreased by using geotextiles made from hyacinth (Maneecharoen *et al.*, 2013). Coir geotextile was investigated by Vishnudas *et al.*, (2012) as a means of increasing soil moisture availability on hillslopes. Based on their research into erosion management, Rao and Balan (2000) concluded that coir geotextile may effectively stop particles from eroding along a surface of the slope and instead let the soil settle onto the bare rock. In a study conducted by Anil (2006), an experiment was conducted using multi-slot devices within a controlled

environment. The findings revealed that when subjected to a 40% slope, the control plot exhibited a soil loss that was 12% greater than the plot treated with coir geotextiles.

2.4 Slope Stabilization using Natural Geotextiles

2.4.1 Slope Failure

Shear stress and shear resistance are influenced by the slope's topography, geology, and climate. Slope failure occurs when shear stress is greater than shear strength. Determining a slope safety factor involves dividing the shear strength by the shear acting along the critical failure surface. Slope movement is often caused by any factor that raises shear stress or lowers shear strength. Table 2.2 displays the classification of slope instability or failure reasons by Varnes (1958).

Table 2.2 Causes of Slope Failure (Varnes, 1958)

Increase in shear stress	Decrease in shear strength
Surcharge load on the slope (Constructions and landfills at top)	Because of the rise in pore water pressure, the effective stress is reduced (the amount of rainwater penetrating a slope).
Elimination of lateral support (excavation-related works at the toe)	Presence of expansive clays (absorption of water accompanied by a breakdown in structural integrity))
Water level changes on a slope abruptly (water table decrease)	Physical and chemical weathering processes (including ion exchange, hydrolysis, and process of solutioning, in which water dissolves and transports minerals such as calcium carbonate and gypsum. This produces voids and changes soil particle bonding, decreasing the shear strength of soil)
Enhanced lateral stress (water filled within the cracks and fissures)	Progressive failure by shear strain softening

The other causes for slope failures are inherently unstable and extremely steep slopes. Until the natural angle of repose is discovered, materials on steep slopes will naturally slide downward. The stability of a slope is affected whenever it is disturbed, either by natural means such as a stream eroding the riverbanks or through manual processes such as the removal of a portion of the base for the construction of roads. According to Khan and Chang

(2006), slopes of several hills (<20m) (Dev hill, Goal Hill, etc.) are prone to the risk of sliding due to excessive sliding.

Compared to air, water has a substantially larger density. The soil on slopes becomes much heavier after heavy rain because the water has filled the air between the soil grains. When retaining walls hold the earth back, this becomes a critical concern. If the amount of soil behind the wall is too high, the wall will buckle and collapse, releasing the soil behind it in a flood disaster. Also, water decreases the angle of repose and soil cohesiveness by decreasing the contact between individual grains. Changes in groundwater hydraulic pressure in slope rocks during the rainy season and the presence of water saturation both increase the likelihood of mass movement of a slope.

Slope failure analysis necessitates examining the soil type on the slope. This is because soils widely vary in their cohesiveness between grains and frictional resistance to erosion. Loose soil or sand, for instance, will have poor cohesiveness and can be eroded quickly when saturated. The swelling behaviour of clay-rich soils upon water contact leads to increased density and instability, particularly in slope conditions, due to the added weight from clay expansion.

Slopes may suddenly experience large displacement of soil for various reasons, including earthquakes, storms, volcanic eruptions, the passage of heavy vehicles, blasting, and other similar shocks. The crucial component of preventing and controlling slope changes is the early detection of these causes. Perhaps the most prevalent cause of instability is removing lateral support, which either natural or human forces may cause. Implementing barriers or structures for retention at the lower portions of slopes is proposed as a remedial measure. The addition of water to a slope may raise stress and reduce strength at the same time. Almost all landslides include water as a contributing element (Chassie and Goughnor, 1976). As a result, drainage and diversion systems are among the most efficient ways to avoid and mitigate slope collapse. According to Patil and Gopale (2018), landslides occur when natural or anthropogenic processes cause the rapid downhill movement of consolidated and unconsolidated soils and rock materials from a geomorphic structure. The terms fall, topple, slide, spread, and flow apply to this motion (Ering and Babu, 2016).

2.4.2 Slope Stability Analysis

Predicting the stability of slopes and embankments is done in various methods. Limit equilibrium analysis and deformation analysis are the two primary methods. Shear stress and

shear resistance are slope properties considered explicitly by limit equilibrium techniques. The safety factor for a particular slope may be calculated using limit equilibrium analysis, which can also be used to examine the impact of a change in one or more factors on the stability of slope. For this reason, many techniques and processes based on the limit equilibrium theory have been developed. The following ideas (Morgenstern and Sangrey, 1978) apply to limit equilibrium analysis across all approaches.

- The schematic diagram presented in Figure 2.4 illustrates the surface failure process, wherein hypothetical slopes are postulated to undergo collapse along planes or circular surfaces that undergo sliding. Complex failure surfaces can be observed and analysed in situations where slope conditions vary.
- The statistical calculation determines the shear resistance necessary to stabilise the mass at risk of failure. It is postulated that the potential failure mass is in a state of "limiting equilibrium," with the shear strength of the soil or rock within the failure mass being fully utilised along the entire slip surface.
- The equilibrium shear resistance is computed and compared to the available shear strength. This evaluation is made relative to a safety factor.
- The least risky mechanism or slipping surface identified through iteration. The least safe surface is the critical slip surface. If the location of the slip surface can be predicted, then it is usually optional to conduct tests in the field.

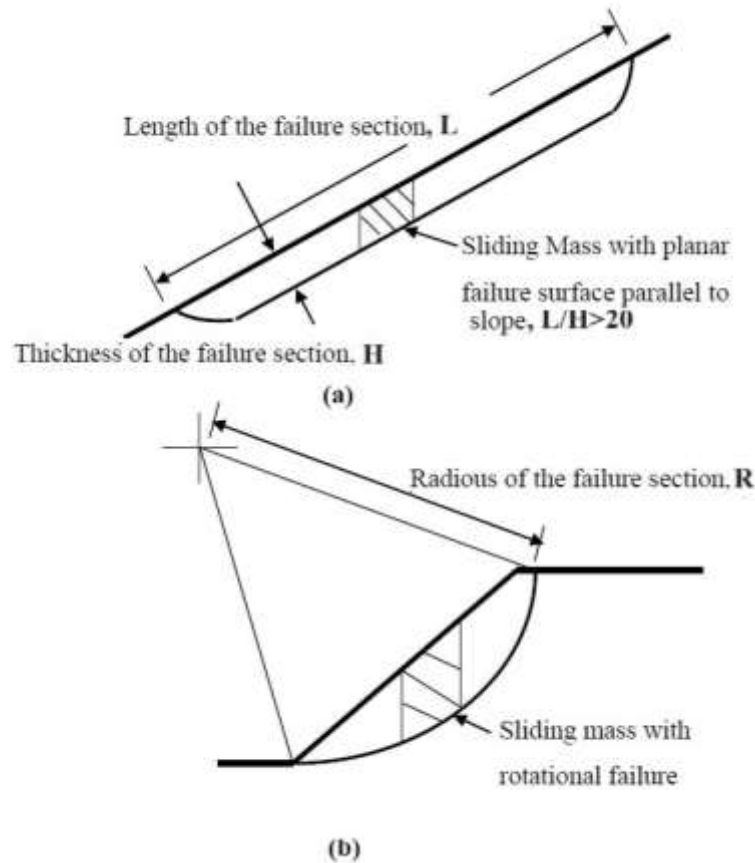


Figure 2.4. Slope failure models or mechanisms for mass stability analysis a) transitional failure infinite slope model; b) rotational failure, circular arc model (Gray and Sotir, 1996)

The following are essential components of a slope stability analysis:

- The slope geometry is accurately described
- Soil properties (c , ϕ , γ)
- External loads including surcharge, line loads, and earthquake loads
- Accurate description of slope hydraulic conditions like ground water table position and seepage condition
- Type of analysis methodology for slope stability

2.4.3 Improvement of Slope stability by Natural Geotextiles

According to Sanyal (2017), JGT is superior to synthetic fibre as a geotextile due to its superior tenacity, initial modulus, low elongation at break, high roughness coefficient, outstanding spinnability, and extremely high thermal stability. Embankment field tests using JGT showed an improvement in the safety factor of 1.26 (or 51%). The safety factor was

determined to be 3.2 after seven months (Sanyal, 2017). In the lab, it was shown to decrease topsoil erosion by 95% and boost slope stability during wet weather when there is no plant cover (Khan and Binoy, 2012). Slope stabilisation and erosion management were much improved when JGT is applied to sandy soil, as Khan and Binoy (2012) reported. Slope stabilisation was best accomplished by using 500 GSM open-weave JGTs with tea plants (up to 90% of the slope) or 700 GSM open-weave JGTs with grass plants (up to 10% of the slope) (Manivannan *et al.*, 2019).

The influence of JGT on the engineering and strength parameters of lime-treated black cotton soil was investigated by Bairagi *et al.*, (2014). Index qualities of soil samples with varying amounts of JGT added (from 0% to 5%) were measured following the IS code requirements. The results of the experiments showed that the black cotton soil's expansive tendency had significantly diminished. The CBR and UCS of black cotton soil were significantly improved if the soil is blended with lime and JGT at a weight ratio of 5% (by weight of black cotton soil). Their experimentation led them to the conclusion that adding lime and JGT into black cotton soil raised the OMC and lowered the MDD. Overall, the results show that incorporating JGT into lime-stabilized soil mitigated swelling and boosted the CBR and unconfined compressive strength values of soil.

Ramesh *et al.*, (2010) conducted an investigation on the compaction and strength characteristics of black cotton soil treated with lime-coir fibres. The researchers made a discovery that black cotton soil, when reinforced with 1.0% coir fibre having an aspect ratio of 20, and 0.5% coir fibre with an aspect ratio of 80, exhibited greater strength compared to black cotton soil treated with alternative combinations of coir fibre. JGT and coir mats were excellent alternative materials to melt-spun thermoplastic fibres for slopes that were not steep ($< 45^\circ$) (Prambauer *et al.*, 2018). Other than just geotextiles, vegetation is also important for slope stabilization. The following sections discuss soil bioengineering (vegetation) methods.

2.5 Improving Soil Strength and Decreasing Surface Erosion by Bioengineering Methods

Soil-bioengineering stabilizes slopes and controls erosion economically and sustainably. Soil bioengineering uses plants or plant components to reduce soil erosion, shallow mass movements, stream-bank protection, etc. Soil bioengineering is a sub-part of biotechnical

engineering. Biotechnical engineering employs plants or plant components alone or with inert materials like steel, concrete, rocks, etc. (Gray and Leiser, 1982; Schiechl, 1980).

Biotechnical engineering methods are divided into categories depending on the environment and the objective. Some categories include surface stabilization, plant-based stabilization methods, and hybrid stabilization strategies that use both living and inert materials (Donat, 1995). Plant components (such as cuttings, roots, and stems) are the primary structural and mechanical elements of a soil bioengineered slope protection system (Coppin and Richards, 2007; Morgan and Rickson, 2003; Schiechl and Stern, 1996; Gray and Sotir, 1995; Schiechl, 1985). Using trees and small retaining walls to protect sloping terrain is an application of biotechnical engineering. Trees are used to improve stability because their roots are capable of doing things like anchor a porous mass of soil to a hard stratum or reinforce a layer of porous soil, all while enabling drainage for surface runoff, stopping debris from moving, and decreasing pore water pressure through absorption of moisture (Mickovski *et al.*, 2009; Howell *et al.*, 2006;).

Soil bioengineering incorporates both the life sciences and conventional engineering practices. It is a broad area that needs input from researchers and engineers in many other disciplines, such as geotechnical engineering, botany, landscape design, hydrology, etc. (Freer R 1991). Protecting soil slopes and reducing erosion by plant cover approach has been employed in numerous regions of the world, mainly Asia and Europe, for a very long time. One of the early uses was reported by Kraebel (1936), who utilised contour wattling to stabilise steep, fill slopes along the Angeles Crest roadway in southern California. Although soil bioengineering has mostly been used for erosion management, recent research has shown its efficacy in preventing shallow earth movements (Mafian *et al.*, 2009). The following section describes the current state of the literature on bioengineering methods for slope stabilization, including plant-soil interaction mechanism, physical modelling, laboratory scale testing, numerical methods for measuring the influence of root system on the tensile strength of soil-root matrix, and challenges in the field of soil bioengineering are described.

2.5.1 Effect of Vegetation on Surface Erosion

The significance of vegetation in reducing the damaging effects of rain is important. Maintaining a thick layer of grass, weeds, or other herbaceous plants on the ground may reduce the soil carried away by rain (USDA Soil Conservation Service, 1978). Here is a

summarizing the results of studies on the effectiveness of grasses and other herbaceous plants in reducing erosion caused by rain.

- **Interception:** The energy of raindrops is absorbed by the foliage and plant debris, and the soil is protected from being washed away.
- **Restraint:** Root systems hold soil particles in place while runoff is cleared of silt by parts above ground.
- **Retardation:** Runoff is slowed by the surface roughness that stems and leaves produce.
- **Infiltration:** Soil porosity and permeability are maintained with the help of plant residues, which in turn delays the beginning of runoff.

Herbaceous plants and grasses that provide a thick ground cover are more effective than woody plants in preventing surficial erosion.

2.5.2 Vegetation influence on Mass Loss

The recognition of the protective role of vegetation in maintaining slope stability is increasing. The subsequent points outline the primary beneficial impacts of woody plants on slope mass stability.

- **Soil Moisture Depletion:** Evaporation and transpiration in the foliage may mitigate negative pore water pressure.
- **Root Reinforcement:** Soil shear stress is converted to tensile resistance in the roots, a mechanism referred to as mechanical reinforcement.
- **Arching and Buttrressing:** Anchored and embedded stems may resist downslope shear stresses by acting as buttress piles or arch abutments.
- **Surcharge:** In some cases, the weight of vegetation may promote stability by increasing the normal confining stress on the failure surface.

Root reinforcement is the most prominent way woody vegetation increases mass stability. Extensive laboratory research on fibre-reinforced sands (Maher and Gray, 1990) suggests that small quantities of fibre may result in large gains in shear strength. The arching and buttressing effect of woody plant roots and stems/trunks is also crucial to slope stability. Plant evaporation and transpiration may also decrease pore water pressures in the soil layer, which may improve slope stability in slopes (Brenner, 1973).

2.5.3 Role of Vegetation in Slope Stability

The factor of safety (FS) quantifies the capacity of a slope to withstand failure. The calculation involves determining the ratio between the resistance to shear along a potential slip plane within the soil mass and the shear force exerted along that same plane. Soil failure occurs when the ratio reaches one. The analysis of infinite slope may investigate the most basic scenario of a translational failure occurring along a sliding surface that is parallel to the ground, situated on a significantly longer and uniformly inclined slope. The smaller portions of the slope, specifically the head and top sections, are disregarded due to their relatively negligible size. Instead, a single element or segment of the slope, as depicted in Figure 2.5, can be considered representative of the entire slope. The safety factor without vegetation may be determined using effective stress analysis.

$$FS = \frac{c' + (\gamma z - \gamma_w h_w) \cos^2 \beta \tan \phi'}{\gamma z \sin \beta \cos \beta} \quad (2.1)$$

Where,

c' = effective soil cohesion (kN/m³)

γ = unit weight of soil (kN/m³)

z = vertical height of soil above slip plane (m)

β = slope angle (degrees)

γ_w = unit weight of water (kN/m³)

h_w = vertical height of ground water table above slip plane (m) and

ϕ' = effective angle of internal friction of the soil (degrees)

Based on the study of Coppin and Richards (1990), Figure 2.6 explains how vegetation affects the stability of vertical profile of the slope. The following may be considered a safety factor.

$$FS = \frac{(c' + c'_R) + \{(\gamma z - \gamma_w h_v) + W\} \cos^2 \beta + T \sin \theta \tan \phi' + T \cos \theta}{\{(\gamma z + W) \sin \beta + D\} \cos \beta} \quad (2.2)$$

where,

c'_R = enhanced effective soil cohesion due to soil reinforcement by roots (kN/m³)

W = surcharge due to weight of vegetation (kN/m²)

h_v = vertical height of groundwater table above the slip plane with the vegetation (m)

T = tensile root force acting at the base of the slip plane (kN/m)

θ = angle between roots and slip plane (degrees) and

D = wind loading force parallel to the slope (kN/m)

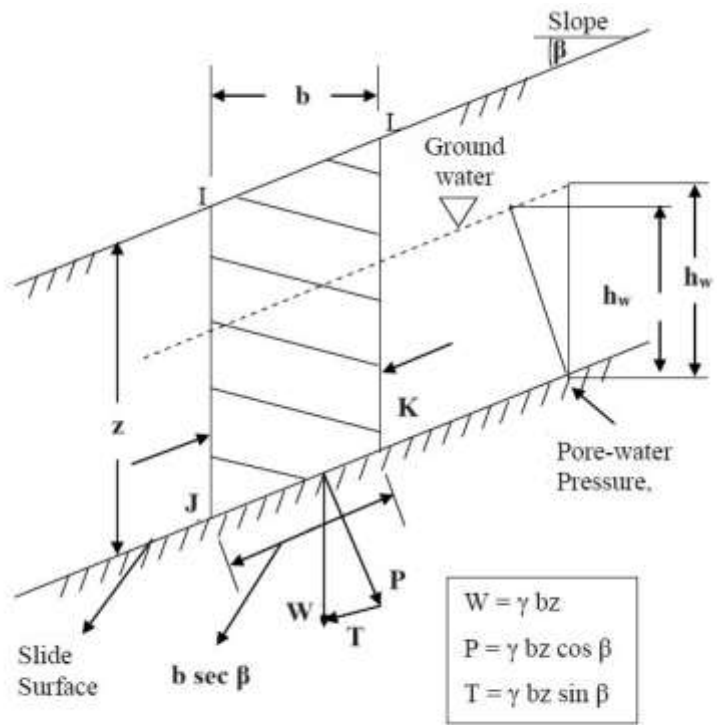


Figure 2.5. Factors involved in the infinite slope method (Styczen and Morgan, 1995)

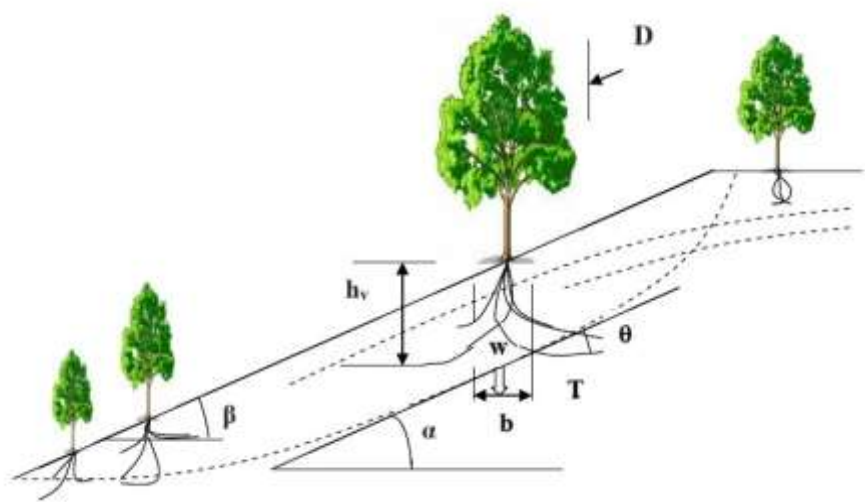


Figure 2.6 Main influences of vegetation on slope stability (Coppin and Richards, 1990)

2.5.4 Root Morphology and Strength

Woody plants significantly affect the stability of shallow mass by increasing its shear strength through root reinforcement. The significance of the root system in this context will be based upon various factors, including the concentration, branching features, spatial distribution of roots within the soil, and root strength and interface properties. The plant species and the soil conditions impact the root's overall structure and strength.

2.5.4.1 Root Architecture

The various constituents of a tree's root system are characterised by distinct terminologies. In the context of discussing tree roots, the terminology employed includes the designation of "taproot" to denote the primary vertical root situated directly beneath the root ball, "sinker root" to refer to vertical roots originating from either the trunk or lateral roots, and "lateral root" to describe the horizontal growth of roots emerging from the central trunk.

The root structure of a tree may also be classified according to its general form or morphology. There are three known root shapes: the taproot, heart, and plate root. It is also possible that variants on these standard forms might emerge as well. Both hereditary and environmental factors influence morphology. The root architecture determines capacity of a tree to contribute to slope stability it develops in response to any of these conditions. The resilience of a root system against shallow sliding may be improved by the presence of strong, vertical or sinker roots that penetrate likely shear surfaces. When improving the shear strength of a root-penetrating soil mass, it has been shown that a greater number of fibrous roots with smaller diameters is more efficient than a smaller number of larger roots. Plants' capacity to withstand shallow sliding is mostly attributable to their deeply penetrating vertical taproots and sinker roots. Mechanical anti-sliding barriers are effective only to the extent that tree roots reach. In order for the roots to have a substantial influence, they must also reach underneath the failed surface.

The majority roots of the loblolly pine plantation are found within the first 0.9 metres, according to research by Patric *et al.*, (1965). Roots near the surface were mostly lateral, whereas those below 0.9 m were often vertical. Watson and O'Loughlin (1990) reported on the root architecture and dispersion of mature Monterey pine (*Pinus radiata*) and other tree species. They showed diagrams of the root structure of an excavated Monterey pine tree that was 25 years old. When the tree was 25 years old, the major laterals reached a maximum

height of 10.4 metres (33 feet) from the bole. The average depth of the vertical roots was around 2.4 m and reached a high of 3.1 m.

2.5.4.2 Root Strength

Despite the challenges, some researchers have attempted to evaluate root tensile strength. Table 2.3 compiles the nominal tensile strengths in the technical literature for a few common types of bushes and trees. There is a large disparity in tensile strength between tests conducted in wet and dry conditions, as well as across different diameters. This means it should consider the numbers in Table 2.3 as approximations at best. Although certain species have been measured as having tensile strengths of up to 70 MPa, the average across all known species is between 10 and 40 MPa. Roots of coniferous trees, in general, are weaker than those of deciduous trees. It seems that the tensile root strengths of shrubs are at least comparable with those of trees. The tensile strength of a plant roots may vary as much due to species as it does due to size variation (diameter).

The effectiveness of vetiver grassroots for slope stabilization was investigated by Hengchaovanich *et al.*, (1996). They found that vetiver roots have a tensile strength that meets or exceeds that of many hardwoods. It is long (2.0 to 3.5 m), and enormous root networks are superior to many other tree species because they are extremely rapidly expanding and important for the stability of embankments. He noted that vetiver root had a mean tensile strength of 75 MPa, about 1/6th that of mild steel. Root tensile strength has decreased with an increase in diameter (Nilaweera, 1994; Burroughs and Thomas, 1977; Wu, 1976; Turmanina, 1965). This is a significant study because it demonstrates that shallow-rooted shrubs may provide the same level of reinforcement as deeper-rooted trees without the latter inherent drawbacks, such as their larger weight, stiffness, and propensity for wind tossing. Root tensile strength may range from around 8 MPa to 80 MPa for root diameters between 2 and 50 mm. Tensile strength may be increased by as much as thrice if the root diameter is reduced from 5 to 2 m. Finer roots may significantly aid in soil reinforcing and shear strength enhancement. As the finer roots have larger specific areas than larger roots with similar area ratios, finer roots have better tensile strengths and greater resistance to pullout.

Table 2.3 Nominal tensile strengths of different Tree Species

Tree Species	Common Name	Mean Tensile Strength (MPa)
<i>Acacia confusa</i>	Acacia	11 (3.99%)
<i>Ficus benjamina</i>	Banyan	13 (4.71%)
<i>Hevea braziliensis</i>	Rubber tree	11 (3.99%)
<i>Populus deltoids</i>	Poplar	37 (13.42%)

Shrub Species	Common Name	Mean Tensile Strength (MPa)
Castanopsis	Golden chinkapin	18 (6.53%)
chrysophylla	Ceanothus	21 (7.61%)
Ceanothus velutinus	Scotch broom	33 (11.97%)
Cytisus scoparius	Scrub lespedeza	71 (25.74%)
Lespedza bicolor	Huckleberry	16 (5.8%)
Vaccinium spp.	Vetiver	75 (27.19%)

Note: The values in the parenthesis indicate % strength compared to 40-grade steel.

2.5.5 Bioengineering

The purpose of vegetation is to stabilize the soil through the hydrological and mechanical properties of roots, which is accomplished by covering the soil with plant communities (Islam and Rahman, 2019). Vegetation is recognized as a more sustainable and cost-effective alternative to artificial structures for improving the stability and durability of hillslopes (Basu *et al.*, 2014; Stokes *et al.*, 2014; National Research Council, 2006). Soil erosion is prevented in two ways by plants: first, by physically protecting the soil surface from erosion agents, and second, by aiding in the growth of a thick protective vegetation cover (Alvarez-Mozos *et al.*, 2014). Plant roots stabilize the soil and prevent shallow slope movements. Plant roots may increase soil stability in several ways, including an increase in cohesion and friction angles. Fine plant roots retain the soil and prevent erosion. The root system of plant helps drain excess water from the soil and provides interlocking properties that make the soil more resistant to shear (Saifuddin and Osman, 2014). Plant leaves not only divert precipitation but also increase the evapotranspiration rate. In contrast, plant roots draw water from the ground and lower pore-water pressure, triggering soil movement on a slope. In addition, they slow

down surface runoff and prevent the transport of fine particles (Mafian *et al.*, 2009; Coppin and Richards, 2007)

When it comes to altering the hydrological properties of a site, plants play a key role. Grass, shrubs, herbs, and trees are all viable options for slope reinforcement, each with unique root systems, mechanical qualities, cost, care requirements, and time required to get established. Where wind speeds and cyclone risks are minimal, deep-rooted trees are more effective at stabilising slopes because the factor of safety is much higher under these conditions (Gupta, 2016). Nevertheless, the impact of herbaceous vegetated slopes on surface mat decreases as depth increases. The hydrological dynamics of soil have minimal impact on vegetation, thereby mitigating shallow slope collapse, which is predominantly associated with increased moisture levels (Lobmann *et al.*, 2020). Vetiver grass (*Vetiveria zizanioides*), a type of grass belonging to the graminaceous family, possesses fibrous roots that have the capacity to reach a height of up to 3 metres. It has been found to be highly effective in mitigating top-soil erosion and providing protection against shallow depth slope failure. Notably, the implementation of vetiver grass for these purposes is cost-efficient, with an estimated expense of only US\$ 4.7 per square metre (Islam *et al.*, 2013) and it attained sufficient height quickly (Islam and Islam, 2018). Rainfall-induced slope failures might be reduced by planting vetiver grass on a slope since this kind of grass was shown to lower surface runoff volume by 18-71% (for varied vegetation intervals) and cumulative sediment production by 312%. (Islam *et al.*, 2021). Although reduced surface runoff might reduce soil erosion, increasing soil permeability can increase the rate of infiltration by as much as 35% in a closed experimental setting; in hilly places, precipitation infiltration and steep slope were two major causes of slope failure (Islam *et al.*, 2021, Islam and Rahman, 2019). Nasrin (2013) compared growth rates of the vetiver grass in silty and clayey soil and found that the former produced much faster results. This finding was similar to an earlier experiment by Islam and Islam (2018). In silty soil, FS contribution for vetiver grass might reach 48%, whereas, in clayey soil, the number is more like 5% - 35% (Suhatriil *et al.*, 2019). Some sample locations in Bangladesh have been treated with artificial grass made from vetiver as part of a bioengineering project meant to reduce the risk of landslides; the participants of the project have embraced this strategy (Dhungana *et al.*, 2020).

Slopes in a subtropical environment that make use of vegetation and JGT for erosion control have less soil erosion and less particle displacement. When natural geotextiles are installed in the ground, they immediately provide a protective layer. First, they do not

negatively affect the environment (Broda *et al.*, 2016; Sarasini and Fiore, 2018; Shavandi and Ali, 2019). Secondly, their progressive biodegradation provides organic matter and nutrients to plants, improving their vegetation growth and taking over the function of geo-JGT. It was found that there was no problem of erosion when the side slope was protected by vetiver and geo-JGT (Islam *et al.*, 2013). Soil particles were kept in place and erosion of the prepared slope was halted after JGT was applied to the shoulder and surface of slope. The vegetation on slopes ensured the slope stability and reduction in soil erosion (Choudhury and Sanyal, 2010). When natural geotextile like JGT is applied, the top layer of soil becomes moist, stimulating fast plant development. A micro-level addition of nutrients to the soil often causes JGT to biodegrade within a year or two. As soon as plants begin to grow, they replace JGT. When plants have matured, their canopy cover acts as a barrier, preventing rain from reaching the ground and eroding the soil. The deep-penetrating root system of vegetation reinforces slopes over the long run. When JGTs biodegrade, they return nutrients to the soil (Choudhury and Sanyal, 2010). Vegetation cover and geotextiles reduce erosion by at least 99 per cent and runoff by 44 to 62 per cent. The combination uses geotextile to assist with growing plant cover and preventing erosion immediately and vegetation cover to protect in the long term. Therefore, according to Liu *et al.*, 2023, the combination is the superior option for protecting road slopes in northern China. According to Kumar and Roy (2023) the use of JGTs on a trench slope helped to retain cohesive soil particles and prevented soil particles from being washed away from the slope surface. Vegetation development stabilized the soil on the trench slope. These types of soil bioengineering method practiced in India by following IS 14986:2001 and EN 13253:2016.

However, plants take around six to nine months to cover a bare surface. Until permanent measures can be taken to prevent top soil erosion, geo JGT, an open mesh naturally biodegradable JGT, may be employed. The vegetation canopy is developed when the geo JGT coating decomposes and becomes a fertilizer for enhanced plant development (Khan *et al.*, 2012). At the same time, JGT biodegrades within a year (Sanyal, 2017). The perpendicular root model and fibre bundle model are two common models for vegetation-based slope stabilisation, and they both primarily consider the impacts of vertical roots. However, vertical and horizontal root impacts might alter slope stability when vegetation produces shallow but dense root systems. In addition, the dynamics of topsoil stabilisation in herbaceous vegetation are poorly explained by existing models designed for woody root

systems. Therefore, further research into the impacts of herbaceous plant roots on horizontal stabilization is required (Lobmann *et al.*, 2020).

People worldwide have turned to live plants and other natural materials to counteract slope erosion for centuries. With the start of the Industrial Revolution, these natural remedies lost their popularity (Evette *et al.*, 2009; Gray and Sotir, 1996; Gray and Leiser, 1982). Soil bioengineering transferability is assessed by examining the current state of affairs in so-called developing nations and weighing the advice of important international cooperation bodies. According to Food and Agriculture Organization (FAO) literature, this method is preferable in a wide range of land reclamation contexts, including watershed management, landslide prevention, vegetation, and soil treatment, and more (Costantinesco, 1976; Sheng 1977a, b, 1979, 1990; Bostanoglou, 1980; Marui, 1988; Schiess, 1994). The widespread use of soil bioengineering in hilly regions of Europe and North America has generated a wealth of information that may be used to plan future operations (Evette *et al.*, 2009) safely. Due to the scarcity of such interventions in developing nations, it is important to emphasize their potential use in the context of technology transfer and sustainable development principles. (Dickerson and Lake, 1989; Anaya *et al.*, 1977; Clyma *et al.*, 1977).

2.6 Durability and Treatment Methods for Natural Geotextiles

Depending on the soil type and where the natural JGT is placed, it may biodegrade within one year (Sanyal, 2017). Researchers developed many chemical treatment procedures to enhance the durability and mechanical qualities of JGTs to address this problem. The following sections elaborate on the different chemical approaches.

2.6.1 Treatment Methods

Researchers have used numerous chemicals to treat JGT to increase its strength and durability. These processes change the chemical composition or the physical properties of the JGT to increase its durability. The following sections provide an in-depth discussion of the effectiveness, treatment procedures, and limitations of a select number of treatment procedures.

Alkali treatment, bleaching, and acetylation are some of the most popular methods to improve the tensile strength of natural fibres (Rosa *et al.*, 2009). Sodium hydroxide and hydrogen peroxide significantly reduce the hemicellulose and lignin content of JGT in an experimental setting. This led to enhanced breaking tenacity and subsequent low moisture

absorption capacity (Saha *et al.*, 2010; Wang *et al.*, 2009). Natural fibres treated with plant oils in conjunction with sodium hydroxide and formaldehyde showed improved resistance to biodegradation. The research concluded that a transesterification process replaced the hydroxyl group with oleic and stearic acid after the treatment (Saha *et al.*, 2012). JGTs treated with 0.5% isothiazolinone and 1.0% fluorocarbon resulted in higher water repellency and rot resistance. However, strength properties were not altered after treatment with these chemicals (Chakrabarti *et al.*, 2016). Alkali steam treatment comprising NaOH solution and steam increased the uniaxial tensile strength of JGT up to 65% by removing non-cellulosic matters of JGT like lignin, pectin, and hemicellulose (Saha *et al.*, 2010). The biological degradation of JGTs was also reduced by bitumen coating. Even after 1.5 years of usage, the tensile strength of JGT treated with bitumen used for river bank protection was high. However, the maximum life span of untreated JGT was reported to be one year (Sanyal and Chakraborty, 1994). However, it was reported that the bitumen coating technique on JGT might lead to leaching (Basu *et al.*, 2009). Treatment of JGT fabric with chemicals like N-vinyl pyrrolidone and ethyl hexyl acrylate in the presence of plasticizers increased the tensile strength up to 80%, with subsequent improvement in durability (Uddin *et al.*, 1997).

2.6.1.1 Scouring and Bleaching

The raw JGT was subjected to two chemical processes scouring with alkali and bleaching with hydrogen peroxide in the investigation by Wang *et al.*, (2009). Using diluted alkali and hydrogen peroxide solutions, they subjected JGT to 90 minutes of treatment at 95°C and 90°C, respectively. Both procedures maintained a constant ratio of 1:20 JGT-to-liquid. Samples were neutralized with diluted sulfuric acid after each treatment. Fourier transform infrared (FTIR) analysis, characteristic surface analysis, the chemical composition of fibre, XRD analysis, breaking tensile strength, breaking elongation, fineness index, moisture regain, and optical properties tests were performed on treated materials after treatment. It was determined by FTIR analysis that both scouring and bleaching remove some part of the hemicellulose and lignin content. To remove non-cellulose material, alkali scouring was more effective than bleaching. After scouring and bleaching, the cellulose content of the sample increased from 62% to 78% and 76%, respectively. As another observation, scouring was more effective than bleach in removing hemicellulose, while bleaching was more effective at removing the lignin content. One additional sample that underwent scouring and bleaching had the greatest cellulose content (82%).

Scanning electron microscopy (SEM) examination of raw JGT revealed the presence of several impurities. Alkali scouring is more effective than bleach in removing surface impurities, as determined by a SEM study of a treated sample. The combined scouring and bleaching of a sample produced the cleanest surface of all tests. X-ray diffraction (XRD) examination did not show crystalline transition or a change in the crystal structure. However, the proportion of different crystals present in raw JGT changed, leading to differences in crystallinity across samples. The crystallinity of the bleached and scoured sample was higher than that of the scoured sample. The crystallinity was lowest in the bleached sample compared to the others. A series of experiments determined the physio-mechanical characteristics of the treated materials. The JGT sample had a higher breaking tenacity due to its enhanced crystallinity and decreased hemicellulose and lignin concentration. The breaking tenacity was highest for the scoured sample, the bleached sample, and the combined scoured and bleached sample. The breaking extension increased for the scoured sample but reduced for the bleached and "scoured and bleached" samples. When lignin was extracted from JGT, the fineness index dropped for all treated samples.

2.6.1.2 Rot Resistant Solution

Both the significance and benefits of chemically treated JGT were highlighted by Prodhan (2008). The author also discussed several treatment methods to extend the durability of JGT. The author claimed that after just six months on the ground, JGT has already degraded significantly. The sensitivity of JGT to both acidic and alkaline conditions was well-documented. To make JGT last for an additional 5-10 years in the ground, Prodhan (2008) suggested a series of chemical treatments. To begin, he suggested spraying JGT with a mixture of copper sulfate, sodium carbonate, and water. This treatment enhanced the ability of JGT to resist rot. In addition, he applied a treatment consisting of a mixture of volatile oil and bitumen, which he had previously emulsified. JGT was brushed with this emulsion to coat it. The treated sample was then put out in the sun to dry. The sample was further processed with silicate solution before being dried one more. Finally, a JGT fabric that had been modified was rubbed with grease made from Ca, carbon black, and volatile oil. After treatment, this material was buried under 500 mm of subgrade.

2.6.1.3 Acetylation

The JGT was treated with acetic anhydride by Anderson *et al.*, (1989). Tensile strength, rot resistance, and hydrophobicity tests were conducted on the treated samples. The authors

submerged a square metre of JGT in acetic anhydride for one minute. After then, the sample was heated between 90 and 120 degrees Celsius for 5 minutes to 24 hours. After heating, excess acetic anhydride and the byproduct acetic acid were removed. Different concentrations of acetic acid were added to the anhydride solution in various experiments conducted by the author. Samples were weighed before and after the treatment to determine the weight increase attributable to acetylation. Acetylation-induced weight gain increased with response time, albeit the rate of increase slowed after 2 hours. Weight increase was higher in the samples heated to 120°C than in those heated to 90°C. JGT acetylation is an endothermic process. A study showed that after 2 hours, weight growth was 11% at 120°C and 7.5% at 90°C. Due to its swelling effect, acetic acid enhances the reaction between JGT and acetic anhydride, resulting in a larger weight gain when added to JGT. The weight gain proportion was reduced only because acetic anhydride was diluted as the concentration was raised.

The stability of JGT samples was evaluated by storing them at 25°C in a fungal cellar with moist soil. Fungi and germs of all kinds were growing in this cellar. After 2, 5.5, and 8 months, samples were visually assessed for signs of deterioration. After two months, the sample with the 11.5% weight rise showed no signs of degradation, as stated by the author. After 5.5 months, the damage was still quite significant. However, after eight months, there were warning signals of extensive degradation. There was no noticeable evidence of decay even after eight months in the samples that gained 14.2% and 16.2% of their initial weight. After two months, untreated JGT samples exposed to the same conditions showed significant degradation, and by 5.5 months, they had completely degraded.

Similarly, treated samples were submerged in water. The weight gain was carefully recorded due to increased water intake. Acetylation resulted in a 16% increase in the weight of the sample and a 30% decrease in water absorption compared to an untreated JGT sample. The treated JGT samples were also less likely to shrink than the untreated ones. Acetylation reduced the tensile strength of JGT textiles. In the weft direction, the sample weight loss was 16% for the 11% weight increase group and 42% for the 16% weight gain group. Similar weakening of about 10% and 33% were seen in the warp direction. There was a significant increase in the life of JGT at the expense of very little loss of strength, leading the author to conclude that the sample with an 11% weight rise is the best.

2.6.1.4 Transesterification

Saha *et al.*, (2012) used a chemical combination derived mostly from natural sources to process the JGT sample. The chemical compound had a 1:8:10:6:2:4 weight ratio of sodium hydroxide, liquid from cashew nut shells, plant tannin, neem oil, resorcinol, and formaldehyde. The pH level of solution was kept constant at 8. The geotextile was soaked for 24 hours and then baked for 1 hour. Two examples were prepared: One sample was made by treating individual jute fibres before weaving them into the fabric, whereas the other was treated after the fabric was already woven. T1 refers to geotextile made with treated fibre, and T2 refers to a fabric-level treated sample for easy reference. The letter JU indicates unprocessed JGT. As soon as samples were ready, testing and analysis were done to understand more about the treated samples' qualities. Freshly produced samples were subjected to a tensile strength test by ASTM D751.

In comparison to the JU sample, the tensile strength of the T1 sample was 13% lower, whereas the tensile strength of the T2 sample was 13% greater. However, there was not much change in the elongation at break. The treated samples were also put through a series of tests to see how well they withstood chemical and biological deterioration. Samples were tested for tensile strength after being stored in a 3% NaCl solution for 120 days. T1 and T2 samples maintained 82% and 64% of their original strength, respectively. JU sample, on the other hand, kept just 17% of its initial potency. The treated samples were also stored in solutions with a range of PH values from 3 to 10. They discovered that 50% of the tensile strength of both T1 and T2 samples was maintained in PH 4-9 solutions, with T1 samples performing somewhat better. The tensile strength test showed that JU samples had just 15% of their original strength.

There had been attempts to simulate real-world conditions in which the resilience of geotextile samples to biological degradation could be tested. Using the right proportions of water, the authors created a combination of black soil, cow dung, and sand. The sample was buried in the compound for 200 days. The temperature and humidity of this set-up were carefully monitored and maintained. Treated samples were shown to be very resistant to biological breakdown. Nearly 40 to 50 % of the original strength was maintained in the T1 and T2 samples, but the UJ sample completely disintegrated after just 90 days. By exposing materials to an artificial weather chamber for 500 hours, we could evaluate their resistance to physical damage. Only 33% of the original intensity of UJ was maintained, whereas T1 and

T2 samples maintained 80% and 75%, respectively. T1 and T2 samples were found to have 66% and 55% less water affinity than their respective controls.

FTIR analysis was performed on JU, T1, and T2 JGT samples to investigate the chemical changes during processing. Alcohol was used to clean up a JU, T1, and T2 sample. A 1% NaOH solution was then used to hydrolyse them. FTIR testing was performed on these modified samples. The FTIR analysis of samples T1 and T2 revealed the presence of stearic acid and oleic acid. Since these acids make up most of the neem oil, this suggested that JGT had been transesterified. FTIR testing also revealed that the hydroxyl groups in the T1 and the T2 samples had been modified. This suggested that JGT that had its fibres altered fared worse than JGT that had just its fabrics altered. The XRD analysis revealed that the crystallinity of the JGT samples had improved. Half-life estimates (the time it takes for a sample to lose half of its original tensile strength) for both T1 and T2 samples were presented in the last section of Saha et al (2012). Survival estimates for JU, T1, and T2 samples were 384, 1584, and 1115 days, respectively.

The aforementioned treatment methods are costly and require very skilled workmanship. To overcome such problems, a novel treatment is required, which is economically friendly and can be applied easily on JGT sheets. It is necessary to estimate the durability of different treated natural fibres also.

2.6.2 Durability Studies of Natural Geotextiles

All natural or artificial geosynthetics are likely to be exposed to sunlight and weathering during construction on-site and must therefore possess the capacity to resist weathering. The chemical bonds of polymers rupture, and the fibres start to disintegrate on exposure to weathering, thereby leading to fading of the natural colour of the fibre. Humid weather conditions and high microbial activities in soil enhanced the degradation process, decreasing its tensile strength (Wahit *et al.*, 2012; Yussuf *et al.*, 2010). Quinoid structures were developed when the lignin content of natural fibre starts absorption of UV rays, and the aging procedure is initiated in the fibres. Most natural and synthetic fibres were buried under the soil during service, but those that would be permanently exposed required a higher level of resistance. One of the primary reasons why natural geotextiles are less often used as reinforcement than manufactured geosynthetics is because of their low durability. The rate of degradation for a natural geotextile is significantly shorter in comparison to an artificial geosynthetic material. Various methods can be employed to evaluate the biodegradability of

natural fibres namely, natural and accelerated weathering tests ((ASTM G 154-16 (2016)) or soil burial tests in natural soils or composts (ASTM D570-98, 1998), resistance to acids & alkalis (BS EN 14030:2001) and hydrolysis of water ((BS EN 12447:2001), microbial attack, etc. (Batista *et al.*, 2010).

Fibres may be evaluated for their long-term performance after 1-2 years of exposure to various environmental conditions (Beninia *et al.*, 2011). Polymer cracking, black spots, bulging, twitching of fibres, and decrease of tensile strength was measured in a JGT or phenolic biocomposite after two years of exposure to natural weathering (Dittenber, 2012). Soil burial studies showed faster degradation of bamboo-reinforced epoxy hybrid composites than accelerated weathering (Chee *et al.*, 2019). Modifying coir geotextiles coated with cashew nut shell liquid (CNSL) increased the tensile strength by 22% compared to unmodified coir geotextiles. The rate of degradation was more for unmodified coir textiles. At the end of 240 days, tensile strength for modified coir was retained up to 76% and decreased by 19% for unmodified coir geotextiles (Sumi *et al.*, 2016). A chemically treated JGT plastic composite showed no change in elongation at breaking strength when immersed in different conditions like soil, semi-mud, and water for up to 150 days. However, for untreated JGT plastic composite, loss in tensile strength was 65% in water and 75% in soil, while the treated composite showed a loss of 5–15% (Uddin, 1997). JGT–polyesteramide composite specimens also showed tendencies of biodegradability with high porosity and lost more than 30% of their original weight when exposed to weathering after 21 days (Dash *et al.*, 2002). Tensile strength increases in treated JGT textiles compared to untreated JGT textiles in both the warp and weft directions after being treated with bitumen emulsion and polyester resin solution. However, long exposure led to a reduction in tensile strength (Akter *et al.*, 2018). In 1 year after installation in tropical climates, the tensile strength of coir geotextiles decreased by 80% (Marques *et al.*, 2014). Balan (1995) observed that in organic-rich sand, coir geotextiles decomposed more rapidly than in clay. Coir in sand had a 63% drop in tensile strength after a year, whereas coir in clay had a 31% decrease. The initial tensile strength of coir netting used for slope stabilization in the field decreased by 78% after seven months (Lekha, 2004). For watershed management embankment applications, coir geotextiles were shown to lose 70% of their tensile strength in only seven months (Vishnudas *et al.*, 2006). Field research by Joy *et al.*, (2011) shows how much time coir geotextiles spend buried and how quickly they degrade. Research indicates that after 90 days in a compost environment, the durability of JGT, another lignocellulosic material, drops to 72% (Saha *et*

al., 2012). Coir geotextile samples had a 77% drop in tensile strength after being exposed to rainfall and sunlight for a year in the tropical area of eastern Brazil. (Marques *et al.*, 2014).

70-80% of the initial tensile strength of modified coir geotextiles is retained after 12 months in soil burial condition. In contrast, unmodified coir geotextiles have lost 88% of tensile strength within four months (Sumi *et al.*, 2016). Tensile and flexural characteristics, as well as impact strength, of oil palm trunk fiber-filled recycled polypropylene composites were found to drop by roughly 38%-47%, 37%-50%, and 47%, respectively, after being buried in soil for 3, 6, and 12 months (Khalil *et al.*, 2010). It was observed that lignin had a slower degradation rate than that hemicellulose when buried in natural soil. The structural integrity of the fibres in windmill palms reduced biodegradation, resulting in an insignificant decrease in the tensile strength following a 90-day exposure to soil. However, a 43% decrease in tensile strength was observed in alkali-treated fibre after 90 days of burial in soil (Chen *et al.*, 2017). The incorporation of vetiver grass fibre as a natural filler material in the composite of natural rubber and polylactic acid resulted in a notable augmentation in the weight loss of the specimens as the duration of burial increased (Juntuek *et al.*, 2014). Experiments showed that the biodegradability of polypropylene-based fibres was greatly enhanced by the addition of 5% each of wood sawdust and wheat flour (Fakhrul and Islam, 2013). Natural fibres like a banana peel and pigeon pea stalk, used in the preparation of the composites, were prone to microbial attack and can be used to prepare polymer composites, thereby replacing the non-biodegradable synthetic fibre. These natural fibres filled polymer composites are a suitable alternative to synthetic fibre-filled polymer composites (Luthra *et al.*, 2020).

Chin *et al.*, (2020) examined how soil burial affects the degradation of an alkali-treated bamboo fibre-reinforced epoxy composite (BFREC). As the amount of time spent buried in the soil increased, the BFREC's ultimate tensile strength declined. Longer periods of soil burial resulted in a lower ultimate tensile strength for the BFREC. The material degradation due to water absorption is probably responsible for the reduction in tensile strength. After 80 days, the tensile strength of BFREC was only 969.95 MPa, a loss of almost 19% from the fresh sample. Rashdi *et al.*, (2010) conducted a soil burial test for Kenaf fibre unsaturated polyester composites. According to their findings, the cellulosic component of fibres decreases their tensile strength when exposed to soil burial conditions. Water absorption also increased, which led to the swelling of fibres. In work done by Rashdi *et al.*, (2009), long kenaf fibres are alkalinized in a 6% NaOH solution and then combined with

unsaturated polyester resin to form a composite buried for four months. Composites' tensile characteristics were measured, including their tensile strength and modulus. As the weight percent of fibre increased, the high cellulose content improved its effectiveness at absorbing water. It observed that when the percentage of moisture absorption in KFRUPC samples increased, the materials' tensile properties decreased. When buried, these composites' water absorption pattern followed a Fickian distribution.

Soil burial degradation tests ranging from one to five months were performed to determine the biodegradability of the biodegradable polyester Bionolle composite material treated with waste flour conducted by Tserki *et al.*, (2005). Within a month of exposure to bacteria, the composite surface changed from brown to white. The surface of the biodegraded composites appeared uneven and damaged, with holes of varied sizes and depths. After 3 and 5 months, biodegradation accelerated, and microorganisms completely degraded the samples. The biodegradation rate was reduced by adding treated flour or a compatibilizer into composites. One possible explanation for this slight decline is the correlation between flour modification and reduced composite hydrophilicity. Sapuan *et al.*, (2013) conducted a study of Soil burial experiments on the kenaf fibre-reinforced thermoplastic polyurethane (TPU) composites to determine how absorbing water affected their mechanical absorption characteristics.

The tensile and flexural properties of composite material were evaluated before and after being buried for 20, 40, 60, and 80 days. The weight gain and moisture absorption percentages after being buried in the ground were calculated. After being buried for 80 days, the tensile strength of a TPU composite reinforced with kenaf fibre decreased to 16.14 MPa. The flexural characteristics of the kenaf fibre-reinforced TPU composite specimens were likewise found to be unaffected by soil burial. The tensile strength, impact strength, and % weight loss of pure HDPE remained unchanged during the compost soil test because it is non-biodegradable, whereas those of pure PBS decreased significantly. In the natural soil burial test, the drop in mechanical characteristics and % weight loss of PBS and bio-composites were much less than in the compost soil test due to the higher warmth and humidity conditions in the chamber (Kim *et al.*, 2006). To investigate and evaluate the characteristics of totally biodegradable poly lactic acid (PLA) composites reinforced with elephant grass fibre, a 90-day soil burial test was conducted (Gunti *et al.*, 2018). Weight loss as a percentage increased linearly with the number of days the composites were buried in the soil.

Composites with the largest percentage of untreated fibres showed the greatest deterioration. About 1.5% of the weight was lost for plain PLA and 16.31% for the PLA composite containing 25% untreated elephant grass fibres. The biodegradability of the coir fibre (CF) and pineapple leaf fibres (PALF) with polylactic acid (PLA) biocomposites was confirmed by burial experiments in soil (Siakeng *et al.*, 2020). The C3P7 (hybrid biocomposites lost the most weight (16.8%), whereas the C7P3 (70% PLA + 21% CF + 9% PALF). Treatment with cashew nut shell liquid on coir geotextiles increased their tensile strength by 22%. After being buried in the ground for 240 days, the treated coir retained 76% of its initial tensile strength (Sumi *et al.*, 2016).

The weight loss of specimens buried in compost soil was used to assess the biodegradability of the material. Twenty per cent water, twenty per cent organic material, thirty per cent decayed leaves, five per cent urea, and five per cent additional materials (sawdust, waste paper) make up compost soil. The evaluation of the biodegradability of poly (butylene succinate) (PBS)/JGT composite is conducted through the analysis of various factors, including fibre content, diameter, surface modification, and arrangement forms. Considering the effect of fibre content biodegradability, higher weight loss is observed for PBS/low JGT composition (Liu *et al.*, 2009).

Coir fibres treated with NaOH showed that the tensile strength increased significantly by 53% compared with composites made with untreated coir fibres (Rosa *et al.*, 2009). Coir geotextiles modified with cashew nut shells have a faster degradation process in alkaline than in acidic conditions (Sumi *et al.*, 2018). When placed in soil, natural nettle fibres biodegrade faster than lactic acid poly fibre. These nettle fibres, which are not treated in any way, have a lower tensile strength (Kumar and Das, 2018). For two geotextiles named Terrafix and Secutex, it is shown that internal hydrolysis damages more than external hydrolysis. The Secutex geosynthetic has more tendency to degrade under the hydrolysis process (Dumitru *et al.*, 2017). From the durability aspect, changes in the surface colour, surface texture, and weight of the treated and untreated samples can be evaluated and compared with the unweathered samples after weathering for a certain period (Siakeng *et al.*, 2020).

2.7 Numerical Studies of Reinforced Soil Slopes

The geometry of a slope and the shear strength of soil are the primary factors in failure resistance. In geotechnical engineering, determining the stability of slopes exposed to precipitation is one of the most critical challenges that must be addressed. Several researchers

have conducted extensive studies on slope stability in wet circumstances (Hossain *et al.*, 2013; Rahimi *et al.*, 2011; Gasmol *et al.*, 2000; Ng *et al.*, 1998). Past research has shown that allowing rainfall to infiltrate the ground decreased slope stability (Chipp *et al.*, 1982; Pitts, 1983). Matrix suction develops in dry soil because unsaturated soil has a negative pore water pressure. This improves the soil's shear strength. Soil matrix suction is mitigated when enough water is absorbed by the soil through infiltration into the slope. A decline in matrix suction weakened the soil shear strength, which in turn brought about the collapse of the slope. There is a direct relationship among the flux parameters like infiltration, evaporation, and slope stability indicators like matrix suction, water flow, and soil strength at the soil-atmosphere interface. During the rainy season, pore water pressure and groundwater level rise, but matrix suction decrease. This combination makes the slopes more prone to collapse (Ali *et al.*, 2021).

According to Zhang *et al.*, (2004), it was revealed that under steady-state conditions, the rainfall intensity was the key component that influenced the matrix suction. However, when flow circumstances are described as transitory, the profile of matrix suction is affected not only by the intensity of rainfall but also by the water storage function, the saturated permeability, and the rainfall infiltration. Yubonchit *et al.*, (2017) conducted many parametric studies. They concluded that the major slope collapse might occur either during the infiltration stage or after the water table rose, depending on the ability of the slope to absorb water in a saturated environment. Due to constant matrix suction, the slope stays stable during the infiltration process. However, the slope could fail if the water table rises above the ability of soil to absorb water. If it rains at a rate that is faster than saturated capacity of the soil, matrix suction will stop while infiltration happens. This could lead to the discovery of slope collapse. Therefore, ground improvement practices must be applied to slopes under rainfall conditions. Geotextile reinforcement is a solution for slope stabilisation that requires little effort and is inexpensive. Geotextile reinforcement is a technique that may be used to stabilise slopes by improving FS value (Ghosh *et al.*, 2012). The impact of vegetation cover on the stability of slopes was examined by Razali *et al.*, 2023. An analysis was conducted on the factor of safety values derived from the Plaxis 2D numerical modeling. Based on the findings of the research, it can be inferred that vegetation will influence the soil's shear strength, as indicated by the increasing factor of safety from the initial slope. The factor of safety exhibited an increase in value from 2.968 to 2.991.

Additionally, the weak layers inside slopes play a crucial role in determining the stability under rainfall. Thus, including reinforcing layers inside the slope, in addition to adequate drainage measures, is a useful strategy for ensuring slope stability against rainwater infiltration (Bhattacharjee and Viswanadham, 2015). Slopes with poor permeability soils exposed to rainfall need a geosynthetic material with drainage and reinforcing qualities to improve their performance. According to Iryo and Rowe (2005), the reinforcing function seems to be more important than drainage in keeping an unsaturated embankment stable. The performance of geotextile structures built with poorly draining backfill is satisfactory, according to several studies, even when subjected to prolonged rainfall. On-site fine-grained backfill materials may be used with the help of nonwoven geotextiles, which have been claimed to result in significant cost reductions. This is because nonwoven geotextiles, when used as reinforcing layers, are predicted to enable internal drainage, which subsequently leads to enhanced stability by dispersing pore water pressures during precipitation events (Portelinha and Zornberg, 2017). When assessing the hydrological response of unsaturated slopes exposed to rainfall infiltration, estimating the slope-specific pore water pressure variation is crucial and difficult. In order to define the physical reactions (i.e., soil shear strength, variation of soil moisture, slope stability, effective stress, and matric suction) of unsaturated soil subjected to infiltration, some recent investigations have utilised coupled and uncoupled hydro-mechanical analyses within the context of unsaturated soil mechanics (Oh and Lu, 2015; Qi and Vanapalli, 2016). Water flow and stress changes in unsaturated soils may be more accurately represented by the coupled analysis (Yang *et al.*, 2017), allowing for a more accurate assessment of slope stability under infiltration circumstances.

Most practical slope stability evaluations are still carried out using limit equilibrium techniques, such as slicing techniques. Regarding slope stability analysis, the finite element technique is a powerful alternative as it is accurate, adaptable, and depends on fewer assumptions, particularly concerning the failure mechanism. In the finite element model, slope failure naturally happens in the areas where shear strength of the soil is inadequate to withstand the shear pressures (Griffiths *et al.*, 2004). Geotechnical engineers have employed a range of methodologies and approaches to analyse earth slopes. These include the Finite Element Method (FEM), which involves reducing cohesion (c) and soil internal friction angle (ϕ), the Limit Equilibrium Method (LEM) or Limit Equilibrium Analysis (LEA), the Finite Difference Method (FDM), the Limit Analysis (LA), and the integration of the Finite Element Method and the FDM (Madhav and Reddy, 2018). Ali *et al.*, (2019) used Plaxis 2D

FEM software to analyze the stability of slopes reinforced with soil nailing exposed to different rainfall intensities. They proved that reinforcing the soil with nailing can reduce soil deformation effectively under high rainfall intensities. Numerous studies have investigated the efficacy of reinforced soil walls and slopes against the penetration of rainfall.

2.7.1 Van Genuchten Model

The analysis used PLAXIS 2D finite element modelling software with fully coupled flow deformation (Brinkgreve 2002). Mohr-Coulomb failure criteria and Bishop's effective stress idea were used to evaluate the shear strength of soil under unsaturated conditions, represented as equation (2.3).

$$\tau = c' + (\sigma_n - u_a)\tan\varphi' + \chi(u_a - u_w)\tan\varphi' \quad (2.3)$$

Where τ = shear strength of unsaturated soil; σ_n = total normal stress; u_a and u_w are pore air pressure and pore-water pressure, respectively; $\sigma_n - u_a$ = net normal stress; $u_a - u_w$ = matric suction; c' = effective cohesion; φ' = internal soil friction angle; and χ = scalar multiplier.

In unsaturated regions, the permeability is denoted by a curve representing the soil water properties (SWCCs). The Van Genuchten equations express the relationship between the pressure head and moisture content, shown in equation (2.4). This relationship is represented by SWCC graphically, as shown in Figure 2.7. The Van Genuchten-Mualem model, as given in the equation, explains the permeability function in equation (2.5).

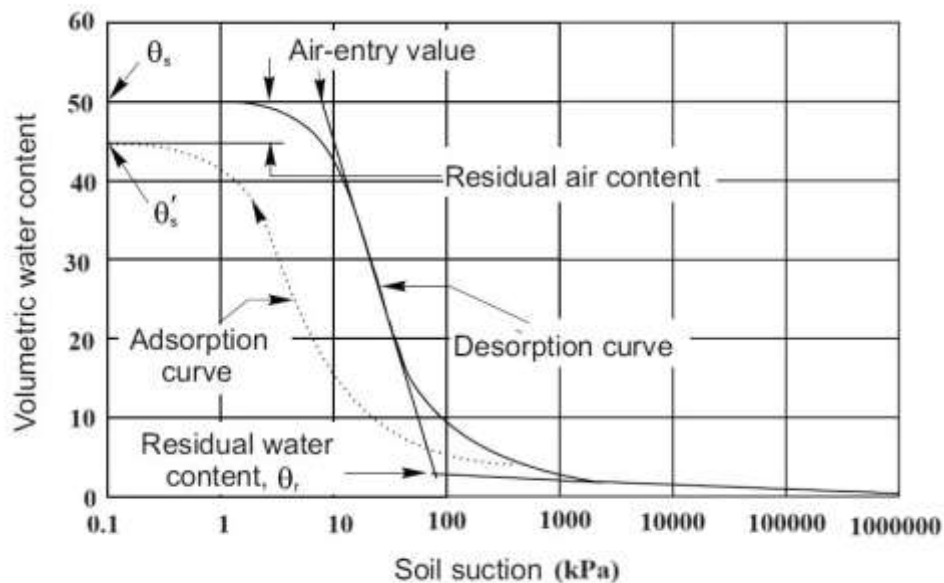


Figure 2.7. Soil Water Characteristic Curve image (Freduland *et al.*, 2012)

$$\theta_e = \frac{\theta_w - \theta_{res}}{\theta_{sat} - \theta_{res}} = \left[\frac{1}{1 + \{\alpha(u_a - u_w)\}^n} \right]^{1-n^{-1}} \quad (2.4)$$

$$k(h) = k_{sat} \times \frac{\left[1 - \{\alpha(u_a - u_w)\}^{n-1} \times [1 + \{\alpha(u_a - u_w)\}^n]^{\frac{1}{n-1}} \right]^2}{[1 + \{\alpha(u_a - u_w)\}^n]^{\frac{1-n}{2}}} \quad (2.5)$$

Where θ_w = volumetric water content; θ_{res} = residual volumetric water content; θ_{sat} = saturated volumetric water content; k_{sat} = saturated permeability of soil; α and n are Van Genuchten fitting parameters.

The hydraulic-related parameters (α , n , k_{sat}) and the strength parameters (c' , ϕ') are required for slope analysis in PLAXIS. Depending on the values of the van Genuchten parameters α , n , the SWCC graph can show a variety of shapes. The simulation of geotextiles in Plaxis 2D used geogrid components, which need the axial rigidity of the material being modelled.

2.7.2 Calculation of Van Genuchten Parameters

The pedo transfer functions (PTFs) approach for determining the Van-Genuchten parameters α and n is derived from the regression equations developed by Benson *et al.*, (2014). The empirical equations utilise the grain size parameters C_u and d_{60} .

- First, using the connection between α , n and d_{60} and assuming $C_u = 1$ for wetting and drying as shown in equations 2.6 to 2.9, determine the α , n values corresponding to wetting (α_{1w} , n_{1w}) and drying (α_{1d} , n_{1d}).
- Before calculating the second step, here, two new parameters are defined: normalised α , i.e., N_α , and normalised n , i.e., N_n . (Normalised $N_\alpha = \frac{\alpha \text{ at given } C_u}{\alpha \text{ at } C_u=1}$, Normalised $N_n = \frac{n \text{ at given } C_u}{n \text{ at } C_u=1}$). Simply put, normalised α or n is the ratio of α at a given C_u to α at $C_u = 1$, which is also applicable for normalised N_n .
- Normalised values of α and n give their corresponding result to the given C_u , which is distinct from the first step.
- Multiplying the α (from the first step) and N_α (from the second step) or n (from the first step) and N_n (from the second step) gives the corrected α and n values, which will be used as Van Genuchten parameters in Plaxis 2D simulation.

For Wetting:

The following equation represents the Van Genuchten air entry fitting parameter for wet conditions.

$$\begin{aligned}\alpha &= \alpha_{1w} \cdot N_{\alpha} \\ \alpha_{1w} &= 1.993 d_{60} \\ N_{\alpha} &= 0.99 C_u^{-0.54}\end{aligned}\tag{2.6}$$

The equation below represents the Van Genuchten water extraction rate from soil fitting parameters for wet conditions.

$$\begin{aligned}n_w &= n_{1w} \cdot N_{nw} \\ n_{1w} &= 8.22 e^{(-0.354 d_{60})} \\ N_{nw} &= -0.0033 C_u + 0.550 \quad (\text{if } C_u > 2.2) \\ N_{nw} &= -0.383 C_u + 1.383 \quad (\text{if } C_u < 2.2)\end{aligned}\tag{2.7}$$

For Drying:

The following equation represents the Van Genuchten air entry fitting parameter for drying conditions.

$$\begin{aligned}\alpha_d &= \alpha_{1d} \cdot N_{\alpha} \\ \alpha_{1d} &= 1.354 d_{60} \\ N_{\alpha} &= 0.99 C_u^{-0.54}\end{aligned}\tag{2.8}$$

The following equation represents the Van Genuchten water extraction rate from the soil fitting parameter for drying conditions.

$$\begin{aligned}n_d &= n_{1d} \cdot N_{nw} \\ n_{1d} &= 14.4 e^{(-0.434 d_{60})} \\ N_{nw} &= -0.0033 C_u + 0.379 \quad (\text{if } C_u \geq 2.2) \\ N_{nw} &= -0.542 C_u + 1.542 \quad (\text{if } C_u < 2.2)\end{aligned}\tag{2.9}$$

Where d_{60} (grain size) and C_u (coefficient of uniformity) are grain size analysis parameters. (α_{1w}, n_{1w}) (α_{1d}, n_{1d}) are Van Genuchten parameters for wetting and drying conditions. N_{α} is a normalised α value with the same empirical formula for wetting and drying. N_{nw} and N_{nd} are normalised n values for wetting and drying conditions.

The empirical equation for finding Van-Genuchten parameters using the PTFs method is the most precise method (Benson *et al.*, 2014). Based on this study, it is observed that there is a range for both α and n values. For α (1/kPa), the values range is from 0.10 to 2.39, and for n values range is from 1.48 to 8.08 based PTF estimation method (Benson *et al.*, 2014). The values of $C_u = 6.6$ and $D_{60} = 2$ mm are obtained after performing the gradation analysis of soil samples used to calculate Van Genuchten parameters.

2.8 Summary of Literature Review and Limitations of Existing Research

A thorough review of existing literature provides a detailed discussion of different types of natural geotextiles and bioengineering methods for improving strength and reducing surface erosion, various treatment methods for natural geotextiles to improve their durability, and numerical studies of reinforced soil slopes. A comprehensive summary of the literature is presented as follows:

- Previous research shows that untreated natural JGTs degrade in the soil within a maximum period of 6 to 12 months. Thus, chemical pretreatment is required to preserve its functioning. Numerous studies have recommended using various treatment methods, including chemical treatments such as alkaline scouring, bleaching, acetylation, and plant-based oil treatment. However, these treatments are unfortunately expensive and cause leaching. To increase the shelf life of JGTs by two to three years, the present research proposes the development of a novel technique for treating jute with an Alkali Activated Binder (AAB).
- A thorough review of past research work highlights that some of the existing chemical treatment methods for natural fibers are expensive and may cause environmental concerns due to leaching. However, the influence of various mediums on the chemical composition of natural fibers has not been adequately quantified or documented, which will differ for different fibers due to their greatly variable composition. Fiber debonding, the influence of corroded fibers, and the effect of exposure circumstances all contribute to a reduction in the strength of composite, which is intended to be used to understand the natural fibers' longevity. The differences in the strength properties of natural fibers in dry and wet conditions, as well as after exposure to various climates may provide further insight into the real degradation process and aid in understanding the deterioration mechanism of natural fibers in these environments.

- From past research, it can be observed that limited studies are available for improving the strength of the soil with the help of vegetation. However, it has been reported that slope erosion triggers before the vegetation grow strong enough to protect the soil. Hence, the present study aims at using the soil bioengineering system i.e. vegetation in conjunction with the AAB-treated jute to increase the strength and durability parameters and decrease surface erosion. Thus, the present research proposes a study on a bioengineered small-scale laboratory model and assessment of the efficiency of AAB reinforcement in conjunction with vegetation on soil erosion using existing empirical models like MUSLE.
- Most of the existing research on modeling a slope against rainfall infiltration is focused on unreinforced soil or soil reinforced with artificial geosynthetics. A systematic numerical study considering the effect of rainfall infiltration on bio-engineered slopes reinforced with treated natural geotextiles is not reported in the literature. Thus, the current work proposes in developing a numerical model that will consider the interaction between soil slopes having different slope angles and reinforcing material subjected to rainwater infiltration.

2.9 Research Significance

The findings (optimal design of natural fibre and plant root stabilised soil or soil slope) of the current research can be innovative solutions for protecting soil erosion on roadways and railroad embankments. Erosion control and slope failure caused by water erosion due to rainfall are the most important aspects which can be addressed effectively by the application of AAB reinforcements in this research. This innovation will benefit the construction industry significantly. India produces enormous volumes of fly ash as an industrial byproduct. Fly ash will be one of the key components of the technique used in the current investigation. Using AAB-treated natural fibre on road/railway embankments, river dykes, and other embankments will be cost-effective and environmentally safe. In addition, the design of embankments, dams, and slopes will benefit greatly from the creation of a numerical model for calculating the impacts of natural fibres on increasing soil strength or providing soil reinforcement. The successful use of natural fibres for slope protection and erosion control will provide a case study of best practices, and the findings may be utilized to educate the public about sustainable slope management and erosion control techniques.

CHAPTER 3

Materials and Experimental Methodology

3.1 General

This chapter presents the basic characterisation of raw materials and the salient experimental procedures used in the thesis. Red soil, Alkali Activated Binder (AAB), Bermuda grass, and natural JGT were the materials employed in this study. The characterisation includes evaluating the geotechnical properties, morphological characteristics, and chemical properties of red soil, untreated and treated JGTs with AAB having different water-to-solids ratios, and Bermuda grass. A comprehensive experimental investigation is conducted, and methodologies concerning the strength and microstructural aspects of red soil and AAB-treated JGTs are examined in detail in this chapter.

3.2 Material Used

3.2.1 Red Soil

The red soil used in the present research is collected from Shameerpet, located in the Medchal-Malkajgiri region of Telangana, India. The soil is obtained from a depth of 300 mm below ground level to ensure no roots or other plant matter are included in the sample. The soil is brownish-red in colour and is fine-textured. The soil samples are prepared for examination by breaking them into little crumbs with a wooden mallet and then dried at 105-110°C in a thermostatically controlled oven. The red soil comprises 4.26% gravel, 60.47% sand, and 35.27% silt and clay and is classified as silty sand (SM) according to Unified Soil Classification System (USCS ASTM D 2487-93). The grain size distribution curve for red soil is shown in Figure 3.1.

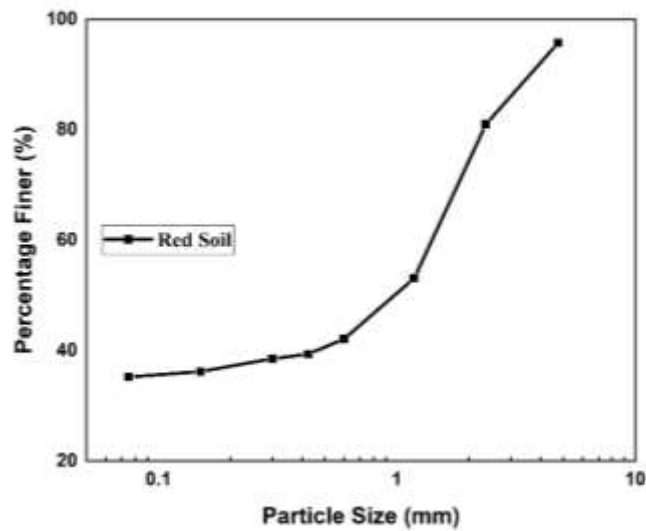


Figure. 3.1 Grain size distribution curve of Red Soil

The following tests are conducted to characterise the red soil:

- Specific gravity (according to IS 2720 - Part 3 (1980)).
- Gradation Analysis (following IS 2720 - Part 4 (1985))
- Atterberg's Limits (following IS 2720 - Part 5 (1985))
- Proctor's Compaction Test (following IS 2720 - Part 7 (1980) and IS 2720 - Part 8 (1983))
- Variable Head Permeability test (following IS 2720 - Part 17 (1986)) on soil using universal permeability apparatus.
- Soaked and Unsoaked California Bearing Ratio (CBR) (according to IS: 2720 - Part - 16 (1987)).
- Strength characteristics using Unconfined Compression Tests (following IS 2720 – Part 10 (1991))
- Large Shear Box test to determine interface friction angle between soil and reinforcing element (jute) (according to IS 2720-13 (1986)).

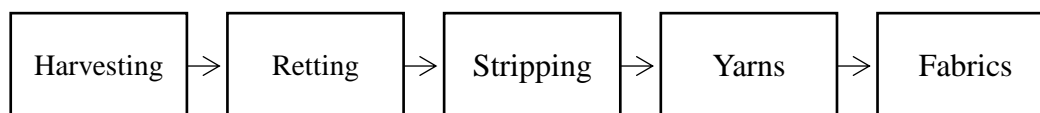
The different properties of the soil are provided in Table 3.1.

Table 3.1 Properties of Red Soil

Properties	Values
Specific gravity, (<i>G</i>)	2.61
Liquid Limit (LL) (%)	31
Plastic Limit (PL) (%)	15
Plasticity Index (PI) (%)	16
Shrinkage Limit (%)	12
Optimum Moisture Content (%)	11.00
Maximum Dry Unit Weight (kN/m ³)	19.40
Permeability (mm/sec)	1.13×10^{-2}
Unsoaked CBR	11.67
Soaked CBR	4.2
Cohesion (kN/m ²)	9.5
Internal Angle of Friction (°)	26.05
Grain Size Analysis	
Gravel (%)	4.26
Sand (%)	60.47
Silt and clay (%)	35.27

3.2.2 Natural Jute Geotextile

Commercially available jute (*Corchorus olitorius* - Tossa Jute) used in the present study is procured from Secunderabad in Telangana state of India as a hessian cloth in a roll of 0.91 m width and 30 m length. The jute sheet is a woven type made from fresh raw jute fibres. The process of obtaining jute fibres from the plant, as mentioned by the manufacturer, is as follows:



It is checked that the jute fabric lacks scouring and bleaching. The aperture opening size, thickness, and mass per unit area of treated and untreated jute sheet are determined confirming to IS 15868 (Parts 1 to 6): 2008. The basic properties of the raw JGT are provided in Table 3.2. The FTIR peaks and corresponding bonds are shown in Table 3.3 and Figure 3.2

shows images of FTIR and XRD patterns of untreated jute. Consistent with the findings of Wang *et al.* (2009) and Gupta *et al.*, (2018), the peaks at 15.1°, 22.8°, and 31.5° (represented by the letter J) in the XRD diffractogram are indicative of unaltered, raw jute fiber. Peaks corresponding to 2θ values of 15.1°, 22.8°, and 31.5° (denoted by "J") indicate the presence of minerals consistent with the composition of jute in Figure 3.2(a). From FTIR spectra, the observed peaks at 2915 cm^{-1} , and 1639 cm^{-1} represent C-H and C–C stretching absorption. The stretching absorptions of the C–O–C bond are detected at 1247 cm^{-1} and 1053 cm^{-1} . These peaks coincide with the FTIR spectra of normal cellulose (Wang *et al.*, 2009).

Table 3.2. Fundamental characteristics of untreated jute

Parameters	Values
Aperture Opening Size	$4.7 \times 10^7 \mu\text{m}^2$
Thickness	$0.62 \times 10^{-3} \text{m}$
Mass per unit area	0.22 kg/m^2
Cellulose content	53%
Hemicellulose content	20%
Lignin content	12.6%
Water absorption	11.6%
Elongation at break	60.38%
Tensile strength (warp direction)	6.68 kN/m
Young's Modulus	20.8 GPa

Table 3.3 FTIR peaks and corresponding for Jute (Merck KGaA, 2022)

FTIR Peak (cm^{-1})	Bonds
3467–3434	O–H Stretching
2930-2910	C–H Stretching
1035-900	C–O-C Stretching
1730	C – O Bending
1700-1644	C=O
1640-1618	C=C

1037.5-1024

Si-O-Si

778-774

Al-OH

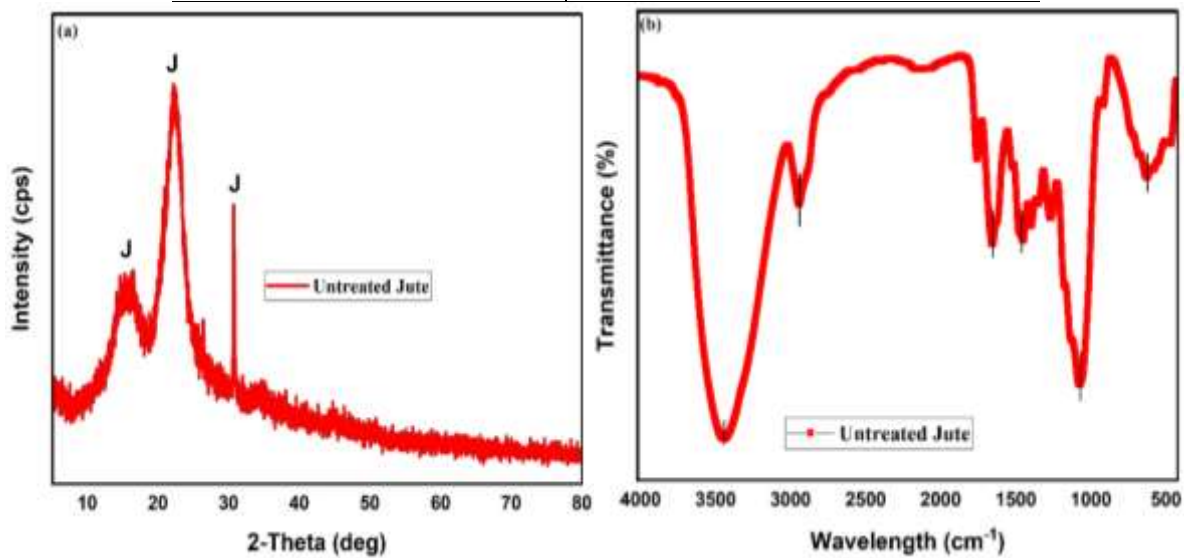


Figure 3.2 a) XRD diffractogram and b) FTIR spectroscopy of untreated Jute.

3.2.3 Alkali Activated Binder (AAB)

Dry aluminosilicate-rich precursor (Class F fly ash) is reacted with an activating solution (consisting of sodium silicate, sodium hydroxide, and water) to create Alkali Activated Binder (AAB). After 24 hours, fly ash is added to the activating solution because of the excessive heat generated by the exothermic reaction between the sodium hydroxide (NaOH) and the sodium silicate (Na_2SiO_3). The Global Warming Potential (GWP) effect of fly ash, sodium silicate and sodium hydroxide on the environment are zero, 0.83 and 1.32 kg CO_2 -eq, respectively (Chottemada *et al.*, 2023). However, the manufacturing process of AAB does not generate any CO_2 emissions as it utilizes already available industrial wastes as raw materials compared to Portland cement (PC), which emits almost to 750-850 kg CO_2 for 1 ton of Portland cement production. Using AAB to treat jute does not lead to the formation of any environmentally harmful volatile compounds. Besides, the heavy metals leaching from the mixture of fly ash and is very negligible. The composition of heavy metals such as chromium (Cr), arsenic trioxide (As_2O_3), lead oxide (PbO), and zinc oxide (ZnO) was not contained in fly ash. The chemical compound of fly ash and slag (such as Cao, MgO) can easily monitor the pH and leachate, which does not impact much too surrounding flora and fauna. The chemicals were procured from Hychem Laboratories Ltd., Hyderabad, Telangana, India. Class F fly ash was obtained from the National Thermal Power Corporation plant in

Ramagundam, Telangana, India. The NaOH is obtained as pellets with 99% purity, whereas the Na₂SiO₃ solution is a mixture of 29.5% SiO₂ and 14.7% Na₂O. In a mass ratio of 1:12.24:37.84 the sodium hydroxide, sodium silicate, and fly ash are mixed to prepare AAB (Gupta *et al.*, 2018; Kar *et al.*, 2014). The detailed mix design procedure is described by Kar *et al.*, (2014). The water-to-solid ratios (w/s) of the AAB mix are varied at 0.35, 0.40, and 0.45 (Gupta *et al.*, 2018). Various amounts of fly ash, NaOH, Na₂SiO₃, and water required to prepare the AAB mix are shown in Table 3.4, along with the corresponding AAB quantity needed per m² of JGT.

Table 3.4. Amount of AAB required treating per sq. meter JGT

Water/Solid Ratio	AAB Applied (kg/m ²)	Fly Ash (kg/m ²)	NaOH (kg/m ²)	Sodium Silicate (kg/m ²)	Water (kg/m ²)
0.35	3.44	2.18	0.058	0.706	0.498
0.40	3.07	1.87	0.049	0.606	0.537
0.45	2.75	1.62	0.043	0.526	0.5611

The hardening characteristic of AAB exhibits similarities to that of hydraulic cement. Therefore, the process of hardening will commence upon the addition of the alkali solution to the fly ash. To optimise resource utilisation and minimise material waste, it is recommended to apply the AAB coating during its workable state, thereby preventing premature hardening. The application of the AAB coating can be accomplished through two methods, either by utilising paint brushes to apply it directly onto the JGT, or by sprinkling the coating over the JGT. Alternatively, the JGT can be soaked in a manner that ensures the entire surface area of the JGT is covered by the coating mixture. The JGT, which is coated with AAB, is maintained at a temperature of 40°C within a controlled environment that regulates humidity for a duration of 24 hours. The treated JGT is subsequently stored at room temperature for seven days to render it appropriate for practical utilisation in ground improvement. During this duration of seven days, the AAB undergoes a hardening process, allowing it to acquire the necessary strength to endure externally imposed loads. Figure 3.3 shows the images of untreated and treated JGT. The treated JGT is then introduced into the soil in horizontal layers. A series of laboratory experiments on permeability, California Bearing Ratio, and

unconfined compressive strength tests are then conducted to compare the properties of the soil before and after the addition of the treated JGT.

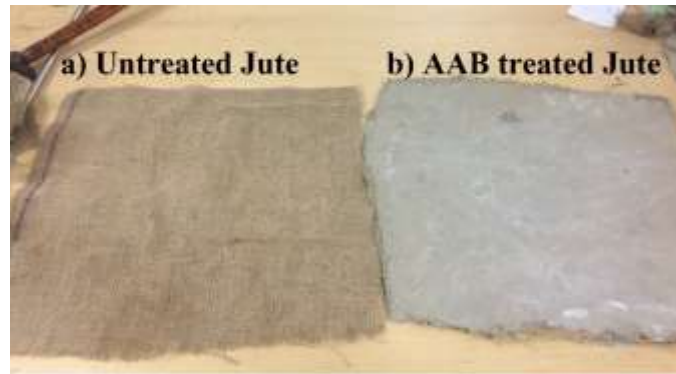


Figure 3.3 JGT before and after AAB treatment

3.2.4 Bermuda Grass

Bermuda grass (*Cynodon dactylon*) is often used for slope stability due to its deep and broad roots. It prevents erosion and stabilises steep slopes, especially in rainy or foot-trafficked areas. The broad, extending root system of Bermuda grass can grow up to 2 metres deep, anchoring the soil and preventing erosion. This is particularly important on slopes, where soil erosion and instability may cause landslides, infrastructure damage, and soil loss. Bermuda grass exhibits adaptability to diverse soil compositions and climatic conditions. It grows on sand, clay, and other soils and resists drought and heat. It may be planted in many conditions, giving it an adaptable slope stabilisation option. Bermuda grass spreads quickly and covers the surface of soil with its deep and spreading roots. This reduces soil erosion and blocks runoff. It is particularly beneficial for stabilising slopes prone to erosion, such as those in areas with heavy rainfall or foot traffic. The image of Bermuda grass is shown in Figure 3.4. Physical observation provided the fundamental characteristics of Bermuda grass, including colour, texture, growth range, length, and width, as listed in Table 3.5.



Figure 3.4. Bermuda grass in laboratory condition

Table 3.5 Basic Properties of Bermuda Grass

Property Type	Values
Colour	Lawn Green
Texture	Smooth texture (lower surface) and jagged texture (upper surface)
Growth Range	Upto 100 cm
Leaf Blade Property	0.02 m to 0.2 m in length and 0.003 m to 0.01 m in width

3.3 Mineralogical, Chemical, and Microstructural Characterizations

Microstructural analyses such as XRD, FTIR, Thermogravimetric analysis (TGA), Stereo microscopy, and SEM are performed on both untreated and AAB-treated jute to quantify the morphological and phase changes caused by the application of AAB to jute fibre. The mechanical properties of jute, including shear strength, volumetric stability, and bearing capacity, can be significantly affected by the microstructural properties of the material. These aforementioned properties play a crucial role in determining the practical implementation of these materials in the field of construction. The chemical composition of materials may be inferred qualitatively using FTIR and XRD data. Qualitative data on the physical properties

of material may also be obtained by stereomicroscopy. SEM examination is used in conjunction with other methods to get quantitative data on treated geotextile-reinforced soils.

3.3.1 Stereomicroscopy

Stereomicroscopy is used to examine the overall structure and any irregularities of the JGTs before and after AAB treatment. Using an Olympus SXZ7 system, the surface texture and physical characteristics of jute samples are examined by collecting stereomicroscopic images at several magnifications. 20 μm is the smallest dimension that can be focused with this microscope. Depending on the topography and shape of the surface, the chosen target area of each stereomicroscope image varies between 4×10^5 and $10 \times 10^5 \mu\text{m}^2$.

3.3.2 X-ray Diffraction (XRD)

Mineralogical analyses using XRD are used to identify the crystallinity of untreated and AAB-treated natural JGTs. The RIGAKU Ultima IV diffractometer is used for the XRD analysis. Powdered samples are analysed using $\text{CuK}\alpha$ rays, produced at 40 mA with a step of 0.02° for 2θ values ranging from 0° to 80° and integrated at a 2 sec/step rate. Preparation of powdered samples for X-ray diffraction (XRD) analysis involves a two-step process, first, the sample is subjected to an oven dry treatment at 105°C for 24 hours to eliminate any moisture content, and second, the resulting sample is crushed into a powder form using a mortar and pestle.

3.3.3 Fourier Transform Infra-Red (FTIR) Spectroscopy

FTIR determines the molecular bond structure of untreated and AAB-treated jute fibre. FTIR is used to study how AAB treatment affects chemical composition of the jute, which can affect performance and durability. The JASCO FTIR 4200 instrument generates FTIR spectra through the KBr pellet technique. All jute samples are analyzed using spectral transmittance from 4000 to 400 cm^{-1} to determine the different vibrational bonds present, such as the stretching vibrations of C-H, O-H, and C=O bonds in jute, which occur in the $4000\text{-}2500 \text{ cm}^{-1}$ range, and the bending vibrations of C-H and O-H, which occur in the $2500\text{-}400 \text{ cm}^{-1}$ FTIR range (Gupta *et al.*, 2018; Kar *et al.*, 2014).

3.3.4 Scanning Electron Microscopy (SEM)

SEM is used to assess the microstructural and morphological characteristics of jute fibre at high resolution. In addition, SEM is used to examine the influence of AAB treatment on the microstructural change, which is beneficial for studying the performance of jute fibres. An

FEI-Thermo Scientific Apreo SEM setup is used to analyse SEM micrographs and elemental compositions. Untreated and AAB-treated jute was dried in an oven at 110° C for 4 hours before sample preparation to remove moisture without causing any significant alteration to composition and SEM analysis is an imaging method with a high resolution that needs a high vacuum environment to function properly. Thus, any remaining moisture or water in the sample might cause pressure changes that can damage the sensitive components of the microscope. The sample adhered to the carbon tape with the help of crushed powder made from a soil-fibre combination. The surface morphology is examined at four distinct spot sizes and magnifications (1000×, 2500×, 5000×, and 10000×). A constant excitation voltage of 20 kV is used for JGTs throughout the investigation with a covering of 10 nm thick platinum coating to prevent the electron cloud and fuzzy condition of SEM pictures and the vacuum pressure of 1.0×10^{-3} Pa is observed to obtain the images. (Gupta *et al.*, 2018). The excitation voltage range of 5kV-15 kV is recommended for AAB-treated JGTs; for this study, 10 kV excitation voltage is used (Kar *et al.*, 2014).

3.3.5 Thermogravimetric Analysis (TGA)

The thermal stability of both untreated and treated jute is assessed using differential TGA on SHIMADZU/DTG-60 equipment. Samples of JGT are typically between 10 and 15 mg in weight. Temperature between 30 to 950 degrees Celsius is used to decompose the materials (Yang *et al.*, 2007). For consistent warmth, the heating rate is maintained constant at 10 C/min.

3.4 Geomechanical Characterisation

3.4.1 Natural Jute Geotextile

The following tests can identify the basic material properties of natural JGTs.

- Aperture size
- Thickness (thickness gauge at 2 KPa pressure)
- Mass Density
- Tensile strength (grab test as per ASTM D 4632/D4632M-15a)

3.4.1.1 Aperture Opening Size

The aperture opening size (AOS) of the untreated JGT is determined by analysing the stereo-microscopic images by direct method for finding the pore size of geotextiles (Babu G.S., 2006). Due to their planar shape and comparatively large pore openings, woven geotextiles

are more effectively examined utilizing a direct method such as image analysis for pore size determination (Ayidlek *et al.*, 2007). The average area of 10 different samples is considered. $AOS = 4.7 \times 10^7$ sq. μm . Figure 3.5 shows the aperture opening size of the jute obtained from the stereomicroscopic image. The aperture opening size of JGTs impacts their performance and functioning in various applications. The aperture opening size is the size of the opening of the fabric, which enable water, air, and other fluids to flow through while retaining soil particles and debris. The application and performance criteria determine JGT aperture opening size. For example, in erosion management applications, a smaller aperture size may be needed to avoid soil erosion and retain soil particles, whereas, in drainage applications, a larger aperture size may be needed to assist water flow and prevent clogging.



Figure 3.5. AOS obtained from the stereomicroscopic image

3.4.1.2 Thickness

The average thickness of the untreated JGT is measured using a thickness gauge under a gradually applied specified pressure. Thickness values were obtained for 1, 3, and 6 months for lab burial conditions. Table 3.5 shows the thickness values of untreated and treated jute at various time durations. The thickness values of untreated and treated JGTs are decreased maximum over the period 6 months due to various reasons including moisture absorption from the environment and biological degradation. From table 3.6 it is observed that the values of thickness reduction are 6.25% and 3.12% for untreated jute 0.35 AAB treated JGTs. Biodegradable untreated JGTs exposed to microorganisms, such as fungi and bacteria, can break down and reduce in thickness. Hysteresis develops when natural geotextiles are regularly wet and dry because the fibres absorb and evaporate moisture from the surrounding environment. This hysteresis may pack the fibres more densely, reducing thickness. The AAB treatment for JGTs protected them from biological degradation and water absorption effect.

Table 3.6 Thickness (in mm) of Untreated and Treated jute at various times

Thickness at	Untreated	0.35 AAB	0.40 AAB	0.45 AAB
jute(mm)	Jute(mm)	Jute(mm)	Jute(mm)	Jute(mm)
0 month	0.64	1.92	1.93	1.84
1 month	0.64	1.92	1.92	1.83
3 months	0.62	1.89	1.88	1.79
6 months	0.60	1.86	1.85	1.76

3.4.1.3 Mass per unit area

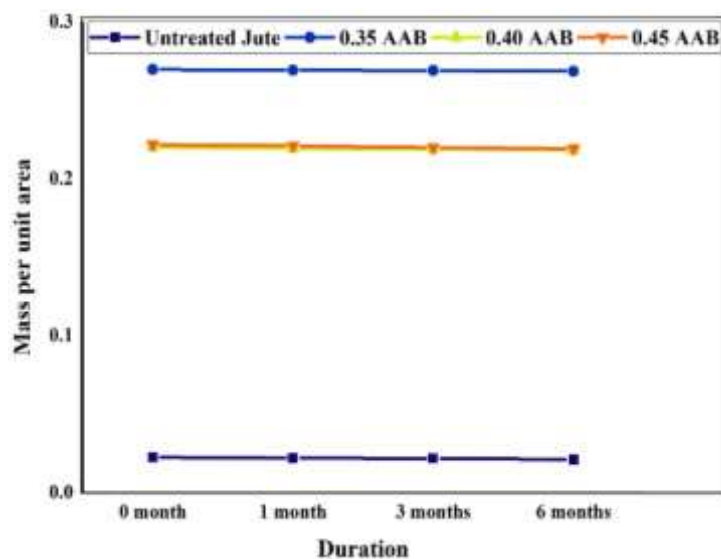


Figure 3.6. Mass per unit area values of Untreated and Treated jute at various times

To determine the mass per unit area of untreated JGT, a total of 10 test specimens with known areas are carefully weighed and collected from various sections of the fabric sample. The calculation of the mean mass per unit area is performed by taking the average of the acquired values. Table 3.6 displays the thickness values of untreated and treated jute at various time durations. The reduction in mass per unit area of untreated and treated JGTs over time is a natural process that occurs as a result of various environmental factors and biological factors. From figure 3.7, it is observed that the reduction values of mass per unit area are 6.66% and 1.13 % for untreated jute 0.35 AAB treated JGTs. The reduction in mass per unit for untreated jute is caused by exposure to moisture and microorganisms in the environment, which breaks down jute fibres and causes the geotextiles to lose mass, whereas AAB coating protects treated JGTs from microorganism attack.

3.4.1.4 Tensile Strength Test (Grab Test)

Grab tensile strength is commonly used for woven fabrics, including JGTs. This is because the test measures the strength of a fabric in both the warp and weft directions simultaneously, providing an overall measurement of strength of the fabric. The grab test is also a quick and simple test that can be performed using relatively small samples of material. The tensile strength of a geotextile strip was evaluated using a Zwick/Roell Z100 testing equipment. The dimensions of a sample were 50mm in width and 200mm in gauge length. The 25 mm grab length was maintained. Narrow strip tensile strength was measured by maintaining a tensile loading at a 100 mm/min deformation rate, as specified by the ISO 13934-1:1999 standards. Ten samples of each geotextile were evaluated for tensile strength in the machine direction (clamps moving direction), and the average of those results was reported. Figure 3.6 shows the image of untreated and treated natural fibre subjected to grab tensile strength test. Table 3.8 displays the tensile strength values of both treated and untreated JGTs. The tensile strength test is a common mechanical test that measures the tensile strength of a material. In the context of JGT, the tensile strength test can provide valuable information on the behaviour of a material under stress and deformation. The tensile strength of 0.35 AAB, 0.40 AAB, and 0.45 AAB treated JGTs is found to be 123.5%, 114.7%, and 107.3% greater than untreated jute. The maximum increase is observed in 0.35 AAB jute, which is attributed to a lower w/s ratio. At a lower w/s ratio, the greater adhesion of AAB paste to jute results in an increase in tensile strength, which can be demonstrated by the specifications of mass per unit area shown in Table 3.7, which indicate that 0.35 AAB, which has a lower w/s ratio than the others, acquires a larger mass per unit area than the other AAB formulations.

Table 3.7. Tensile Strength of Untreated and Treated Jute

Type of Sample	Tensile Strength(kN/m)
Untreated Jute	6.8
0.35 AAB treated jute	15.2
0.40 AAB treated jute	14.6
0.45 AAB treated jute	14.1

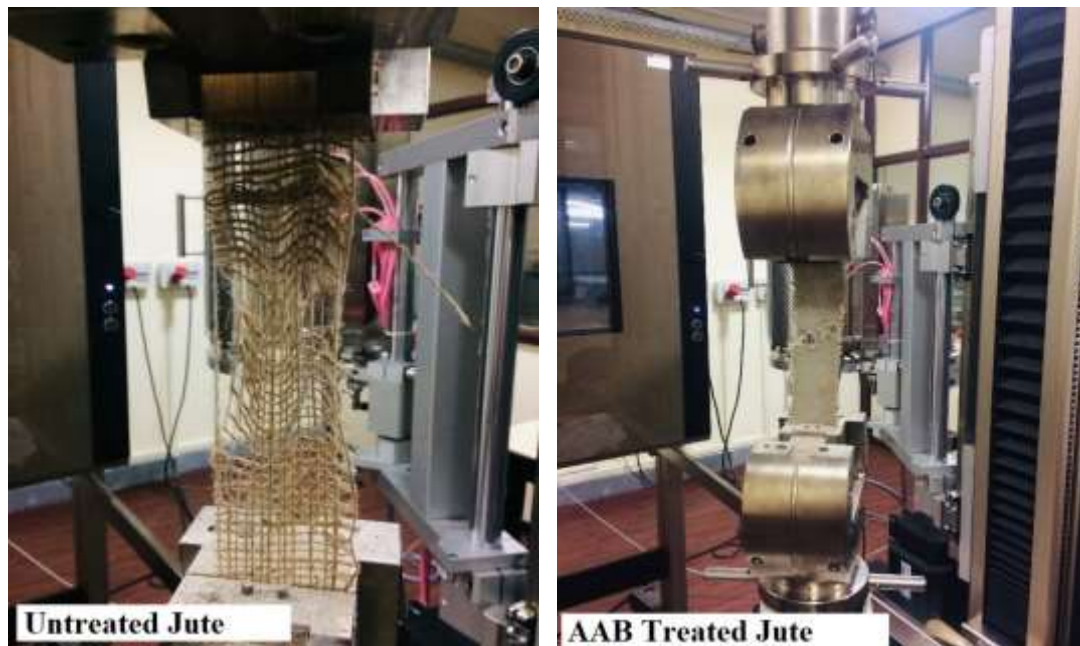


Figure 3.7. Tensile Strength Test of Untreated and AAB Treated JGT

3.4.2 Permeability of jute-reinforced soil

The permeability test is essential for determining the water movement rate through the soil. The purpose of the permeability test for jute-reinforced soil is to measure the influence of jute reinforcement on the hydraulic conductivity of soil. Soil reinforced with untreated and treated jute fibres is subjected to falling head permeability tests following IS 2720 (Part 18):1986. The corresponding schematic diagram for the permeability test is shown in Figure 3.7, and the obtained permeability values are shown in Table 3.9. Since AAB partly blocks the pores of the jute and obstructs the flow of water, it is clear that the permeability reduces for the soil reinforced with treated jute samples.

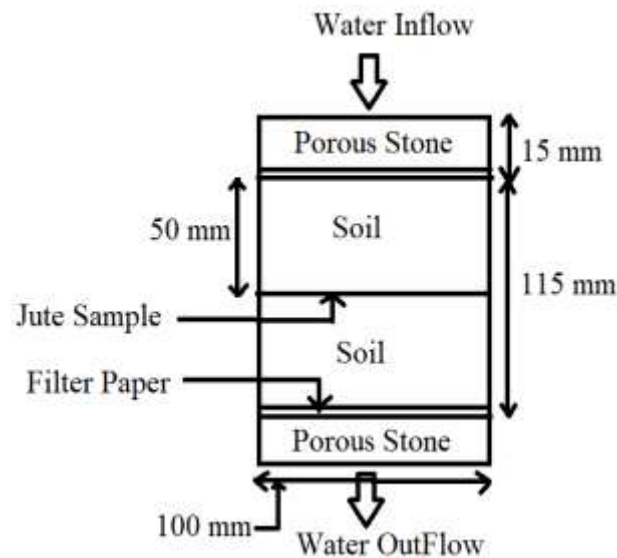


Figure 3.8. Schematic diagram of permeability test of jute-reinforced soil

Table 3.8. Permeability of jute-reinforced soil

Types of reinforcement	k (mm/sec)
No reinforcement	11.3×10^{-2}
Untreated Jute	1.94×10^{-2}
0.35 AAB treated jute	2.32×10^{-3}
0.40 AAB treated jute	3.12×10^{-3}
0.45 AAB treated jute	5.90×10^{-3}

3.4.3 CBR of jute-reinforced soil

Soil reinforced with untreated and treated jute fibres undergoes a series of wet and dry CBR tests following ASTM D-1883. At respective MDD-OMC values, different fibres are compacted at varying depths in a CBR mould with a 15 cm diameter and 17.5 cm height. For the soaking condition, compacted soil samples are submerged in water for 96 hours with a 5 kg surcharge before being tested at 1.25 mm/min with a loading frame coupled to a 50 mm plunger. The obtained CBR values are shown below in Tables 3.10 and 3.11. Figure 3.8 shows the images of jute-reinforced CBR samples at various positions from the top. The CBR values of treated jute samples are more than untreated jute samples. 0.35 AAB jute has a higher CBR value among all because more material is applied to the surface of 0.35 AAB jute. It has a CBR value of 105% more than untreated jute samples in unsoaked conditions at two thirds of total height of the specimen.

Table 3.9. CBR of jute-reinforced soil (Unsoaked)

	1 st layer (2H/3 from top)	2 nd layer (H/2 from top)	3 rd layer (H/3 from top)
No reinforcement	11.67	11.67	11.67
Untreated Jute	13.4	13.0	12.6
0.35 AAB treated jute	24.02	23.0	21
0.40 AAB treated jute	22	21	20
0.45 AAB treated jute	20.43	20.35	20.11

Table 3.10. CBR of jute-reinforced soil (Soaked)

	1 st layer (2H/3 from top)	2 nd layer (H/2 from top)	3 rd layer (H/3 from top)
No reinforcement	4.2	4.2	4.2
Untreated Jute	6.6	5.8	5.04
0.35 AAB treated jute	12.8	12.4	12.25
0.40 AAB treated jute	11.65	11.54	11.23
0.45 AAB treated jute	11.27	10.98	10.86



Figure 3.9. Images of jute-reinforced CBR samples at H/3, H/2, and 2H/3 positions from top

3.4.4 UCS of jute-reinforced soil

According to ASTM D-2166, multiple UCS tests are conducted on red soil with untreated and treated jute reinforcement using a typical three-split cylindrical UCS mould with a diameter of 38 mm and a height of 76 mm at corresponding MDD-OMC values. Soil samples

are dried out in a vacuum chamber for 30 minutes before being tested to ensure they are mature. This experiment used a strain-controlled, fully-automated 20 KN compression machine that applied a constant strain rate of 1.25 mm/min. Further tests are conducted using the identical three specimens if there is more than a 10% disparity between the peak stress values for any combination. The obtained UCS values are shown in Table 3.12. The failure patterns of soil samples reinforced with jute at various heights are shown in Figure 3.9. The UCS value of treated jute is greater than that of untreated jute. Among all, 0.35 AAB jute has the highest UCS value. The failure pattern of an unreinforced sample is 45° degrees to the horizontal, whereas untreated and treated jute reinforcements prevented the failure at the reinforcement location.

Table 3.11. UCS values red soil reinforced with different jute fibres

Type of Reinforcement	q_u (kN/m ²)
No Reinforcement	268.45
Untreated Jute	286.8
0.35 AAB treated jute	323.48
0.40 AAB treated jute	304.70
0.45 AAB treated jute	293.62

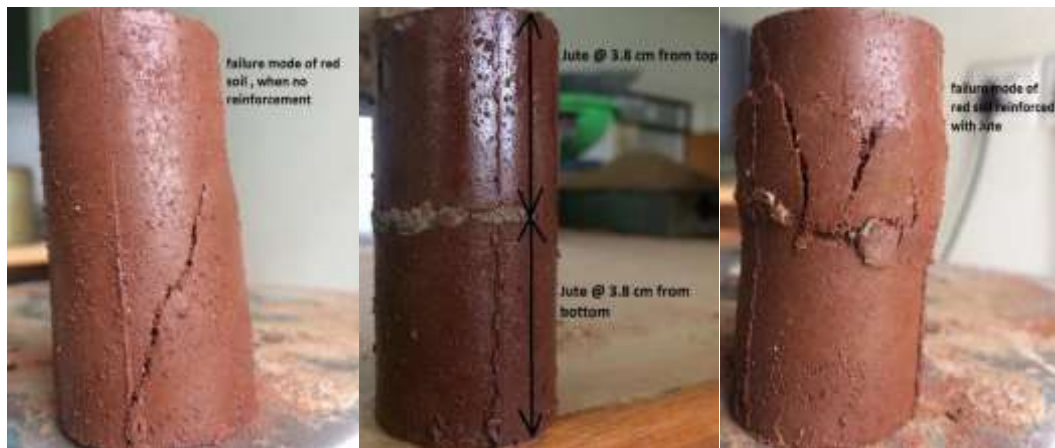


Figure 3.10. Untreated and jute-reinforced UCS samples at 38mm position from the top

3.4.5 Interface Friction Angle between soil and untreated / treated jute

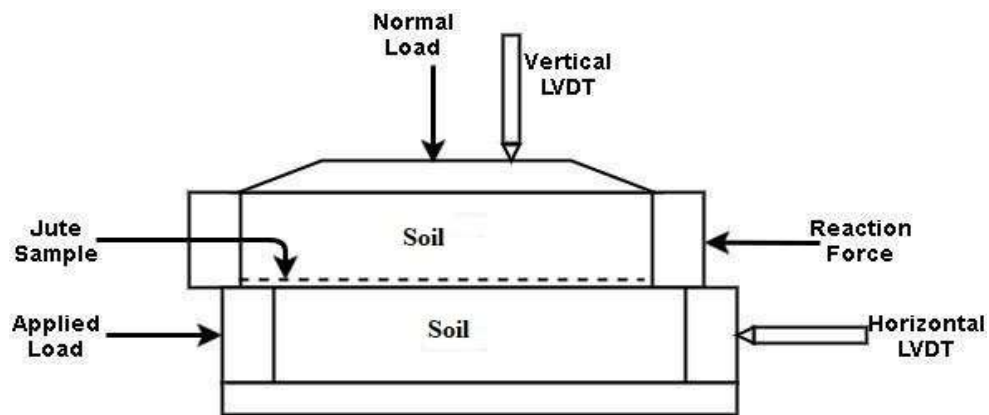


Figure 3.11. Schematic Diagram of Large Shear Box Test

To investigate the interface properties between the soil and the reinforcing material, a Heico automated large-size direct shear apparatus is utilised. The schematic diagram of a typical large shear box is shown in Figure 3.10. The procedure for experimenting is determined following IS 2720-13 (1986). The soil sample is compacted to the required density in the large shear box of 300 mm length, 300 mm width, and 150 mm depth. The top of the lower shear box is fitted with untreated and treated JGTs. Sufficient care is taken to attach the geotextiles to the sides properly so they do not move while applying shear.

To evenly distribute the normal load, a thick rigid loading pad is installed on top of the upper shear box. Using the hydraulic jack arrangement, the normal load is applied on the loading pad through the reaction frame of 100kN capacity. Both horizontal and vertical displacements are measured using LVDTs (Linearly Variable Differential Transformers) of 100mm capacity. The strain rate used in this experiment is 1.2617 mm/min. It is observed that the angle of internal friction between jute and red soil is 8.78% higher than the internal friction of red soil. In contrast, the value decreased between red soil and jute sample by 2%, 7%, and 10% after treating the jute with AAB solution with w/s ratios of 0.35, 0.40, and 0.45, respectively. The possible reason for this is the formation of smoothness on the surface of JGTs due to AAB solution application. The values of the friction angle between red soil and different reinforcements are shown in Figure 3.11.

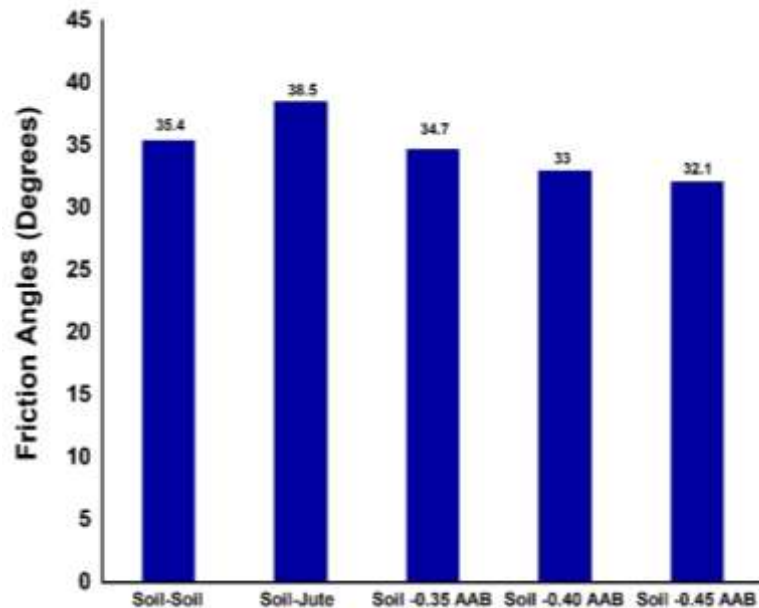


Figure 3.12. Friction angle between red soil and different reinforcements

3.5 Mechanical Properties of Bermuda Grass

3.5.1 Growth Mechanism of Bermuda Grass

The Bermuda grass growth mechanism starts with sowing seeds in a seeding tray for healthy seed germination. The soil is mixed with compost for the healthy germination of plants from seed. The seed containers provide the optimal environment for the healthy germination of seeds, including appropriate drainage and protection from parasitic organisms and diseases. Seed containers make identifying and preventing signs of unhealthy seed growth easier because they are easily recognisable in closed proximity. The seeds started growing after three days of sowing with regular watering intervals. The seed-sowing process is shown in Figure 3.12, and germinated Bermuda grass plants are shown in Figure 3.13. The observed crop period is six months to get a root length of 34 cm and plant length of approximately 100 cm in laboratory conditions. The grown Bermuda grass and its root system are shown in Figure 3.14.



Figure 3.13. Seed sowing process for healthy germination of Bermuda grass



Figure 3.14. Germinated plant from Bermuda grass after 25 days from the sowing date



Figure 3.15. Length of Bermuda Grass Plant and Root System

The grass forms a dense mat by creeping along the ground with its stolons and roots wherever a node touches the ground. Bermuda grass reproduces through seeds, stolons, and rhizomes. The Bermuda grass regrowth mechanism is shown in Figure 3.15.

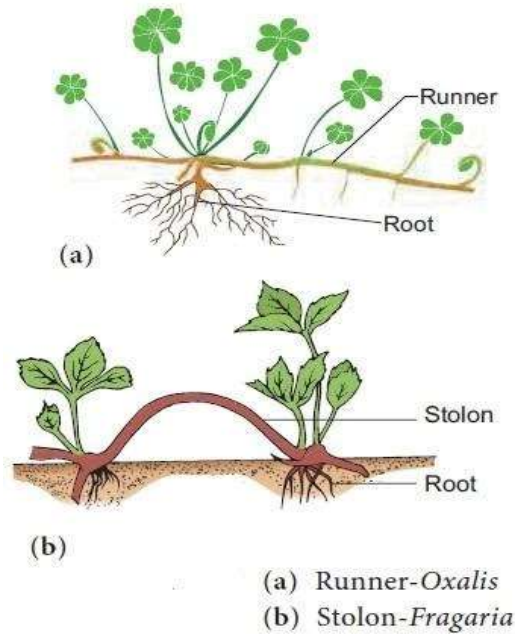


Figure 3.16. Grass regrowing mechanism (Department of School Education, TN, 2020)

3.5.2 Root Matrix of Bermuda Grass

Bermuda grass used in the present study falls under thin, hairy roots. Figure 3.16 shows the Bermuda grass root matrix, which has three distinct root systems: primary, secondary, and tertiary. The root samples are then analysed to study their properties. Vernier Callipers are used to measure the average length and width of the roots. The root system and root matrix of Bermuda grass are shown in Figure 3.17.

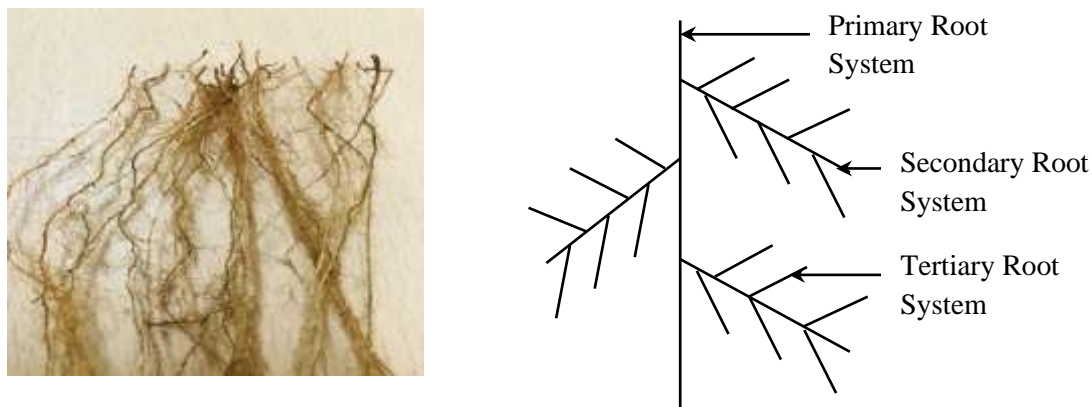


Figure 3.17. Root Matrix for Bermuda Grass

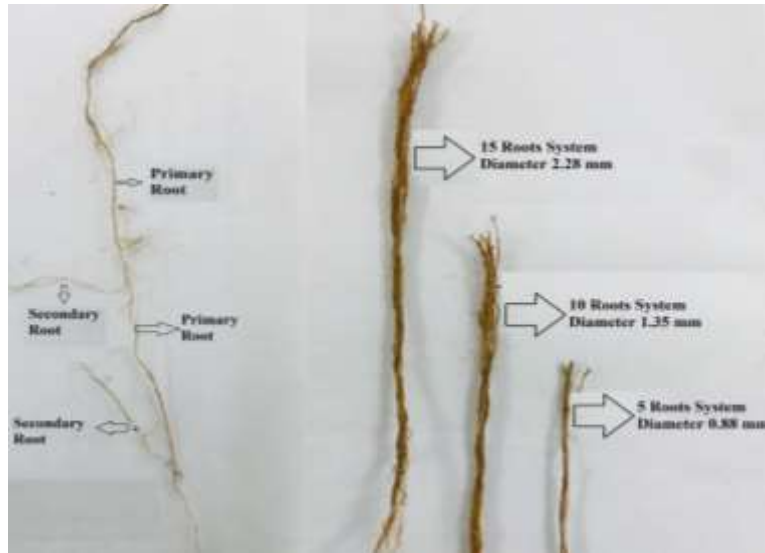


Figure 3.18. Root Matrix and Root System Diameter for Bermuda Grass

3.5.3 Tensile Strength of Roots

A Zwick/Roell Z100 with 100KN capacity testing equipment is used to measure the tensile strength of the root matrix. The tests are carried out on individual root systems consisting of approximately 5, 10, and 15 numbers of roots (Noorasyikin and Zainab, 2016). The tensile strength values of different root matrix systems are shown in Table 3.13. The tensile strength of 15-root 67% and 30% higher than that of the 5-root and 10-root systems, respectively, due to the increased thickness of the overall system. The tensile strength test for Bermuda grassroots is shown in Figure 3.18.

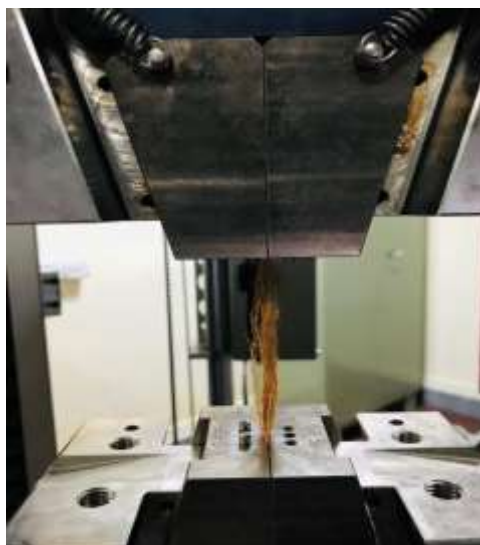


Figure 3.19. Tensile Strength Test of Bermuda Grass

Table 3.12. Tensile Strength of different Root Matrix Systems

Root Matrix System	Root Diameter (mm)	Root Length (mm)	Tensile Strength (MPa)
5 root	0.88	226	27.13
10 root	1.35	215	34.86
15 root	2.28	210	45.30

3.5.4 Shear strength of soil infused with roots

The determination of the shear strength of vegetated soil, where roots have germinated, is found out through the measurement of the apparent cohesion value using a direct shear test. The size of the sample is $60 \times 60 \times 25 \text{ mm}^3$. The initial step involves extracting soil infused with roots using a sampler, as shown in Figure 3.19. Subsequently, the soil is manually transferred into the shear box setup, in which the test is conducted. It is conducted for soil with any root as standard for comparison, and other samples consist of roots in the soil. The obtained shear strength values are shown in Table 3.14.



Figure 3.20. Sample collection from root-penetrated soil

Table 3.13. Shear strength of soil infused with roots

Sample	Shear Strength (kN/m ²)
Bare Soil	9.5
Soil infused with grassroots	29.97

3.6 Soil Erosion Model Set up

In this investigation, a 0.9×0.9×0.3 m³ soil erosion model is built in the laboratory to simulate real-world conditions. Untreated and AAB-treated JGTs reinforce the entire top surface of the slope. The slope is also exposed to a rainfall impact due to an artificial rainfall setup. Soil erosion tests are performed before and after various reinforcements have been installed on the slope to evaluate how effectively they prevent erosion when exposed to rainfall. Similarly, vegetation consisting of Bermuda grass is transplanted onto the surface of a slope to examine soil erosion caused by rainfall.

3.6.1 Artificial Rainfall Simulating Assembly

A robust rainfall-simulating system (Figure. 3.21) is designed and developed to induce low and high-intensity rainfall. To estimate the rainfall intensity, a non-recording type rain gauge is used as the Indian Meteorological Department mostly uses it according to the guidelines of IS 5225 (1992). The non-recording type rain gauge image is shown in Figure. 3.22. The water flow system is set up with 12 pipes at a spacing of 7.5 cm, which is arranged using the grid-iron system methodology. Drippers having 2.97 mm diameter holes are inserted into the pipe with a centre-to-centre spacing of 5 cm. This grid pipe network is built before the main water line is connected, and it is then attached to the wooden rod frame system to keep rainfall height at no less than 1 meter. A water pump motor with a capacity of 0.5 hp is used to supply the water. An L-shaped connector links the motor pump outlet to the inlet of grid pipe. The water flow via the pump and drip system is verified after this setup to avoid operational mistakes. A rotameter (Figure. 3.23) is used to control the water flow rate. The rotameter exhibits predetermined flow rate levels. Through multiple experimental iterations, two distinct flow rates, namely low and high, have been established. These two flow rates are applied on the soil slope to estimate the soil erosion due to the rainfall effect. Rainfall intensities of 10.2 mm/min and 23.4 mm/min are measured at low and high flow rates using a

non-recording rain gauge. According to the Telangana State Development Planning Society (Government of Telangana, 2022) these rainfall intensities are considered to simulate the average rainfall in the Medchal-Malkajgiri District in the Telangana region for the past three years. To maintain consistency, all experiments are conducted in the fixed position of the model slope and with fixed flow rates. The collection of runoff and sediment occurs at regular 5-minute intervals over a span of 12 periods, from its initiation to the completion of the hour duration. To determine sediment generation, collected samples are oven-dried for 48 hours at 105 °C. The average value of sediment is calculated using an average of at least ten samples.

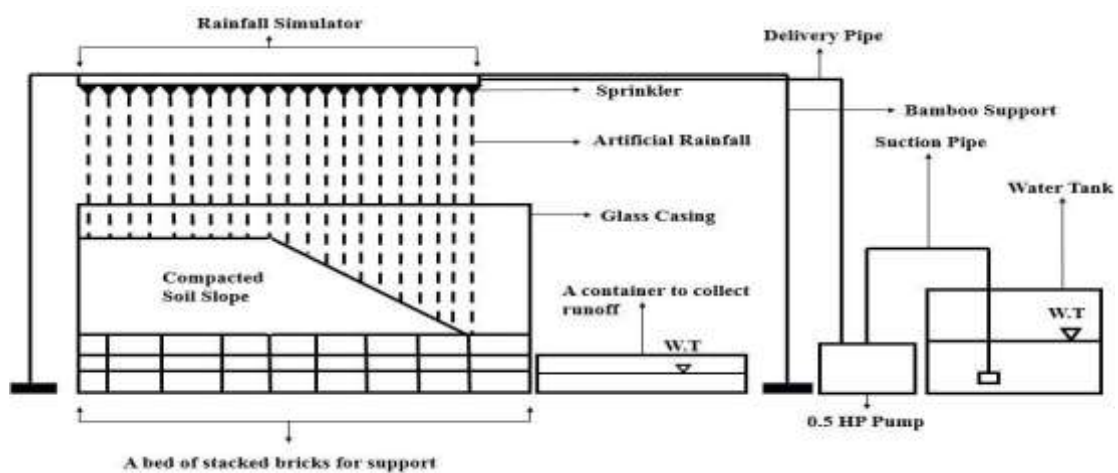


Figure. 3.21. Schematic Diagram of Experimental Setup for Surface Erosion

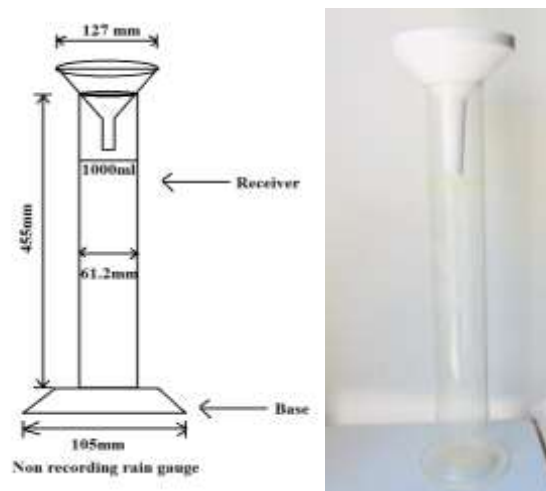


Figure. 3.22. Non-recording type rain gauge



Figure. 3.23. Rotameter

3.7 Summary

The material characterisation of red soil and the chemical and mechanical characterisations of natural JGTs are presented in this chapter. After applying the AAB chemical treatment, natural JGT is examined for its capability as a soil-reinforcing material. Furthermore, the detailed methodology for the determination of microstructural and geotechnical properties of materials is described in this chapter. The root matrix system of Bermuda grass is also discussed, in addition to the fundamental characteristics of Bermuda grass. The laboratory scale slope model and the artificial rainfall set-up are also discussed in the present chapter. This information can establish the theoretical basis for the subsequent research and the context of the study. It is also useful in understanding the properties of the tested materials and how they may influence the results of subsequent analyses and the methodology for determining microstructural and geotechnical properties of materials can help in understanding how the research was conducted and how the results were obtained.

CHAPTER 4

Durability Studies of Untreated and Treated Jute

4.1 General

This chapter deals with the durability studies of untreated jute and AAB-treated JGT (JGT). Natural geotextiles undergo decay and the surface colour gets faded on exposure to sunlight and weathering at the time of construction or during the service period as the chemical bonds present in the fibers start disintegrating. The microorganisms present in soil enhance this process, resulting in significant strength reduction. Previous research related to the durability of jute indicates that there are limited studies in this area, and there is a need for further investigation. Typically, durability assessments of natural geotextiles involve conducting experiments to evaluate their resistance to soil burial, weathering, weight loss, exposure to acid and alkali, and microbial attack. These experiments primarily focus on observing changes in fibre tensile strength. Determination of weight loss and elongation at break are also essential to estimate the extent of durability under different exposure conditions. Characterizations of surface texture, crystallinity, molecular bond, morphology, and thermogravimetry are conducted to demonstrate the effect of different exposure conditions on JGTs. The relevant findings on untreated and AAB-treated jute fibres are analyzed and discussed in detail in this chapter.

4.2 Methodology of Durability Tests

4.2.1 Soil Burial Test

To assess the durability criteria for JGT, a soil burial test is performed following ASTM G 160-12. Untreated and AAB-treated jute specimens are cut into strips of 25 cm length and 5 cm width. For the laboratory test, a large container with dimensions of 1 m × 1 m × 0.25 m is filled with red soil [classified as silty sand (SM) by Unified Soil Classification System (USCS)] consisting of 2.36% gravel, 55.47% sand, and 42.17% fines (silt and clay). Small holes at specific intervals are punctured at the bottom and four sides of the container for sufficient air and water circulation. During the entire test period, the moisture level for the soil is maintained between 20 to 30 % of its dry weight, to ensure consistency moisture level of soil is periodically evaluated and any water lost via evaporation is restored and kept outside under the sun at an average temperature of 27 °C and relative humidity of around

75% (Sumi *et al.*, 2016). The untreated and treated jute specimens are implanted in the soil to a depth of 15 cm below the soil surface, exposing them to the behaviour of microorganisms often present in the soil to replicate field settings. In the same manner, a soil burial test is carried out in the field to find out the durability of the JGT in-situ conditions. Untreated and AAB-treated JGT specimens of 25 cm length and 5 cm width are buried at a depth of 30 cm in the ground. Figure 4.1 shows the images of buried JGT samples in the laboratory and field conditions. At fixed intervals of 30, 60, and 90 days, the samples are taken out and cleaned with the help of a brush to remove the adhered soil on the surface before performing the post-burial characterization tests. All the samples are air-dried till constant weight is reached. Loss of strength due to biodegradability after soil burial may be evaluated by performing a tensile strength test and using the average of three findings. Tests were conducted on untreated and AAB-treated JGT by burying them in soil for 30, 60, 90, and 180 days, as shown in Figure 4.2.



Figure 4.1. Images of JGTs in (a) Lab burial condition; (b) Field burial condition

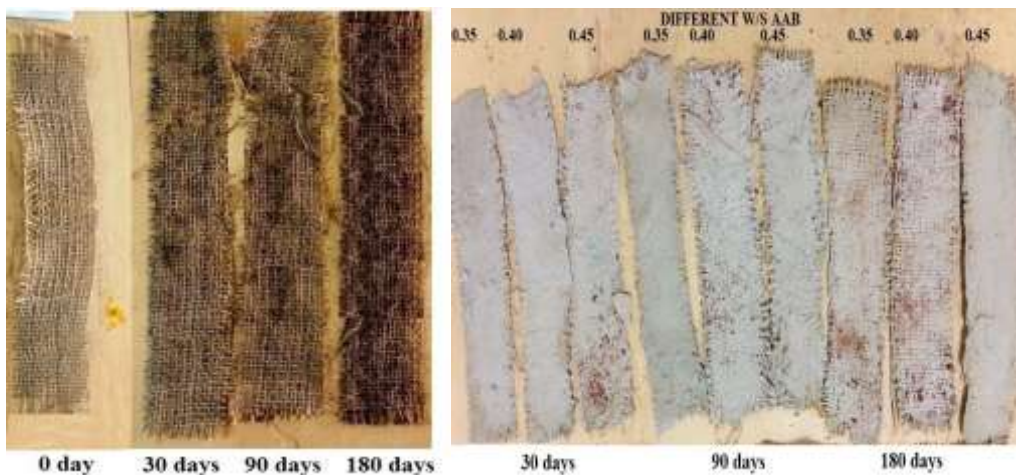


Figure 4.2. Images of (a) Untreated and (b) AAB-treated JGTs subjected to soil burial under lab conditions at 30, 90, and 180 days duration

4.2.2 Resistance to Acid and Alkali Test



Figure 4.3. Images of (a) AAB-treated jute immersed in acidic and alkaline solution, (b) Raw Jute, and (c) AAB-treated jute after 30 days of HCl and NaOH treatment

In almost all geotechnical engineering applications, geotextiles can come in contact with dilute solutions of acids, alkalis, or dissolved oxygen. Hence, the resistance of jute against acid and alkaline attacks is also an important durability parameter. The tests for exposure to acid and alkali are conducted as per the guidelines of BS EN 14030. In this experiment, the acidic solution is prepared by using 8 ml of 0.01 N HCl having pH 2. The 1 N alkaline solutions having pH 13.3 are prepared with 40 gm of NaOH (99% pure) pellets. These conditions are selected to represent strongly acidic and alkaline environments. The untreated and treated jute samples are immersed in acid and alkaline solutions for an interval of 30, 60, 90, and 180 days at room temperature. The quantity of chemical solutions is chosen to be greater than 30 times the weight of the samples, and care is taken to ensure that the liquids cover the specimens completely. At the end of the respective exposure periods, the samples are rinsed thoroughly with water, immersed in water for 1 hour, and then dried to remove the

excess deposition of acid and alkali on the sample surface. Figure 4.3a presents the treated jute just after immersion, while Figures 4.3(b-c) and 4.4(a-b) present the untreated and AAB-treated jute samples immersed in the acidic and alkaline solution after 30 days and 90 days.



Figure 4.4. Images of (a) Raw Jute after 90 days of HCl and NaOH treatment and (b) AAB-treated jute after 90 days of NaOH

4.2.3 Resistance to Hydrolysis

Hydrolysis degradation have an impact on the performance of fiber in two ways, internally and externally. Both internal and external hydrolysis reduce the molecular weight of polyethylene by damaging the polymer chain along the cross section. In the present study, an external hydrolysis degradation test is carried out according to BS EN 12447:2001. As shown in Figure 4.5a, both untreated and treated jute samples are submerged in 95°C deionized water for 30, 60, 90, and 180 days throughout the test. The pH level is regularly monitored on a weekly basis, and if it surpasses a value of 8, as measured under ambient conditions, the water is subsequently replaced. Figures 4.5b and 4.5c show the untreated and 0.40 AAB jute samples after 90 days of hydrolysis.



Figure 4.5. (a) Hydrolysis Test; (b) Raw Jute and (c) AAB treated jute after 90 days of Hydrolysis Test

4.2.4 Compost Burial method

The compost burial test is a type of soil burial used to assess the impact of microorganisms such as endospore-forming *Bacillus*, *Enterococcus*, and protozoa resulting from cow dung (Siakeng *et al.*, 2020). The application of cow dung manure enriches the mineral content of the soil and boosts the plant's ability to withstand diseases and pests (Tomar *et al.*, 2020). Compost is often used to augment plant development, while jute geotextiles are employed with plants to provide slope stability. Hence, a compost burial test is conducted to assess the impact of these bacteria on jute. The untreated and treated jute specimens are placed in a soil bed that was previously produced using a 2:1:1:1 ratio of garden soil, cow dung, dried leaves, and sand (Figure 4.6a). According to ASTM G160-12, the soil shall be composed of equal parts of fertile topsoil, well-rotted and shredded horse manure, and coarse sand. Due to the unavailability of horse manure, cow dung, and dried leaves are used. It is ensured that the mixture is made homogeneous and that moisture content is maintained at around 25% throughout the test. Although ASTM G160-12 recommends a minimum of 60 days of exposure for the compost burial test (Sumi *et al.*, 2016), this test was conducted for 30 days to compare results to those of other kinds of durability tests, such as acid and alkali tests. At the end of 30, 60, 90, and 180 days, the samples are removed, cleaned thoroughly with a brush, and air-dried to achieve a constant weight. Figures 4.6(b-d) show the images of AAB-treated JGT subjected to compost burial test at different time intervals.



Figure 4.6. (a) Fresh Compost, (b) AAB-treated jute at 0 days (c) Compost after 180 days
(d) AAB Treated Jute after 180 days

4.3 Determination of Mechanical Properties

4.3.1 Weight Loss Test

Calculation of loss in weight at different stages of durability tests is considered a significant aspect of all durability analyses and it is conducted according to IS 15868 (Part 1): 2008. For the calculation of loss in weight, care is taken to ensure the removal of all soil particles entrapped within fibres without causing physical damage. All samples are gently washed with a brush and air-dried until the weights were consistent. The weights of each sample are measured before and after degradation, and weight loss is calculated by comparing the loss in weight before and after burial using the following equation.

$$\text{Weight Loss (\%)} = \frac{W_i - W_f}{W_i} \times 100 \quad (4.1)$$

where W_i and W_f are the initial (before soil burial) and final (after soil burial) weight of the jute samples, respectively.

4.3.2 Tensile Strength

The tensile strength of treated and untreated jute samples after 30, 60, 90, and 180 days of soil burial test are determined by Zwick/Roell Z100 tensile strength testing machine. The width, gauge, and grip length of the samples are kept at 50 mm, 200 mm, and 25 mm, respectively. Each sample is clamped in the top and bottom jaw in such a way that the pressure of clamping is optimum to avoid slippage at the back of the jaws. The tensile loading is maintained at a constant strain rate of 100 mm/min according to ISO 13934-1:1999 standards. The estimated tensile strengths for each sample are taken as an average of 10 specimens of each untreated and treated jute sample. The procedure is repeated 10 times

for all sets of untreated and treated samples, in the warp direction, and the average result of the peak load is reported for each sample.

4.3.3 Elongation at Break

Elongation at break, also called fracture strain, is defined as the percentage increase in length relative to initial length after a jute sample has been broken. The capability of a fibre to resist changes of shape without crack formation can be assessed by this method. The elongation at break is determined from the tensile testing results following EN ISO 527.

4.4 Determination of Chemical Characteristics

4.4.1 Surface Texture

In order to analyse the surface texture and physical characteristics of both untreated and treated jute sheets, a stereomicroscopy technique is employed utilising an Olympus SXZ7 configuration. Different locations and magnifications are used to acquire the images, with the smallest dimension being 20 μ m. The areas of interest in each image are selected with proper care to include the prominent features of all the samples.

4.4.2 Crystallinity

XRD is performed for qualitative identification of chemical structure along with determining the degree of crystalline nature of untreated and treated geotextile. To determine which minerals are present in raw and treated JGT, an XRD analysis is carried out using a RIGAKU Ultime IV diffractometer. At 40 mA and 40 kV, CuK rays are used to analyse the powdered materials. With a 0.02° 2 θ step and a 2-second integration time, considering operating 2θ range is from 0° to 100° .

4.4.3 Molecular Bonds

To identify the changes in the chemical bonds of untreated and treated jute fibre, FTIR is carried out using JASCO FTIR 4200 setup. The transmittance spectral range having wavenumbers in the mid-Infrared range of 4000 to 400 cm^{-1} is maintained for all the samples. Jute samples are shredded into powdered form for this test. The excess moisture content in the powdered samples is removed by oven-drying at 105 $^\circ\text{C}$ for 24 h. KBr powder is mixed with the dried powdered samples for the preparation of pellets.

4.4.4 Morphology

A heated field emission scanning electron microscope (FE-SEM JSM-7600F) from FEI Apreo is used for SEM examination to distinguish between untreated and treated jute sheets by means of surface morphology and elemental content. In general, if the raw materials are collected from an unknown source, a thorough analysis is recommended to identify its components. For a complete analysis, an excitation voltage of 20 kV is commonly used. However, electron clouds tend to develop due to such high voltage, thereby blurring the obtained image. Cellulose and hemicellulose are the prominent components of raw jute. Since AAB-treated jute contains fly ash, the existence of elements with atomic numbers greater than iron is quite unlikely. Three distinct locations are selected at random for each sample. At each designated location, three distinct regions are selected randomly. Subsequently, five distinct points are examined at varying magnification levels within each of these regions. Before analysis, the geotextile fibres undergo a drying process at a temperature of 105 °C for 24 hours to eliminate any internal moisture present. To provide electrical conductivity upon the jute fibres, a layer of platinum with a thickness of 15 nm was applied in an argon gas environment.

4.4.5 Thermogravimetric Analysis

Thermal stability of untreated and treated jute is measured using TGA using a SHIMADZU/DTG-60 setup. The 4 to 10 mg geotextile samples are stored in a nitrogen-rich atmosphere on a platinum pan. Following the decomposition range of jute the samples are heated progressively from 30°C to 950°C (Yang *et al.*, 2007). For even heating, the temperature rise rate is controlled to 10°C/min.

4.5 Results and Discussions on Durability Tests

4.5.1 Soil Burial Test

The untreated and treated JGTs exposed to soil burial tests are explained in weight loss, tensile strength, and elongation at break perspectives.

4.5.1.1 Weight Loss for Soil Burial

Figure 4.7(a) shows the percentage of weight loss of untreated and treated jute at different exposure times of 30, 60, 90, and 180 days for soil burial durability studies. The mass per unit area of untreated jute is found to be 225 gm/m². Treatment of jute by 0.35, 0.40, and 0.45

AAB increases the mass per unit area to 2690 gm/m², 2200 gm/m² and 2220 gm/m² respectively. Figure 4.5(a) shows that treated jute exhibits less than 0.3% of weight loss, the minimum being that of 0.35 AAB treated jute, while this weight loss increases to 2.2% for untreated jute on exposure to natural soil after 30 days. Considering the soil burial test after 90 days weight loss of untreated jute, 0.35AAB, 0.40AAB, and 0.45AAB treated jute sheets are 0.4%, 0.7%, 36.30%, and 1.12% respectively. After 180 days of soil burial, the weight loss of untreated jute, 0.35AAB, 0.40AAB, and 0.45AAB treated jute sheets are 11.2%, 0.9%, 1.12%, and 1.67%.

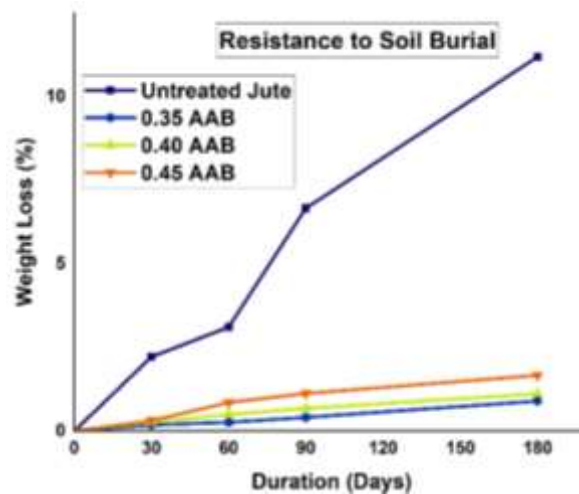


Figure 4.7(a). Weight loss of untreated and treated jute with time in soil burial test

4.5.1.2 Tensile Strength for Soil Burial

The tensile strength of jute specimens of size 25 cm x 5 cm is measured at 30,60, 90, and 180 days duration after lab soil burial condition. Figure 4.7(b) shows the change in tensile strength of different jute sheets after 30,60, 90, and 180 days. From the tensile strength test, it is observed that after 90 days soil burial period, the reduction in tensile strength of untreated jute, 0.35AAB, 0.40AAB, and 0.45AAB treated jute sheets are 50.72%, 24.57%, 27.57%, and 29.57% respectively. Considering the 180 days soil burial period, the reduction in tensile strength of untreated jute, 0.35AAB, 0.40AAB, and 0.45AAB treated jute sheets are 85%, 32.23%, 35.23%, and 36.83% respectively. Table 3.4 states that the quantity of AAB paste decreases from 0.35 to 0.45 w/s, specifically from 3.44 kg/m² to 2.75 kg/m². The main factor contributing to the weight of AAB paste is the fly ash used in its preparation. For the 0.35 w/s ratio, the fly ash weight is higher at 2.18 kg/m², while for the 0.45 w/s ratio, it is lower at 1.62 kg/m². The high porosity of the 0.45 AAB treated jute is the reason for the decrease in tensile strength observed in the 0.45 AAB treated jute compared to the 0.35 AAB treated jute, as

well as the decrease in mass per unit area from 0.35 to 0.45 w/s. Higher water content leads to lower strength due to the formation of greater porosity.

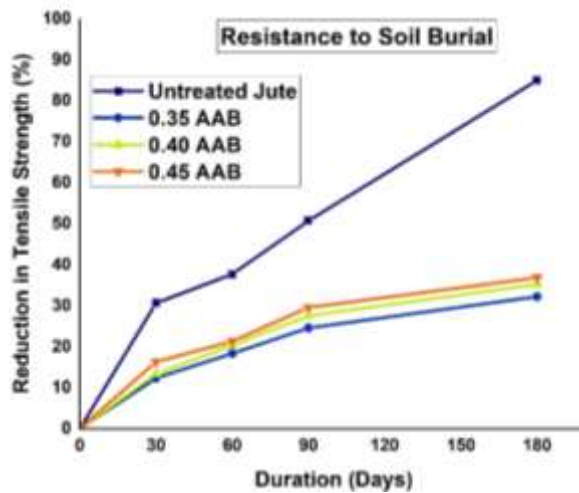


Figure 4.7(b). Reduction in Tensile Strength of untreated and treated jute with time in soil burial test

4.5.1.3 Elongation at Break for Soil Burial

Figure 4.7(c) displays the percentage reduction in elongation at breaking of untreated and AAB-treated JGT subjected to different durability tests after periods of 30, 60, 90, and 180 days. From the elongation at break result, it is observed that after 90 days soil burial period, reduction in elongation at break of untreated jute, 0.35AAB, 0.40AAB, and 0.45AAB treated jute sheets are 61.85%, 22.25%, 26.47%, and 31.75% respectively. After 180 days soil burial period, reduction in elongation at break of untreated jute, 0.35AAB, 0.40AAB, and 0.45AAB treated jute sheets are 85%, 32.1%, 33.45%, and 35.6% respectively.

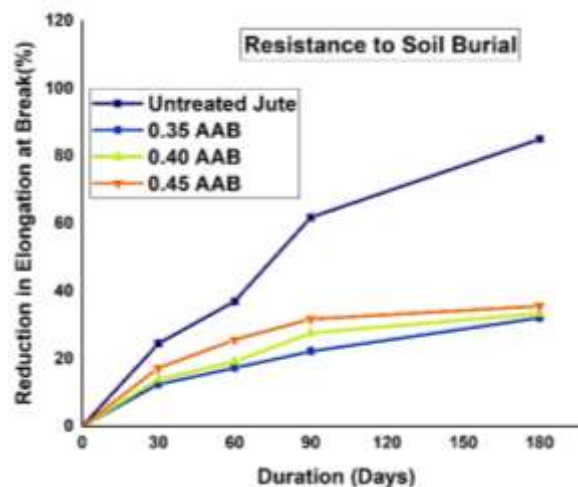


Figure 4.7 (c). Reduction in Elongation at Breaking of untreated and treated jute with time in soil burial test

4.5.2 Resistance to Acid and Alkali Test

The untreated and treated JGTs exposed to acid and alkali tests are explained in weight loss, tensile strength, and elongation at break perspectives.

4.5.2.1 Weight Loss for Acid and Alkali Test

Figures 4.8(a-b) show the percentage of weight loss of untreated and treated jute at different exposure times of 30, 60, 90, and 180 days for acid and alkali durability studies. The maximum weight loss is observed when the fibres are exposed to the acid test. After being exposed to acid for a period of 90 and 180 days, the weight loss is around 77.7% and 91.38% for the untreated fibres, while the same reduces to 33.25% and 42.67% for 0.35 AAB treated fibres. Considering the alkaline test for a period of 90 and 180 days, the weight loss is around 35.22% and 68.97% for the untreated fibres, while the same reduces to 24.09% and 31.07% for 0.35 AAB treated fibres.

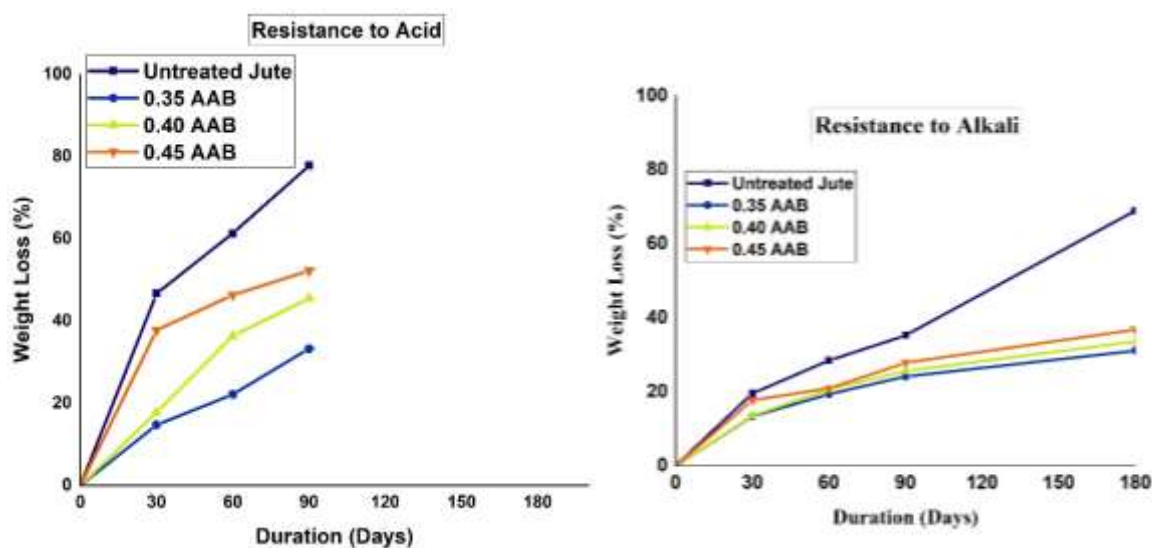


Figure 4.8(a-b). Weight loss of untreated and treated jute with time in acid test (left) and alkali test (right)

4.5.2.2 Tensile Strength for Acid and Alkali Test

The tensile strength of jute specimens of size 25 cm x 5 cm is measured at 30, 60, 90, and 180 days duration after acid and alkali tests. Figures 4.8(c-d) show the change in tensile strength of different jute sheets after 30, 60, 90, and 180 days exposed to acid and alkali tests. For the acid exposure test, after 90 days, the reduction in tensile strength of untreated jute, 0.35AAB, 0.40AAB, and 0.45AAB treated jute sheets are 97%, 82%, 85.37%, and 87.08%

respectively. For the alkaline test, after 90 days, the reduction in tensile strength of untreated jute, 0.35AAB, 0.40AAB, and 0.45AAB treated jute sheets are 71.30%, 36.57%, 38.57%, and 39.89% respectively. For the alkaline test, after 180 days, the reduction in tensile strength of untreated jute, 0.35AAB, 0.40AAB, and 0.45AAB treated jute sheets are 80.78%, 43.23%, 45.23%, and 46.23 respectively. HCL degrades the microfibrils in natural fiber during chemical treatment, resulting in a reduction in lignin and hemicellulose content. Because HCl was an acidic medium, the chemical reaction was more severe, resulting in a substantial reduction in cellulose, hemicellulose, and lignin (Vijay *et al.*, 2021). Tensile strength decreases when cellulose chains decrease. Acidic environments may destroy hydrogen bonds and other intermolecular interactions that strengthen cellulose fibers. Tensile strength might decrease due to cellulose bond breakdown. Strong NaOH alkaline solutions hydrolyze cellulose, the primary component of jute fibers, swelling them. Swelling increases cellulose chain intermolecular gaps, making fibers weaker and more susceptible to mechanical stress. Prolonged exposure of jute to HCl acid and NaOH may have caused additional tensile strength loss in 30 days, resulting in a steep slope. Jute geotextiles without AAB coating lose tensile strength more than those with it.

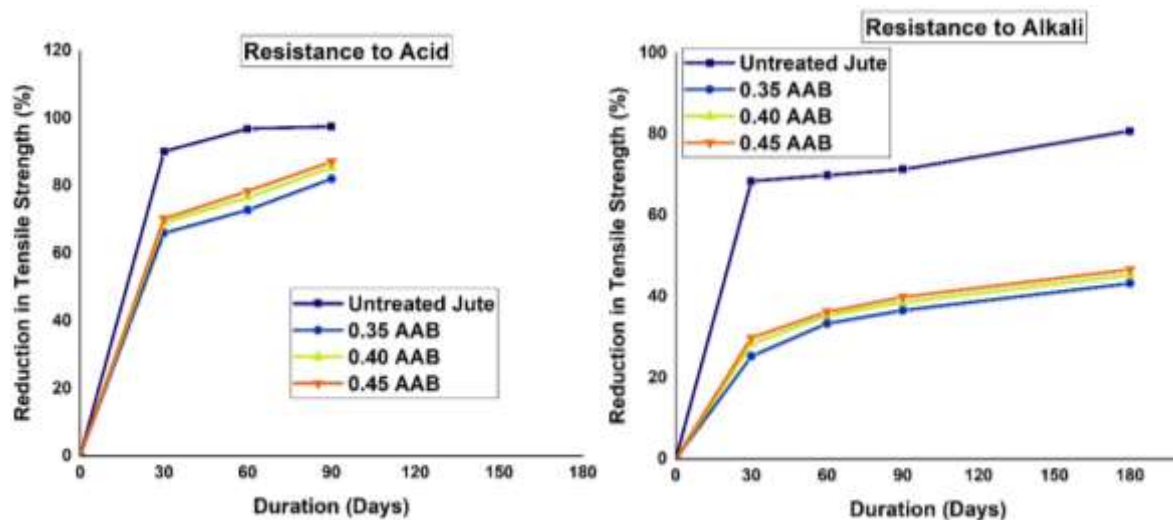


Figure 4.8(c-d). Reduction in Tensile Strength of untreated and treated jute with time in acid test (left) and alkali test (right)

4.5.2.3 Elongation at Break for Acid and Alkali Tests

Figures 4.8(e-f) display the percentage reduction in elongation at breaking of untreated and AAB-treated JGT subjected to acid and alkali durability tests after periods of 30, 60, 90, and 180 days. For the acid exposure test after 90 days, reduction in elongation at break of untreated jute, 0.35AAB, 0.40AAB, and 0.45AAB treated jute sheets are 92%, 80.5%,

82.9%, and 84.62% respectively. For the alkaline test, after 90 days, reduction in elongation at break of untreated jute, 0.35AAB, 0.40AAB, and 0.45AAB treated jute sheets are 74.56%, 40.2%, 42.24%, and 43.24% respectively. For the alkaline test, after 180 days, reduction in elongation at break of untreated jute, 0.35AAB, 0.40AAB, and 0.45AAB treated jute sheets are 89.72%, 42.75%, 43.15%, and 44.75%.

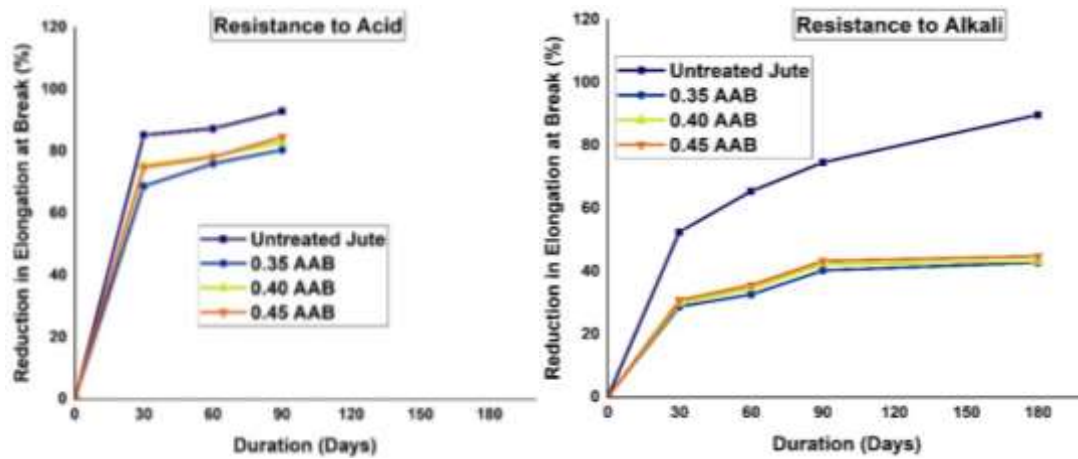


Figure 4.8(e-f). Reduction in Elongation at Breaking of untreated and treated jute with time in acid test (left) and alkali test (right)

4.5.3 Resistance to Hydrolysis

The untreated and treated JGTs exposed to hydrolysis tests are explained in weight loss, tensile strength, and elongation at break perspectives.

4.5.3.1 Weight Loss for Hydrolysis Test

Figure 4.9(a) shows the percentage of weight loss of untreated and treated jute at different exposure times of 30, 60, 90, and 180 days towards resistance to hydrolysis. Considering the hydrolysis test for a period of 90 and 180 days, the weight loss is around 39% and 61% for the untreated fibres, while the same reduces to 21.98% and 31.67% for 0.35 AAB treated fibres

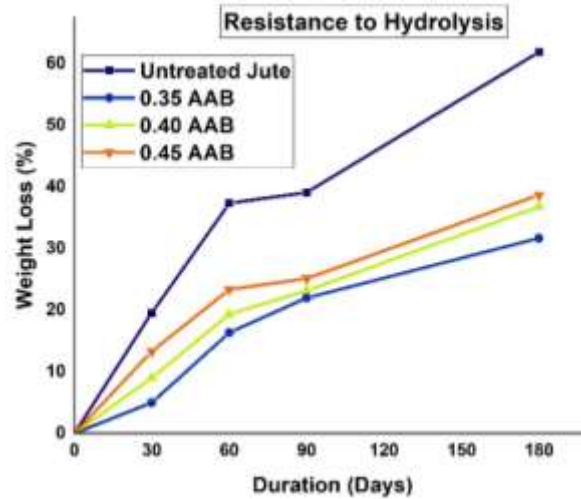


Figure 4.9(a). Weight loss of untreated and treated jute with time in hydrolysis test

4.5.3.2 Tensile Strength for Hydrolysis Test

The tensile strength of jute specimens of size 25 cm x 5 cm is measured at 30, 60, 90, and 180 days duration after the hydrolysis test. Figure 4.5(b) shows the change in tensile strength of different jute sheets after 30, 60, 90, and 180 days. Considering the hydrolysis test after 90 days reduction in tensile strength of untreated jute, 0.35AAB, 0.40AAB, and 0.45AAB treated jute sheets are 58.04%, 32.57%, 34.57%, and 35.57% respectively. For the hydrolysis test, after 180 days, the reduction in tensile strength of untreated jute, 0.35AAB, 0.40AAB, and 0.45AAB treated jute sheets are 89%, 37.23%, 39.23%, and 41.23% respectively.

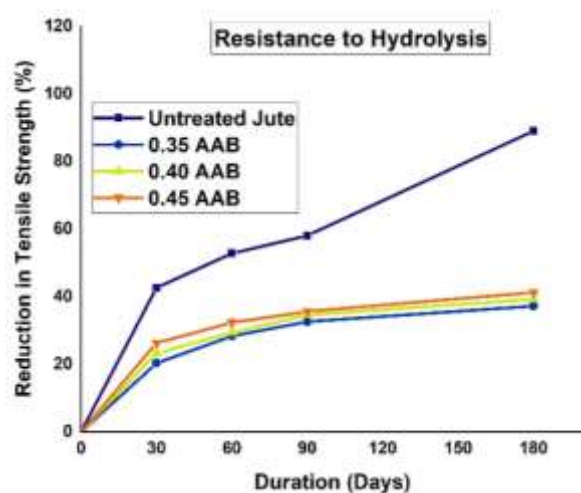


Figure 4.9(b). Reduction in Tensile Strength of untreated and treated jute with time in hydrolysis test

4.5.3.3 Elongation at Break for Hydrolysis Test

Figure 4.9(c) displays the percentage reduction in elongation at breaking of untreated and AAB-treated JGT subjected to hydrolysis test after periods of 30, 60, 90, and 180 days. Considering the hydrolysis test after 90 days reduction in elongation of untreated jute, 0.35AAB, 0.40AAB, and 0.45AAB treated jute sheets are 68.02%, 35.93%, 36.30%, and 38.79% respectively. Considering the hydrolysis test after 180 days reduction in elongation of untreated jute, 0.35AAB, 0.40AAB, and 0.45AAB treated jute sheets are 88%, 41.45%, 42.76%, and 43.87%. Jute fibers are hygroscopic. Prolonged exposure to water may result in elevated moisture levels inside the fibers, hence impacting the mechanical characteristics of natural fibers. The primary component of jute fibers is cellulose. Water absorption causes the cellulose microfibrils within the fibers to swell. This swelling may lead to an expansion of the fiber structure, limiting the ability of the fibers to elongate during stress. With an increase in time, untreated jute experienced a greater decrease in elongation at breaking compared to AAB treated jute. This may account for the similar trend observed in the graphs of untreated and AAB-treated jute geotextiles for the 60 days, followed by a trend change for the subsequent 120 days.

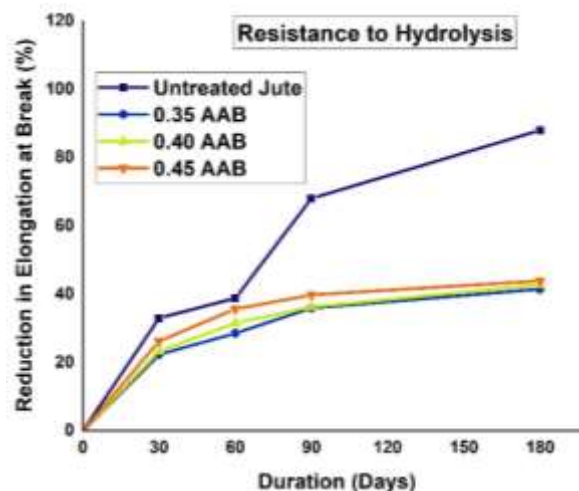


Figure 4.9 (c). Reduction in Elongation at Breaking of untreated and treated jute with time in Hydrolysis test

4.5.4 Compost Burial Test

The durability of untreated and treated JGTs exposed to compost burial tests is explained in weight loss, tensile strength, and elongation at break perspectives.

4.5.4.1 Weight Loss for Compost Burial Test

Figure 4.10(a) shows the percentage of weight loss of untreated and treated jute at different exposure times of 30, 60, 90, and 180 days towards resistance to hydrolysis durability study. Considering the soil burial test after 90 days weight loss of untreated jute, 0.35AAB, 0.40AAB, and 0.45AAB treated jute sheets are 20%, 14%, 18%, and 18.35% respectively. After 180 days of soil burial, the weight loss of untreated jute, 0.35AAB, 0.40AAB, and 0.45AAB treated jute sheets are 35%, 22%, 24.78%, and 25.12%.

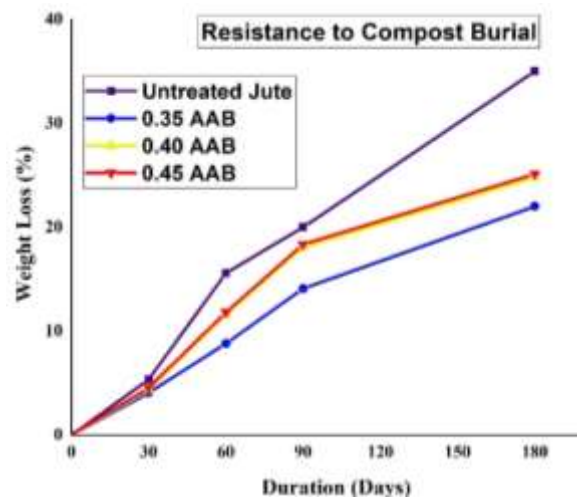


Figure 4.10(a). Weight loss of untreated and treated jute with time in hydrolysis test

4.5.4.2 Tensile Strength for Compost Burial Test

The tensile strength of jute specimens of size 25 cm x 5 cm is measured at 30, 60, 90, and 180 days duration after the compost burial test. Figure 4.10(b) shows the change in tensile strength of different jute sheets after 30, 60, 90, and 180 days. For the compost burial test, the reduction in tensile strength of untreated jute, 0.35AAB, 0.40AAB, and 0.45AAB treated jute sheets are 56.23%, 27.57%, 29.57%, and 31.57% respectively after 90 days. For the compost burial test, after 180 days, the reduction in tensile strength of untreated jute, 0.35AAB, 0.40AAB, and 0.45AAB treated jute sheets are 88%, 35.13%, 37.43%, and 38.53% respectively.

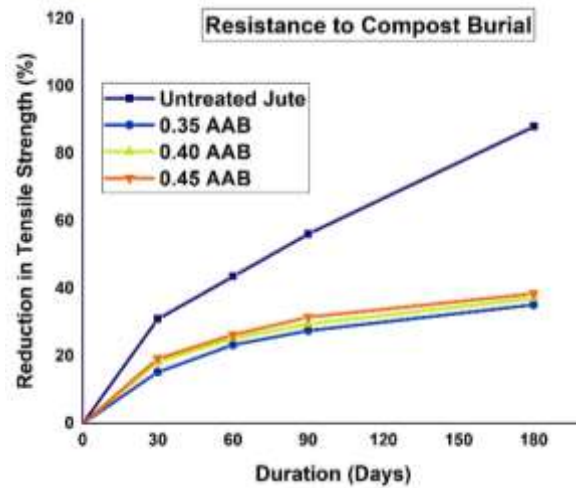


Figure 4.10(b). Reduction in Tensile Strength of untreated and treated jute with time in compost burial test

4.5.4.3 Elongation at Break for Compost Burial Test

Figure 4.10(c) displays the percentage reduction in elongation at the break failure of untreated and AAB-treated JGT subjected to compost test after periods of 30, 60, 90, and 180 days. For the compost burial test after 90 days, reduction in elongation at break of untreated jute, 0.35AAB, 0.40AAB, and 0.45AAB treated jute sheets are 55.67%, 28.67%, 32.27%, and 34.31% respectively. For the compost burial test after 180 days, reduction in elongation at the break of untreated jute, 0.35AAB, 0.40AAB, and 0.45AAB treated jute sheets are 87%, 33.78%, 35.98%, and 36.78% respectively.

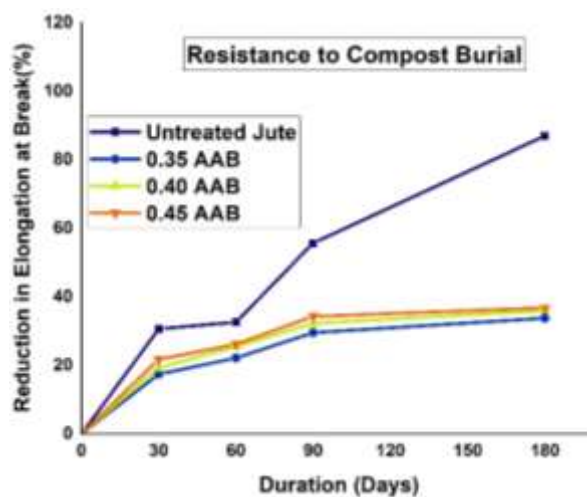


Figure 4.10 (c). Reduction in Elongation at Break of untreated and treated jute with time in Compost burial test

4.5.5 Reasons for Strength Reduction in JGT

In the case of soil burial and compost burial tests, the weight loss of untreated jute fibres is discussed from biological degradation perspective. The rate of decomposition of cellulosic fibres is dependent on the presence of microorganisms. Bacteria and fungi are the two primary microorganism groups responsible for the enzymatic breakdown of cellulose. In the presence of bacteria, cellulosic fibers degrade from the outside to the inside. The moisture content in soil and compost burial experiments creates favourable conditions for microorganisms to degrade untreated fibre surfaces, resulting in weight loss (Arshad *et al.*, 2011; Bordoloi *et al.*, 2017). Moisture is absorbed by natural fibre because the cellulose, hemicellulose, and lignin components all include an OH- group in their amorphous regions, which is the main reason for the degradation of jute in the hydrolysis of water experiment, and also it enhances the bacterial activity in case of compost and soil burial tests (Jafrin *et al.*, 2014). For AAB-treated fibers, the direct interaction between cellulose and microorganism is restricted by applying a coating of AAB paste which leads to a delayed biodegradation process (Gupta *et al.*, 2018). Cellulose in lignocellulosic fibres provides them strength. Glucose units are linked together in a linear polymer by β -1, 4 glycosidic bonds making this a linear polymer. Cellulose consists of long polymer chains of glucose units covalently bonded together by hydrogen bonds. Microfibrils are formed when cellulose chains bind together inside a hemicellulose matrix. A microfibril is composed of several microfibrils organised in a helical pattern. Such a collection of microfibrils is responsible for the formation of the plant fibril matrix (Bordoloi 2017). Considering the acidic effect on JGT the degradation of cellulosic fibres occurs when they are exposed to acid, which breaks the glucosidic bonds in the cellulose and reduces the degree of polymerisation, which is important in increasing the mechanical properties of cellulosic fibres (Palme *et al.*, 2016). The reduction in weight loss in AAB-treated fibres might be due to the improved interfacial bonding owing to the reduced hydrophilic tendency of alkali-treated fibres.

The primary factor contributing to the reduction in the tensile strength of the untreated fibres in soil burial and compost burial is damage to the cellulose microfibrils structure from microorganisms and breaking of cellulose bonds in case of acidic exposure, as the tensile strength of natural fibres is mostly due to cellulose (Arunavathi *et al.*, 2017). The reduction tensile strength of AAB-treated fibres is not much affected because of the strength-enhancing nature of NaOH present in AAB. When jute fibre reacted with sodium hydroxide (NaOH) present in AAB, the hydroxyl group on the alkoxide is ionised, affecting the cellulose fibril

directly (Valadez-Gonzalez *et al.*, 1999; Jähn *et al.*, 2002). NaOH, which is included in AAB treatment, increases the surface roughness of cellulosic fibres, increasing their tensile strength by mechanically interlocking the fibres with the matrix (Bordoloi *et al.*, 2017).

The main reason for the maximum reduction in elongation at break for the untreated fiber-exposed acid test is the breakdown of cellulosic structure from the fibre because it is the main component contributing to the mechanical properties of jute (Arunavathi *et al.*, 2017; Methacanon *et al.*, 2010).

4.6 Results and Discussions on Chemical Characteristics

4.6.1 Surface Texture

Significant changes are observed in surface texture after treatment with AAB as shown in Figure 4.11. Before treatment with AAB, untreated jute fabric shows the presence of voids interspersed between fibres. The presence of voids is confirmed by permeability test results shown in Table 3.9. However, these voids are filled with AAB mix after treatment. The observations indicate that the particles of AAB adhere to the jute fibrils and provide strength by acting as an adhesive medium between different fibres (Figure 4.11 b). The change in the surface texture of jute fabric is discernible as the visible spaces between the fibres disappear after AAB treatment, although the permeability of soil reinforced with treated jute remains roughly unaffected. A surface study of AAB-treated jute fibres shows the attachment of the AAB layer to the fibres. There is a possibility of reducing the permeability of the soil if these treated fibres are used as reinforcement. However, results have shown that this attachment does not have a significant influence on the permeability of the soil.

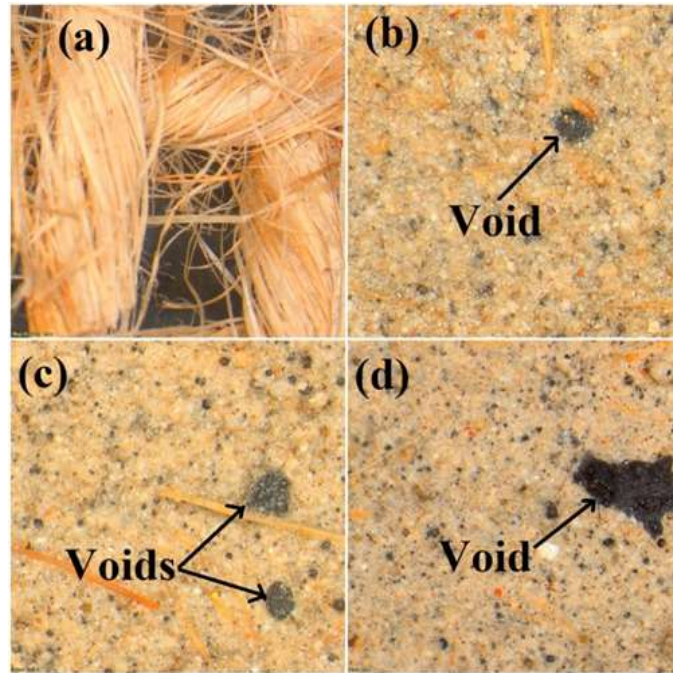


Figure 4.11. Stereomicroscopic images of (a) untreated jute, (b) 0.35 AAB jute, (c) 0.40 AAB jute, (d) 0.45 AAB jute at magnification 1.5 x

Figures 4.12(a-f) and 4.13 (a-f) display the stereomicroscopic images of untreated and AAB-treated jute after 90 and 180 days of exposure to different durability tests. After 90 days, there is no difference in the surface texture or colour of treated or untreated fibres, as shown in Figure 4.12(b-c). In Figure 4.13(b-c), untreated jute fibre changes colour and surface texture after 180 days in the soil and compost burial. Still, AAB-coated fibre remains unchanged due to AAB coating under the same conditions. The compost burial and soil burial effects do not show a remarkable change in the surface texture of treated jute fibres even after 180 days. It is observed that the untreated jute fibre becomes brittle and easily disintegrates into pieces after 180 days of soil and compost burial. The AAB treatment, hardens the jute fibre and increases its resistance to exposure to various chemicals. It is observed from Figure 4.13c that due to the compost burial effect, a black-coloured fungus develops on the surface of the jute, but it does not alter the internal structure of the jute. This is confirmed by FTIR, XRD, and SEM images of compost burial jute at 180 days duration.

Figure 4.12d shows that the outer surface of the untreated jute becomes darker in colour and exhibits signs of disintegration due to the acid effect. Similar observations are reported by Ghosh *et al.*, (2021). AAB-treated jute is more resistant to HCl than the untreated jute, as the applied AAB paste protects the internal structure of jute fibres from acidic attack. However, with an increase in exposure time, the AAB coating becomes thin and the volume

of voids increases, leading to enhanced disintegration. In Figure 4.12d, it is observed that 0.40 AAB and 0.45 AAB jute sheets show the removal of some amount of AAB paste due to the acidic effect, whereas, for 0.35 AAB jute, the removal of paste is not observed because of more AAB paste at the time of sample preparation (Gupta *et al.*, 2018). Because of the acidic effect after 180 days, the untreated jute fibre completely loses its original texture and becomes darker in colour. Whereas the AAB treatment protects the jute against the acidic effect, due to the high concentration of acidic nature (i.e. pH=2), it loses its original surface texture. Considering Figures 4.12e and 4.13e, the alkali treatment on jute fibre deposits white colour patches on the surface of untreated and treated jute fibre which changes the outer surface into a completely white patched nature, referred to as efflorescence. Efflorescence is a layer of salts, often white, that has developed on a surface, as shown in Figure 4.13e. Efflorescence is more likely to arise in AAB prepared with sodium-based activators. Efflorescence is said to be worse in formulations where the Na₂O is more in the solution (Allahverdi *et al.*, 2015). Due to the hydrolysis of water, except for untreated jute fibre, the surface of treated fibres does not change, which is observed in Figures 4.12f and 4.13f. From Figures 4.12 and 4.13, it is observed that AAB treatment on jute fibres protects them from the degradation effect from soil burial, compost burial, and hydrolysis of water, acid, and alkali effect. It is concluded from the stereomicroscopic images, that the 0.35 AAB jute is most effective in protecting it from the bio-degradation process.

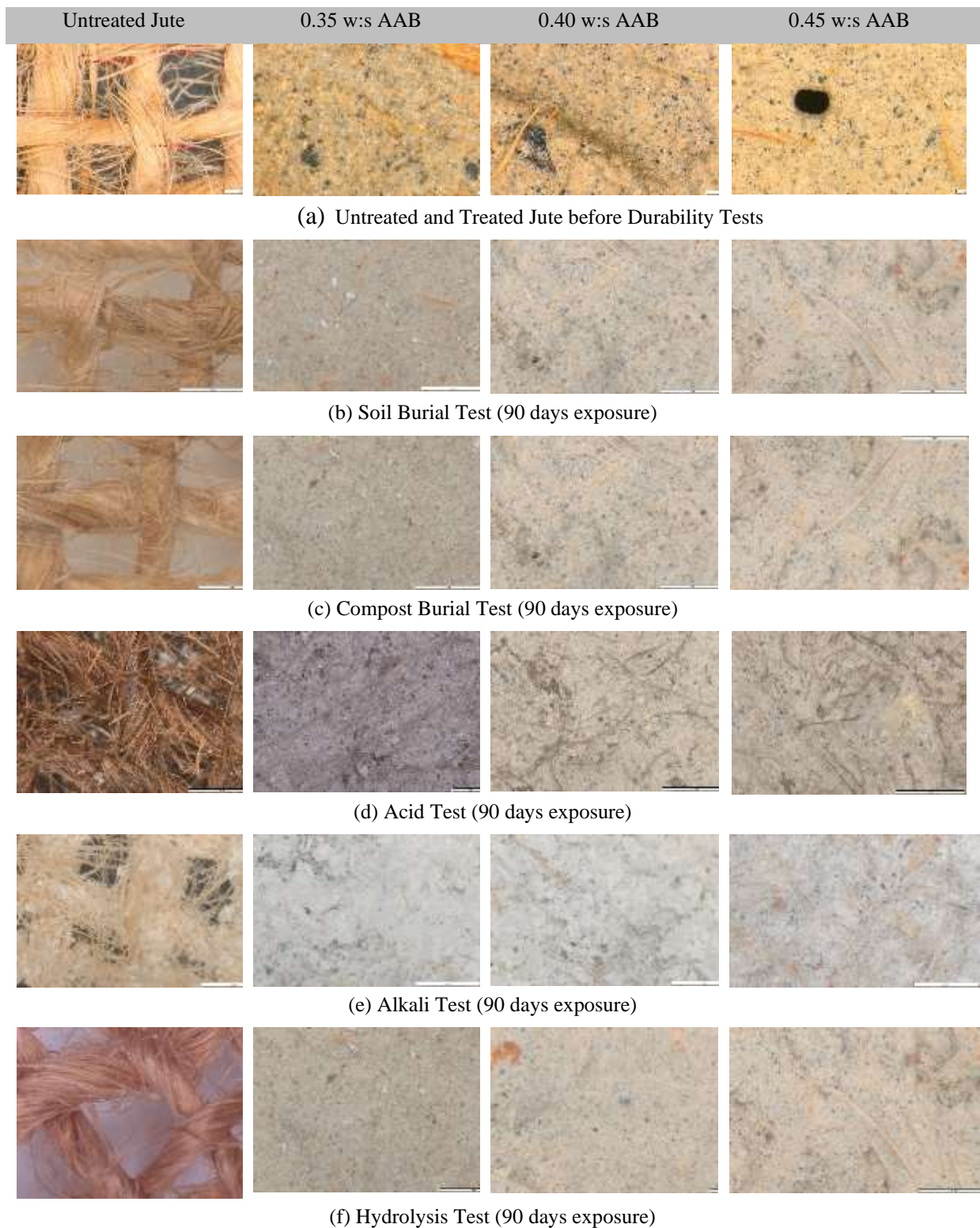


Figure 4.12. Stereomicroscopic Images of Untreated and Treated Jute (a) before durability tests and in (b) Soil Burial (c) Compost Burial (d) Acid (e) Alkali and (f) Hydrolysis Tests after 90 days of exposure

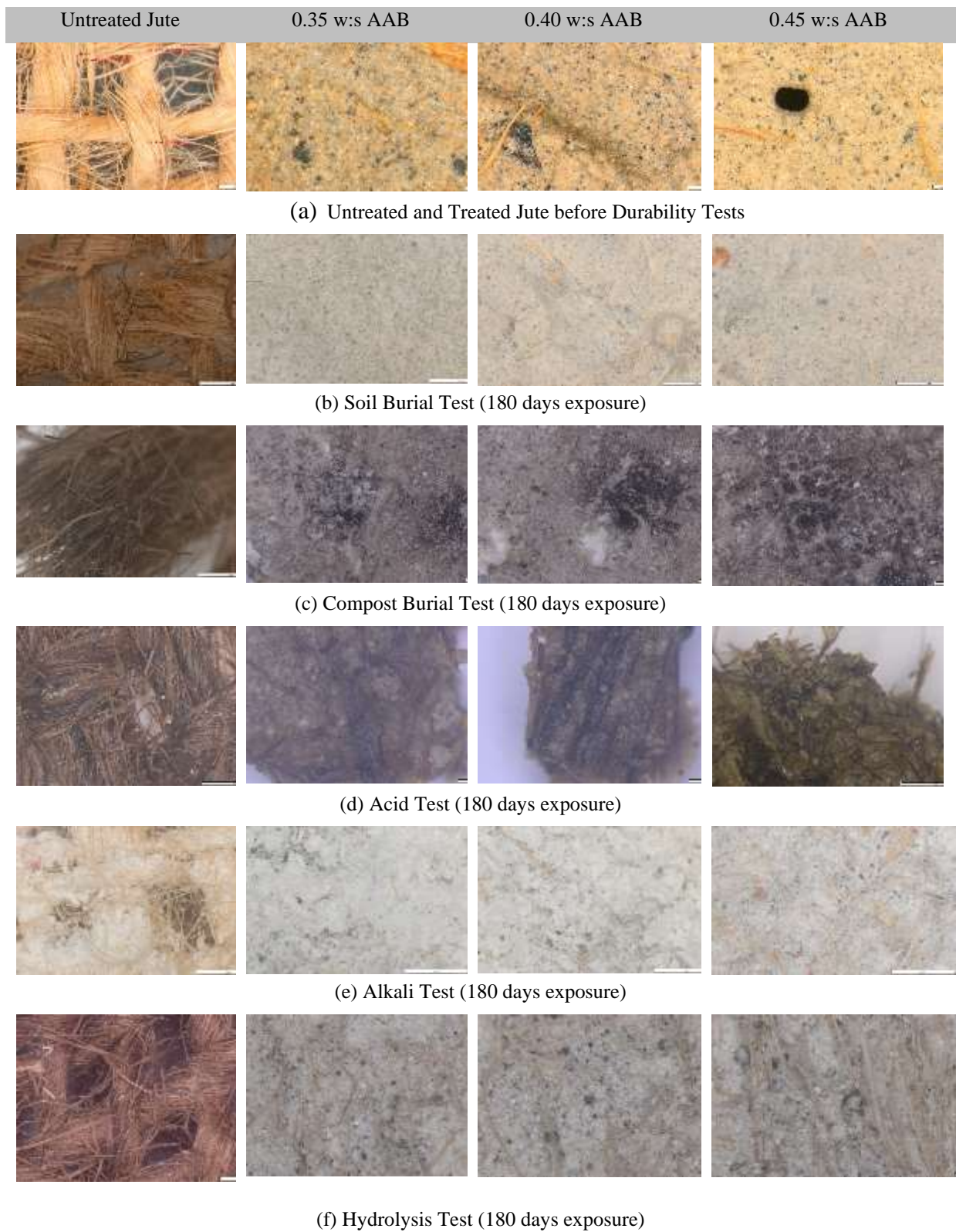


Figure 4.13. Stereomicroscopic Images of Untreated and Treated Jute (a) before durability tests; (b) Soil Burial (c) Compost Burial (d) Acid (e) Alkali and (f) Hydrolysis Tests after 180 days of exposure

4.6.2 Crystallinity

If the peaks are sharp, the crystallinity was strong, and if they are flat or humped, it is poor. The presence of pure portions suggests the existence of amorphous materials. Samples of untreated and treated jute are shown in their XRD patterns, respectively, in Figure 4.14. Raw jute shows XRD peaks at 15.9° , 21.3° , and 33.5° , all indicated by 'J' as reported by Wang *et al.*, (2009). Quartz (SiO_2), analcime ($\text{NaAlSi}_2\text{O}_6 \cdot \text{H}_2\text{O}$), mullite ($\text{Al}_6\text{Si}_2\text{O}_{13}$), and hydroxyl sodalite ($\text{Na}_6(\text{Si}_6\text{Al}_6\text{O}_{24}) \cdot 8\text{H}_2\text{O}$) are all identified as present in the XRD pattern of AAB treated jute. These minerals are unique to the cured AAB paste, as studied by Kar (2013). In addition, the diffractograms of all treated jute samples show the presence of the peaks typical of jute, demonstrating that jute retains its individuality. Following treatment, a coating of AAB paste is found to have solidified and developed over the jute fibres, which is observed from these mineral findings. The findings of XRD are supported by the SEM analysis (Figure 4.16b). In addition, the proportion of amorphous material in the treatment solution is shown to grow when the water-to-cement ratio is raised. This occurs because an increased quantity of sodium aluminosilicate hydrate matrix is formed as a consequence of the higher water content.

The XRD pattern is not changed for treated jute fibres when exposed to soil burial and compost burial effects after 180 days, as shown in Figures 4.14 (b-c). Applying AAB treatment to jute fibers effectively protected jute geotextiles against biodegradation induced by microorganisms in soil burial and compost burial experiments. This might be a possible reason for the absence of any alteration in the XRD pattern for both experiments. For the untreated jute fibre, the peak pattern is slightly changed for the compost burial, alkaline effect, and hydrolysis tests but does not alter the amorphous material (Figure 4.14 c). Under the effect of acid, the XRD pattern is completely changed; whereas similarity in the XRD pattern is observed for AAB-treated jute. AAB jute XRD pattern for the hydrolysis test is matched with AAB jute before durability, which is a clear indication that the hydrolysis test does not affect the AAB jute. From XRD analysis, it is observed that AAB treatment protected them against changing XRD patterns.

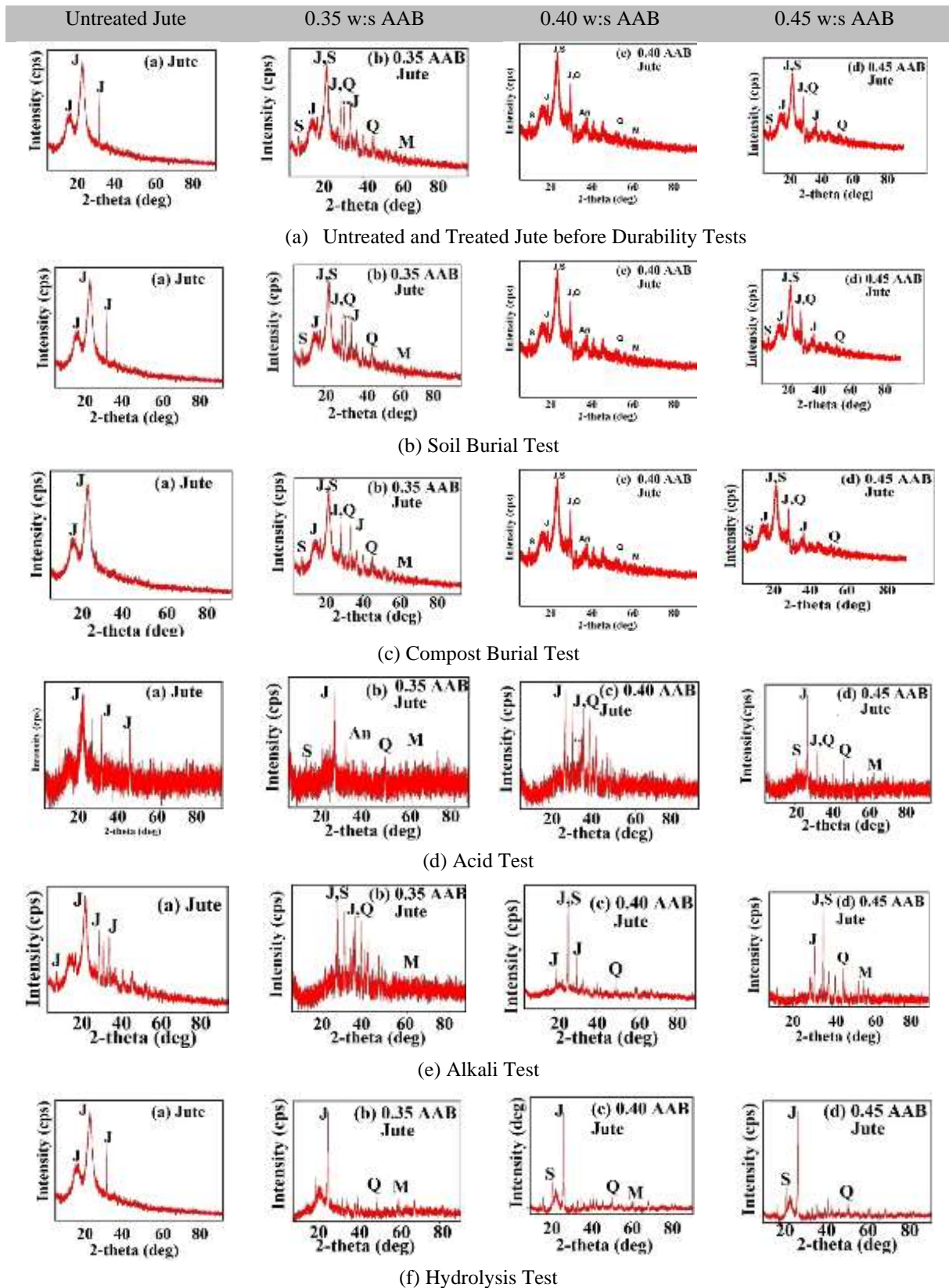


Figure 4.14. XRD diffractogram images of Untreated and Treated Jute (a) before durability tests and in (b) Soil Burial (c) Compost Burial (d) Acid (e) Alkali and (f) Hydrolysis Tests after 180 days of exposure (J= Jute, S= Hydroxy sodalite, M= Mullite, Q= Quartz, An= Analcine)

4.6.3 Molecular Bonds

The transmittance spectra of untreated and treated jute before and after 180 days of durability tests are presented in Figures 4.15 (a-f). The transmittance peaks at 3427 cm^{-1} , 3476 cm^{-1} , 3465 cm^{-1} , and 3474 cm^{-1} presented in Figure 4.15(a) constitute the O-H stretching absorption for untreated, 0.35 AAB, 0.40 AAB, and 0.45 AAB jute fibres respectively. In the case of untreated jute, the peaks are shown at 2915 cm^{-1} and 1639 cm^{-1} , indicating the C-H absorption and C-C stretching, respectively. Absorption peaks at 1247 cm^{-1} and 1053 cm^{-1} are attributed to C-O-C stretching and are consistent with the typical cellulose FTIR spectra (Wang *et al.*, 2009). The peaks at 1737 cm^{-1} and 1442 cm^{-1} are associated with C-O bending and symmetric CH_2 bending vibration, respectively (Abderrahim *et al.*, 2015). Hemicellulose may be identified by its unique spectral peaks at 1700 cm^{-1} and 1644 cm^{-1} , which represent acetyl groups and C=O bonds (Abdulkhani *et al.*, 2013). As a result of C=C in-plane aromatic vibrations, lignin exhibits a peak in the 1542 cm^{-1} band (Neto *et al.*, 2013). These observations indicate the presence of lignin and hemicellulose. After being treated with AAB, cellulose and hemicellulose are no longer present, therefore the peaks at 2820 cm^{-1} to 1784 cm^{-1} and 1490 cm^{-1} to 1214 cm^{-1} disappear. The siloxane unit (Si-O-Si) of the AAB system is observed in 0.35 AAB, 0.45 AAB, and 0.45 AAB for corresponding peaks of 1063 cm^{-1} , 1074 cm^{-1} , and 1038.5 cm^{-1} , respectively. Al-OH stretching vibrations were identified in the peaks at 786.8 cm^{-1} , 787 cm^{-1} , and 777.7 cm^{-1} in treated jute. The AAB treatment on jute fibres does not alter the cellulose component present in them, as the same peaks are observed in both untreated and treated jute fibres. Hemicellulose acetyl groups and C=O bonds may be seen as peaks at 1644 cm^{-1} and 1649 cm^{-1} in AAB-treated samples. This is a strong indication of jute identity even after AAB treatment. In Figure 4.15d, due to the acidic effect, most of the bonds present in it are nullified in untreated jute fibres, with the corresponding graph showing amorphous peaks. The same phenomenon is observed in the case of treated jute fibres with few bonds existing at around 787 cm^{-1} , indicating Al-OH stretching vibration. In the case of alkali treatment, peaks observed at 1037.5 cm^{-1} in 0.40 and 0.45 AAB jute fibre indicate the siloxane unit (Si-O-Si) of the AAB system. Sharp peaks are observed in alkali treatment, whereas in acidic attack, bonds are nullified at transmittance around 3400 cm^{-1} , which is an indication of O-H stretching absorption. From Figures 4.15 (b-c), it is observed that the exposure of jute fibres for soil burial and compost burial conditions does not have a significant effect on the molecular bonds. Transmittance peaks are identified at 3465 cm^{-1} .

indicating the O-H stretching bond, which is observed in untreated and 0.45 AAB-treated JGTs.

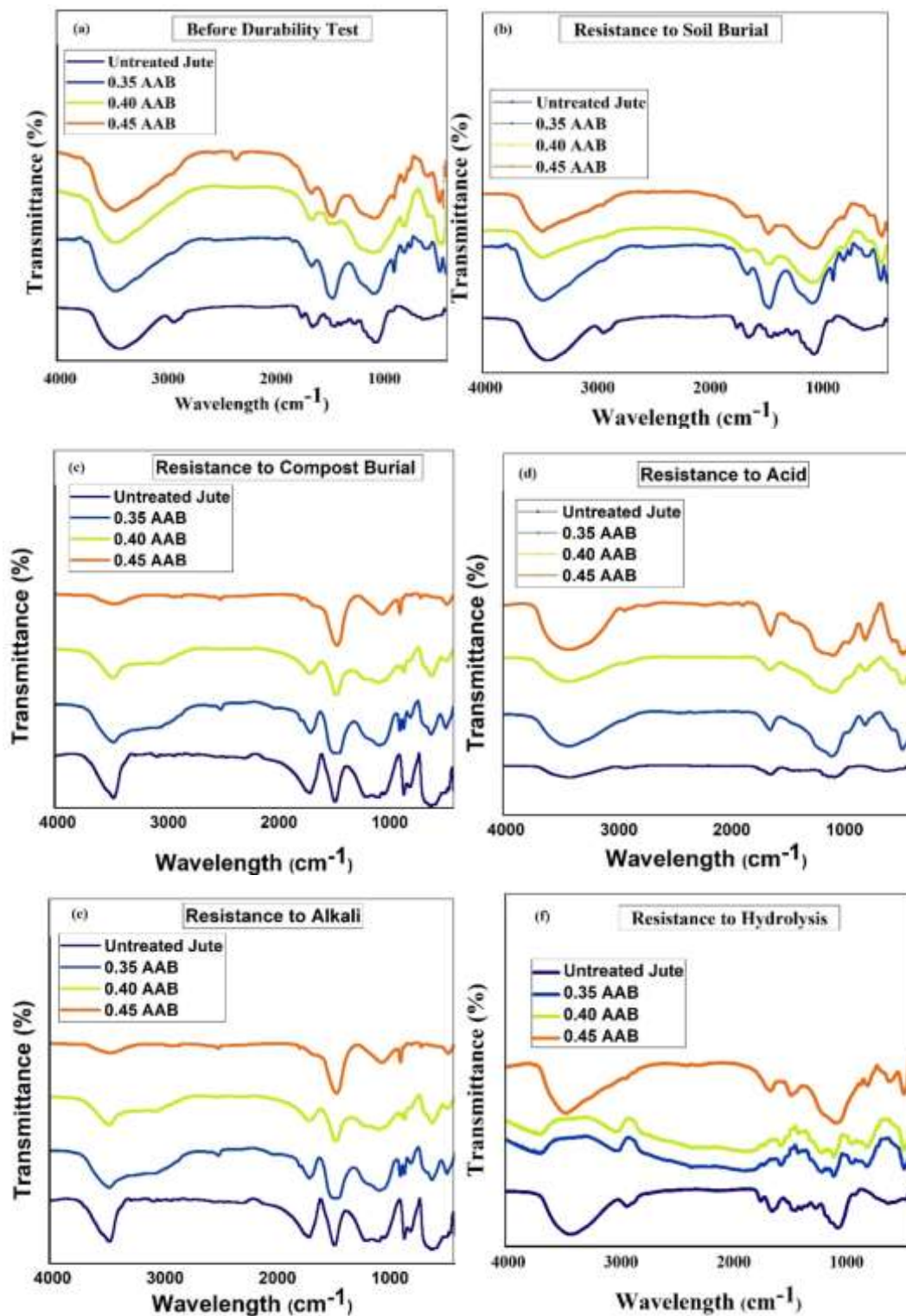


Figure 4.15. FTIR spectral image profile of Untreated and Treated Jute (a) before durability tests (b) Soil Burial (c) Compost Burial (d) Acid (e) Alkali and (f) Hydrolysis Tests after 180 days of exposure

4.6.4 Morphology

Figures 4.16(a–d) show the SEM images of untreated jute, 0.35 AAB, 0.40 AAB, and 0.45 AAB-treated jute. After 90 and 180 days of exposure to various durability tests, the SEM micrographs of untreated and AAB-treated jute are shown in Figures 4.17(a-f) and 4.18(a-f), respectively. SEM micrographs of longitudinal sections of untreated jute fibres (Figure 4.16(a) and 4.17(a-d)) reveal the presence of several grooves. Raw jute, as shown in a SEM image, is contaminated with hemicellulose, lignin, and pectin (Wang et al., 2009). Uneven voids may be seen throughout the 0.35 AAB-treated jute fibre. Therefore, it may be concluded that a matrix of sodium aluminosilicate hydrate (N-A-S-H), characterised by vitreous networks, becomes partly smeared over the fibre surface (Kar, 2013). AAB treatment of jute fibres leads to the formation of smooth spherical shape morphology particles varying from small to large size, which are unreacted fly ash particles as shown in Figures 4.16c and 4.17. According to Figures 4.16(c) and (d), more of the alkali-activating solution reacts with the fly ash, resulting in a larger matrix of sodium aluminosilicate hydrate and fewer unreacted fly ash particles formed as the w/s ratio rises. The figures reveal an increase in the N-A-S-H matrix and a corresponding decrease in the unreacted fly ash residue.

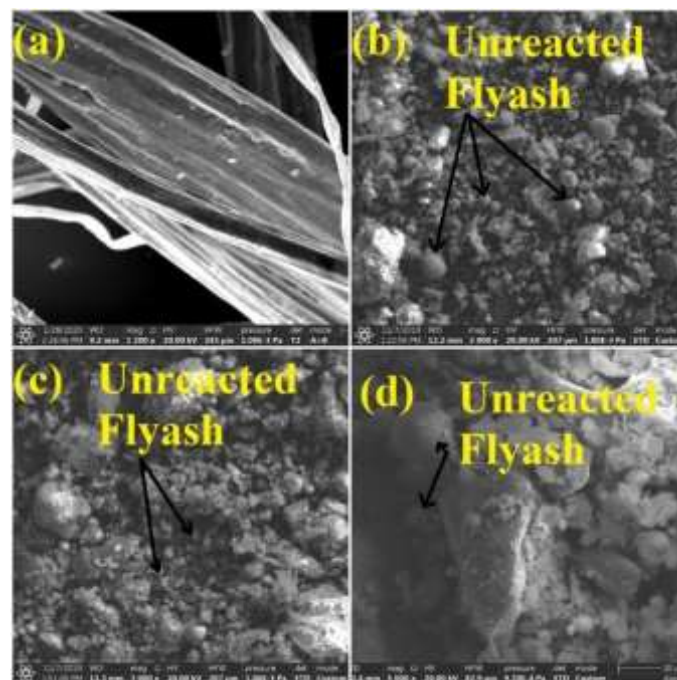


Figure 4.16. SEM images of a) untreated jute; b) 0.35 AAB Jute; c) 0.40 AAB Jute; d) 0.45 AAB jute

Several pores and grooves appear on the surface of both untreated and treated jute after the soil burial, compost burial, and exposures to acidic and alkaline environments as

well as hydrolysis for 90 and 180 days, as observed in Figures 4.17(a-d) and 4.18(b-c). This is attributed to the erosion of the jute. It is observed that the degree of erosion of the untreated jute is higher than that of the treated jute. Traces of fibre peeling off and breakage are observed on the surface of jute fibre, along with the increased concentration of pores around the fibres. This is ascribed to the adsorption of water by the hydrophilic groups of jute, thereby aggravating the erosion effect. From Figures 4.17(c) and 4.18(c), the spherical shape of fly ash particles is observed, which is a clear indication that soil burial and compost burial effects do not alter the internal structure of AAB-treated jute at the end of 90 and 180 days. In the hydrolysis test at 180 days also, fly ash particles are observed.

In Figures 4.17(d) and 4.18(d), a large crack is observed in jute fibre due to the acidic effect. It is observed when hydrochloric acid comes into contact with the cellulosic fibre of jute, it increases the number of pores on the surface and makes the fibre very rough, and formation of large cracks, which damages the surface as shown in Figures 4.17(d) (Vijay *et al.*, 2021). In Figure 4.17e, some white spots are observed due to efflorescence (Allahverdi *et al.*, 2015). It is concluded from SEM images that AAB treatment protects the jute fibres from various biodegradation effects and chemical attacks. Among all the AAB jute fibres, 0.35 AAB is observed to be most effective in protecting the internal morphology of jute by its thick paste application on the surface of the jute.

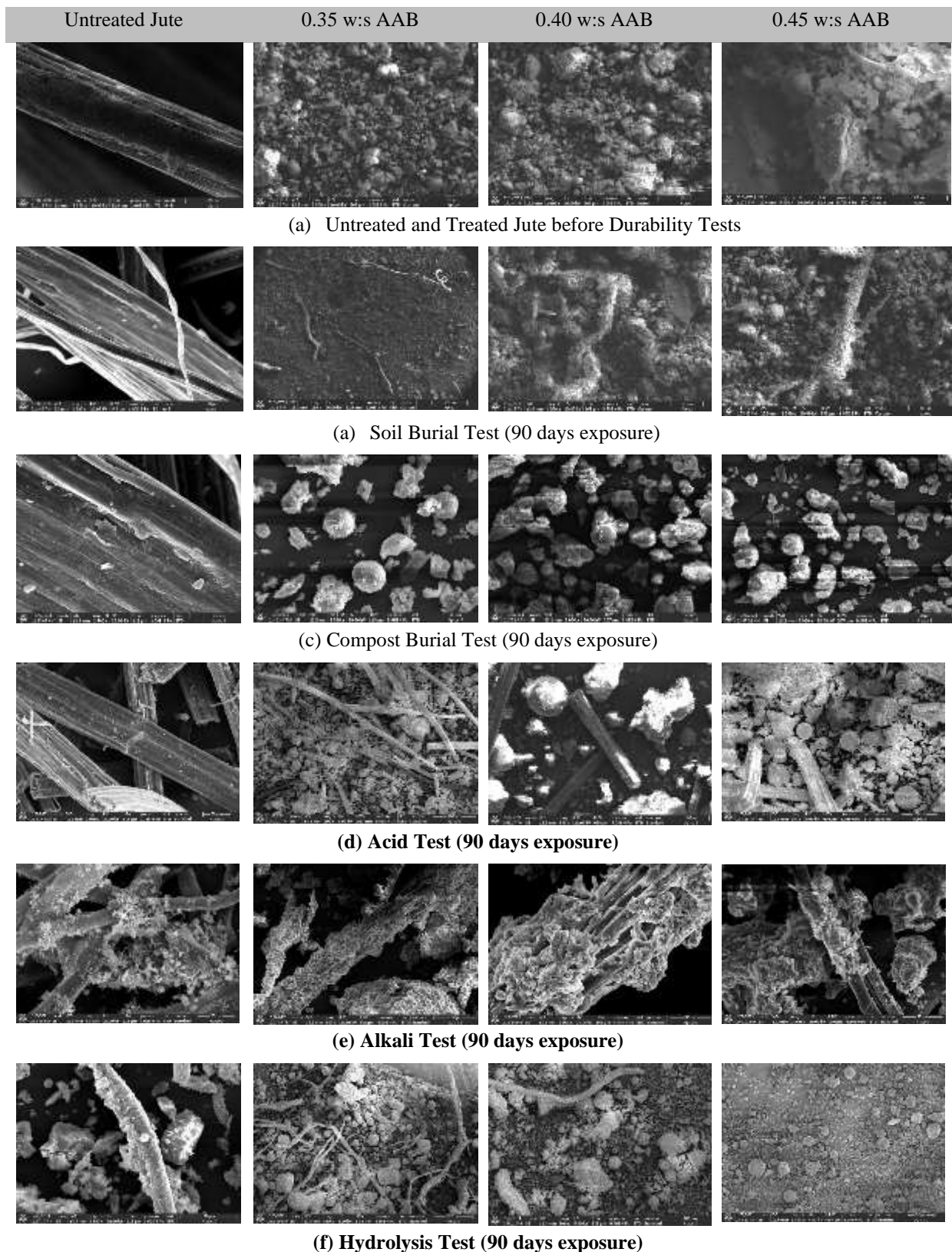


Figure 4.17. SEM Images of Untreated and Treated Jute (a) before durability tests (b) Soil Burial (c) Compost Burial (d) Acid; (e) Alkali (f) Hydrolysis Tests after 90 days of exposure

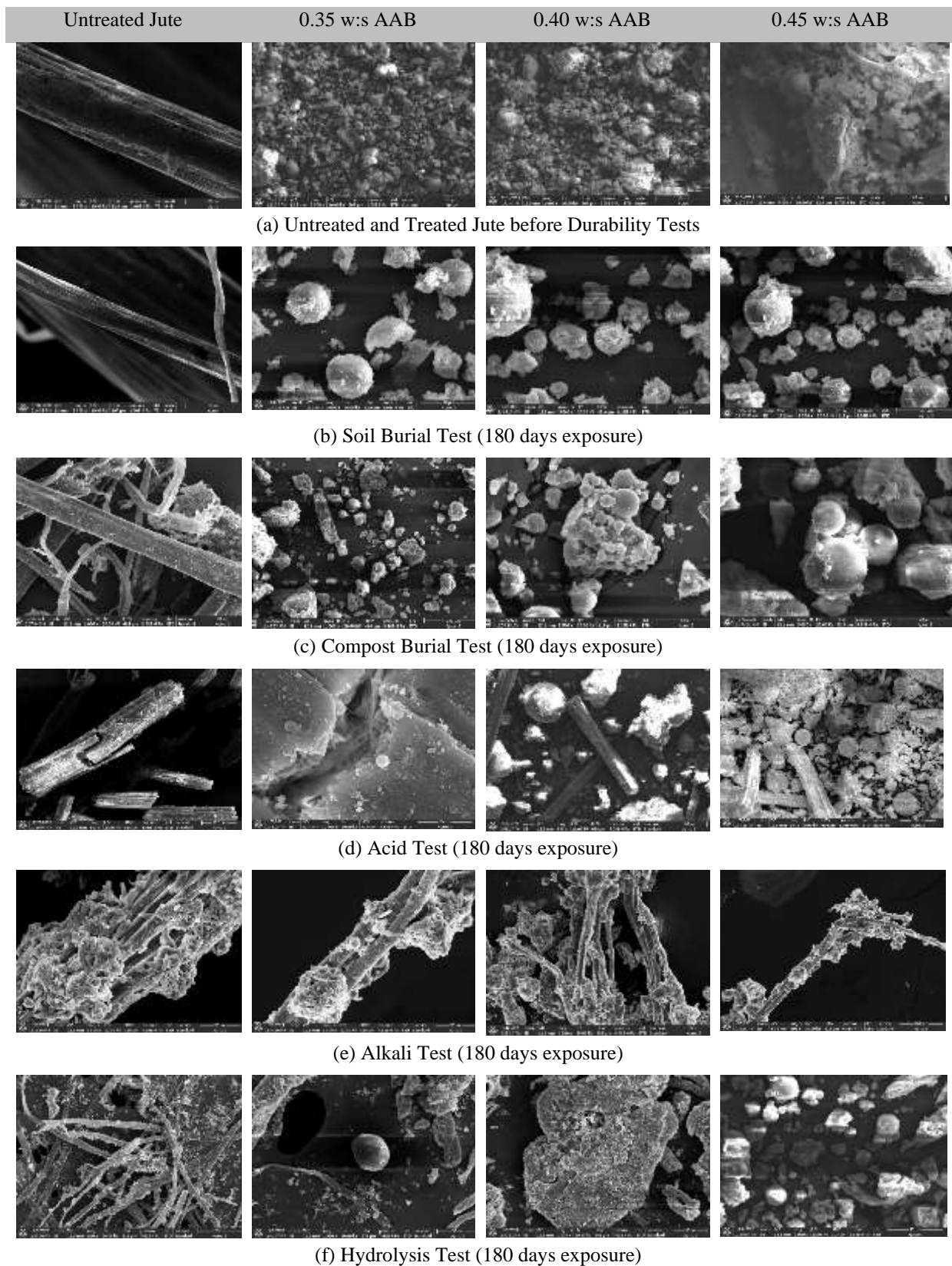


Figure 4.18. SEM Images of Untreated and Treated Jute (a) before durability tests (b) Soil Burial (c) Compost Burial (d) Acid (e) Alkali (f) Hydrolysis Tests after 180 days of exposure

4.6.5 Thermogravimetric Analysis

The thermal stability of both the untreated and treated jute is shown on the thermogravimetric curve (Figure 4.19). At 950 °C, different parts of the sample begin to break down, resulting in a shift in weight of the sample and, ultimately, its composition. The initial weight loss at 100°C owing to evaporation of the water is shown by the TGA curve of the untreated jute sample. Lignin decomposition, hemicellulose decomposition, and cellulose decomposition are the three stages of thermal degradation of untreated jute. At temperatures between 270°C and 310°C, the hemicellulose in untreated jute is decomposed, causing the material to lose mass. After the hemicellulose is broken down, the cellulose breakdown causes a significant loss of mass between 321°C and 390 °C, and the process is carried on up to 525°C. Though lignin degradation begins between 155 and 169 °C, composition of lignin at different aromatic branches gives it more heat stability than cellulose and hemicellulose. Lignin is broken down at temperatures ranging from around 150 °C to about 550 °C. Similarly, Yang *et al.*, (2007) noted that the degradation of cellulose, hemicellulose, and lignin occurred between 315 °C and 400 °C, 220 °C and 315 °C, and 100 °C and 900 °C, respectively. Nunn *et al.*, (1985) conducted an alternate investigation and found that cellulose breakdown might occur between 200 °C and 400 °C, whereas lignin decomposition could occur between 150°C and 750°C.

Figure 4.19 shows in the case of AAB jute, there is a rapid weight loss of up to 250 °C in the TGA curves of treated samples, attributable to the evaporation of water. As temperatures rises up to 700 °C, the lignin, hemicellulose, and cellulose in the jute continue to decompose, causing the jute to lose weight steadily. In addition, after 700 °C, there is almost no noticeable shift in weight. These observations are similar to the work done by Al Bakri *et al.*, (2012). It is observed from the finding that jute fibre loses its weight after 700 °C and but AAB paste does not decompose fully. Each treated jute sample hardly changes in weight after being heated to temperatures above 700 °C. From these findings, it can be concluded that AAB paste is effective against thermal heating.

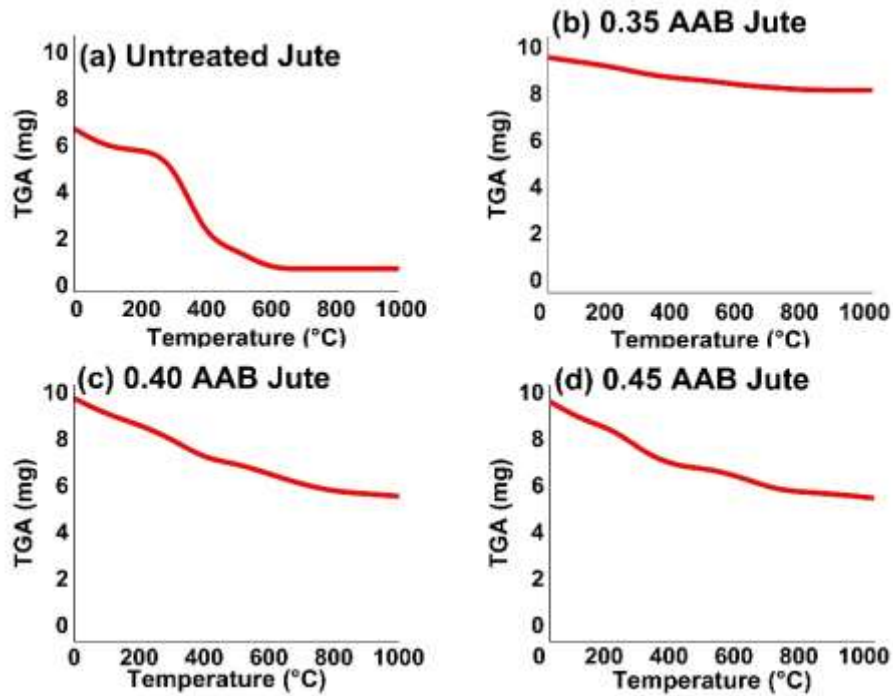


Figure 4.19: TGA images of a) Untreated (b) 0.35 AAB Treated Jute (c) 0.40 AAB Treated Jute (d) 0.45 AAB Treated Jute

4.7 Summary

The present chapter describes a method for treating natural JGTs with an alkaline binder to improve their durability and strength for ground improvement that is both sustainable and environmentally benign. The durability of natural geotextiles is primarily assessed by conducting experiments that examine the resistance of fibres to various factors such as soil burial, weathering, weight loss, exposure to acid and alkali, and microbial attack. These experiments primarily focus on observing changes in fibre tensile strength. Determination of weight loss and elongation at break is also carried out to estimate the extent of durability under different exposure conditions. Characterizations of surface texture, crystallinity, molecular bond, morphology, and thermogravimetry are conducted to demonstrate the effect of different exposure conditions on JGTs. The results reflect that the treatment of raw jute with AAB helps to improve its durability to a considerable extent.

CHAPTER 5

Experimental Assessment of Erosion Control of Treated Soil Slopes

5.1 General

The use of soil bioengineering techniques to reduce soil erosion and stabilise the soil is discussed in this chapter. Soil bioengineering is a method that combines living plant materials with inert materials to address soil erosion and slope stability issues. This approach is gaining popularity as a sustainable and cost-effective alternative to conventional engineering methods. One of the primary advantages of soil bioengineering is that it employs the natural resilience of plants to reinforce soil structures and reduce erosion. Plant roots can bond soil particles together, thereby decreasing the likelihood of wind and rainfall erosion. Additionally, plant growth can enhance soil structure, making it more resistant to erosion. According to the research on soil erosion, only a few studies in this sector are discussed, and there is a need for further in-depth research. The MUSLE (Modified Universal Soil Loss Equation) was used to calculate soil erosion in a laboratory environment for this investigation. The applied erosion control measurements using AAB-treated JGTs and Bermuda grass plants are discussed thoroughly. The applied reinforcement provides immediate protection against soil erosion, while Bermuda grass gradually starts to impart strength to the slope. The effect of variation in rainfall intensities on soil erosion is also discussed.

5.2 Laboratory Scale Soil Erosion Model setup

5.2.1 Laboratory Scale Slope Model

A laboratory-scale slope model is constructed in a transparent glass box to visually observe the eroding process of various slope angles. The tests are conducted in a 1.8 m (L) × 1.0 m (B) × 0.3 m (H) acrylic glass box (refer to Figure. 5.1). A 0.15 × 0.15 m² aperture is fabricated on the front side of the test setup to collect eroded soil and runoff water. The erosion slope model is designed using the scale factor 1:10 to replicate the real embankment. This model is based on past research that was carried out by Kumar and Roy, (2023) on laboratory-scale erosion models. It is ensured that no water leakage occurs through the sides during rainfall on the soil slope, by applying waterproof adhesive gel on all sides of the glass

box. The soil slope, measuring 0.3 metres in height, is constructed by compacting soil into six layers using a Proctor hammer. The amount of soil compacted in each layer is predetermined to achieve a relative density of 70, thereby simulating medium-dense conditions. A total of six containers are employed to mix water with soil to produce a uniform and well-balanced soil mixture and then to store the soil mixture. The containers are then used sequentially to prevent moisture loss.

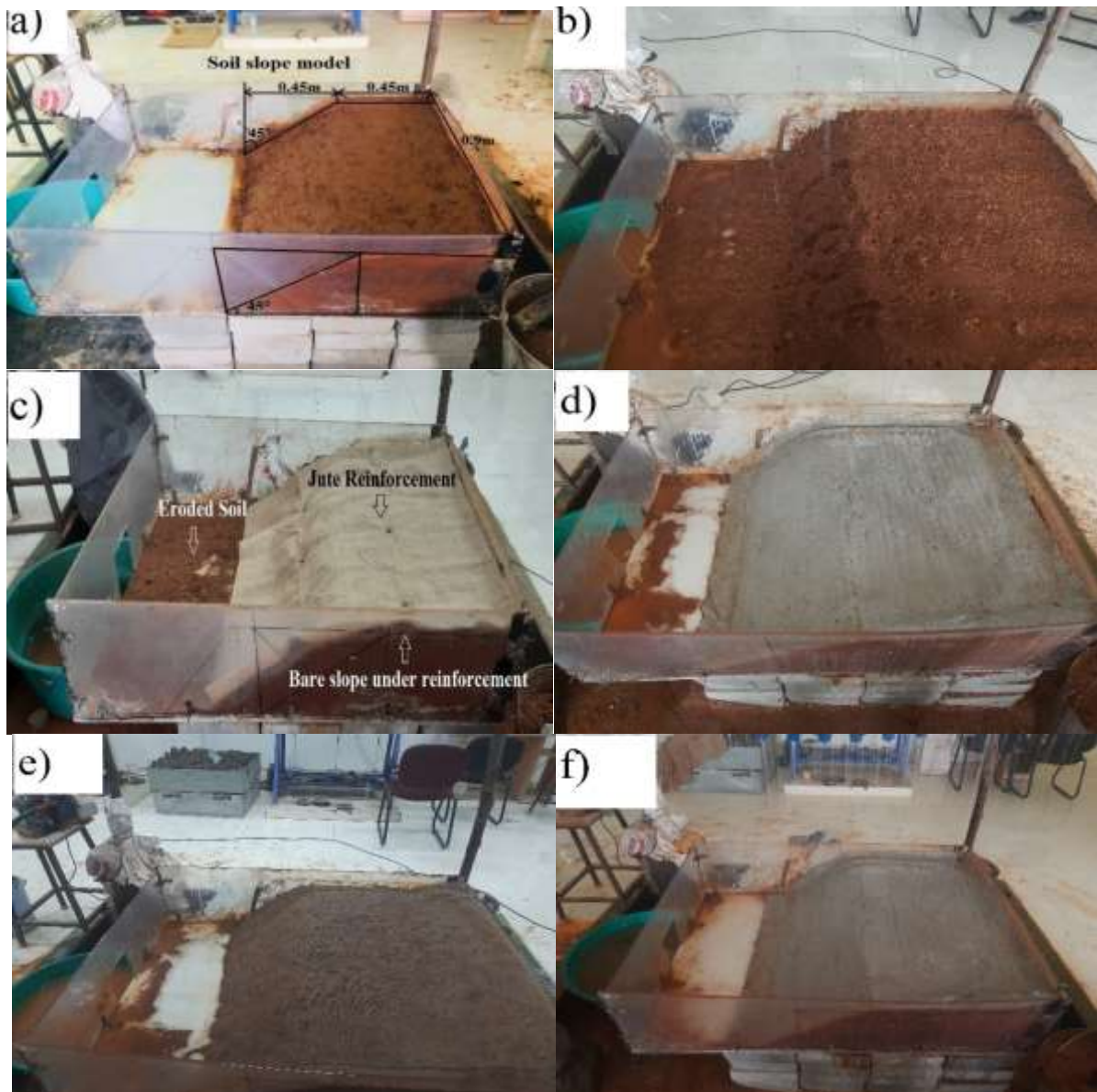


Figure. 5.1. (a) Bare soil slope; (b) Unreinforced Slope exposed to rainfall; (c) Slope reinforced with jute; (d) Slope reinforced with 0.35 AAB jute reinforcement; (e) Slope reinforced with untreated jute after one month of rainfall exposure; (f) Slope reinforced with 0.35 AAB jute after one month of rainfall exposure

The soil slope model is constructed in a right-angle trapezoidal shape having a long base of 0.90 m and a short base of 0.45 m, with a 45° angle between the long base and the slope side. Supporting wooden plates are used to prepare the slope at the desired inclination and angle in 6 layers. The soil surface is smoothed with a wooden trowel after compaction, which helped to reduce the number of voids or fractured lines in the soil. Grease is spread evenly on the interior walls of the box to reduce friction between the walls of the test chamber and the soil model within the box. Five experiments are conducted on the slopes with varying angles of 30°, 45°, and 60° with no reinforcement and a slope reinforced with untreated, 0.35, 0.40, and 0.45 AAB JGTs. JGTs are pinned to the slope at different points to avoid slippage from the surface. Figures 5.1 (a-f) depict bare soil slopes and slopes covered with untreated jute.

5.2.2 Sediment Yield Calculation from Experimental Investigation

When a raindrop hits the soil surface from a given height, it detaches the soil particles, causing displacement of the soil particles and runoff water as shown in Figure 2.3. In the present study, after applying the desired rainfall intensities of 10.2 mm/hr and 23.4 mm/hr on the slope for 5 minutes, the corresponding runoff water is collected in a container, and the runoff volume is measured. Then the collected runoff is stored along with sediment in a container to settle sediment particles. Using the tap arrangement, clean water is expelled from the storage container. Finally, the remaining sediment and water content are kept in an oven for 48 hours at 105 °C. After the sample becomes dry, the weight of the sediment is calculated using a weighing balance. A similar procedure is followed for all other types of slopes and reinforcements. The sediment yield values from the experimental investigation are shown in Table 5.1.

Table 5.1 shows that the intensity of rainfall directly affects soil erosion. This is because the amount of rain that falls per unit of time and area increases with the intensity of rainfall, so the time it takes for the soil to become saturated decreases, which results in more rainwater being converted into a runoff. A large quantity of fine sand, clay, and silt is quickly washed away by the runoff water (Mohamadi *et al.*, 2015; Wu *et al.*, 2018). From the perspective of slope steepness, it is obvious that the quantity of sediment yield increases along with the increase in slope steepness. There will be increased erosion due to more soil particles being washed away when runoff velocity increases as slope steepness increases (Siswanto *et al.*, 2019). As a cover for slopes, jute can be applied to reduce the impact of raindrops and the detachment of soil particles. Jute reinforcement slows runoff that might

pass through and acts as a partial receptor for soil particles that have been separated (Sanyal, 2017). Although alkali-activated binder jute sheets are an effective alternative to conventional jute sheets, they reduce soil erosion even more. Due to the AAB coating, the rough and thick outer surface of AAB jute significantly decreases raindrop impact and runoff velocity.

Table 5.1. Soil Yield Values Obtained from Laboratory Slope Model Set-up

Slope Inclination	Sediment Yield (Kg) for 10.2 mm/hour Rainfall	Sediment Yield (Kg) for 23.4 mm/hour Rainfall	Type of Reinforcement
30°	2.08	3.93	No reinforcement
	0.645	1.45	Untreated Jute
	0.397	0.66	0.35AAB Jute
	0.471	0.74	0.40 AAB Jute
	0.509	0.83	0.45 AAB Jute
45°	3.2	5.32	No reinforcement
	1.01	1.344	Untreated Jute
	0.67	1.10	0.35AAB Jute
	0.73	1.32	0.40 AAB Jute
	0.795	1.428	0.45 AAB Jute
60°	5.48	7.64	No reinforcement
	1.854	2.404	Untreated Jute
	0.936	1.436	0.35AAB Jute
	1.01	1.59	0.40 AAB Jute
	1.3	1.75	0.45 AAB Jute

5.3 Soil Loss Prediction Models

Soil erosion may be modelled in various ways, depending on the underlying causes. Since the 1930s, researchers have been attempting to forecast and detect soil erosion accurately. This has resulted in the development of several models (Lal, 2001). Empirical, semi-empirical, and physical process-based models are the three main types. Field research is costly, time-consuming, and must be conducted over several years to predict and assess soil erosion. Despite the valuable insights that field studies offer in understanding erosion processes, their efficacy is constrained by the intricate interactions involved and the challenges associated with developing the findings. Models of soil erosion may replicate how erosion typically occurs in a drainage basin and can account for a number of the complex interconnections that influence erosion rates. Figure 5.2 shows the different types of soil erosion models.

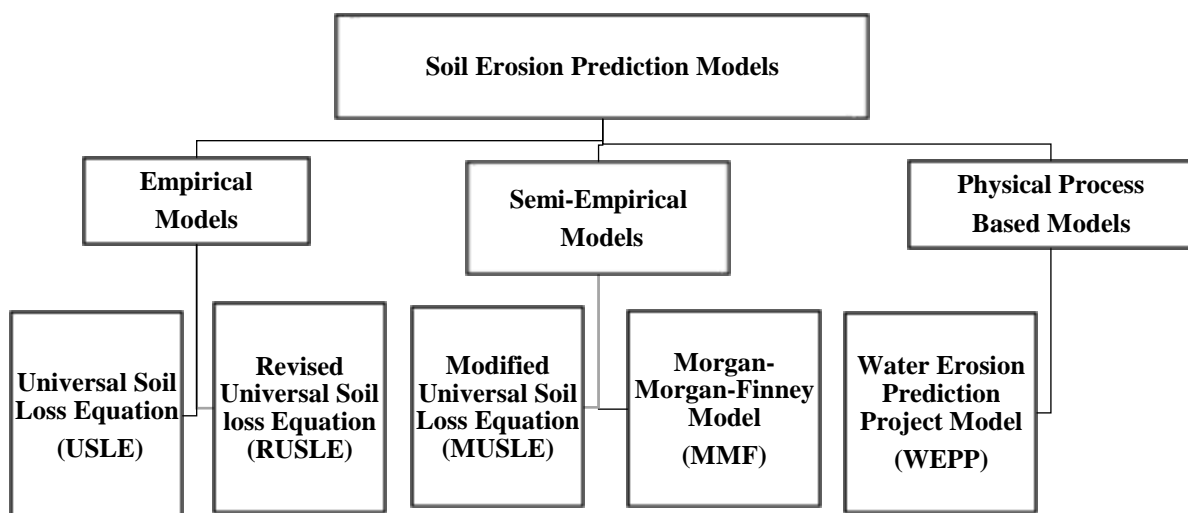


Figure. 5.2 Flow chart showing different types of soil erosion models

5.3.1 Empirical Models

5.3.1.1 The Universal Soil Loss Equation (USLE) Model

Estimating the rate of soil loss over several area scales using the empirical formula Wischmeier and Smith (1978) developed is one option being considered. Quantifying soil losses is a common method, often used with GIS approaches. This model is built in a way that takes into account the patterns of rainfall, land use, topography, soil erodibility, and anti-erosion techniques as follows.

$$A = R \times K \times LS \times C \times P \quad (5.1)$$

Where, A is the calculated average soil loss (t/ha/year), R (MJ-mm ha⁻¹ h⁻¹ y⁻¹) is the rainfall-runoff erosivity factor, calculated based on average rainfall over a lengthy period. The credibility factor of the soil is calculated based on soil properties such as texture, organic matter, permeability, and other unique characteristics, and it is denoted by the letter K (t ha h ha¹ MJ⁻¹ mm⁻¹); LS is topographic where the slope length (L) and slope gradient (S) factor are calculated based on length of the slope and gradient irrespective of land usage, and both of these factors are dimensionless. C is the cropping management component. It is calculated based on six crop stages, cropping sequence, surface residue cover, surface roughness, and canopy cover, weighted by the proportion of erosive precipitation. P is the supporting conservation practice element, calculated based on installing techniques that decrease soil movement by slowing runoff. P factors vary based on slope ranges, with a difference made for ridge heights. These factors are dimensionless and range from 0 to 1 (Sandeep *et al.*, 2021).

5.3.1.2 The Revised Universal Soil Loss Equation (RUSLE) Model

The RUSLE model estimates the typical soil loss that occurs each year. This is an updated universal soil loss equation model, sometimes known as the USLE (Wischmeier & Smith, 1978). According to Roose and Noni (2004), erosion occurs as a result of the multiplication of rainfall-runoff erosivity (R) and environmental resistance, which can be described as a multiplicative function. The environmental resistance includes the soil erodibility factor (K), the topographical component (LS), the anti-erosion practises (P), and the plant cover factor (C). This model is written in a manner that is comparable to the USLE in equation number 5.1.

$$A_{RUSLE} = R \times K \times LS \times C \times P \quad (5.2)$$

The involved parameters and their units are the same as in the USLE model. Still, the method of finding the respective parameters' values differs from the conventional USLE model. R is calculated based on the same criteria as the USLE but with minor adjustments using some additional data and weather stations. The erodibility factor (K) of soil is calculated similarly to USLE but with some adjustments made to allow for seasonal shifts such as freezing and thawing and soil consolidation. LS is calculated by redefining the LS value of USLE model by considering the type of land used. The calculation of the C factor involves the

consideration of several distinct subfactors that are independent of each other. These subfactors include past land use, canopy cover, surface cover, surface roughness, and soil moisture. The USLE is modified by partitioning each calendar year into discrete intervals of 15 days, followed by the calculation of a soil loss ratio for each respective time period. It calculates a new soil loss ratio every time one of the subfactors is altered due to a tillage operation. The calculation of the P factor values involves the utilisation of various factors, including the soil hydrologic groups, slope, row grade ridge height, cover-management condition, and the 10-year single storm index (Roose & Noni, 2004).

5.3.1.3 The Modified Universal Soil Loss Equation (MUSLE) Model

It is necessary to accurately anticipate the sediment production from watersheds to support sustainable land management practices and environmental protection. According to Williams (1975), the USLE was modified to create the Modified Universal Soil Loss Equation (MUSLE) by replacing the rainfall erosivity component with a runoff energy factor (Wischmeier *et al.*, 1960). This was done to calculate the amount of soil lost due to runoff. The total runoff volume and peak flow rate during a specific storm determine the energy component of MUSLE. Williams (1982) points out that MUSLE has various advantages over USLE when modelling sediment production from a watershed. The advantages are as follows:

- Applicability of individual storm.
- Because the runoff component captures the energy needed in sediment transport and detachment, sediment delivery ratios are no longer required.
- Higher accuracy because runoff accounts for a larger fraction of the variation in sediment output than rainfall.

In the development of MUSLE, the runoff energy component was originally computed from reported runoff rates and volumes (Williams, 1975). Smith *et al.*, (1984) obtained the prediction equation by substituting this runoff energy component for the rainfall energy element in the USLE using an optimisation method (DeCoursey and Synder, 1969). The MUSLE equation is written as follows.

$$Y = 11.8 \times (Q \times q_p)^{0.56} \times K \times LS \times C \times P \quad (5.3)$$

where,

Y = sediment yield in metric tons,
 Q = runoff volume in m³,
 q_p = peak runoff rate in m³/sec,
 K = soil erodibility factor,
 C = crop management factor,
 P = erosion control-practice factor, and
 LS = Topographic factor

All the factors in the above equation are the same as in the USLE model except runoff volume and peak flow rate. By figuring out how much runoff volume was collected for each type of rainfall intensity, it is possible to get the value for Q (Arekhi *et al.*, 2012; Pandey *et al.*, 2009). The flow rate (q_p) of a rotameter can be used to figure out the peak flow rate. Since the experiment is carried out in a lab, the rain rate is kept constant for both types of rain throughout the process.

Calculation of soil erodibility factor (K):

The soil erodibility factor (K) corresponds to the erosion rate of various soils. When the slope, rainfall, vegetation cover, and soil management techniques are the same, some soils may erode more readily than others because of their intrinsic soil properties. The measurement of K on unit runoff plots directly captures the collective impact of all factors that substantially affect soil erosion susceptibility. The soil qualities that significantly impact soil loss include soil permeability, infiltration rate, soil texture, size and stability of soil structure, organic content, soil depth, precipitation, runoff, seepage, and the properties of soil (Kanito *et al.*, 2021). Typically, they are calculated by specialized experimental runoff plots or by employing empirical erodibility equations that establish a relationship between various soil parameters and the factor K. The formula calculating soil erodibility is given as

$$K = \frac{A_0}{S \times (\sum EI)} \quad (5.4)$$

Where A₀= observed soil loss, S= Slope Factor, $\sum EI$ = Total rainfall erosivity index. Table 5.2 shows K values for many Indian sites. The soil erodibility factor (K) quantitatively measures the intrinsic erodibility of a certain soil. Greater values of K indicate more vulnerability to erosion, while smaller values indicate less vulnerability. The factor considers soil characteristics such as texture, structure, organic matter content, and permeability, all of which affect the soil's capacity to resist erosion.

Table 5.2. Soil Erodibility factor values (Subramanya, 2008)

Station	Soil	Value of K
Agra	Loamy sand, alluvial	0.07
Dehradun	Dhulkot silt, Loam	0.15
Hyderabad	Red chalk sandy loam	0.08
Kharagpur	Soils from lateritic rock	0.04
Kota	Kota clay loam	0.11
Ootakamund	Laterite	0.04
Rehmankhara	Loam,alluvial	0.17

Calculation of Topographic Factor (LS):

The geography of a region is one of the most significant factors contributing to water erosion. The inclination of the soil slope plays an important role in soil particles detaching, migrating, and settling on new sites. The topographic factor is determined by equation (5.4).

$$LS = \left(\frac{\lambda}{22.13} \right)^m [65.41 \times \sin^2(\theta) + 4.58 \times \sin(\theta) + 0.65] \quad (5.4)$$

Substituting the slope length and θ values corresponding to each slope gives the topographic values (Kanito *et al.*, 2021).

Table 5.3. Topographic Factor Values

Angle	30°	45°	60°
Slope Length (m)	$\lambda=0.545$	$\lambda=0.3676$	$\lambda=0.3052$
LS (m)	3.02	4.7	6.3

Values of Cropping Management Factor

The values of the cropping management factor (C) for different soil conditions, like bare soil slopes, reinforced soil slopes, and plantation, were adopted from the study of Jena *et al.*, (2018).

Table 5.4. Cover Management factors for different conditions

S. No.	Type of Cover Management	C -Factor
1	Agriculture, Crop Land	0.5
2	Current shifting cultivation	0.8
3	Terrace cultivation	0.5
4	Plantations	0.02
5	Scrub level	0.6
6	Land with open scrub	0.7
7	Wasteland	1.0
8	Built up	1.0
9	Evergreen forest	0.004
11	Deciduous forest	0.008
12	Scrub forest	0.05
13	Dense scrub forest	0.08
14	Water bodies	0

The values for the C factor for other types obtained from the source are listed in Table 5.5 (Ganasri and Ramesh, 2016).

Table.5.5 Cover Management Factors for reinforcement

Type of Cover Management	C -Factor
Jute	0.3
Straw Mulch (Assumed for AAB)	0.2

Values of Support Practice Factor

The support practice factor (P) values for different types of soil conditions and slope conditions, like bare soil slopes, reinforced soil slopes, and plantation, are adopted from the study of Jena *et al.*, (2018).

Table 5.6. Support Practice Factor (P) Values

S. No.	Type of Cover Management	P-Factor
1	Agriculture, Crop Land	0.5
2	Current shifting cultivation	1.0
3	Terrace cultivation	0.5
4	Plantations	0.8
5	Scrub level	1.0
6	Land with open scrub	1.0
7	Wasteland	1.0
8	Built up	1.0
9	Evergreen forest	1.0
11	Deciduous forest	1.0
12	scrub forest	1.0
13	Dense scrub forest	1.0
14	Water bodies	1.0

Empirical models are simpler and easy to apply, with fewer input data requirements and less computational demand. They may be more appropriate in situations where quick assessment of erosion risk is needed. Process-based models estimate the soil erosion by explicitly considering the underlying physical and biological processes that drive erosion. MUSLE is an empirical model that uses simplified parameterization to estimate soil erosion. MUSLE is a scalable model that can be applied at different scales. Soil loss due to water erosion may be estimated based on data like erodibility, slope length, and slope steepness. At the plot level, MUSLE can be used to assess the erosion potential of individual locations or other small areas. It allows for consistent assessment of erosion risk across different scales, using a common set of input parameters and assumptions. This can be useful for comparing erosion risk across different regions or tracking changes in erosion risk over time. In addition, MUSLE has an advantage over USLE/RUSLE because it can predict sediment yield from a single storm (Ketema and Dwarakish, 2021). Many past research works indicate the application MUSLE model resulted appropriate estimation of sediment yield. The effectiveness of MUSLE in forecasting the sediment yield from storm events in the Khanmirza watershed in Iran was assessed by Sadeghi and Mizuyama (2007). The results from MUSLE are compared to those from sediment analysis. The results showed that the MUSLE is able to accurately estimate the sediment yield from storm events in the study

region ($R^2 = 0.99$). This study uses the MUSLE model to assess sediment yield due to the simple parameterization compared to process-based models and its applicability from plot to catchment scale.

5.3.2 Sediment Yield Calculation Using MUSLE Model

The following calculation is carried out using equation (5.3):

The parameter values $C = 1$ and $P = 1$ are used in the equation for unreinforced slopes of 45° inclinations under low rainfall conditions, and other parameter values are taken from Tables 2 to 6. The same calculation process is completed for other reinforced slopes, but values of $C=0.30$ are used for jute reinforcement, and $C=0.20$ are used for AAB-treated jute reinforcement, as AAB is considered as type of straw mulching cover as shown in Table 5.5. The P value is taken as 1 for all reinforcements. All other parameters required for reinforced slope calculations are taken from Tables 2 to 6. For each experiment, the peak flow rate and runoff volume are measured manually. Similar substitutions are made for the values of all other conditions in the MUSLE model, and the resulting sediment yield estimates are shown in Table 5.7.

$$Y = 11.8 \times (Q \times q_p)^{0.56} \times K \times LS \times C \times P$$

For 45° slope with no reinforcement and low rainfall condition

$K=0.08$ for the current research region (Hyderabad)

$LS= 4.7, C=1 P=1$

$$Y = 11.8 \times (0.04914 \times 0.000176)^{0.56} \times 0.08 \times 4.7 \times 1 \times 1$$

$$Y=3.86 \text{ Kg}$$

Table. 5.7 Sediment Yield Values Calculated from the MUSLE Model

Slope Inclination	Sediment Yield (Kg) for 10.2 mm/hour Rainfall	Sediment Yield (Kg) for 23.4 mm/hour Rainfall	Type of Reinforcement
30°	2.48	4.16	No reinforcement
	0.745	1.24	Untreated Jute
	0.497	0.83	0.35AAB Jute
	0.512	0.89	0.40 AAB Jute
	0.539	0.95	0.45 AAB Jute
	3.86	6.48	No reinforcement

45°	1.158	1.944	Untreated Jute
	0.772	1.296	0.35AAB Jute
	0.785	1.40	0.40 AAB Jute
	0.83	1.47	0.45 AAB Jute
60°	5.18	8.68	No reinforcement
	1.554	2.604	Untreated Jute
	1.036	1.736	0.35AAB Jute
	1.12	1.89	0.40 AAB Jute
	1.2	1.98	0.45AB Jute

5.4 Effect of Vegetation on Slope Stability

Erosion is the movement and depositing of soil and rock particles in new areas after being removed from the surface of earth as a result of wind and water flow. Conventional methods of protecting soil from erosion involve using costly and, in some circumstances, ineffective measures such as dumping cement concrete blocks and stones, providing wood revetments, and using geotextile, etc. The use of vegetation to protect the soil from erosion is, on the other hand, economical, eco-friendly, and effective in the long run. It prevents soil erosion and helps recharge groundwater, also. Grasses, shrubs, and trees are used as vegetation types for slope stability. These may be planted either from seed or from live plants. Special approaches called soil biotechnology, or bioengineering systems have been developed for growing plants on slopes (Islam, 2013). According to the definition provided by Morgan and Rickson (1995), bioengineering encompasses the utilisation of vegetation in various forms, including individual plants or groups of plants, as a material for engineering purposes. In general, plant roots can be divided into two groups. Generally thin and thick roots differ in their structure, function, and location.

- Thin, hairy roots increase the apparent cohesion of soil by binding soil particles, thus improving the shear strength of the composite. Soil particles, bonded with hairy roots, form a natural protective layer that protects the ground surface from erosion.
- Thick, woody plant roots act like soil nails across the failure zones.

The primary difference between thin and thick roots is their size, structure, function, and location in the plant. Thin roots are smaller, less complex, and typically associated with taproot systems, whereas thick roots are larger, more complicated, and may have additional

functions and locations within the plant. The diameter of thin and thick roots can vary widely based on the species and developmental stage of the plant.

5.4.1 Laboratory Scale Vegetated Slope Model



Figure 5.3. Soil erosion test for Vegetated Slope with Jute reinforcement (Left) and 0.35 AAB treated Jute Reinforcement (Right)

The laboratory scale vegetated slope model is constructed following the mechanism described in section 5.6.2. The vegetation is transplanted into the bare soil with an optimal spacing of 150 mm centre-to-centre to accommodate more plants in a given space and to facilitate the growth of plants without disrupting neighbouring plants, resulting in a higher plant density. First, several 0.05- to 0.1-meter-deep holes with 0.15 meter-apart spacing are dug to renew plant regrowth from the stolon of the mother plant. For reinforced slopes with needed holes, reinforcing material is cut without damaging adjacent jute threads for transplanting. Figure 5.3 shows the vegetation on the reinforced slope.

5.4.2 Sediment Yield Calculation for Vegetation Applied Slope

Table 5.8. Experimental Values of Soil Yield

Slope Inclination	Sediment Yield (Kg) for 10.2 mm/hour Rainfall	Sediment Yield (Kg) for 23.4 mm/hour Rainfall	Type of Reinforcement
30°	1.68	2.87	No reinforcement
	0.525	1.15	Untreated Jute
	0.267	0.46	0.35AAB Jute
	0.291	0.54	0.40 AAB Jute
	0.36	0.63	0.45 AAB Jute
45°	2.42	4.13	No reinforcement
	0.92	1.31	Untreated Jute
	0.47	0.78	0.35AAB Jute
	0.51	0.82	0.40 AAB Jute
	0.59	0.861	0.45 AAB Jute
60°	3.48	5.64	No reinforcement
	1.454	1.804	Untreated Jute
	0.73	0.936	0.35AAB Jute
	0.786	0.94	0.40 AAB Jute
	0.81	0.98	0.45AB Jute

The sediment yield estimation was calculated in section 5.7 without any vegetation. This section calculated sediment yield for different angles slopes applied with vegetation and AAB-treated jute reinforcement. A similar procedure in section 5.7 was also followed for all other types of vegetated slopes. The sediment yield values from the experimental investigation are shown in Table 5.8.

5.4.3 Sediment Yield Calculation for Vegetated Slope Using MUSLE Model

Table 5.9 shows the sediment yield values calculated from MUSLE model for different inclinations of slope and different rainfall conditions.

Table. 5.9. Sediment Yield Values calculated from MUSLE model

Slope Inclination	Sediment Yield (Kg) for 10.2 mm/hour Rainfall	Sediment Yield (Kg) for 23.4 mm/hour Rainfall	Type of Reinforcement
30°	1.38	2.32	No reinforcement
	0.41	0.69	Untreated Jute
	0.278	0.46	0.35AAB Jute
	0.29	0.49	0.40 AAB Jute
	0.30	0.532	0.45 AAB Jute
45°	2.16	3.62	No reinforcement
	0.64	1.088	Untreated Jute
	0.43	0.726	0.35AAB Jute
	0.44	0.78	0.40 AAB Jute
	0.46	0.82	0.45 AAB Jute
60°	2.9	4.86	No reinforcement
	0.87	1.45	Untreated Jute
	0.58	0.97	0.35AAB Jute
	0.62	1.05	0.40 AAB Jute
	0.67	1.10	0.46AB Jute

The following calculation was carried out using equation (5.3):

The parameter values $C = 0.7$ and $P = 0.8$ were used in the equation or calculation of sediment yield for plantation criteria.

$$Y = 11.8 \times (Q \times q_p)^{0.56} \times K \times LS \times C \times P$$

For 45° slope with no reinforcement and low rainfall condition

$K = 0.08$ for the current research region (Hyderabad)

$LS = 4.7$, $C = 0.02$ $P = 0.8$

$$Y = 11.8 \times (0.04914 \times 0.000176)^{0.56} \times 0.08 \times 4.7 \times 0.02 \times 0.8$$

$Y = 2.16 \text{ Kg}$

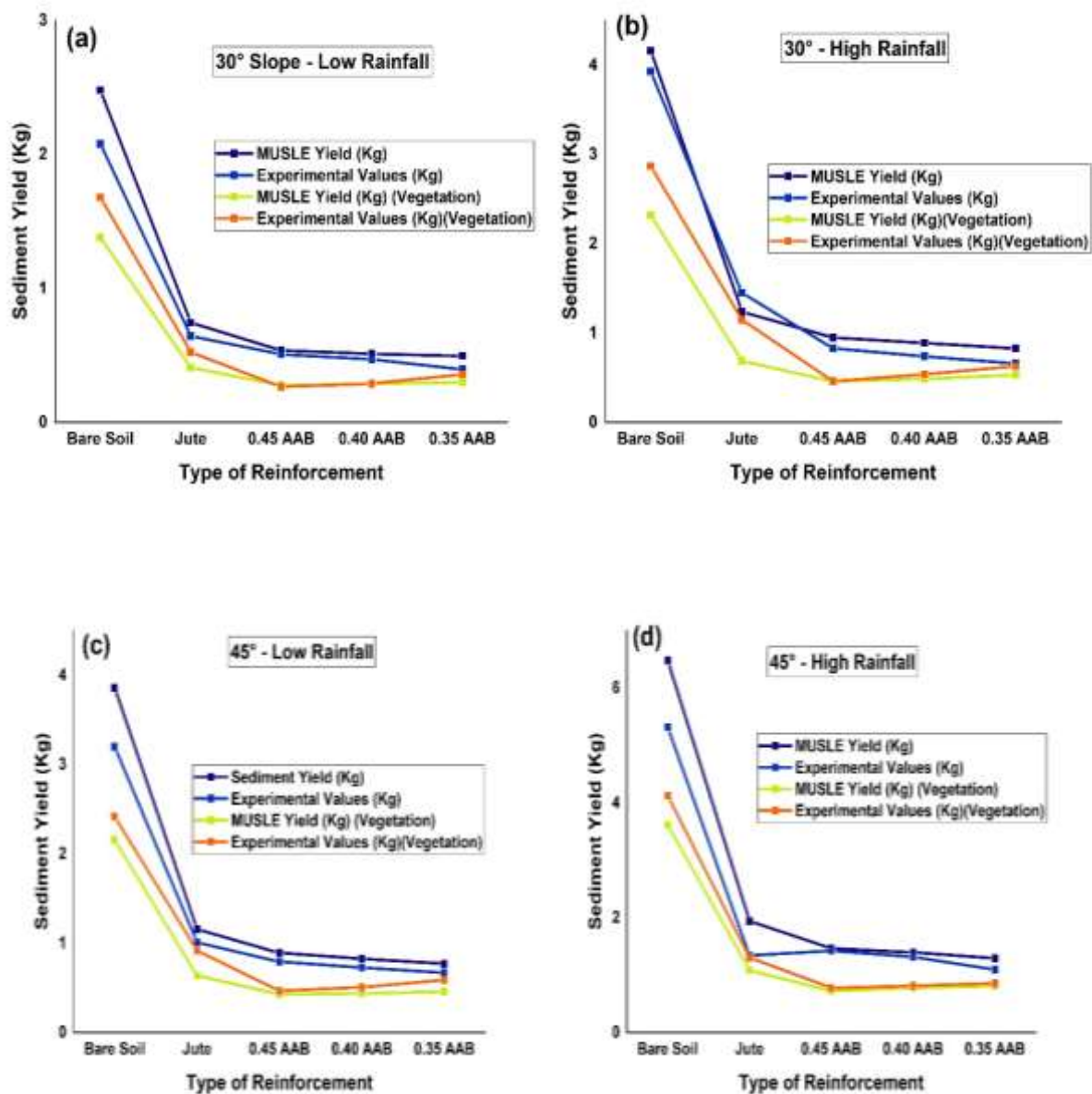
5.5 Results and Validation of Models with Experimental Data

From the sediment yield values obtained from the experimental procedure, as shown in Tables 5.1 and 5.8, it is observed that the surface erosion is greater on bare slopes without any reinforcement and vegetation in both low and high rainfall conditions. These values are used as a reference for comparing the results of various types of reinforcements and vegetation. Untreated jute-reinforced slopes experience more soil erosion during rainfall than treated jute-reinforced and vegetated slopes. When the jute sheet is treated with AAB treatment, the performance varies considerably from 0.35 AAB to 0.45 AAB. Figures 5.1(c-d) and 5.3 demonstrate that the 0.35 AAB is more capable of reducing surface displacements than any other form of reinforcement. It is more effective when combined with applied vegetation than standalone reinforcement. While 0.40 and 0.45 AAB treatments on jute also provide good displacement control, they do so to a lesser extent than 0.35. It is observed from the mix design of AAB that the quantity of AAB solution to treat the jute sheet is more for 0.35 w/s when compared to w/s of 0.40 and 0.45 (Chakravarthy *et al.*, 2021). Since there is enough AAB solution to treat and effectively cover the full jute sheet, the 0.35 AAB treated jute can control erosion more effectively than other reinforcements. It is observed from the experimental work that after one month of exposure to rainfall, the untreated jute reinforcement started to change its colour along with the initiation of the decay process, as shown in Figure 5.1e. However, even after one month of rainfall exposures, AAB-treated jute remains the same as the initial condition, as shown in Figure. 5.1f, which confirms that AAB treatment is more reliable in improving durability.

According to the results from laboratory-scaled model experiments (Figure. 5.1a), soil erosion is directly proportional to the model slope angle. It essentially means that slope steepness significantly impacts soil erosion (Ganasri *et al.*, 2016). Without reinforcement, the sediment yield on a 30° slope is calculated to be lower than on 45° and 60° slopes. Jute reinforcement on soil slopes reduces erosion by 69%, 68.4%, and 66.16% for 30°, 45°, and 60°, respectively, under low rainfall conditions. The highest erosion reduction is 84.10%, 80.5%, and 79% for 30°, 45°, and 60° slopes, respectively, when the slope surface is reinforced with 0.35 AAB jute and vegetation under low rainfall conditions. The second highest erosion reduction is obtained at 80.98%, 79%, and 82% for 30°, 45°, and 60° slopes, respectively, when the slope surface was reinforced with 0.35 AAB jute under low rainfall conditions. Under high rainfall conditions for 30°, 45°, and 60° slopes, applying jute reinforcement reduces erosion by 63%, 74%, and 76%, respectively. For 30°, 45°, and 60°

slopes, the largest reduction in erosion was 84%, 81%, and 83%, respectively, when the slope surface is reinforced with 0.35 AAB treated jute under high rainfall conditions. For 30°, 45°, and 60° slopes, the second largest reduction in erosion is 83.2%, 79%, and 83%, respectively, when the slope surface is reinforced with 0.35 AAB-treated jute under high rainfall conditions. In each case, the reduction percentages are calculated by comparing the bare slope erosion value to the corresponding reinforced angled slope erosion value.

The MUSLE model results are used to validate the findings of the experiments. Figure. 5.4(a-f) illustrates the results of the validation.



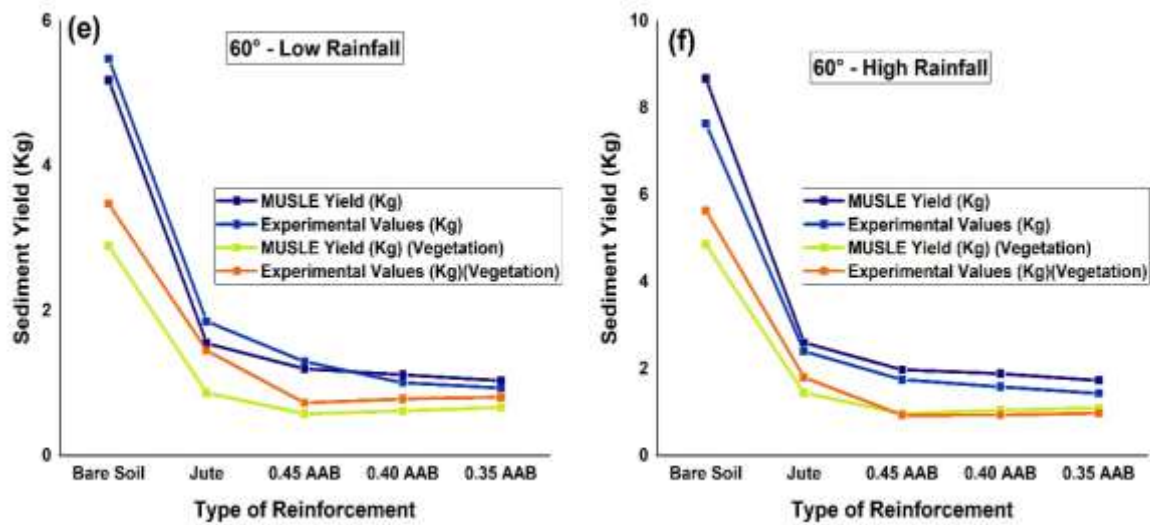


Figure. 5.4. Sediment yield data of (a) 30° slope - low rainfall condition (b) 30 ° slope - High rainfall condition (c) 45 ° slope - Low rainfall condition (d) 45 ° slope - High rainfall condition (e) 60 ° slope - Low rainfall condition (f) 60 ° slope - High rainfall condition

The results of a 45° slope with high rainfall conditions are shown in Figure. 5.4(d). For the bare slope values, 0.35AAB treated the MUSLE model overestimates jute reinforced slope values against experimental values by 21.8% and 17.81%. For 0.45 AAB, treated jute-reinforced slope values are underestimated by the MUSLE model against experimental values by 12.5%. For both 45° normal and vegetated slopes with high rainfall conditions, the linear regression R^2 values for experimental and MUSLE are observed to be 0.98 and 0.99.

The results of the 60° slope with low rainfall conditions are shown in Figure. 5.4(e), The 0.40 AAB and 0.35AAB treated jute reinforced slope values are overestimated by the MUSLE model against experimental values by 10.8% and 10.6%. For the jute, reinforced slope values are underestimated by the MUSLE model against experimental values by 16.18%. Results for untreated jute reinforcement are understated by 17% by MULE calculation. For both 60° normal and vegetated slopes with low rainfall conditions, the linear regression R^2 values for experimental and MUSLE are observed to be 0.99 and 0.97. The results of the 60° slope with high rainfall conditions are shown in Figure. 5.4(f). For the bare slope, 0.45 AAB, 0.40 AAB, and 0.35AAB treated jute reinforced slope values are overestimated by the MUSLE model against experimental values by 13.6%, 13.14%, 18.36%,

and 20.89%. For both 60° normal and vegetated slopes with high rainfall conditions, the linear regression R^2 values for experimental and MUSLE are observed to be 0.99 and 0.99.

The findings indicate that a significant number of results were both underestimated and overestimated. This can be attributed to site-specific factors, such as precipitation parameters, watershed size, land use, and the accuracy of observed sediment data (Kandrika & Venkataratnam, 2005; Sadeghi *et al.*, 2007; Pongsai *et al.*, 2010). The under-prediction and over-prediction limits of the MUSLE model simulation, according to Bingner *et al.*, (1989), are within 20% of the actual values for all analysed storms. These limits are assumed to be good enough for the accuracy of the simulations. In other words, the modelling processes used for natural events can handle an average estimation error of 16.34% for the rainfall events examined (Das, 2000). The major variation in the hydrological response of the soil slope during the rainfall event in terms of the volume of sediment generated is mostly due to geographic and temporal variations in rainfall distribution (Arekhi *et al.*, 2012). The MUSLE model does not consider the change in previous hydrological conditions or the availability of eroded material throughout the watershed in its calculations. Many other related models support this (Arekhi *et al.*, 2012). The sediment yield of this region can still be estimated using the MUSLE model, even if the differences between predicted and actual sediment yields include some errors. Both Walling and Webb (1982) report similar results. Soil erosion prediction may be confidently based on the results of the MUSLE performance evaluation, which concluded that the MUSLE does not need any modifications. It was previously said that the MUSLE calibration was necessary for this conclusion. However, this is directly contradicted by its implementation in locations other than where it was initially established (Nicks *et al.*, 1994; Kinnell & Risse 1998; Khajehee *et al.*, 2001; Rezaeifard *et al.*, 2001; Sadeghi *et al.*, 2007). Other researchers have shown that runoff is a stronger predictor of silt than rainfall (ASCE, 1970; Williams, 1975a, 1975b; Foster *et al.*, 1977; Beasley *et al.*, 1980; Hrissanthous 2005; Sadeghi *et al.*, 2004). It is suggested that using the MUSLE model to predict the sediment yield is acceptable till an estimation error of a maximum of 20%, based on this and past research. It is the best method to implement when compared to USLE and RUSLE models.

5.6 Summary

This chapter discusses the impact of varying rainfall intensities on a laboratory-scale slope model. The slope is reinforced with untreated and treated JGTs of 0.35 AAB, 0.40 AAB, and 0.45 AAB, with and without vegetation. For each case, the soil erosion values are calculated experimentally. The soil erosion values for each case are calculated using the MUSLE model and compared with experimental values. When reinforced with treated JGTs, the experimental soil erosion values decrease more than those of untreated JGTs. The MUSLE model underestimates, for instance, a 60° slope with 0.40 AAB-treated jute by 10.8% and overestimates for 60° slope with jute reinforcement by 17%. Observations indicate that the estimation lies between 0 to 20% for both under and over estimation. The study observed that MUSLE model can help in assessing the soil erosion on slopes, which could assist in implementing preventative measures such slope reinforcement.

CHAPTER 6

Numerical Modelling of Slope Using Finite Element Method

6.1 General

Parametric laboratory investigations can be challenging due to the need for skilled human resources. Numerical models are low-cost methods for understanding experimental data and effectively analysing boundary conditions. Numerical models are utilised to identify slope failure mechanisms through various perspectives, including soil properties, slope geometry, and loading conditions. Numerical models can predict potential failure modes, such as rotational slides, and facilitate efforts towards stabilisation and mitigation strategies. They predict slope stability under different rainfall intensities by determining failure time and critical rainfall intensity and helping to choose the most cost-effective slope stabilisation methods. This study aims to assess the failure behaviour of a reinforced soil slope under different rainfall conditions by employing the commercially available finite element software PLAXIS 2D (V2021).

Due to the complexity of the detachment, movement, and deposition of soil particles, Plaxis 2D has limitations in simulate slope erosion. The Plaxis 2D software lacks erosion models to accurately simulate erosion's effects on slope stability and cannot predict soil erosion based on sediment yield (Tjie, 2014). Hence, to simulate slope failure behaviour due to erosion, it is necessary to consider slope failure time, as discussed in the following sections. Due to the complex interactions between roots, soil, and water, simulating the behaviour of roots in PLAXIS 2D is difficult. It requires discrete elements with orientation, age, and plant health, which is unavailable in Plaxis 2D. To model root behaviour, apparent soil cohesion due to roots can be considered, but this method is inadequate for accurately simulating root structure, orientation, length, and health conditions (Elahi, 2019).

6.2 Formulation of PLAXIS 2D model

Utilizing Plaxis 2D and the plane strain model, a soil slope with similar geometry to the experimental one is simulated. A soil slope, having similar geometry as the experimental one, is modelled using Plaxis 2D, by selecting a model of plane strain. The strength of the slope, having three different slope angles and different reinforcements, is analysed when subjected to two different rainfall conditions.

6.2.1 Geometric Configuration of Model

Various angled soil slopes, such as 30°, 45°, and 60°, are used in the simulation. These slopes are reinforced with untreated jute, 0.35, 0.40, and 0.45 AAB treated jute, and they are exposed to rainfall infiltrations of 10.2 mm/hr and 23.4 mm/hr. The basic laboratory soil slope with 0.9m×0.9m ×0.3m (L x W x H) is constructed, as shown in Figure 5.1. Plaxis 2D model simulates the failure behaviour of slopes of the laboratory scale model in terms of failure time. A scale factor is considered approximately 1:1 in this study.

Plaxis 2D uses plane-strain or axisymmetric 2D finite element models to simulate real-world problems (Figure 6.1). The plane strain model may be effectively used with a uniform cross-section, uniform loading, and a large extent in the z-direction. The normal stresses are evaluated in the Z-direction, whereas displacements and strains are neglected or assumed to be zero. Axisymmetric modelling performs effectively with systems loaded uniformly along a central axis with a constant radial cross-section. The stresses and deformations are assumed to be equal in all directions (Plaxis 2D, 2021).

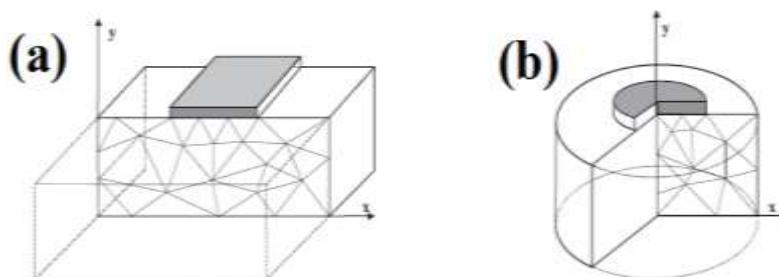


Figure 6.1 Images of (a) plane strain (b) axisymmetric models (PLAXIS 2D, 2021)

To evaluate element deformations, PLAXIS 2D uses triangular elements with 6 or 15 nodes (Figure 6.2). The calculation uses 12 Gauss points for the triangle element with 15 nodes for fourth-order displacements and 3 Gauss points for the triangular element with six nodes for second-order displacements. When a load is applied, the resulting triangular finite element deformations and stresses are aggregated to reflect the overall response of the structure (Brinkgreve *et al.*, 2016). In this investigation, the triangular element with 15 nodes and 12 Gaussian integration points is chosen because of the improved precision in results.

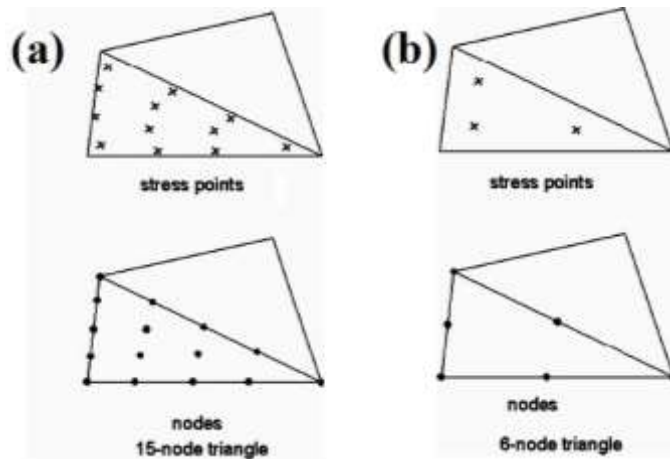


Figure 6.2 Images of (a) 15- Node (b) 6-Node triangular elements (PLAXIS 2D, 2021)

6.2.2 Geogrid Element

Geogrids are characterised by their slender configuration, possessing axial stiffness, whereas they do not have bending stiffness. Geogrids are not capable of withstanding compression and can only endure tension. In most cases, these things represent various types of soil reinforcements. To simulate the JGT in Plaxis 2D, a geogrid element is applied. Reinforcement is laid on the slope's surface to find its ability to protect the slope against rainfall. The jute reinforcements used in this simulation are untreated jute, 0.35, 0.40 and 0.45 AAB treated jute. Axial Stiffness (EA) is the input parameter for the geogrid element. These axial stiffness values are obtained by performing the tensile strength test for geotextiles using Zwick/Roell Z100 testing machine. The properties of geogrid elements are listed in Table 6.1.

Table 6.1. Axial stiffness of untreated and AAB treated jute used in PLAXIS 2D

Parameter	Value (kN/m)
Untreated Jute	17
0.35 AAB Jute	60.2
0.40 AAB Jute	59.21
0.45 AAB Jute	57.4

6.2.3 Soil Properties and Constitutive Model

When stressed or strained, soils exhibit non-linear behaviour. In actuality, soil stiffness is determined by stress, stress path, and strain. These features are part of PLAXIS 2D soil models. One such model is the Mohr-Coulomb material model, used as the constitutive

model in this work. The initial evaluation of soil behaviour is conducted using the well-established Mohr-Coulomb model, which is based on linear elasticity and perfect plasticity. The linear elastic portion of the Mohr-Coulomb model depends upon Hooke's law of isotropic elasticity. The Mohr-Coulomb failure criterion is employed to analyse the fully plastic component within a plasticity framework (Plaxis 2D, 2021). Young's modulus (E), cohesion (c), friction angle (ϕ), unsaturated (γ_{unsat}) and saturated unit weights (γ_{sat}) are input parameters required for this model. To more accurately represent the complex nature of soil behaviour in Plaxis 2D, the Mohr coulomb material model implemented the non-associated plasticity flow rule to ensure a constant dilatancy angle during the simulation procedure. In the case of modelling soil strength as undrained shear strength, the dilatancy angle is set up to zero (Brinkgreve *et al.*, 2016; Tschuchnigg *et al.*, 2016). These parameters are obtained from basic soil tests, as presented in Chapter 3. An undrained condition is considered for the analysis. In an undrained analysis, it is assumed that the rate at which the load is applied is faster than the rate at which excess pore water pressures can dissipate. Hence, the behaviour of undrained conditions is significantly impacted by the characteristics of the soils and the prevailing drainage system (Brinkgreve *et al.*, 2016). Table 6.2 shows the general and mechanical characteristics of the soil.

6.2.4 Ground Water Parameters

To understand the slope failure mechanism caused by rainfall infiltration, mechanical modelling and flow simulation are essential, especially when the groundwater flows in unsaturated soil. Various factors, such as the hydraulic properties of the soil, the initial volumetric moisture content, the intensity of rainfall, and the duration of rainfall, influence the water pressure exerted on slopes (Cai and Ugai, 2004). To assess the hydraulic characteristics of groundwater flow in unsaturated soil zones, a Soil Water Characteristic Curve (SWCC) is defined. The SWCC measures the ability of the soil to retain water under various stress conditions. Various models can be employed to illustrate the hydraulic characteristics of unsaturated soils. In PLAXIS 2D, fully coupled flow-deformation analysis is conducted using Van Genuchten's (1980) model, as described in Chapter 2. The Van Genuchten model is a widely used empirical model for estimating the hydraulic properties of unsaturated soils. The Van Genuchten model is essential for Plaxis 2D because it enables accurate simulation of unsaturated soils, facilitates simulation of different types of soil, accurately simulates the behaviour of unsaturated soil in complex geotechnical scenarios and enhances the accuracy of simulation results. The required input parameters for this model are

the rate of water extraction (g_n), air entry value (g_a), saturated permeability (k_{sat}), residual volumetric water content (S_{res}), and saturated volumetric water content (S_{sat}). The hydraulic properties of soil are listed in Table 6.2.

Table 6.2. Soil and Ground Water Parameters used in Plaxis 2D

Material property	Parameter	Symbol	Value	Unit
	Mechanical Model		Mohr-Coulomb	-
	Material Type		Undrained A	-
Mechanical	Cohesion	c	9.5	kPa
	Friction Angle	ϕ	36°	-
	Modulus of Elasticity	E	25000	kPa
	Poisson's ratio	ν	0.3	-
	Hydraulic Model	-		-
Hydraulic	Saturated Permeability	k_{sat}	1.13x10 ⁻²	mm/s
	rate of water extraction	g_n	2.16	-
	air entry value	g_a	0.91	kPa ⁻¹
General	Dry unit weight	γ_d	17	kN/m ³
	Total unit weight	γ_{sat}	18	kN/m ³

6.2.5 Interface Elements

Interface elements must be created for the reinforcing material to interact fully with the soil. Interface elements model the friction between the geotextile and soil. The modelling of interaction roughness involves the modification of the strength reduction factor (R_{inter}) at the interface. If the soil and geotextile are not sliding relative to one another, $R_{inter} = 1$. When the reinforcement material experiences greater deformation or sliding compared to the soil body, the value of the R_{inter} is less than one. The present soil and geotextile interaction experiment considered R_{inter} 0.9 for untreated jute-soil interaction and 0.8 for AAB-treated jute-soil interaction (Beju and Mandal, 2017). The R_{inter} values for different interfaces are adopted from past research works conducted by Waterman (2006) and Beju and Mandal., (2017). Table 6.3 provides R_{inter} values for different combinations.

Table 6.3. R_{inter} values for different interfaces (Beju and Mandal, 2017)

Interface	R_{inter}
Sand – steel	0.6 – 0.7
Clay - steel	0.5
Sand - Concrete	0.8
Clay - Concrete	0.7
Soil - geogrid	1.0
Soil - geotextile	0.9 – 0.5

6.2.6 Boundary Conditions and Mesh Convergence Study

Approximate results are obtained, and simulation process errors are reduced by applying boundary constraints to the model. The boundary conditions used in the numerical modelling include full fixity at the soil's base and horizontal fixity on all other sides. The problem domain is segmented into finite elements during the mesh generation process. These components are connected at particular points called nodes. The creation of each node contributes a new degree of freedom (DOF) to the structure. Mesh convergence study examines how many elements must be included in the model to minimise the influence of mesh size on the final result. This study uses mesh convergence to identify ideal mesh size for the simulation. Five primary meshing strategies are available in Plaxis 2D: 'very coarse', 'coarse', 'medium', 'fine', and 'very fine', each governed by a 'mesh coarseness factor'. To get accurate numerical results, it is essential to ensure that the mesh is suitably fine. When the very coarse mesh is used, the unique properties of the model are lost. Using a very fine mesh is not a good idea because it will take longer to calculate.

Convergence studies involve varying the number of mesh components to assess the influence of such variations on the obtained outcomes (Fig 6.3) for the 30° unreinforced soil slope model exposed to low rainfall conditions. From Fig. 6.3, it is observed that the results for fine and very fine meshing vary by less than 5%. Hence, in the present study, fine meshing is adopted. The number of elements and nodes generated with variation of mesh coarseness for different inclinations of the slope is provided in Table 6.4. The typical boundary conditions and generated mesh for soil slope are shown in Figure 6.4.

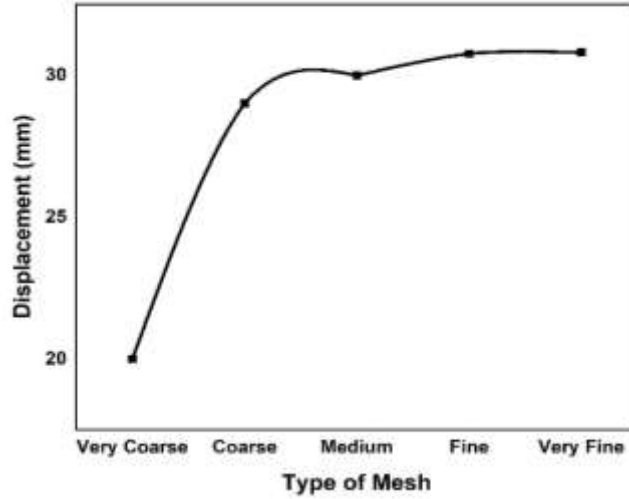


Figure 6.3 Mesh convergence study of 30° unreinforced soil slope

Table 6.4 Number of elements and nodes generated with the variation of mesh fineness

Mesh Fineness	Elements generated for slope angles			Nodes generated for slope angles		
	30°	45°	60°	30°	45°	60°
Very Coarse	68	74	80	597	649	693
Coarse	155	155	164	1315	1319	1393
Medium	242	249	279	2037	2095	2335
Fine	541	591	661	4479	4887	5443
Very Fine	1042	1089	1115	8541	8919	9127

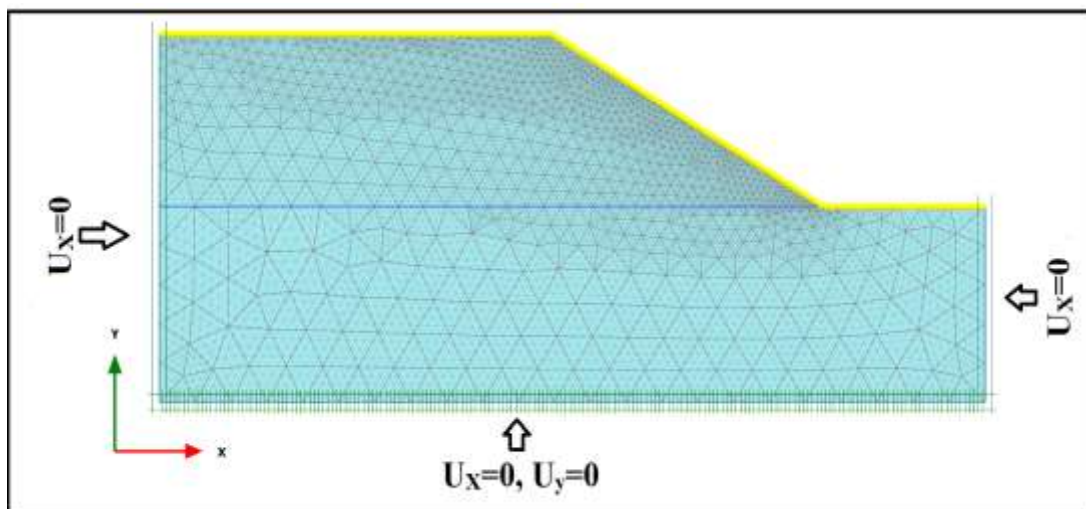


Figure 6.4 Meshing and boundary condition of 30° soil slope reinforced with jute

6.2.7 Ground Water Flow Boundary Condition

Applying groundwater flow boundary conditions to the model enables the simulation of the effects of rainfall in real-world scenarios. Similarly, conducting the same simulation on a 30° slope produces the outcomes depicted in Figure 6.5. The steady-state flow is computed before the appropriate rainfall intensity is applied. Soil ground is supposed to be indicated by a shift in pore water pressure from -100 kPa at top of the slope to 0 kPa at the bottom before the application of precipitation. Precisely the right amount of rainfall intensity is used as a boundary flux along the sides of FE, DC, and ED inclines to replicate the laboratory scale slope model. The boundaries between AB are fixed in all directions, whereas BC and FA are vertically fixed, as shown in Figure 6.5.

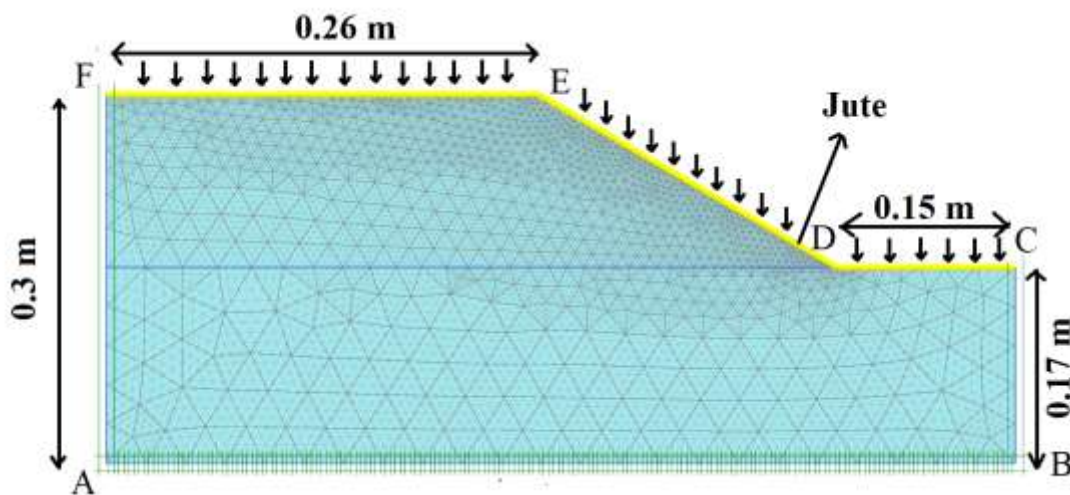


Figure 6.5 Groundwater flow boundary condition applied for 30° slope

6.2.8 Staged Construction

ΣM_{stage} in Plaxis 2D is a load intensity indicator that begins at 0 and is supposed to reach one after calculation. This number has to be established concerning the difficulty of the problem. If ΣM_{stage} is 1, then the load is being applied normally. In the initial phase, stresses are calculated using the gravity loading type calculation and the construction is carried out in two phases:

Phase-1: Generation of initial stresses (Gravity loading)

Phase-2: Application of rainfall infiltration (Fully coupled flow-deformation)

6.2.9 Factor of Safety Analysis

When performing the design of a slope, it is of greatest significance to take into account the stability considerations of the slope, specifically the factor of safety (FOS). Using reduced parameters, Plaxis 2D determines FOS. A multiplier called ΣM_{sf} is used and gradually raised to reduce the strength parameters until failure occurs. If the value of ΣM_{sf} at failure is reasonably consistent over a series of load steps with continuous deformations, it is called the safety factor (Brinkgreve *et al.*, 2016).

6.3 Validation of Plaxis 2D Results with Past Research Work

The model validation is carried out by validating the deformation values of slopes subjected to low rainfall intensity under unreinforced conditions. A literature study by Ali *et al.* (2019) has been utilised to validate the methods for assessing unreinforced slopes under low rainfall intensity using a 60° unreinforced slope. The boundary conditions were kept constant, as mentioned in the literature. This study's slope was analysed using experimentally obtained soil characteristics, whereas Ali *et al.* (2019) work soil properties were used as a reference. The rainfall intensities of 13.75 and 10.2 mm/hr, as reported by Ali *et al.* (2019) and in the present study, are employed. Maximum deformational values of the unreinforced slope were compared with data obtained from the literature study after performing the numerical simulation, as shown in Figure 6.6. The validation demonstrated high concordance with previous research. The trend for the obtained results was the same for both literature and present simulation works, i.e., the deformation values increased as the duration increased, as observed from the literature. In the present study, various untreated and 0.35, 0.40 and 0.45 AAB-treated jute were considered as reinforcement, whereas soil nailing was taken as reinforcement in the literature. However, in Figure 6.6, in both the reference and the present study, unreinforced soil was considered.

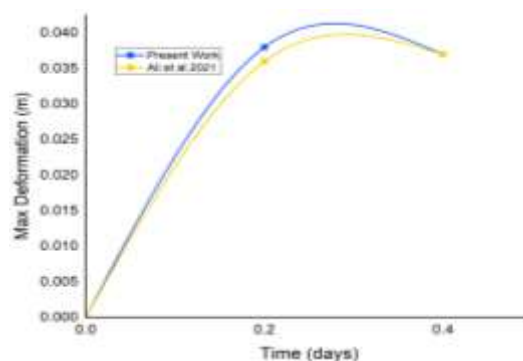


Figure 6.6. Validation of Plaxis 2D Results

6.4 Results and Discussions

Ten cases with different combinations of unreinforced and reinforced slope and rainfall intensities were experimentally analysed in the laboratory-scale slope model. Figures 6.7 and 6.8 show the failure situations at the end of experiments. Following a one-hour exposure to continuous rainfall, the 45° angled unreinforced slope shown in Figure 6.8(a) experiences the formation of gullies, ultimately leading to slope failure after 1.5 hours. Conversely, the 45° angled slope reinforced with jute shown in Figure 6.8(b) does not exhibit any gully formation, but the slope failure occurred after 2.2 hours due to development of gullies. These pictures were taken diagonally above the slopes. Initially, no run-off was observed in any of the cases because of the infiltration of rainwater into the soil. After that, red soil mixed with rainwater started flowing from the slopes and small holes started developing on the surface of slopes, which eventually turned into gullies. The highest sediment yield values reported during this failure process were 65, 72, and 85 kilogrammes for slopes of 30°, 45°, and 60°, respectively. After reaching these maximum sediment yield values, slope collapse occurred. These maximum sediment yield values were used as a reference to calculate failure times for other reinforced slopes. For instance, a 30° angled slope resulted in sediment yield value of 65Kgs in 6.37 hours, which is considered as slope failure time. The sediment yield and failure time values for slopes of 30°, 45°, and 60° are presented in Table 6.5(a). The data indicates that a slope without reinforcement, with inclinations of 30°, 45°, and 60°, experienced failure after 2.5, 1.5, and 1.17 hours, respectively, when exposed to uninterrupted low-intensity rainfall. Similarly, the slope failed after 1.54, 1.3, and 1.06 hours, respectively, when subjected to continuous high rainfall intensities under unreinforced conditions.

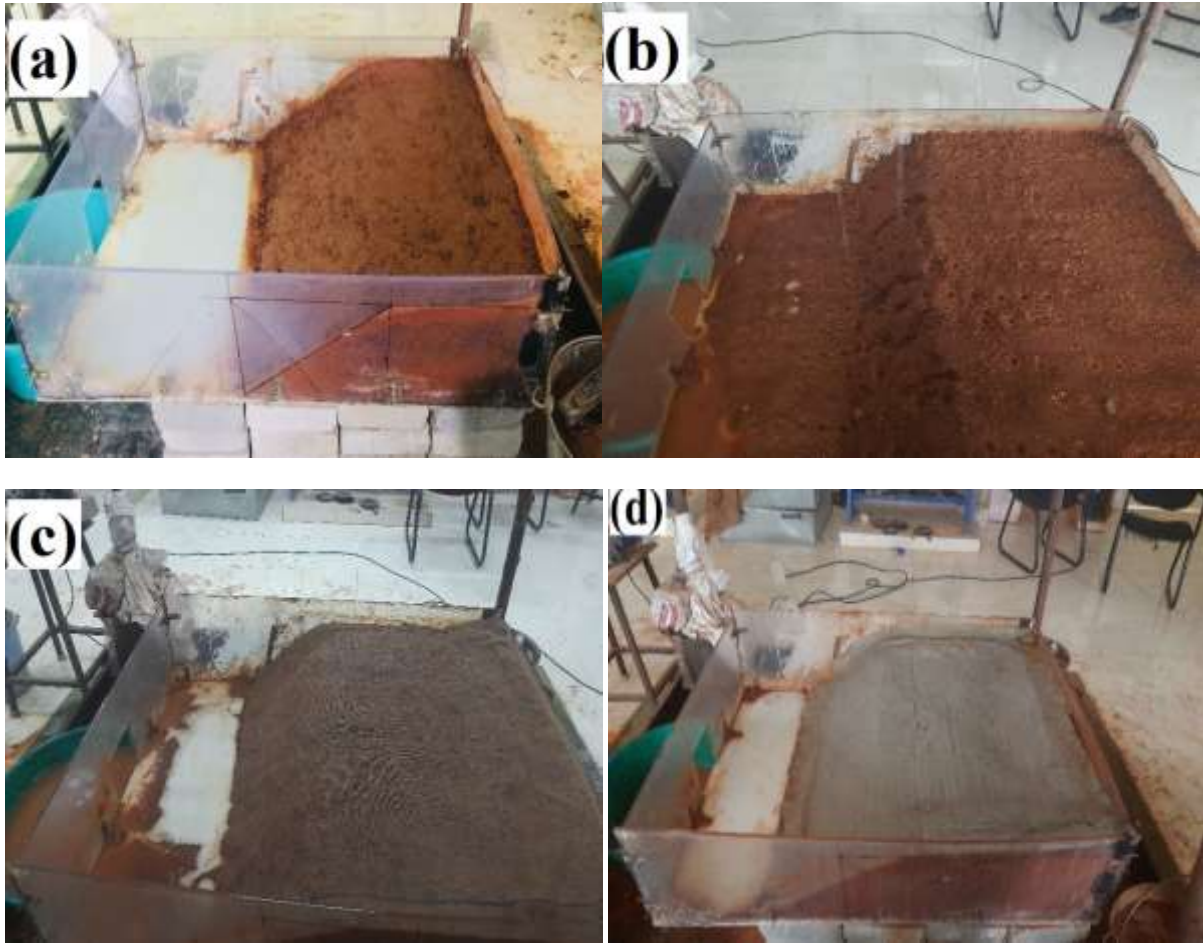


Figure 6.7. Images of a) 45° slope before rainfall; b) 45° slope exposed to 23.4 mm/hr rainfall; c) slope reinforced 0.35 AAB jute; d) slope reinforced with untreated jute



Figure 6.8. Images of a) 45° unreinforced slope; b) 45° jute reinforced slope after exposure to high rainfall for a period of 1 hr

Table 6.5(a) Sediment yield at the time of slope failure for reinforced slopes under rainfall

Condition	Low Rainfall (Hours)		High Rainfall (Hours)	
	Time	Sediment Yield (Kg)	Time	Sediment Yield (Kg)
30° - Unreinforced	2.5	65	1.54	65
30° - Jute	4.32	64	3	64
30° -0.35 AAB Jute	6.37	65	5.81	65
30° -0.40 AAB Jute	6.21	66	5.4	66
30° -0.45 AAB Jute	5.95	64	5.1	64
45° - Unreinforced	1.5	72	1.3	72
45° - Jute	2.2	72.5	2	72.5
45° -0.35 AAB Jute	2.87	71	2.3	71
45° -0.40 AAB Jute	2.65	72	2.1	72
45° -0.45 AAB Jute	2.46	71.9	2.05	71.9
60° - Unreinforced	1.17	85	1.06	85
60° - Jute	1.65	83	1.60	83
60° -0.35 AAB Jute	1.81	82	1.73	82
60° -0.40 AAB Jute	1.75	82.8	1.54	82.8
60° -0.45 AAB Jute	1.72	83.1	1.53	83.1

Failure behaviour of unreinforced and reinforced slopes was simulated when exposed to rainfall by numerical modelling of various angled slopes using the Plaxis 2D software. The simulation was carried out on 30°, 45°, and 60° slopes under unreinforced and reinforced conditions when exposed to low and high rainfall conditions. In the simulation, the slopes failed due to low and high rainfall intensities after a certain exposure period, as shown in Table 6.5(b). These periods were considered as slope failure times for numerically modelled slopes. The deformed shapes of the numerically modelled slope are shown in Figure 6.7.

Table 6.5(b) Slope failure times for both experimental and numerical simulation

Condition	Low Rainfall (Hours)		High Rainfall (Hours)	
	Numerical	Experimental	Numerical	Experimental
30° - Unreinforced	2.41	2.5	1.60	1.54
30° - Jute	4.84	4.32	2.63	3
30° -0.35 AAB Jute	5.81	6.37	5.51	5.8
30° -0.40 AAB Jute	5.74	6.21	5.37	5.4
30° -0.45 AAB Jute	5.68	5.95	5.15	5.1
45° - Unreinforced	1.94	1.5	1.55	1.3
45° - Jute	2.13	2.2	2.08	2
45° -0.35 AAB Jute	2.39	2.87	2.18	2.3
45° -0.40 AAB Jute	2.32	2.65	2.14	2.1
45° -0.45 AAB Jute	2.31	2.46	2.13	2.05
60° - Unreinforced	1.17	1	1.06	0.9
60° - Jute	1.65	1.5	1.60	1.2
60° -0.35 AAB Jute	1.81	2.4	1.73	2
60° -0.40 AAB Jute	1.75	2.15	1.54	1.89
60° -0.45 AAB Jute	1.72	2.1	1.53	1.75

The analysis of slope failure behaviours is described from various perspectives, such as slope angle, rainfall intensity, and reinforcement criteria. Table 6.5(b) shows duration for slope failure decreased with an increase in slope angle for both low and high rainfall events. Factors contributing to this reduction include increased gravitational force, reduced shear strength, and increased soil erosion. The gravitational force on a soil mass and slope inclination angle are directly proportional. The increased gravitational force can cause higher soil stresses, potentially leading to shear failure along weak planes. Increased pore water pressure caused by rainwater penetration into a slope may decrease its effective stress and shear strength. This reduction in slope stability makes it more vulnerable to failure. Runoff erosion, positively correlated with slope angle, can displace soil sediment and expose

weakened layers, decreasing slope stability and potentially causing slope failure (Jing et al., 2019).

In the design of slopes, considering rainfall intensity is a crucial factor. Using PLAXIS 2D for numerical simulation of slope failure behaviour under different rainfall intensities allows engineers to model and assess slope stability effectively. The results of this study indicate that an increase in rainfall intensity is associated with a decrease in the time it takes for slopes of varying angles to experience failure. The change from low to high rainfall intensity reduced the failure time of a 30° unreinforced slope from 2.5 to 1.54 hours. High rainfall can increase the driving forces on a slope, making it more vulnerable to collapse. Additionally, high-intensity rainfall can affect groundwater conditions, raising the groundwater table and imposing additional pressure on the slope. Slope failure was caused by increased infiltration, increased unsaturated zone moisture content, and decreased matric suction. (Hossain *et al.*, 2013).

The increase in slope failure time for various angled slopes can be attributed to factors such as installing geotextiles on the soil's top surface. Geotextiles act as a barrier to dissipate tensile stresses, reducing the likelihood of soil movement and slope failure. They also enhance soil's cohesive properties and improve the internal resistance of soil particles against shear deformation. Geotextile material reduces soil particle detachment and erosion during rainfall events, ultimately prolonging the time for slope failure. The 30° slope with 0.35 AAB jute reinforcement had maximum slope failure times of 6.37 hours and 5.81 hours, while the 60° slope with 0.35 AAB jute reinforcement had maximum failure times of 1.81 hours and 1.73 hours, in the numerical simulation and experimental works as shown in Table 6.5(b). Unreinforced slopes with a 45° inclination experienced failure after 1.5 hours, while reinforced slopes resisted failure by mitigating the failure zone in the numerical simulation, as shown in Figure 6.7.

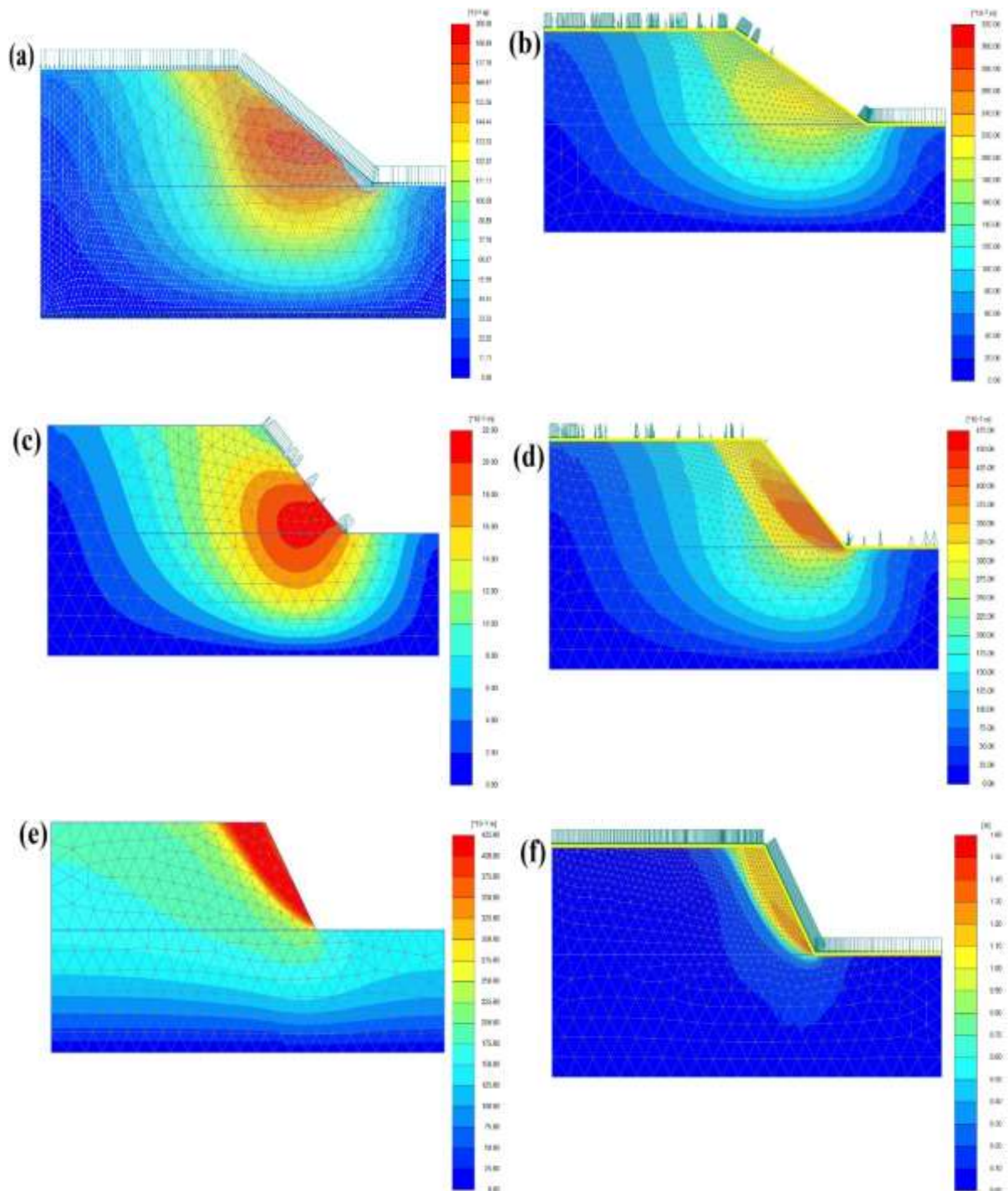


Figure 6.9. Deformed images of a) 30° slope without any reinforcement; b) 30° with jute reinforcement; c) 45° slope without any reinforcement; d) 45° slope with jute reinforcement; e) 60° slope without any reinforcement; f) 60° slope with jute reinforcement under low rainfall condition

Geotextiles absorb rainwater, reducing its impact on soil surfaces and preventing erosion. 0.35 AAB-treated jute reinforcement significantly increases slope failure time when exposed to rainfall, making it suitable for steeper slopes to mitigate the impact of slope angle and

intensity on stability, because of its high tensile strength and physical properties like more thickness than 0.40 and 0.45 AAB jute (Chakravarthy *et al.*, 2021). According to Vibha et al. (2021), adding reinforcements has mitigated the likelihood of failure by facilitating water drainage from the pores during rainfall. As a conclusion from this study, it can be stated that less angled slopes, such as 30° slopes, showed more slope failure time than 60° slopes. However, 60° slopes exposed to low and high rainfall intensities significantly increase slope failure time when reinforced with untreated and various w/s AAB-treated JGTs, primarily with 0.35 AAB jute.

The face-type rotational slope failure is observed in simulation results, as shown in Figure 6.7 (a, c, and e), which is caused by several factors, such as soil saturation, increased pore water pressure, and reduced soil cohesion. Rainfall intensity can cause soil to become saturated, losing its shear strength. Increased rainfall duration and intensity can increase pore water pressure, making the soil more susceptible to failure. Rainfall can cause soil particles to disperse, reducing cohesiveness, and when water infiltrates, they detach and move apart, reducing interlocking forces between particles and soil cohesion. Figure 6.7 (b, d, and f) reveals that the applied reinforcement protected it from rotational failure due to the rain effect. These reinforcements act as a barrier to the effect of rainfall on the slope's surface towards saturation, pore water changes, and protection of soil cohesion by preventing soil particle detachment caused by rainfall.

The slope failure durations for both numerical simulation and experimental procedures are shown in Figure 6.10, which indicates a difference between the numerical simulation and the experimental outcomes. The difference in the slope failure time can be attributed to basic assumptions, material characteristics, boundary conditions, and modelling techniques.

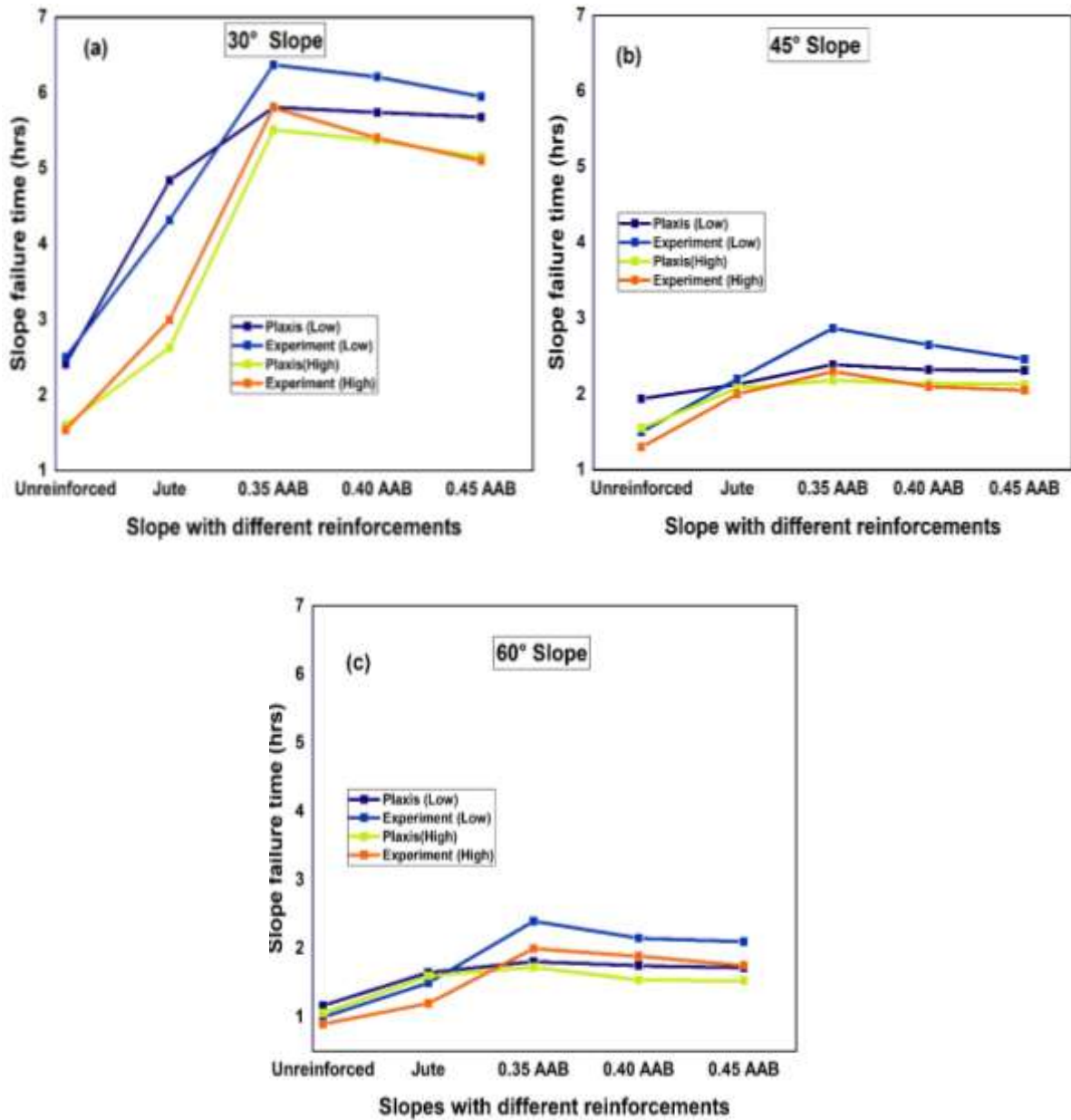


Figure 6.10. Slope failure time images of a) 30° unreinforced slope, b) 45° jute reinforced slope, c) 60° jute reinforced slope

The above assumptions may not comprehensively account for complex characteristics and variations of real-life situations. As a result, differences can develop between the numerically simulated and experimentally observed behaviours, leading to fluctuations in the duration of slope failure. The Plaxis 2D software relies upon many input parameters, including soil strength, stiffness, and cohesion. Variability in the slope's material properties is possible because of its heterogeneity and anisotropy, and these variations can potentially affect the timing of slope failure. Establishing boundary conditions, including constraints and applied

loads, for Plaxis 2D simulations may not precisely align with the real-world scenario, and modifying boundary conditions can affect the slope response, influencing the failure time.

As shown in Table 6.6, the FOS value is important when analysing the stability of various slopes. First, based on the low rainfall conditions, the maximum FOS value obtained for the 30° slope is 2.72, while the minimum FOS value obtained for the 60° slope is 1.476 without any reinforcement. With 0.35 AAB treated jute reinforcement, the 30° slope was highly stabilised with a higher FOS value of 3.88 under low rainfall conditions. It was observed from the results that the angle, rainfall intensity, rainfall duration, and reinforcement had a major impact on slope stability. Considering the slope angle criterion, 30° slopes are more stable than 45° and 60° slopes. In consideration of reinforcement criteria, reinforced slopes have a higher FOS value than unreinforced slopes. 0.35 AAB-treated jute reinforcement has the greatest FOS value among all applied reinforcements for all slope angles. However, as the duration of rainfall increases, reinforcement can stabilise the soil compared to its unreinforced condition. 0.35 AAB-treated jute reinforcement has been observed to be more stable than 0.40 and 0.45 AAB-treated jute reinforcements.

Table 6.6 Factor of Safety Values of Slopes

Type of Slope	Type of reinforcement	Low Rainfall	High Rainfall
30° Slope	Unreinforced condition	2.72	2.29
	Untreated jute	3.35	3.15
	0.35 AAB treated jute	3.88	3.66
	0.40 AAB treated jute	3.80	3.58
	0.45 AAB treated jute	3.70	3.48
45° Slope	Unreinforced condition	1.89	1.79
	Untreated jute	2.63	2.53
	0.35 AAB treated jute	3.19	3.02
	0.40 AAB treated jute	3.07	2.95

	0.45 AAB treated jute	2.98	2.86
	Unreinforced condition	1.476	1.45
	Untreated jute	1.98	1.927
60° Slope	0.35 AAB treated jute	2.474	2.36
	0.40 AAB treated jute	2.38	2.28
	0.45 AAB treated jute	2.33	2.23

6.5 Parametric Analysis

Parametric analysis using Plaxis 2D provides numerous benefits, such as sensitivity analysis, design optimisation, risk assessment, informed decision-making, and robustness analysis. Design optimisation focuses on economically efficient designs, mitigating construction risks, and enhancing overall performance, whereas sensitivity analysis examines the effect of input parameters on slope structures. Risk assessment helps identify critical parameters that contribute to unfavourable outcomes, allowing for informed decisions regarding risk mitigation and the maintenance of stability and safety. Analysis of robustness evaluates the stability and robustness of slope systems, identifying potential failure mechanisms and vulnerabilities. In this study, parametric analysis is carried out from different perspectives, such as the effect of variation in rainfall intensities and the effect of variation in slope geometry.

6.5.1 Effect of Variation of Rainfall Intensities

This parametric analysis considers a slope of 8 meters, taking reference from the Udaipur railway embankment, constructed in 2016 (IRICE, 2023). The findings of the Plaxis 2D simulation indicated that the slope, which had undergone reinforcement using 0.35 AAB treated jute, exhibited the highest level of stability among the simulated slopes when subjected to rainfall. According to the data, the optimal slope angle for maximum safety is 30°. Therefore, in this parametric study, the slope angle of 30°, along with the 0.35 AAB treated jute reinforcement, is considered. The slope is exposed to various rainfall intensities ranging from 10mm/hr to 100mm/hr. These rainfall ranges are obtained from Zope et al. (2016) study, which reflects rainfall occurrences in the Colaba area, Mumbai, Maharashtra,

India. The Plaxis 2D simulation is conducted on a slope with the above-mentioned rainfall intensities, and the FOS values of the slope are shown in Figure 6.11. The figure demonstrates a correlation between rainfall intensity and the FOS values. Specifically, when there is an increase in rainfall, the FOS values consistently decrease. However, it is important to note that the application of 0.35 AAB-treated jute reinforcement has a notable effect on the FOS values. Results from this study suggest that the utilisation of 0.35 AAB reinforcement is considered safe, even when employed on slopes exposed to rainfall of up to 100 mm/hr.

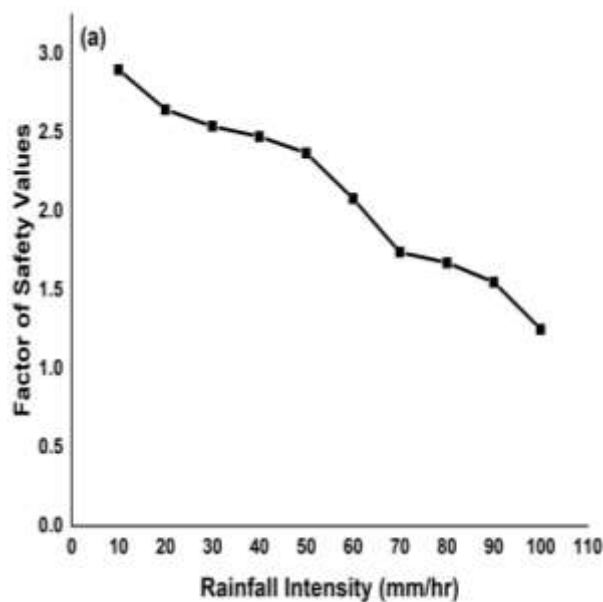


Figure 6.11. Factor of safety values of 8m height 30° slope reinforced with 0.35AAB jute

6.5.2 Effect of Variation of Geometry of Slope

This study examines the effect of slope angle variation on slope stability by constructing eight meters height slope at varying angles (30°, 45°, 55°, 60°, and 70°). The slope is reinforced with a jute reinforcement of 0.35 AAB. The maximum safety factor obtained with 10mm/hr rainfall intensity in the Plaxis 2D simulation, this rainfall is applied in this analysis on different angled slopes. The FOS values after performing the Plaxis 2D simulation is shown in Figure 6.12. The results show that a decrease in the FOS value can be observed as the slope angle increases. Among all different angled slopes, the 30° slope angle is observed to be more stable, with the highest FOS value of 2.9. Using 0.35 AAB-treated jute reinforcement has also resulted in a FOS value greater than 1, even for a 70° slope. Results

from this study suggest that the utilisation of 0.35 AAB reinforcement is considered safe, even when employed on slopes with steep angles of up to 70°.

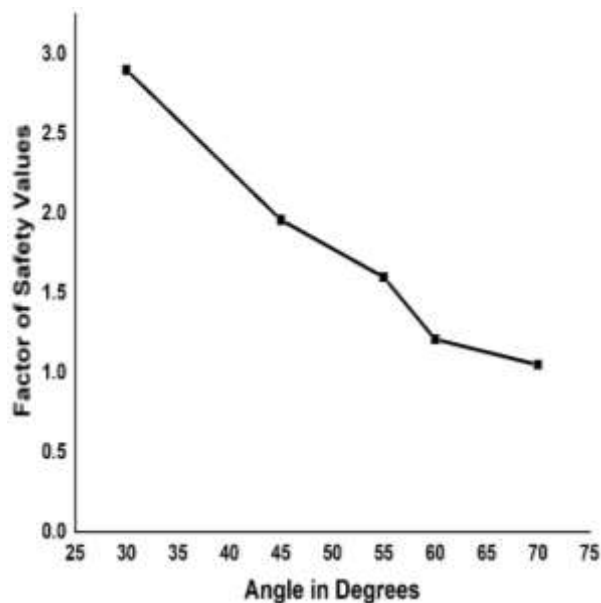


Figure 6.12. Factor of safety values of 8m high slopes with varying slope angles

6.6 Summary

The slope angle and rainfall intensity are critical parameters in designing slopes, as it affects slope stability, shear strength analysis, deformation behaviour, design optimization, a saturation of slope material, seepage behaviour, time-dependent behaviour, construction phasing, all of which can impact the stability and performance of the slope. This chapter discusses the simulation of slope stability under rainfall effects using a finite element method software called Plaxis 2D. The stability behaviour of the slope with the various untreated and treated reinforcements exposed to rainfall is discussed in detail in this chapter. In this simulation process, the slope is reinforced with untreated and 0.35 AAB, 0.40 AAB, and 0.45 AAB treated JGTs. The slopes with varying angles of 30°, 45°, and 60° are used for simulation. The slope stability is discussed regarding slope failure time with respect to variations in slope angle, rainfall intensity and reinforcement criteria. Analyses of slope stability can be utilized to make informed decisions regarding the design of slopes and mitigation of risks. This analysis is useful to design safe and cost-effective slopes and embankments which are exposed to rainfall, as well as to identify vulnerable sections of the slope. The results demonstrated that including 0.35 AAB reinforcement could help improve the stability slope by increasing the failure time due to the rainfall effect.

CHAPTER 7

Conclusions

7.1 General

The use of natural materials for slope stabilisation is justified by the need to utilise environmentally acceptable materials in the construction sector to prevent environmental contamination. Natural geotextiles face biodegradability problems, which limit their use in geotechnical structures including retaining walls, slopes, and river bank protection. Controlling the potentially harmful impacts of geosynthetic materials on the environment, while also utilising construction industry wastes like fly ash is of utmost importance in modern times, especially in developing nations.

The goal of the current study is to create a technique for the environmentally responsible and sustainable use of natural materials in slope stabilisation. This dissertation comprehensively explores the study of the durability of JGTs and the applicability of treated JGTs for reducing soil erosion and improving the strength of soil slopes. The research findings are explained in the subsequent sections, providing specific conclusions.

7.2 Summary and Conclusions

Using plant roots and natural fibres to stabilise slopes and reducing surface erosion has recently gained popularity. Natural geotextiles such as coir, jute, and sisal provide immediate protection when installed in the ground. There are no negative environmental impacts associated with their use and their slow biodegradation contributes essential nutrients to the soil. As the vegetation grows, it helps to anchor the soil and prevent erosion. Plant roots, particularly those of certain grasses and shrubs, can stabilize slopes effectively and reduce erosion.

However, natural fibres have a relatively limited lifespan. Therefore, it is essential to take the appropriate measures to extend the service life of these fibres. It is necessary to develop a new environmentally and economically friendly treatment methodology for improving the durability of JGTs. The present study proposes to utilize the alkali activate binder (AAB) treatment to improve the durability and shelf life of natural geotextiles. This AAB treatment uses fly ash as the main ingredient.

In the beginning, a critical review of different treatment methods available for natural geotextile along with their durability studies and application of the same to reduce surface erosion and improve the strength of soil slopes has been carried out and presented in Chapter 2. This review has given a broad insight into the existing knowledge and limitations of different studies related to erosion and strength of soil slopes, which brought out the scope of the present study. The effect of AAB treatment on the mechanical and microstructural properties of jute, when subjected to different durability tests, is studied in detail. The effect of untreated and treated JGTs on the erosion of soil slopes due to rainfall is studied extensively by constructing a laboratory-scale artificial rainfall set-up. Furthermore, detailed numerical analysis using Plaxis 2D, a commercially available finite element software, is conducted to study the improvement in the strength of soil slopes using untreated and treated JGTs under different rainfall conditions. The specific conclusions of the research work are presented chronologically in the following sections.

7.2.1 Microstructural Characterization of Untreated and Treated Jute

Natural geotextiles are preferable to synthetic geotextiles since they have less environmental impact and are less expensive. Additionally, using fly ash as a treatment element helps the environment by reducing the disposal of fly ash and the accompanying costs. Treating jute to increase strength, durability, and performance requires laborious processes and expensive chemicals. Therefore, the current research develops a novel method for treating JGT with an AAB solution of varying w/s ratios (0.35–0.45) to enhance the soil strength. A series of microstructural tests using a stereomicroscope, FTIR, SEM, XRD, and TGA are carried out on untreated, and AAB-treated soil JGTs. The important findings may be highlighted as follows:

- According to the stereomicroscopic tests, the colour of untreated JGTs darkened after exposure to an acidic test. In contrast, AAB-treated jute was able to withstand this change. Due to the efflorescence effect of the alkaline test, both untreated and AAB-treated JGTs exhibit white patches on their surfaces. As a result of the AAB coating, the roughness of the jute fabric surface is reduced. As the w/s ratio rises, the AAB coating layer becomes soft, limiting JGTs flexibility.
- According to the SEM/EDS analysis, more N-A-S-H is generated at higher w/s ratios. These aluminosilicates have more pores than others, which increased their permeability. However, at lower w/s ratios, this aluminosilicate occurs in much smaller quantities. As a

result, the porosity is reduced, leading to increased load bearing capacity and decreased permeability. The results of the permeability and tensile strength tests confirm these observations.

- FTIR and TGA analysis indicate that after AAB coating, the characteristics of untreated jute are maintained to a large extent. According to XRD findings, the amorphous quality of sodium aluminate silicate hydrate from alkali-activated fly ash becomes more prominent with increasing w/s ratio.
- Compared to untreated jute, AAB-treated jute forms a new crystalline phase (Quartz, Mullite, Hydroxy sodalite and Analcine) due to the predominant behaviour of alkali-activated fly ash observed from XRD analysis.

7.2.2 Durability Studies of Untreated and Treated Jute

Different durability tests, including soil burial, compost burial, acid and alkali exposure, and water hydrolysis, are conducted on untreated and treated natural geotextiles for 30, 60, 90 and 180 days. Surface texture, morphology, chemical bond changes, weight loss, tensile strength, and elongation at failure (fibre breaking) are examined to evaluate durability performance. The important findings are summarised as follows:

- It has been shown that untreated jute degrades at a faster rate than treated jute. It has been noticed that untreated jute threads become brittle and readily dissolved into fragments after being buried in soil and compost for 180 days. However, after undergoing AAB treatment, the jute fabric becomes rigid and chemically resistant.
- After being exposed to acid for 180 days, the weight loss is around 91.38% for the untreated samples, while the same is reduced to 42.67% for 0.35 AAB jute samples. It is observed that 0.35 AAB jute textile exhibits the minimum weight loss after 180 days when exposed to acid and soil burial tests. After 180 days, the same treatment shows minimum weight loss for soil burial, compost burial, and acid and alkali exposure.
- The reduction in elongation at break for untreated jute is more when compared to other treated JGTs. Among all the treated samples, reduction in elongation at breakage is observed to be lowest for 0.35 AAB. The highest reduction of 92.9% in elongation is observed for untreated jute when exposed to an acidic attack. It is also observed that elongation at breakage decreases with increased w/s ratio and exposure time.

- When all of the findings are considered, it can be stated that jute treated with AAB containing 0.35 w/s outperforms the other treatment ratios. However, compared to other w/s values, the workability this ratio is lower and tends to harden quickly.

7.2.3 Experimental Assessment of Erosion Control of Treated Soil Slopes

An artificial rainfall setup has been built to evaluate the stability of a laboratory scale model when reinforced with natural geotextiles. To verify the experimental findings, MUSLE numerical modelling is used. The following conclusions were drawn from the artificial rainfall in the investigation.

- Soil slopes without any reinforcement are at high risk of severe soil erosion because of the direct effect of rainfall on bare soil, which causes soil particles to separate and subsequently create gullies.
- Soil erosion is more likely to occur when there is more rain and it lasts longer. High-intensity rainfall on a 30° bare slope causes 47% more soil erosion. Rain causes soil erosion due to increased runoff, flow velocity, and soil structure deterioration. Runoff carries soil particles when it rains heavily because soil cannot absorb the excess water. Water velocity increases as more water flows over the soil surface, causing erosion. Heavy rains can dislodge soil particles from their original position and cause them to lose their structure, making them more prone to erosion. When the slope angle increases from 30° to 60°, additional erosion occurred at 62.2% in low and 48.2% in high rainfall conditions. This excess increase in soil erosion results from increased discharge and flow velocity as water flows with increased gravitational force from the top to the bottom of a slope. On steeper slopes, raindrops travel longer distances and obtain more momentum in contact with the soil surface.
- When jute reinforce is placed on soil slopes, it works as a mesh-like structure that retains soil particles and prevents erosion. Additionally, jute fibres can absorb water and swell, forming a barrier that slows water passage down the slope. This reduces the danger of erosion by slowing down the movement of water and soil particles. Untreated jute reinforcement on soil slopes reduces erosion by 68.6%, 68%, and 66 % on slopes of 30°, 45°, and 60° under conditions of low precipitation respectively, but it was also prone to a biodegradability risk. Before using JGTs to reinforce soil on slopes, it is best to treat the geotextiles appropriately to improve their durability.

- Treated JGTs can help reduce soil erosion more effectively than untreated JGTs when exposed to rainfall. They have an AAB coating that repels water, reducing the amount of water absorbed by the material. Additionally, they have improved tensile strength, allowing them to better resist the forces of water flow and prevent soil erosion. They can also be made to have a higher density, which improves their ability to filter sediment and prevent soil particles from being carried away by water flow. 0.35 AAB jute reinforcement effectively minimised erosion compared to 0.40 and 0.45 AAB JGTs. 0.35 AAB jute treatment reduced 81% of erosion for a 60° slope under high rainfall conditions.
- Bermuda grass can be used in conjunction with geotextiles to reduce soil erosion on slopes exposed to rainfall. The combination of Bermuda grass and geotextiles can provide a synergistic effect, providing both immediate and long-term protection against soil erosion. Bermuda grass is a drought-resistant grass species that can grow well on slopes and provide effective soil cover to prevent erosion. Its root system can bind soil particles together and create a stable soil structure, making it a good complement to geotextiles. Bermuda grass vegetation with 0.35 to 0.45 AAB JGTs substantially reduced erosion. 0.35 AAB jute treatment along with Bermuda grass was the most efficient reinforcement, reducing erosion by 84% and 83.4% for 30° and 60° slopes, respectively, under high rainfall conditions.
- The MUSLE (Modified Universal Soil Loss Equation) model is useful for estimating soil erosion under variable rainfall intensities. Observations based on the MUSLE model showed that the MUSLE-calculated sediment yield values are comparable to those from experiments. 79.9% to 95.8% of MUSLE results and experimental data are matching each other. Based on the results, the MUSLE model can design soil slopes to estimate soil erosion under various rain intensities.

7.2.4 Numerical Modelling of Strength of Treated Soil Slopes

Plaxis 2D, a finite element program, is used to execute the numerical simulation and determine the stability of a slope. This numerical modelling is performed on a slope subjected to varying rainfall intensities and reinforced with untreated and AAB-treated JGTs. The subsequent findings are derived from the Plaxis 2D simulation employing a fully coupled flow deformation analysis.

- The analysis demonstrates a significant correlation between the intensity of rainfall and the duration of slope failure. Slope instability is caused by rainwater infiltration, which increases pore water pressure and reduces effective stress in the soil. As the intensity of rainfall increased from 10.2 mm/hr to 23.4 mm/hr, the duration of slope failure decreased. For a 30° unreinforced slope, the time interval for slope failure decreased from 2.5 hours to 1.54 hours.
- Slope failure time is prolonged by reinforcing the slope to counteract the effects of rainfall. The reinforcement can enhance the shear strength of the soil and add tensile strength to resist failure time. When rainfall occurs, the reinforcement can distribute external loads more uniformly across the slope, decreasing the likelihood of localised failure and increasing the slope failure time. With 0.35 AAB-treated jute reinforcement, failure time under low rainfall intensity increased from 2.5 to 6.37 hours for a 30° slope, and 1.54 to 5.8 hours for high rainfall intensity. The 0.35 AAB jute reinforcement was the most effective in enhancing the lifespan of slopes under varying rainfall conditions, by increasing the slope failure time.
- The degree of steepness of the slope is an important factor in the aspect of slope failure time, as observed in numerical simulations. As the slope's angle increases, the slope failure initiation occurs within a shorter duration. The gravitational force exerted on a soil mass is directly proportional to the angle of inclination of the slope. The increased gravitational force can induce increased stresses within the soil, potentially leading to slope failure. The time required for slope failure decreased from 2.41 to 1.17 hours as the slope angle increased from 30° to 60°. However, the implementation of 0.35 AAB treated jute reinforcement measures reduced the impact of steepness on the occurrence of slope failure, by increasing the slope failure time up to 5.81 to 1.81 hours 30° to 60° angled slopes.
- The 0.35 AAB treated jute reinforcement application improved the slope's stability by increasing the soil's shear strength and providing additional tensile strength to increase the slope failure time. Under lower rainfall conditions, a 30° slope with a reinforcement resulted in a maximum slope failure time of 6.37 hours.
- A parametric study evaluated the effectiveness of 0.35 AAB-treated jute reinforcement in stabilising a large slope with a height of 8 metres. The study involved varying the slope angle from 30° to 70° and changing the rainfall intensity from 10 mm/hr to 100 mm/hr.

The objective was to assess the suitability of the 0.35 AAB treated jute reinforcement in enhancing the stability of the slope. The results indicate that increased rainfall intensity and slope angle decreases the safety factor. Still, the slope remains stable with a safety factor greater than one even when exposed to 100 mm/hr rainfall and a slope inclined at 70°.

7.3 Contributions made by the scholar

The proposed treatment method for treating natural geotextiles employs fly ash as a binder. India produces approximately 106.37 to 133.9 million tonnes of extremely fine fly ash annually (CEA 2022), according to (IRC SP:20-2002). In developing nations such as India, the dispersal of industrial waste byproducts (such as fly ash) is a significant issue. Using this waste material AAB treatment enhances the durability properties of natural geotextiles by eliminating the need for disposal. These techniques eliminate the need for traditional treatment methods and reduce the costs associated with landfill disposal. As the majority of thermal plants donate fly ash, the price of producing AAB is also lesser. India is one of the greatest producers of natural fibre in the world. Many slope stabilisation and embankment works are reinforced with natural JGTs, but this material and other geotextile such as coir, sisal, and hemp are naturally biodegradable. AAB improves the strength and durability properties of jute. This technique will provide a sustainable and cost-effective method for enhancing the durability of natural geotextiles through the use of fly ash as the primary component.

The present study concentrates on increasing the service life of natural geotextiles through the use of environment-friendly and cost-effective applications. Durability experiments are conducted to determine the effect of AAB treatment on JGTs. In addition, a comprehensive microstructure analysis is performed to understand the chemical reaction between jute and AAB. Using various untreated and treated JGTs, an attempt is made to reduce soil erosion and stabilizing the variously angled soil slopes that are exposed to rainfall. To reduce soil erosion and stabilize the slope in the long term, the slope is bio engineering with Bermuda grass in conjunction with this AAB-treated JGT. To understand the reinforcement effect on the stability behaviour of the slope, numerical modelling is conducted using the finite element software Plaxis 2D. Perhaps this will be a novel study in which the durability and strength of natural geotextiles are enhanced. This treated natural

material is the best alternative to synthetic geotextiles for enhancing slope stability and reducing surface erosion. The proposed technique can be used by construction professionals to increase the durability of natural geotextiles and improve the stability of slopes by reducing surface erosion. It is hoped that the purpose of this thesis is to convince geotechnical engineers and practitioners to adopt the usage of waste materials, enviro-safe AAB as an ecologically preferable alternative to the conventional binder used in ground improvement methodologies.

7.4 Recommendations for Future Research

This research focuses on using industrial by-products in construction technology and highlights the microstructural, physical, and durability features of untreated and treated JGTs. Carbon dioxide (CO₂), nitrous oxide (N₂O), and methane (CH₄) are some of the greenhouse gases that may be minimized by restricting the use of conventional binders to increase the durability of natural geotextiles. The features will change, however, if the location and origin of the samples are changed. There has to be more work done to support and improve the results of the existing investigations. The suggestions for further study are as follows.

- Application of AAB treatment to other natural geotextiles (coir, hemp, sisal) to enhance their durability before soil slope reinforcement.
- Numerical modelling of erosion and comparison with experimental results.
- The effectiveness of AAB-treated natural geotextiles in preventing soil erosion can be evaluated using a field-based slope erosion model.
- Research on the influence of earthquakes or seismic forces on soil bioengineering.
- Dimensional study for untreated and treated jute

7.5 Design Procedure and Practical Application of Vegetation along with AAB Treated Jute

The design procedure for the practical application of treated jute with vegetation is described below. The first stage involves the preparation and cost of AAB jute. The mass ratio of 10.57:129.43:400 between sodium hydroxide, sodium silicate, and fly ash is considered in this study (Gupta et al., 2018). The cost for a 1 square metre jute sheet is 35 Indian Rupees. Fly ash, sodium silicate, and sodium hydroxide costs are 4.8/-, 81/- and 106.2/- Indian Rupees per kg (Chottemada et al., 2023).

Quantities of components required to cover 1 m² for addressing erosion = 1 m² jute + 2.18 kg of fly ash + 0.058 kg of NaOH + 0.706 kg of Na₂ SiO₃ + 0.498 kg of H₂O

Cost for treated jute to cover 1 m² area = 35 + 4.8*2.18+0.058*106.2+81*0.706= 108.8/-

The second stage involves the application of vegetation along with reinforcement. Once the AAB-treated jute sheets have been acquired, they should be evenly laid down on a soil slope and fixed properly using nails. For vegetative purposes, it is necessary to create holes with a diameter of 0.05m and 0.05 to 0.1m deep holes on an AAB jute sheet. The fully-grown plants are taken as a bunch and transplanted at a distance of 0.15m on the jute sheet. Water is regularly sprayed over the plants until vigorous plant regrowth occurs.

Combining alkali-activated binder-treated jute with plant growth for soil slope stabilization entails treating jute fibers with a specially produced alkali-activated binder to improve strength and durability. This treated jute is then used to protect slopes from erosion. The establishment of root networks on these stabilized slopes adds to long-term stability. Jute treated with alkali-activated binder strengthens the soil and prevents erosion, while planted plants provide ecological advantages. This ecologically friendly method offers instant stabilization while also ensuring long-term slope stability. Regular monitoring and maintenance are essential for this integrated solution's sustained efficacy.

References

- Abderrahim B, Abderrahman E, Mohamed A, Fatima T, Abdesselam T, Krim O (2015) Kinetic thermal degradation of cellulose, polybutylene succinate and a green composite: a comparative study. *World J Environ Eng* 3:95–110.
- Abdulkhani, A., E. H. Marvast, A. Ashori, Y. Hamzeh, and A. N. Karimi. 2013. "Preparation of Cellulose/Polyvinyl Alcohol Biocomposite Films Using 1-N-Butyl-3-Methylimidazolium Chloride." *International Journal of Biological Macromolecules* 62: 379–386.
- Aggarwal, P. and Sharma, B. (2010). Application of jute fiber in the improvement of subgrade characteristics. In *Proceeding of international conference on advances in civil engineering, Trabzon, Turkey* (pp. 27-30).
- Akhtaruzzaman, M., Roy, S., Mahmud, M. S., & Shormin, T. (2020). Soil Properties Under Different Vegetation Types in Chittagong University Campus, Bangladesh. *Journal of Forest and Environmental Science*, 36(2), 133–142.
- Akter N, Saha J, Das SC, Khan MA. (2018). Effect of bitumen emulsion and polyester resin mixture on the physic mechanical and degradable properties of jute fabrics. *Fibers* 6(3):44
- Allen, S.R. (1996). Evaluation and standardization of rolled erosion control products. *Geotextiles and Geomembranes* 14, 207–221.
- Al Bakri, A. M., H. Kamarudin, M. Bnhussain, I. K. Nizar, A. R. Rafiza, and Y. Zarina. 2012. "The Processing, Characterization, and Properties of Fly Ash Based Geopolymer Concrete." *Reviews on Advanced Materials Science* 30: 90–97.
- AL-Hameidawi, B. H., Aodah, H. H., & Shala, H. (2016). Experimental And Numerical Evaluation for Improvement of Underlying Layers of Road's Pavement Using Jute Fibre Sheets. *Al-Qadisiya Journal for Engineering Sciences*, 9, 461-478.
- Allahverdi, A., Kani, E.N., Hossain, K.M.A. and Lachemi, M., 2015. Methods to control efflorescence in alkali activated cement-based materials. In *Handbook of alkali activated cement, mortars and concretes* (pp. 463-483). Woodhead Publishing.
- Álvarez-Mozos, J., Abad, E., Giménez, R., Campo, M. A., Goñi, M., Arive, M., & Diego, I. (2014). Evaluation of erosion control geotextiles on steep slopes. Part 1: Effects on runoff and soil loss. *Catena*, 118, 168-178.

- Andersson, M. and Tillman, A.M. (1989). Acetylation of jute: Effects on strength, rot resistance, and hydrophobicity. *Journal of applied polymer science*, 37(12), pp.3437-3447.
- Anil, K.R. (2006). The study on use of geotextile for soil and water conservation under varying slopes. Kerala Agriculture University, Kerala, India, Coir Board.
- Angulo-Martínez, M., Begueria, S., Navas, A., Machín, J. (2012). Splash erosion under natural rainfall on three soil types in NE Spain. *Geomorphology* 175-176, 38-44.
- Arshad, Khubaib, and Muhammad Mujahid. Biodegradation of textile materials. University of Borås/Swedish School of Textiles, 2011.
- Arekhi, S., Shabani, A. and Rostamizad, G. (2012). Application of the modified universal soil loss equation (MUSLE) in prediction of sediment yield (Case study: Kengir Watershed, Iran). *Arabian Journal of Geosciences*, 5(6), pp.1259-1267.
- Arunavathi, S., Eithiraj, R.D. and Veluraja, K., 2017, May. Physical and mechanical properties of jute fiber and jute fiber reinforced paper bag with tamarind seed gum as a binder-An eco-friendly material. In *AIP Conference Proceedings* (Vol. 1832, No. 1, p. 040026). AIP Publishing LLC.
- ASCE (American Society of Civil Engineers). (1970). Sediment sources and sediment yields. *J Hydraul Div ASCE* 96 (HY6):1283–1329.
- ASTM D 4595. (2017). Standard Test Method for Tensile Properties of Geotextiles by Wide-Width Strip Method. West Conshohocken, PA: American Society for Testing and Materials.
- ASTM G160-12 (2019) Standard practice for evaluating microbial susceptibility of non-metallic materials by laboratory soil burial. ASTM, West Conshohocken.
- Avni, Y. (2005). Gully incision as a key factor in desertification in an arid environment, the Negev highlands, Israel. *Catena* 63:185–220.
- Aydilek, A.H., D Hondt, D. and Holtz, R.D., 2007. Comparative evaluation of geotextile pore sizes using bubble point test and image analysis. *Geotechnical Testing Journal*, 30(3), p.173.
- Babu, G.S., 2006. An introduction to soil reinforcement and geosynthetics. Universities Press.

- B. Pandey, K. Bajaj, A.P Singh. (2013) Soil Stabilization Using Pozzolanic Material And Jute Fibre, Proceedings of Indian Geotechnical Conference, December 22-24, Roorkee.
- Balan K .(1995). Studies on engineering behaviour and uses of geotextile with natural fibres. Ph.D. Thesis, Indian Institute of Technology Delhi, India.
- Balan, K., Venkatappa Rao, G. (1996). Erosion control with natural geotextiles. In: Rao, G.V. Banerjee, P.K. (1996). Development of new synthetic products through blends of natural fibres. In: Rao, G.V., Banerjee, K. (Eds.), Environmental Geotechnology with Geosynthesis. The Asian Society for Environmental Geotechnology and CBIP, New Delhi, pp. 337–346.
- Basu G, Roy AN, Bhattacharyya SK, Ghosh SK .(2009). Construction of unpaved rural road using jute synthetic blended woven geotextile. A case study. *Geotext Geomembr* 27(6):506–512.
- Batista KC, Silva DAK, Coelho LAF, Pezzin SH, Pezzin APT. (2010). Soil biodegradation of PHBV/peach palm particles bio composites *J Polym Environ* 18(3):346–354.
- Beguería, S., Angulo-Martínez, M., Gaspar, L., Navas, A. (2015). Detachment of soil organic carbon by rainfall splash: Experimental assessment on three agricultural soils of Spain. *Geoderma* 245-246, 21-30.
- Baroghel-Bouny, V., Basset-Mens, C., & Gautier, J. (2017). Soil reinforcement with natural fibers: Laboratory experiments on jute and coir geotextiles. *Geotextiles and Geomembranes*, 45(1), 56-64.
- Beasley DB, Huggins LF, Monke EJ. (1980). ANSWERS: a model for watershed planning. *Trans Am Soc Agri Eng* 23:938–944.
- Beju, Y.Z. and Mandal, J.N., 2017. Combined use of JGT-EPS geofoam to protect flexible buried pipes: Experimental and numerical studies. *International Journal of Geosynthetics and Ground Engineering*, 3(4), pp.1-20.
- Beninia KCCC, Voorwald HJC, Cioffi MOH. (2011). Mechanical properties of HIPS/sugarcane bagasse fiber composites after accelerated weathering. *Proc Eng* 10:3246–3251.
- Bewket, W., Sterk, G. (2003). Assessment of soil erosion in cultivated fields using a survey methodology for rills in the Chemoga watershed, Ethiopia. *Agric. Ecosyst. Environ.* 97,

81–93.

- Bingner RL, Murphee CE, Mutchler CK. (1989). Comparison of sediment yield models on various watersheds in Mississippi. *Trans ASAE* 32(2):529–534.
- Bhattacharyya R., Smets T., Fullen M.A., Poesen J., Booth C.A. (2010). Effectiveness of geotextiles in reducing runoff and soil loss: a synthesis. *Catena* 81:184-95.
- Bhattacharjee, D. and Viswanadham, B.V.S. (2018). Effect of geocomposite layers on slope stability under rainfall conditions. *Indian Geotechnical Journal*, 48(2), pp.316-326.
- Booth, C. A.; Fullen, M. A.; Sarsby, R. W.; Davies, K.; Kurgan, R.; Bhattacharyya, R.; Poesen, J.; Smets, T.; Kertesz, A.; Toth, A.; Szalai, Z.; Jakab, G.; Kozma, K.; Jankauskas, B.; Trimirka, V.; Jankauskienė, G.; Bühmann, C.; Paterson, G.; Mulibana, E.; Nell, J. P.; van der Merwe, G. M. E.; Guerra, A. J. T.; Mendonça, J. K. S.; Guerra, T. T.; Sathler, R.; Zheng, Y.; Li, Y.; Panomtarachichigul, M.; Peukrai, S.; Thu, D. C.; Cuong, T. H.; Toan, T. T.; Jonsyn-Ellis, F.; Jallow, S.; Cole, A.; Mullholland, B.; Dearlove, M.; Corkill, C. (2007). The BORASSUS Project: aims, objectives and preliminary insights into the environmental and socio-economic contribution of biogeotextiles to sustainable development and soil conservation, in *Proc of the 3rd International Conference on Sustainable Development and Planning III (2)*. Ed. by Kungolos, A. G.; Brebbia, C. A.; Beriatos, E. 25–27, Algarve, Portugal. WIT Press, 601–610. ISBN 978-1-84564-102-3.
- Bordoloi, S., Garg, A. and Sekharan, S., 2017. A review of physio-biochemical properties of natural fibers and their application in soil reinforcement. *Advances in Civil Engineering Materials*, 6(1), pp.323-359.
- Bouazza, A., Freund, M. and Nahlawi, H.(2006). “Water retention of nonwoven polyester geotextiles,” *Polymer Testing*, Vol. 25, No. 8, pp.1038-1043.
- B. Pandey, K. Bajaj, A.P Singh. (2013).” Soil Stabilization Using Pozzolanic Material And Jute Fibre”, *Proceedings of Indian Geotechnical Conference*, December 22-24,2013, Roorkee.
- Brinkgreve RBJ, Swolfs WM, Engine E (2016) *PLAXIS user’s manual*, PLAXIS bv, The Netherlands.
- Broda, J., Przybyło, S., Kobiela-Mendrek, K., Binias, D., Rom, M., Grzybowska-Pietras, J., Laszczak, R. (2016). Biodegradation of sheep wool geotextiles. *Int.Biodeterior.*

Biodegrad. 115, 31e38. <https://doi.org/10.1016/j.ibiod.2016.07.012>.

Broda J, Gawłowski A, Przybyło S, Biniaś D, Rom M, Grzybowska- Pietras J, Laszczak R .(2018). Innovative wool geotextiles designed for erosion protection. *J Ind Text* 48(3):599–611.

Broda, J., Gawłowski, A., Przybyło, S., Biniaś, D., Rom, M., Grzybowska-Pietras, J. and Laszczak, R. (2018). Innovative wool geotextiles designed for erosion protection. *Journal of Industrial Textiles*, 48(3), pp.599-611.

Brown III WM, Sitar N, Saarinen TF, Blair M. (1982). Overview and summary of debris flows, landslides, and floods in the San Francisco Bay region, January 1982. In: Conference on debris flows, landslides, and floods in the San Francisco Bay region, Stanford University, Stanford, CA, USA, pp 1–66.

Browne, M. A., Galloway, T., & Thompson, R. (2007). Microplastic-an emerging contaminant of potential concern? Learned discourses. *Integrated Environmental Assessment and Management*, 3, 559–561. <https://doi.org/10.1002/ieam.5630030412>.

Brunton, D.A., Bryan, R.B. (2000). Rill network development and sediment budgets. *Earth Surf. Process. Landf.* 25, 783–800. BS EN 14030:2001 Geotextiles and geotextile-related products. Screening test method for determining the resistance to acid and alkaline liquids (ISO/TR 12960:1998, modified).

Buhmann, C., Paterson, D.G., Pienaar, G.M.E., Nell, J.P., Mulibana, N.E., Deventer, P.W., Fullen, M.A., Subedi, M. & Sarsby, R.W. (2010). Rainfall simulator study of the erosion control potential of palm geotextiles for mine dam slope stabilization. In: *Construction for a sustainable environment* (eds. R.W. Sarsby & T. Meggies), pp. 443–452. Taylor & Francis Group, London.

Buragadda V, Thyagaraj T .(2019). Bearing capacity of JGT-reinforced sand bed. *Int J Geosynth Ground Eng* 5(4):1–14.

Cai, Q.G., Zhu, Y.D., Wang, S.Y. (2004). Research on processes and factors of rill erosion. *Adv. Water Sci.* 15 (1), 12–18 (in Chinese, with English Abstract).

Cai, F. and Ugai, K. (2004). Numerical analysis of rainfall effects on slope stability. *International Journal of Geomechanics*, 4(2), pp.69-78.

Chottemada, Pujitha Ganapathi, Arkamitra Kar, and Patricia Kara DeMaeijer."Environmental Impact Analysis of Alkali-Activated Concrete with Fiber

- Reinforcement." *Infrastructures* 8, no. 4 (2023): 68.
- Choudhury, P. K., Arindam Das, D. N. Goswami, and T. Sanyal.(2009). "Bio-engineering approach with JGT for slope stabilization." In *Geosynthetics in Civil and Environmental Engineering: Geosynthetics Asia 2008 Proceedings of the 4th Asian Regional Conference on Geosynthetics in Shanghai, China*, pp. 863-867. Springer Berlin Heidelberg.
- Costantinesco, I.(1976). Soil conservation for developing countries, *FAO Soil Bulletin*, 30, 74–86.
- Coppin NJ, Richards IG. (2007). Use of vegetation in civil engineering. Construction Industry Research and Information Association, London
- Choudhary, A. K., Gill, K. S., & Jha, J. N. (2011). Improvement in CBR values of expansive soil subgrades using Geo synthetics. *Guru Nanak Dev Engineering College Ludhiana (Punjab)-141006*, 155.
- Chakrabarti SK, Saha SG, Paul P, Dewan AR, Das K, Chowdhury PK, Gon DP, Ray P .(2016). Specially treated woven JGTs for river bank protection. *Indian J Fibre Text Res (IJFTR)* 41(2):207–211.
- Chakrabarti, S.; Saha, S.; Paul, P.; Dewan, A.; Das, K.; Chowdhury, P.; Gon, D.; Ray, P.(2016). Specially treated woven JGTs for river bank protection. *IJFTR* 41, 207–211.
- Chakravarthy, G.S., GuhaRay, A. and Kar, A. (2021). Effect of soil burial exposure on the durability of alkali activated binder-treated JGT. *Innovative Infrastructure Solutions*, 6(2), pp.1-10.
- Chauhan, N., Singh, R., & Patel, R. K. (2019). Slope stability analysis using geotextile. *Journal of Geotechnical Engineering and Geosciences*, 5(1), 27-33.
- Chee SS, Jawaid M, Sultan MTH, Alothman OY, Abdullah LC. (2019). Accelerated weathering and soil burial effects on colour, biodegradability and thermal properties of bamboo/kenaf/epoxy hybrid composites. *Polym Test* 79:106054.
- Chen C, Yin W, Chen G, Sun G, Wang G. (2017). Effects of biodegradation on the structure and properties of windmill palm (*Trachycarpus fortunei*) fibers using different chemical treatments. *Materials* 10(514):1–10.
- Chen, X., Wang, Y., & Zhang, Z. (2021). Study on the stability of slopes covered with flax

- geotextile. *Journal of Soil and Water Conservation*, 66(1), 23-29.
- Chen CY, Chen TC, Yu FC, Tseng CC. (2005). Rainfall duration and debris -Flow initiated studies for real monitoring. *Environ Geol* 47(1):715–724.
- Chin, S. C., Tong, F. S., Doh, S. I., Lim, K. S., & Gimbun, J. (2020). Effect of Soil Burial on Mechanical Properties of Bamboo Fiber Reinforced Epoxy Composites. In IOP Conference Series: Materials Science and Engineering (Vol. 736, No. 5, p. 052016). IOP Publishing.
- Cho, S. E. (2014). Probabilistic stability analysis of rainfall induced landslides considering spatial variability of permeability. *Engineering Geology*, 171, 11–20.
- Choudhury P K and Sanyal T. (2010). Embankment slope stabilization with JGTs – A case study in NH-2 Allahabad by-pass. (In) Indian Geotechnical Conference – 2010, Mumbai, pp 731-4ghosh.
- Daria, M., Krzysztof, L. and Jakub, M. (2020). Characteristics of biodegradable textiles used in environmental engineering: A comprehensive review. *Journal of cleaner production*, 268, p.122129.
- Das G. (2000). Hydrology and soil conservation engineering. Prentice-Hall, India.
- Dasgupta T. (2014). “Soil Improvement By Using JGT And Sand,” *Int. J. Sci. Eng. Technol.*, vol. 884, no. 3, pp. 880–884.
- Datta, U. (2007). “Application of JGTs.” *Journal of Natural Fibers* 4 (3): 67–82.
- Dash BN, Sarkar M, Rana AK, Mishra M, Mohanty AK, Tripathy SS . (2002). A study on biodegradable composite prepared from jute felt and polyesteramide (BAK). *J Reinf Plast Compos* 21(16):1493–1503
- Das, P. & Biswas, D. (2017). Study on the use of JGT in retaining wall construction. *International Journal of Engineering Research and Technology*, 6(9), 534-538.
- Davidovits, J. (1994). “Properties of geopolymer cements.” *Alkaline Cements and Concretes*, Kiev, Ukraine, 1–19.
- Davies, K., Fullen, M.A. & Booth, C.A. (2006). A pilot project on the potential contribution of palm-mat geotextiles to soil conservation. *Earth Surface Processes and Landforms*, 31, 561–569.
- Dawit Kanito, Samuel Feyissa. (2021). Comparison and Applicability of Selected Soil

- Erosion Estimation Models. *Hydrology*. Vol. 9, No. 4, pp. 79-87. doi: 10.11648/j.hyd.20210904.12
- Day RW and Axten GW. (1989). Surficial stability of compacted clay slopes. *Journal of Geotechnical Engineering*, ASCE 115(4): 577–580.
- Dayte, K.R., Gore, V.N. (1994). Application of natural geotextiles and related products. *Geotextiles and Geomembranes* 13, 371–388.
- Debnath, M. C., & Bhowmick, D. (2011). An experimental investigation on the effect of JGT on the stability of slopes. *Indian Geotechnical Journal*, 41(4), 391-402.
- Decoursey, D.G. and Snyder, W.M. (1969). Computer-oriented method of optimizing hydrologic model parameters. *Journal of Hydrology*, 9(1), pp.34-56.
- Department of School Education, Tamil Nadu. (2020). Higher Secondary First Year Botany.
- Dixon, N., Raja, J., Fowmes, G. and Frost, M., 2016. Sustainability aspects of using geotextiles. In *Geotextiles* (pp. 577-596). Woodhead Publishing.
- Dittenber DB. (2012). Effect of alkalization on flexural properties and moisture absorption of kenaf fiber reinforced composites. In: International SAMPE technical conference.
- Dhungana, N., Silwal, N., Upadhaya, S., Khadka, C., Regmi, S. K., Joshi, D., & Adhikari, S. (2020). Rural coping and adaptation strategies for climate change by Himalayan communities in Nepal. *Journal of Mountain Science*, 17, 1462-1474.
- Donat M. (1995). Bioengineering techniques for stream-bank restoration. A review of central European practices. Watershed restoration program. Ministry of Environment, Lands and Parks, and Ministry of Forests, Vancouver.
- Elahi, T.E., Islam, M.A. and Islam, M.S., 2019, January. Effect of vegetation and nailing for prevention of landslides in Rangamati. In *Proceedings, international conference on disaster risk mitigation (ICDRM 2019)*, Dhaka, Bangladesh (pp. 193-197).
- EN ISO 13934-1:1999, Textiles — Tensile properties of fabrics —Part 1: Determination of maximum force and elongation at maximum force using the strip method.
- Erpul, G., Gabriels, D., Cornelis, W.M., Samray, H., Guzelordu, T. (2009a). Average sand particle trajectory examined by the Raindrop Detachment and Wind-driven Transport (RD806 WDT) process. *Earth Surface Processes and Landforms* 34, 1270-1278.
- Erpul, G., Gabriels, D., Cornelis, W.M., Samray, H., Guzelordu, T. (2009b). Sand transport

under increased lateral jetting of raindrops induced by wind. *Geomorphology* 104, 191-202.

Ering, P., & Babu, G. S. (2016). Probabilistic back analysis of rainfall induced landslide-A case study of Malin landslide, India. *Engineering Geology*, 208, 154–164.

Fakhrul T, Islam MA. (2013). Degradation behavior of natural fiber reinforced polymer matrix composites. *Proc Eng* 56:795–800.

Faruk, O., Bledzki, A. K., & Fink, H. P. (2010). MohiniSain,,,. Biocomposites reinforced with natural fibers: 200-2010, 1552-1596.

Freer R. (1991). Bio-engineering: the use of vegetation in civil engineering. *Constr Build Mater* 5(1):23–26.

Fredlund, D.G. and Rahardjo, H. (1993). *Soil mechanics for unsaturated soils*. John Wiley & Sons.

Foster GR, Meyer LD, Onstad CA. (1977). A runoff erosivity factor and variable slope length exponents for soil loss estimates. *Trans Am Soc Agri Eng* 20(4):683–687.

FTIR LINKS- <https://www.sigmaaldrich.com/IN/en/technical-documents/technical-article/analytical-chemistry/photometry-and-reflectometry/ir-spectrum-table>

Ftir link 2- Merck KGaA, IR Spectrum Table & Chart, Merck KGaA, Darmstadt, Germany (2022). <https://www.sigmaaldrich.com/IN/en/technical-documents/technical-article/analytical-chemistry/photometry-and-reflectometry/ir-spectrum-table>. Accessed: 29 June 2022

Fullen, M.A., Booth, C.A., Sarsby, R.W., Davies, K., Kugan, R., Bhattacharyya, R., Subedi, M., Poesen, J., Smets, T., Kertesz, A., Toth, A., Szalai, Z., Jakab, G., Kozma, K., Jankauskas, B., Jankauskiene, G., Böhmann, C., Paterson, G., Mulibana, E., Nell, J.P., van der Merwe, G.M.E., Guerra, A.J.T., Mendonça, J.K.S., Guerra, T.T., Sathler, R., Bezerra, J.F.R., Peres, S.M., Yi, Z., Yongmei, Li, T., Panomtarachichigul, M., Peukrai, S., Thu, D.C., Cuong, T.H., Toan, T.T., Jonsyn-Ellis, F., Jallow, S., Cole, A., Mulholland, B., Dearlove, M., Corkill, C. (2007). Contributions of biogeotextiles to sustainable development and soil conservation in developing countries: the BORASSUS Project. *Ecosystems and Sustainable Development*. WIT Press, Southampton, UK, pp. 123–141.

Fullen, M. A.; Booth, C. A.; Sarsby, R. W.; Davies, K.; Bhattacharyya, R.; Poesen, J.; Smets,

- T.; Kertesz, A.; Toth, A.; Szalai, Z.; Jakab, G.; Kozma, K.; Jankauskas, B.; Trimirka, V.; Jankauskienė, G.; Bühmann, C.; Paterson, G.; Guerra, A. J. T.; Mendonça, J. K. S.; Zheng, Y.; Li, Y.; Panomtarachichigul, M.; Dao, C. T.; Tran, H. C.; Truong, T. T.; Jonsyn-Ellis, F.; Corkill, C.; Mulholland, B., Dearlove, M. (2006). The potential contribution of palm mat geotextiles to soil conservation and sustainable development, *Soil and Water Conservation under Changing Land Use*. Universitat de Lleida Press, 303–306.
- Ganasri, B.P. and Ramesh, H. (2016). Assessment of soil erosion by RUSLE model using remote sensing and GIS-A case study of Nethravathi Basin. *Geoscience Frontiers*, 7(6), pp.953-961.
- García-Díaz, A., Bienes, R., Sastre, B., Novara, A., Gristina, L. & Cerdà, A. (2017). Nitrogen losses in vineyards under different types of soil groundcover. A field runoff simulator approach in central Spain. *Agriculture, Ecosystems & Environment*, 236, 256–267.
- Gimenez-Morera, A.; Ruiz-Sinoga, J.D.; Cerdà, A.(2010). The impact of cotton geotextiles on soil and water losses from Mediterranean rainfed agricultural land. *Land Degrad. Dev.* 21, 210–217. [CrossRef].
- Ghosh B., Ramesh V., and Vibhuti R. B. (2014). “Improvement of Soil Characteristics Using Jute,” *Int. J. Sci. Eng. Technol. Res.*, vol. 3, no. 7, pp. 1983–1986.
- Ghosh M, Saha R, Das M. (2021). Application of jute-polypropylene blended geotextile in black cotton soil subgrade for low volume road construction. *Int J Geosynth Ground Eng* 7(3):1–18.
- Ghosh, S. K., Bhattacharyya, R., & Mondal, M. M. (2014). A review on JGT-Part 1. *Int. J. Res. Eng. Technol*, 3(2), 378-386.
- Ghosh, S.K., Ray Gupta, K., Bhattacharyya, R., Sahu, R.B. and Mandal, S., 2014. Improvement of life expectancy of jute based needle punched geotextiles through bitumen treatment. *Journal of The Institution of Engineers (India): Series E*, 95(2), pp.111-121.
- Ghosh P, Samanta A K and Das D. (1994). Effect of selective pretreatments and different resin post-treatments on jute-viscose upholstery fabric. *Indian Journal of Fibre and Textile Research* 19(4): 277–280.
- Gray DH, Sotir RB. (1995). Biotechnical stabilization of steepened slopes, *Transportation*

- research record. Transportation Research Board, National Research Council, Washington, DC, pp 23–29.
- Gray, D. H. and Leiser, A. T.(1982). *Biotechnical Slope Protection and Erosion Control*, Van Nostrand Reinold Company, New York, 271 pp., 1982.
- Gray, D. H. and Sotir, R. B. (1996). “Biotechnical and Soil Bioengineering Slope Stabilization”, J. Wiley & Sons Inc., 605 Third Avenue, New York.
- Gray DH, Leiser AT.(1982). *Biotechnical slope protection and erosion control*. Van NostrandReinhold Company, New York.
- Gray, D. H., and Ohashi, H. (1983). “Mechanics of fiber reinforcement in sand.” *J. Geotech. Engrg.*, 1093, 335–353.
- Gong, X., Liu, X., & Wang, Z. (2019). Study on the stability of slopes covered with vegetation using geotextile. *Soil and Water Conservation*, 64(6), 305-310.
- Government of Telangana Planning Department. (2022). *Annual Rainfall 2021-22 District wise Rainfall(mm)*, Telangana State Development Planning Society, Available at: <https://www.tsdps.telangana.gov.in/annualrf.jsp>. Last accessed 10 March 2023.
- Gunti, R., Ratna Prasad, A. V., & Gupta, A. V. S. S. K. S. (2018). Mechanical and degradation properties of natural fiber-reinforced PLA composites: Jute, sisal, and elephant grass. *Polymer Composites*, 39(4), 1125-1136.
- Gupta, S., GuhaRay, A., Kar, A. and Komaravolu, V.P. (2018). Performance of alkali activated binder-treated JGT as reinforcement for subgrade stabilization. *International Journal of Geotechnical Engineering*.
- Gupta, A. (2016). Relative effectiveness of trees and shrubs on slope stability. *Electron. J. Geotech Eng*, 21, 737-53.
- Harshita Bairagi, R.K. Yadav, R. Jain,” Effect of Jute Fibres on Engineering Properties of Lime Treated Black Cotton Soil”.(2014). *International Journal of Engineering Research & Technology (IJERT)* ISSN: 2278-0181, Vol. 3 Issue 2.
- Hann CT, Barfield BJ, Hayes JC. (1996). *Design hydrology and sedimentology for small catchments*. Academic, San Diego.
- Hassan, A., Al-Mamun, A., & Islam, M. R. (2020). Study on the effectiveness of using geotextile in slope stability. *International Journal of Earth Sciences and Engineering*,

13(6), 595-600.

Henderson, M.S. (1982). The potential use of a degradable erosion control membrane in the United Kingdom. *Journal of Engineering Geology* London 15, 233–234.

Heras, M.M.-d.l., Espigares, T., Merino-Martín, L., Nicolau, J.M. (2011). Water-related ecological impacts of rill erosion processes in Mediterranean-dry reclaimed slopes. *Catena* 84, 114–124.

Hrissanthou V. (2005). Estimate of sediment yield in a basin without sediment data. *Catena* 64:333–347.

<https://www.deccanherald.com/state/karnataka-districts/landslide-to-affect-rail-movement-in-dharwad-874233.html>

Http://iraj.in/journal/journal_file/journal_pdf/13-321-148283034113-18.pdf.

Hossain, J., Hossain, M.S. and Hoyos, L.R., 2013. Effect of rainfall on stability of unsaturated earth slopes constructed on expansive clay. In *Geo-Congress 2013: Stability and Performance of Slopes and Embankments III* (pp. 417-425).

Howell JH, Sandhu SC, Vyas N et al. (2006). Introducing bio-engineering to the road network of Himachal Pradesh. *J Indian Roads Congr* 67(3):84. W07025 (1–11).

Hudson, N. (2006). *Conservación del suelo*. Ed. Reverte, Barcelona. 304 pp.

Huang, J., Yang, X., & Chen, Y. (2021). The effectiveness of using natural geotextiles in slope stability. *International Journal of Earth Sciences and Engineering*, 14(2), 180-185.

Indian Railways Institute of Civil Engineering Pune (2023), IPWE Seminar Year Wise, 2016, Available at : <https://www.ircen.gov.in/ircen/IpweSeminar.jsp>. Last access on 04/07/2023.

Ingold, T.S. (1996). Market study. In: CFC/IJO, Technical specification and market study of potentially important JGTs. Project Completion Report by Silsoe College, Cranfield University (Project Executing Agency).

Ingold T S. (1994). *Geotextiles and Geomembranes Manual*, p 199. Elsevier Science Publishers Ltd, Oxford.

IS 2720-4 (1985): Methods of test for soil, Part 4: Grain size analysis.

IS 2720-3-1 (1980): Methods of test for soils, Part 3: Determination of specific gravity.

- IS 2720-5 (1985): Methods of test for soils, Part 5: Determination of liquid and plastic limit.
- IS 2720-7 (1980): Methods of test for soils, Part 7: Determination of water content-dry density relation using light compaction.
- IS 2720-8 (1983): Methods of test for soils, Part 8: Determination of water content-dry density relation using heavy compaction.
- IS 2720-17 (1986): Methods of test for soils, Part 17: Laboratory determination of permeability.
- IS 2720-16 (1987): Methods of test for soils, Part 16: Laboratory determination of CBR.
- IS 2720-10 (1991): Methods of test for soils, Part 10: Determination of unconfined compressive strength.
- IS 2720-13 (1986): Methods of test for soils, Part 13: Direct shear test.
- IS Code 5225. (1992). Indian Standard Code for Meteorology -Raingauge, Non Recording Specification.
- ISO 527–1:2019 (2019) Plastics. Determination of tensile properties– Part 1: general principles. ISO, Geneva.
- Islam, M. S., & Rahman, A. (2019). Slope stability problem and Bio-engineering approach on slope protection: a case study of Cox's Bazar area, Bangladesh. *Geotechnical Engineering Journal of the SEAGS & AGSSEA*, 49(4).
- Islam, M. A., Islam, M. S., Chowdhury, M. E., & Badhon, F. F. (2021). Influence of vetiver grass (*Chrysopogon zizanioides*) on infiltration and erosion control of hill slopes under simulated extreme rainfall condition in Bangladesh. *Arabian Journal of Geosciences*, 14(2), 1-14.
- Islam, M. S., & Islam, M. A. (2018). Reduction of landslide risk and water-logging using vegetation. In *E3S web of conferences* (Vol. 65, p. 06003). EDP Sciences.
- Islam, M. S., Shahriar, B. A. M., & Shahin, H. M. (2013). Study on growth of vetiver grass in tropical region for slope protection. *International Journal of GEOMATE*, 5(2), 729-734.
- Jadhav, S. P., & Damgir, R. M. (2011). Use of jute geo textile for strengthening of sub grade of road work. *Innovative Systems Design and Engineering*, 2(4), 40-47.
- Jähn, A., Schröder, M. W., Fütting, M., Schenzel, K., and Diepenbrock, W., “Characterization

- of Alkali Treated Flax Fibres by Means of FT Raman Spectroscopy and Environmental Scanning Electron Microscopy,” *Spectrochim. Acta, Part A*, Vol. 58, No. 10, 2002, pp. 2271–2279, [https://doi.org/10.1016/S1386-1425\(01\)00697-7](https://doi.org/10.1016/S1386-1425(01)00697-7).
- Jain, R. & Singh, A. (2019). Effect of Jute Fiber on Soil Stabilization. *Journal of Geotechnical Engineering and Geosciences*, 9(2), 1-5.
- Jafrin, S., Shahinur, S., Khayer, M.M.A., Dilruba, A.F., Assaduzzaman, M. and Dhali, S.K., 2014. Effect of weak acid and weak alkali on jute fibre and fabrics in physical properties. *Indian J. Nat. Fibers*, 1, pp.83-90.
- Jain, P.K., and Tewari, V. (2010). "Performance of JGT in Slope Stabilization." *International Journal of Geotechnical Engineering*, 4(1), pp. 13-20.
- Jain, V. K., & Mishra, B. (2010). Strength and stability improvement of soil by jute fiber reinforcement. *International Journal of Engineering Science and Technology*, 2(4), 865-870.
- Jankauskas, B.; Jankauskiene, G.; Fullen, M. Soil conservation on road embankments using palm-mat geotextiles: Field studies in Lithuania. *Soil Use Manag.* (2012). 28, 266–275.
- Jankauskas, B., Jankauskien_e, G., Fullen, M.A. & Booth, C.A. (2008b). The effects of biogeotextiles on the stabilization of roadside slopes in Lithuania. *The Baltic Journal of Road and Bridge Engineering*, 3, 175–180.
- Jing, X., Chen, Y., Pan, C., Yin, T., Wang, W. and Fan, X.: Erosion failure of a soil slope by heavy rain: laboratory investigation and modified GA model of soil slope failure. *International Journal of Environmental Research and Public Health*, 16(6), p.1075.2019.
- Jomaa, S., Barry, D.A., Brovelli, A., Heng, B.C.P., Sander, G.C., Parlange, J.Y., Rose, C.W. (2012). Rain splash soil erosion estimation in the presence of rock fragments. *Catena* 92, 38- 48.
- Joy S, Balan K, Jayasree PK .(2011). Biodegradation of coir geotextile in tropical climatic conditions. In: *Proceedings of the golden jubilee Indian geotechnical conference, Kochi, India*, pp 604–606.
- Juntuek P, Chumsamrong P, Ruksakulpiwat Y, Ruksakulpiwat C. (2014). Effect of vetiver grass fiber on soil burial degradation of natural rubber and polylactic acid composites. *Int Polym Process J Polym Process Soc* 3:379–388.

- Kandrika, S. & Venkataratnam, L. (2005). A spatially distributed event based model to predict sediment yield. *Journal of Spatial Hydrology* 5(1), 1–19.
- Kar, A., Ray, I., Halabe, U. B., Unnikrishnan, A., and Dawson-andoh, B. (2014). “Characterizations and Quantitative Estimation of Alkali Activated Binder Paste from Microstructures.” *International Journal of Concrete Structures and Materials*, 8(3), 213–228.
- Kar, A. (2013). Characterizations of concretes with alkali activated binder and correlating their properties from micro-to specimen level. West Virginia University.
- Keesstra, S., Pereira, P., Novara, A., Brevik, E.C., Azorín-Molina, C., Parras-Alcántara, L., Jordán, A., Cerdà, A. (2016). Effects of soil management techniques on soil water erosion in apricot orchards. *Science of The Total Environment* 551-552, 357-366.
- Ketema, A. and Dwarakish, G.S., 2021. Water erosion assessment methods: a review. *ISH Journal of Hydraulic Engineering*, 27(4), pp.434-441.
- Kiffle, Z.B., Steele, S.E., Bhatia, S.K. and Smith, J.L. (2017). Use of jute as a sustainable alternative for PP in geotextile tubes. In *Geotechnical Frontiers 2017* (pp. 369-378).
- Kim, H. S., Kim, H. J., Lee, J. W., & Choi, I. G. (2006). Biodegradability of bio-flour filled biodegradable poly (butylene succinate) bio-composites in natural and compost soil. *Polymer degradation and stability*, 91(5), 1117-1127.
- Kinnell PIA. (2005). Why the universal soil loss equation and the revised version of it do not predict event erosion well. *Hydrological Processes* 19:851–854.
- Kinnell PIA, Risse LM .(1998). USLE-M: empirical modeling rainfall erosion through runoff and sediment concentration. *Soil Sci Soc Am J* 62:1662–1672.
- Kirschbaum DB, Adler R, Hong Y, Hill S, Lam AL. (2010). A global landslide catalogue for hazard applications: method, results, and limitations. *Nat Hazards* 52:561–575.
- Kimaro, D.N., Poesen, J., Msanya, B.M., Deckers, J.A. (2008). Magnitude of soil erosion on the northern slope of the Uluguru Mountains, Tanzania: interrill and rill erosion. *Catena* 75, 38–44.
- Kinnell, P.I.A. (2005). Raindrop-impact-induced erosion processes and prediction: a review. *Hydrological Processes* 19, 2815-2844.
- Khajehee A, Broshkeh A, Sokouti R, Arzabkhedri M. (2001). Study on application of

- empirical model of MUSLE in Shahrchai watershed, In: Proceedings National Seminar on Land Management, Soil Erosion and Sustainable.
- Khalil HPSA, Poh BT, Jawaid M, Ridzuan R, Suriana R, Said MR, Ahmad F, Fuad NAN .(2010). The effect of soil burial degradation of oil palm trunk fiber-filled recycled polypropylene composites. *J Reinf Plast Compos* 29(11):1653–1663.
- Khan, A. J., & Binoy, T. H. (2012). Top soil erosion control Using Geojute. In Proceedings of international conference on advances in civil engineering, Delhi, India (Vol. 2829).
- Khan YA, Chang C. (2006). Landslide Potentialities in Low Hills in Chittagong, Bangladesh; Proc Korean Soc Eng Geol Conf; Daejeon, South Korea, 2006; 79–88p.
- Kolathayar S, Sowmya S, Priyanka E. (2020). Comparative study for performance of soil bed reinforced with jute and sisal geocells as alternatives to HDPE Geocells. *Int J Geosynth Ground Eng* 6(4):1–8.
- Kossai, R., Hamdi, M., & Debez, A. (2016). Effect of coconut fiber on soil shear strength and erosion control. *Soil and Tillage Research*, 162, 55-64.
- Kumar N, Das D. (2018). Nonwoven geotextiles from nettle and poly (lactic acid) fibers for slope stabilization using bioengineering approach. *Geotext Geomembr* 46(2):206–213.
- Kumar, D., Nigam, S., Nangia, A., & Tiwari, S. (2015). California bearing ratio variations in soil reinforced with natural fibres (a case study Bhopal Bypass Road). *International Journal on Emerging Technologies*, 6(2), 95.
- Kumar R. (2012). “Effect of Geotextile on CBR Strength of Unpaved Road with Soft Subgrade,” *Electron. J. Geotech. Eng.*, vol. 17, pp. 1355–1363.
- Kumar, S. and Roy, L.B., 2023, January. Case study on soil-reinforced embankment slope stability with natural fibre additives. In Proceedings of the Institution of Civil Engineers-Engineering Sustainability (Vol. 176, No. 5, pp. 270-284). Thomas Telford Ltd.
- Lagmay AMF, Ong JBT, Fernandez DFD, Lapus MR, Rodolfo RS, Tengonciang AMP, Soria JLA, Baliatan EG, Quimba ZL, Uichanco E, Paguican A. (2006). Scientists investigate recent Philippine landslide. *Am Geophys Union* 87(12):121–128.
- Lal, R.A.T.T.A.N. (2001). Soil degradation by erosion. *Land degradation & development*, 12(6), pp.519-539.
- Langford, R.L., Coleman, M.J. (1996). Biodegradable erosion control blankets prove

- effective on Iowa wildlife refuge. XXVII Int. Erosion Control Assoc. Proceedings of Conf., Seattle, USA, pp. 13–20.
- Lekha, K.R.(2004). “Field instrumentation and monitoring of soil erosion in coir geotextile stabilised slopes—A case study,” *Geotextiles and Geomembranes*, Vol. 22, No. 5, pp.399-413.
- Liu, H., Liu, L., Zhang, K. and Geng, R., 2023. Effect of combining biogeotextile and vegetation cover on the protection of steep slope of highway in northern China: A runoff plot experiment. *International Journal of Sediment Research*, 38(3), pp.387-395.
- Li, J., Wang, Z., & Liu, L. (2021). Study on the stability of slopes covered with JGT. *Journal of Geotechnical Engineering*, 56(3), 407-413.
- Liu, T., Zhang, L., & Chen, H. (2021). The environmental impact of using natural geotextiles in slope stability. *Environmental Science and Technology*, 45(5), 2022-2027.
- Löbmann, M. T., Tonin, R., Wellstein, C., & Zerbe, S. (2020). Determination of the surface-mat effect of grassland slopes as a measure for shallow slope stability. *Catena*, 187, 104397.
- Luthra P, Vimal KK, Goel V, Singh R, Kapur GS. (2020). Biodegradation studies of polypropylene/natural fiber composites. *SN Appl Sci* 2:512. <https://doi.org/10.1007/s42452-020-2287-1>.
- Mafian S, Huat BBK, Ghiasi V. (2009). Evaluation on root theories and root strength properties in slope stability. *Eur J Sci Res* 30(4):594–607.
- Maitra, S. and Pramanick, B., Causes and Effect of Soil Erosion and its Preventive Measures. *Advanced Agriculture New Delhi Publishers, New Delhi: 2020, 376-387. ISBN: 978-93-88879-99-6, DOI: 10.30954/NDP-advagr.2020.19*
- Mahabaleshwara, H. and Nagabhushan, H.M. (2014). A study on soil erosion and its impacts on floods and sedimentation. *International Journal of Research in Engineering and Technology*, 3(03), pp.443-451.
- Maher, M. H., and Gray, D. H. (1990). “Static response of sand reinforced with randomly distributed fibers.” *J. Geotech. Engrg.*, 11611, 1661–1677
- Maiti, S. & Roy, P. (2015). Effect of JGT on the Stability of sandy soil slopes. *Journal of Geotechnical Engineering*, 11(2), 82-86.

- Mancilla, G.A., Chen, S., McCool, D.K. (2005). Rill density prediction and flow velocity distributions on agricultural areas in the Pacific Northwest. *Soil Tillage Res.* 84, 54–66.
- Maneecharoen J., Htwe W., Bergado D.T., Baral P. (2013). Ecological erosion control by limited life geotextiles (LLGs) as well as with Vetiver and Ruzi grasses. *Ind. Geotech. J.* 43:388-4
- Manivannan, S., Khola, O. P. S., Kannan, K., Choudhury, P. K., & Thilagam, V. K. (2018). Efficacy of open weave JGTs in controlling soil erosion and its impact on hill slope stabilization. *Indian Journal of Agricultural Sciences*, 88(5), 679-84.
- Marques AR, de Oliveira Patri'cio PS, dos Santos FS, Monteiro ML, de Carvalho Urashima D, de Souza Rodrigues C. (2014). Effects of the climatic conditions of the south eastern Brazil on degradation the fibers of coir-geotextile: evaluation of mechanical and structural properties. *Geotextile Geomembrane* 42(1):76–82. doi:10.1016/j.geotextmem.2013.07.004.
- Methacanon, P., Weerawatsophon, U., Sumransin, N., Prahsarn, C. and Bergado, D.T., 2010. Properties and potential application of the selected natural fibers as limited life geotextiles. *Carbohydrate Polymers*, 82(4), pp.1090-1096.
- Menon AR, Konnur S, Bhasi A. (2021). Model tests on coir geotextile-encased stone columns with tyre crumb-infilled basal coir geocell. *Int J Geosynth Ground Eng* 7(2):1–13.
- Merck KGaA, IR Spectrum Table & Chart, Merck KGaA, Darmstadt, Germany (2022). <https://www.sigmaaldrich.com/IN/en/technical-documents/technical-article/analytical-chemistry/photometry-and-reflectometry/ir-spectrum-table>. Accessed: 9 May 2023
- Mesut, G.Ö.R., TAHER, N.R., AKSOY, H.S. and AWLLA, H.A., EFFECT OF GEOGRID INCLUSION ON THE SLOPE STABILITY.
- Michael Tobias Löbmann, Rita Tonin, Camilla Wellstein, Stefan Zerbe(2020). Determination of the surface mat effect of grassland slopes as a measure for shallow slope stability. *CATENA*, Volume 187, 104397, ISSN 0341-8162.
- Mickovski SB, Hallett PD, Bransby MF. (2009). Mechanical reinforcement of soil by willow roots: impacts of root properties and root failure mechanism. *Soil Sci Soc Am J* 73 (4):1276–1285.
- Mitchell, D.J., Barton, A.P., Fullen, M.A., Hocking, T.J., Zhi, Wu.Bo., Yi, Zheng. (2003).

- Field studies of the effects of JGTs on runoff and erosion in Shropshire, UK. *Soil Use & Management* 19, 182–184.
- Mitra, B. C.(1999). *Data Book on Jute*. 1st Edn. National Institute of Research on Jute and Allied Fibre Technology, Kolkata, India.
- Mishra SK, Tyagi JV, Singh VP, Singh R. (2006). SCS-CN-based modeling of sediment yield. *J Hydrol* 324:301–322.
- Mohamadi, M.A. and Kavian, A. (2015). Effects of rainfall patterns on runoff and soil erosion in field plots. *International soil and water conservation research*, 3(4), pp.273-281.
- Mondal, A., & Saha, S. K. (2015). Seismic behavior of jute fiber reinforced soil slopes. *Arabian Journal of Geosciences*, 8(11), 11199-11207.
- Morgan, R.P.C. (2005). *Soil erosion and conservation*. Blackwell Publishing, Oxford.
- Morgan RP, Rickson RJ. (2003). *Slope stabilization and erosion control: a bioengineering approach*. Taylor & Francis, Madras.
- Müller, W. W., & Saathoff, F. (2015). Geosynthetics in geoenvironmental engineering. *Science and Technology of Advanced Materials*, 16, 034605. <https://doi.org/10.1088/1468-6996/16/3/034605>.
- Naeini S. A. (2008). “The Effect of Geotextile and Grading on the Bearing Ratio of Granular Soils,” *Electron. J. Geotech. Eng.*, vol. 13, no. 1996, pp. 1–10.
- Nam, S. and Netravali, A.N., 2006. Green composites. I. Physical properties of ramie bers for environment-friendly green composites. *Fibers and Polymers*, 7(4), pp.372-379.
- NDMG. (2009). *National disaster management guidelines—management of landslides and snow avalanches*, a publication of the national disaster management authority. Government of India, New Delhi.
- Neto, A. R. S., M. A. Araujo, F. V. Souza, L. H. Mattoso, and J. M. Marconcini. 2013. "Characterization and Comparative Evaluation of Thermal, Structural, Chemical, Mechanical and Morphological Properties of Six Pineapple Leaf Fiber Varieties for Use in Composites." *Industrial Crops and Products* 43: 529–537.
- Ng CWW, Shi Q. (1998). A numerical investigation of the stability of unsaturated soil slopes subjected to transient seepage. *Comput Geotech* 22(1):1–28.

- Ng, L.Y., Wong, T.J., Ng, C.Y. and Amelia, C.K.M., 2021. A review on cellulose nanocrystals production and characterization methods from *Elaeis guineensis* empty fruit bunches. *Arabian Journal of Chemistry*, 14(9), p.103339.
- Nicks AD, Williams RD, Williams JR, Gander GA. (1994). Estimating erosion with models having different.
- Noorasyikin, M.N. and Zainab, M., 2016, July. A tensile strength of Bermuda grass and Vetiver grass in terms of root reinforcement ability toward soil slope stabilization. In *IOP conference series: materials science and engineering* (Vol. 136, No. 1, p. 012029). IOP Publishing.
- Novotny V, Olem H. (1994). *Water quality: prevention, identification, and management of diffuse pollution*. Wiley, New York.
- Nunn, T. R., J. B. Howard, J. P. Longwell, and W. A. Peters. 1985. "Product Compositions and Kinetics in the Rapid Pyrolysis of Sweet Gum Hardwood." *Industrial & Engineering Chemistry Process Design and Development* 24 (3): 836–844.
- Nyssen, J., J. Poesen, J. Moeyersons, J. Deckers, H. Mitiku, and A. Lang. (2004). Human impact on the environment in the Ethiopian and Eritrean highlands: A state of the art. *Earth Science Reviews* 64 (3–4): 273–320.
- Palme, A., Theliander, H. and Brelid, H., 2016. Acid hydrolysis of cellulosic fibres: comparison of bleached kraft pulp, dissolving pulps and cotton textile cellulose. *Carbohydrate polymers*, 136, pp.1281-1287.
- Patil, V., & Gopale, R. (2018). A geographical study of landslide: A case study of malin village of ambegaon tahsil in Pune district, Maharashtra. *Peer Reviewed International Research Journal of Geography*, 35, 55–60.
- Pandey, A., Chowdary, V.M. and Mal, B.C. (2009). Sediment yield modelling of an agricultural watershed using MUSLE, remote sensing and GIS. *Paddy and Water Environment*, 7(2), pp.105-113.
- Panigrahi, B., & Pradhan, P. K. (2019). Improvement of bearing capacity of soil by using natural geotextile. *International Journal of Geo-Engineering*, 10(1), 1-12.
- Philip A. S. and Charly K. K. (2016). "Study on Strength Behaviour of Soil Using Geotextile," *Int. J. Engineering Res. Sci.*, vol. 2, no. 7, pp. 30–37.

- Phillips C, Marden M. (2006). Use of plants for ground bioengineering and erosion sediment control in New Zealand. In: Proceedings of soil water. Too good to lose. Joint annual conference NSW Stormwater Industry Association and the International Erosion Control Association.
- PLAXIS 2D 2021.PLAXIS 2D Manuals 2021.
- Poesen, J., J. Nachtergaele, G. Verstraeten, and C. Valentin. (2003). Gully erosion and environmental change: importance and research needs. *Catena* 50 (2): 91–133.
- Pongsai, S., Schmidt Vogt, D., Shrestha, R. P., Clemente, R. S. & Eiumnoh, A. (2010). Calibration and validation of the Modified Universal Soil Loss Equation for estimating sediment yield on sloping plots: A case study in Khun Satan catchment of northern Thailand. *Canadian Journal of Soil Science* 90(4), 585–596.
- Prambauer M, Wendeler C, Weitzenbock J, Burgstaller C. (2019). Biodegradable geotextiles An overview of existing and potential materials. *Geotext Geomembr* 47(1):48–59.
- Prakash, V., Singh, A., and Yadav, R. (2015). "Slope Stabilization Using JGT: A Review." *International Journal of Engineering Research and Technology*.
- Provis, J. L. (2018). "Alkali activated materials." *Cement and Concrete Research*, Elsevier Ltd, 114, 40–48.
- Rao, G.V., Balan, K. (2000). *Coir Geotextiles–Emerging Trends*. Kerala State Coir Corporation, Kerala, India.
- Rashdi, A. A. A., Sapuan, S. M., Ahmad, M. M. H. M., & Khalina, A. (2009). Water absorption and tensile properties of soil buried kenaf fibre reinforced unsaturated polyester composites (KFRUPC). *Journal of Food, Agriculture & Environment*.
- Rashdi, A. A. A., Sapuan, S. M., Ahmad, M. M. H. M., & Khalina, A. J. I. J. (2010). Combined Effects of Water Absorption Due to Water Immersion, Soil Buried and Natural Weather on Mechanical Properties Of Kenaf Fibre Unsaturated Polyester Composites (KFUPC). *International Journal of Mechanical and Materials Engineering*, 5(1), 11-17.
- Ramagiri KK, Kar A (2019) Effect of precursor combination and elevated temperatures on the microstructure of alkali activated binder. *Indian Concr J* 93(10):34–43.
- Ramesh, H. N., Manoj Krishna, K. V., & Mamatha, H. V. (2010). Compaction and strength

- behavior of lime-coir fiber treated Black Cotton soil. *Geomechanics & engineering*, 2(1), 19-28.
- Ranganathan, S.R. (1992). JGTs in soil erosion control. *International Erosion Control Association Proceedings of Conference XX111, Indianapolis, (USA)*, pp. 343–351.
- Rawal, A. and Anandjiwala, R.(2007). “Comparative study between needlepunched nonwoven geotextile structures made from flax and polyester fibres,” *Geotextiles and Geomembranes*, Vol. 25, No. 1, pp.61-65.
- Razali, I.H., Taib, A.M., Abd Rahman, N., Hasbollah, D.Z.A., Dan, M.F.M., Ramli, A.B. and Ibrahim, A., 2023. Slope stability analysis of riverbank in Malaysia with the effects of vegetation. *Physics and Chemistry of the Earth, Parts A/B/C*, 129, p.103334.
- Rezaeifard M, Telvari AR, Arzabkhedri M. (2001). Study on application of MUSLE in estimation of storm-wise sediments in Afjeh, Latian Basin. In: *Proceedings national seminar on land management, soil erosion and sustainable development* 534–542.
- Rickson, R.J. (2006). Controlling sediment at source: an evaluation of erosion control geotextiles. *Earth Surface Processes and Landforms* 31, 550–560.
- Rickson, R.J. (1995). Simulated vegetation and geotextiles. In: Morgan, R.P.C., Rickson, R.J. (Eds.), *Slope Stabilization and Erosion Control: A Bioengineering Approach*. Taylor & Francis, Abingdon, UK.
- Rickson R J. (1988). The use of JGTs in soil erosion control. *Proceedings of the Fifth International Soil Consolidation Conference, Bangkok, Thailand*, pp 627–33.
- Rosa MF, Chiou BS, Medeiros ES, Wood DF, Williams TG, Mattoso LH, Imam SH. (2009). Effect of fibre treatments on tensile and thermal properties of starch/ethylene vinyl alcohol copolymers/ coir biocomposites. *Bioresour Technol* 100(21):5196–5202.
- Roose, É. and De Noni, G. (2004). Recherches sur l ‘érosion hydrique en Afrique: revue et perspectives. *Science et changements planétaires/Sécheresse*, 15(1), pp.121-129.
- Ryżak, M., Bieganowski, A., Polakowski, C. (2015). Effect of soil moisture content on the splash 1165 phenomenon reproducibility. *Plos One* 1, 1-15.
- Sadeghi SHR, Mizuyama T. (2007). Applicability of the modified universal soil loss equation for prediction of sediment yield in Khanmirza watershed, Iran. *Hydrol Sci J* 52(5):1068–1075.

- Sadeghi SHR, Singh JK, Das G. (2004). Efficiency of annual soil erosion models for storm-wise sediment prediction: a case study. *Int Agric Eng J* 13:1–14.
- Saha, S. K., Hossain, A. B. M. S., & Hossain, M. A. (2013). Jute fiber reinforced soil for slope stability improvement. In *Proceedings of the International Conference on Soil Mechanics and Geotechnical Engineering* (pp. 2417-2420).
- Saha, P., Roy, D., Manna, S., Adhikari, B., Sen, R. and Roy, S. (2012). Durability of transesterified JGTs. *Geotextiles and Geomembranes*, 35, pp.69-75.
- Saha P, Manna S, Chowdhury SR, Sen R, Roy D, Adhikari B. (2010). Enhancement of tensile strength of lignocellulosic jute fibers by alkali-steam treatment. *Bioresour Technol* 101(9):3182–3187.
- Saha, B., Mondal, S., and Banerjee, S. (2009). "Utilization of JGT for Slope Stabilization: An Experimental Study." *International Journal of Geotechnical Engineering*, 3(2), pp. 141-149.
- Saifuddin, M., & Osman, N. (2014). Evaluation of hydro-mechanical properties and root architecture of plants for soil reinforcement. *Current Science*, 845-852.
- Sandeep, P., Kumar, K.A. and Haritha, S., 2021. Risk modelling of soil erosion in semi-arid watershed of Tamil Nadu, India using RUSLE integrated with GIS and Remote Sensing. *Environmental Earth Sciences*, 80(16), p.511.
- Sanyal, T. (2017). *JGTs and Their Applications in Civil Engineering*. Singapore: Springerjadhav.
- Sanyal, T. (2017). Application of JGT and a Few Case Studies. In *JGTs and their Applications in Civil Engineering* (pp. 181-211). Springer, Singapore.
- Sanyal, T.(2017) Control of Soil Erosion Caused by Rain and Wind with JGTs. In *Jute Geotext. Their Applications in Civil Engineering*; Springer: Berlin/Heidelberg, Germany, pp. 41–63.
- Sanyal T. (2011). Control of bank erosion naturally – A pilot project in Nayachar island in the river Hugli and performance appraisal, JGTs. National Jute Board, Ministry of Textiles, Government of India, Kolkata, pp 219–26.
- Sanyal, T. (2004). Proc. - Seminar workshop Geosynthetics India Indian Institute of Technology, New Delhi, India: 362.

- Sanyal T, Chakraborty K. (1994). Application of a bitumen-coated JGT in bank-protection works in the Hooghly estuary. *Geotext Geomembr* 13(2):127–132.
- Sarasini, F., Fiore, V. (2018). A systematic literature review on less common natural fibres and their biocomposites. *J. Clean. Prod.* 195, 240e267. <https://doi.org/10.1016/j.jclepro.2018.05.197>.
- Sapuan, S. M., Pua, F. L., El-Shekeil, Y. A., & AL-Oqla, F. M. (2013). Mechanical properties of soil buried kenaf fibre reinforced thermoplastic polyurethane composites. *Materials & Design*, 50, 467-470.
- Savindra, S., and S. Prakash. (1987). Rill and gully erosion in the subhumid tropical riverine environment of Teonthar Tahsil, Madhya Pradesh, India. *Geographical Analysis* 69A (1): 227–236.
- Schiechtl HM, Stern R. (1996). *Ground bioengineering techniques for slope protection and erosion control*. Blackwell Science Ltd., London.
- Schiechtl, H. M.(1985). *Vegetative and soil treatment measures, FAO watershed management field*.
- Schiechtl H. M. (1980). *Bioengineering for land reclamation and conservation*. University of Alberta Press, Edmonton.
- Schuster RL, Salcedo DA, Valenzuela L. (2002). Overview of catastrophic landslides of South America in the twentieth century. *Rev Eng Geol* 15:1–34.
- Schurholz H. (1992). Use of woven coir geotextiles in Europe. In: *Proceedings of the United Kingdom coir geotextile seminar, West Midlands*.
- Shavandi, A., Ali, M.A. (2019). Keratin based thermoplastic biocomposites: a review. *Rev. Environ. Sci. BioTechnol.* 18, 299e316. <https://doi.org/10.1007/s11157-019-09497-x>.
- Shavandi, A., Carne, A., Bekhit, A.A., Bekhit, A.E.-D.A., 2017. An improved method for solubilisation of wool keratin using peracetic acid. *J. Environ. Chem. Eng.* 5, 1977e1984. <https://doi.org/10.1016/j.jece.2017.03.043>.
- Shaia, H., H Aodah, H., & H AL-Hameidawi, B. (2016). Improvement of Sub-grade Soil using Natural Jute Fiber Sheet at Various Layers. *journal of kerbala university*, 12(1), 170-177.
- Shavandi, A., Carne, A., Bekhit, A.A., Bekhit, A.E.-D.A. (2017). An improved method for

- solubilisation of wool keratin using peracetic acid. *J. Environ. Chem. Eng.* 5, 1977e1984. <https://doi.org/10.1016/j.jece.2017.03.043>.
- Sheng, T. C.(1979). L'ensemencement par pulvérisation: procédés, exemples et perspectives à la Jamaïque, Techniques spéciales de conservation, Cahier FAO: Conservation des sols, 4, 75–83.
- Sheng, T. C.(1977). Approche d'aménagement intégré dans l'établissement d'un projet de développement d'un bassin versant, Aménagement des bassins versants, Cahier FAO: Conservation des sols, 1, 11–18.
- Sheng, T. C.(1977). Protection des versants cultivés, Aménagement des bassins versants, Cahier FAO: Conservation des sols, 1, 179–213.
- Shukla SK. (2021). Geosynthetics and ground engineering: sustainability considerations. *Int J Geosynth Ground Eng.* <https://doi.org/10.1007/s40891-021-00256-z>.
- Shtykov, V.I., Blazhko, L.S. and Ponomarev, A.B.(2017). “The Performance of Geotextile Materials Used for Filtration and Separation in Different Structures as an Important Part of Geotextiles Requirements,” *Procedia Engineering*, Vol. 189, pp.247-251.
- Sempere-Torres, D., Porrá, J.M., Creutin, J-D. (1994). A general formulation for raindrop size 1183 distribution. *Journal of Applied Meteorology* 33, 1494-1502.
- Sengupta A, Gupta S, Anbarasu K. (2010). Rainfall thresholds for the initiation of landslide at Lanta Khola in north Sikkim, India. *Nat Hazards* 52:31–42.
- Siakeng, R., Jawaid, M., Asim, M., & Siengchin, S. (2020). Accelerated weathering and soil burial effect on biodegradability, colour and texture of coir/pineapple leaf fibres/PLA biocomposites. *Polymers*, 12(2), 458.
- Singhvi, G. M. (2003). Proc. - International Jute Symposium on Indian Jute Sector and Its Relevance in 21st Century, Kolkata, India: 22.
- Singh H. P. and Bagra M., (2013). “Improvement in CBR Value of Soil Reinforced With Jute Fiber,” *Int. J. Innov. Res. Sci. Eng. Technol.*, vol. 2, no. 8, pp. 3447–3452.
- Singh H. P., (2013), “Strength and Stiffness of Soil Reinforced with JGT Sheets,” *Intenatiol J. Curr. Eng. Technol.*, vol. 3, no. 3, pp. 1143–1146.
- Singh, H. and Yachang, O. (2012). Use of fly ash reinforced with JGT as a pavement subgrade. *International Journal of Earth Science and Engineering*, 5(4), 562-567.

- Siswanto, S.Y. and Sule, M.I.S. (2019). The Impact of slope steepness and land use type on soil properties in Cirandu Sub-Sub Catchment, Citarum Watershed. In IOP Conference Series: Earth and Environmental Science (Vol. 393, No. 1, p. 012059). IOP Publishing.
- Smets, T.; Poesen, J.; Fullen, M.A.; Booth, C.A. (2007). Effectiveness of palm and simulated geotextiles in reducing run-off and inter-rill erosion on medium and steep slopes. *Soil Use Manag.* 23, 306–316. [CrossRef].
- Smith, S.J., Williams, J.R., Menzel, R.G. and Coleman, G.A. (1984). Prediction of sediment yield from southern plains grasslands with the modified universal soil loss equation. *Rangeland Ecology & Management/Journal of Range Management Archives*, 37(4), pp.295-297.
- Sprague, C.J., Paulson, J.N. (1996). Project-specific selection of erosion control geosynthetics. *Erosion control technology: bringing it home*, Proceedings of Conference XXVII, International Erosion Control Association, 27 February–1 March, Seattle, Washington, pp. 213–226.
- Suhatri, M., Osman, N., Sari, P. A., Shariati, M., & Marto, A. (2019). Significance of surface eco protection techniques for cohesive soils slope in Selangor, Malaysia. *Geotechnical and Geological Engineering*, 37(3), 2007-2014.
- Sumi, S., Unnikrishnan, N. and Mathew, L. (2016). Experimental Investigations on Biological Resistance of Surface Modified Coir Geotextiles. *International Journal of Geosynthetics and Ground Engineering*, 2(4), p.31.
- Sutherland, R.A., Ziegler, A.D. (1996). Geotextile effectiveness in reducing interill runoff and sediment flux. *International Erosion Control Association Proceedings of Conference XXVI*, 1995, Atlanta, USA, pp. 359–370.
- Tapas D. and Baleshwar S. (2014). “Deformation And Strength Characteristics of JGT Reinforced Soil,” *J. Environ. Res. Dev.*, vol. 8, no. 4, pp. 987–995.
- Tauro, F.; Cornelini, P.; Grimaldi, S.; Petroselli, A. (2018). Field studies on the soil loss reduction effectiveness of three biodegradable geotextiles. *J. Agric. Eng.* 49, 117–123. [CrossRef].
- Terry, J.P., Shakesby, R.A. (1993). Simulated rainfall and photographic evidence. *Earth Surface Processes and Landforms* 18, 519-525.
- Tjie-Liong, G., 2014. Common mistakes on the application of Plaxis 2D in analyzing

- excavation problems. *International Journal of Applied Engineering Research*, 9(21), pp.8291-8311.
- T.H. Wu. Investigation of landslides on prince of Wales Island, Alaska.(1976). *Geotechnical Engineering Report 5*, Ohio State University, Department of Civil Engineering, 20, 44, 45, 57, 61, 63.
- Thomson J C. (1988). The role of natural fibres in geotextile engineering. *Proceedings of the First Indian Geotextile Conference, Vol 1. Bombay, India*, pp G25 – G29.
- Tserki, V., Matzinos, P., Kokkou, S., & Panayiotou, C. (2005). Novel biodegradable composites based on treated lignocellulosic waste flour as filler. Part I. Surface chemical modification and characterization of waste flour. *Composites Part A: Applied Science and Manufacturing*, 36(7), 965-974.
- Theisen, M.S. (1992). The role of geosynthetics in erosion and sediment control: an overview. *Geotextiles and Geomembranes* 11, 535–550.
- Tomar, A., Choudhary, S., Kumar, L., Singh, M., Dhillon, N. and Arya, S., 2020. Screening of Bacteria Present in Cow Dung. *Int. J. Curr. Microbiol. App. Sci*, 9(2), pp.584-591.
- Uddin MK, Khan MA, Ali KI. (1997). Degradable jute plastic composites. *Polym Degrad Stab* 55(1):1–7.
- Valadez-Gonzalez, A., Cervantes-Uc, J. M., Olayo, R. J. I. P., and Herrera-Franco, P. J., “Effect of Fiber Surface Treatment on the Fiber-Matrix Bond Strength of Natural Fiber Reinforced Composites,” *Compos. Part B: Eng.*, Vol. 3, No. 3, 1999, pp. 309–320, [https://doi.org/10.1016/S1359-8368\(98\)00054-7](https://doi.org/10.1016/S1359-8368(98)00054-7).
- Van Sint Jan, M. and Talloni, P. (1993). Flujo de sedimentos del 18 de Juniode 1991 en Antofagosta: La Serena, Chile. In *Tercer Congreso Chileno de Ingenieria Geotecnia (Vol. 1, pp. 247-265)*.
- Venkatappa Rao, G., Balan, K. (2000). *Coir Geotextiles—emerging trends*, The Kerala State Coir Corporation Ltd., Alappuzha, Kerala.
- Vibha, S. and Divya, P.V., 2021. Performance of Geosynthetic Reinforced Steep Soil Slopes at the Onset of Rainfall Infiltration. In *Proceedings of the Indian Geotechnical Conference 2019 (pp. 167-176)*. Springer, Singapore (2021).
- Vijay, R., Vinod, A., Singaravelu, D.L., Sanjay, MR and Siengchin, S., 2021.

- Characterization of chemical treated and untreated natural fibers from Pennisetum Orientale grass-A potential reinforcement for lightweight polymeric applications. *International Journal of Lightweight Materials and Manufacture*, 4(1), pp.43-49.
- Vishnudas, S., Savenije, H.H., Van der Zaag, P. and Anil, K.R. (2012). Coir geotextile for slope stabilization and cultivation—A case study in a highland region of Kerala, South India. *Physics and Chemistry of the Earth, Parts A/B/C*, 47, pp.135-138.
- Vishnudas S, Savenije HHG, Van der Zaag P, Anil KR, Balan K. (2006). The protective and attractive covering of a vegetated embankment using coir geotextiles. *Hydrol Earth Syst Sci* 10(August):565–574. doi:10.5194/hess-10-565-2006.
- Wahit MU, Akos NI, Laftah WA. (2012). Influence of natural fiber on the mechanical properties and biodegradation of poly (lactic acid) and poly (ε-caprolactone) composites. A review. *Polym Compos* 33(7):1045–1053.
- Walling DE, Webb BW. (1982). Sediment availability and the prediction of storm-period sediment yields. In: *Proceedings of the Exeter Symposium*, 327–337. IAHS Publ. 137. IAHS Press, Wallingford, UK.
- Wang, Y., Liu, X., & Chen, Z. (2021). The influence of coir geotextile on the stability of soil slopes. *Soil and Water Conservation*, 67(2), 89-94.
- Wang, Z., Li, Q., Zhang, N., Jin, Y., Qin, H. and Ding, J., 2020. Slope failure of biotreated sand embankments under rainfall conditions: Experimental investigation and numerical simulation. *Bulletin of Engineering Geology and the Environment*, 79, pp.4683-4699.
- Wang, W.M., Cai, Z.S., Yu, J.Y. and Xia, Z.P., 2009. Changes in composition, structure, and properties of jute fibers after chemical treatments. *Fibers and Polymers*, 10, pp.776-780.
- Wang WM, Cai ZS, Yu JY, Xia ZP. (2009). Changes in composition, structure, and properties of jute fibers after chemical treatments. *Fibers Polym* 10(6):776–780.
- Wiewel, B. V., & Lamoree, M. (2016). Geotextile composition, application and ecotoxicology: a review. *Journal of Hazardous Materials*, 317, 640–655. <https://doi.org/10.1016/j.jhazmat.2016.04.060>.
- Williams, J.R. (1982). Testing the Modified Universal Soil Loss Equation [Runoff energy factor, small watersheds, Texas, Nebraska]. *Agricultural reviews and manuals*.

- Williams JR, Berndt HD. (1977). Sediment yield prediction based on watershed hydrology. *Trans Am Soc Agric Eng* 20(6):1100–1104.
- Williams, J.R. (1975). Sediment-yield prediction with Universal Equation using runoff energy factor, present and prospective technology for predicting sediment yield and sources. ARS-S-40. Brooksville, FL: US Department of Agriculture, Agricultural Research Service, 244–252.
- Williams JR. (1975a). Sediment routing for agricultural watersheds. *Water Resour Bull* 11:965–975.
- Williams JR. (1975b). Sediment yield prediction with Universal Equation using runoff energy factor. In: Present and prospective Technology for predicting sediment yields and sources, 244–252, Agricultural Research Service, US Department of Agriculture.
- Wischmeier WH, Smith DD. (1978). Predicting rainfall erosion losses. USDA Agricultural Research Services Handbook 537. USDA, Washington, p 57.
- Wischmeier, W.H. (1960). Cropping-management factor evaluations for a universal soil-loss equation. *Soil Science Society of America Journal*, 24(4), pp.322-326.
- Wu, S., Wu, D., Jing, X., Chen, X., Wang, Y. and Ye, L. (2021). Rainfall Erosion Predictions for Artificial High-Filled Embankment with Reinforcement. *Advances in Materials Science and Engineering*, 2021.
- Wu, H., Yao, C., Li, C., Miao, M., Zhong, Y., Lu, Y., & Liu, T. (2020). Review of application and innovation of geotextiles in geotechnical engineering. *Materials*, 13(7), 1774.
- Wu, L., Peng, M., Qiao, S., Ma, X. (2018). Effects of rainfall intensity and slope gradient on runoff and sediment yield characteristics of bare loess soil. *Environ. Sci. Pollut. R.* 25(4), 3480-3487.
- Xu Q, Zhang L. (2010). The mechanism of a railway landslide caused by rainfall. *Landslides* 7:149–156.
- Yamauchi, IN.(1962). Proc.-2nd International Conference on Structural Design of Asphalt Pavements (Ann. Arbor, Michigan, USA): 381
- Yang, H., Yan, R., Chen, H., Lee, D.H. and Zheng, C. (2007). Characteristics of hemicellulose, cellulose and lignin pyrolysis. *Fuel*, 86(12), pp.1781-1788.

- Yussuf AA, Massoumi Hassan A. (2010). Comparison of polylactic acid/kenaf and polylactic acid/rise husk composites: the influence of the natural fibers on the mechanical, thermal and biodegradability properties. *J Polym Environ* 18(3):422–429
- Zhang, L.L., Zhang, J., Zhang, L.M. and Tang, W.H. (2011). Stability analysis of rainfall-induced slope failure: a review. *Proceedings of the Institution of Civil Engineers-Geotechnical Engineering*, 164(5), pp.299-316.
- Zheng YR, Zhao SY, Deng CJ, Liu MW, Tang XS, Zhang LM (2006) Development of finite element limit analysis method and its applications in geotechnical engineering. *Eng Sci* 8(12):39–61.
- Zope, P.E., Eldho, T.I. and Jothiprakash, V., 2016. Development of rainfall intensity duration frequency curves for Mumbai City, India. *Journal of water resource and protection*, 8(07), p.756.

List of Publications

Journals

1. **G. Sachin Chakravarthy**, Anasua GuhaRay and Arkamitra Kar (2021), "Experimental Investigations on Strength and Durability of Alkali Activated Binder Treated Natural JGT", International Journal of Geosynthetics and Ground Engineering, Springer, 7: 97, doi: 10.1007/s40891-021-00341-3.
2. **G. Sachin Chakravarthy**, Anasua GuhaRay and Arkamitra Kar (2021), "Effect of Soil Burial Exposure on Durability of Alkali Activated Binder Treated JGT", Innovative Infrastructure Solutions, Springer, 6 (62), <https://doi.org/10.1007/s41062-020-00441-5>.
3. **G. Sachin Chakravarthy**, Anasua GuhaRay and Arkamitra Kar (2023) "Reduction of Soil Slope Erosion using Natural Jute treated with Alkali Activated Binder". Soil Science Society of America Journal. (Under 2nd Review)

Conference Proceedings

1. **Chakravarthy, G.S.**, GuhaRay, A. (2022), "Numerical Investigation on Stability of Slope Reinforced with Alkaline Binder Treated Jute under Different Rainfall Conditions ", Indian Geotechnical Conference (IGC) - 2022, Kochi, 15-17 December 2022.
2. **Chakravarthy, G.S.**, GuhaRay, A. (2020), "Effect of Soil Burial on Durability of Alkali Activated Binder treated JGT", Indian Geotechnical Conference (IGC), Andhra University, 17-19 December 2020.
3. **Chakravarthy, G.S.**, GuhaRay, A. (2021), "Reduction Of Surface Erosion Of Soil Slopes Using Alkali Activated Binder Treated Jute Fibers", Indian Geotechnical Conference (IGC), NIT Trichy, 16-18 December 2021.
4. **Chakravarthy G.S.**, GuhaRay, A., Kar, A. (2020), "Strength Characterisation of Alkali Activated Binder treated Jute for Ground Improvement", 2nd ASCE India Conference on Challenges of Resilient and Sustainable Infrastructure Development in Emerging Economics (CRSIDE 2020), Kolkata, 2-4 March.

Book Chapters

1. **Chakravarthy G.S.**, GuhaRay, A., Kar, A. (2020), "Strength Characterisation of Alkali Activated Binder treated Jute for Ground Improvement", 2nd ASCE India Conference on Challenges of Resilient and Sustainable Infrastructure Development in Emerging Economics (CRSIDE 2020), Kolkata, 2-4 March (accepted as book chapter "*Innovative Civil Engineering Materials*", Cambridge Scholars publication)

Biography of Candidate

Mr. Gunde Sachin Chakravarthy was born on the 13th January 1991, in Deekshakunta, Warangal, Telangana, India. He received his Bachelors in Civil Engineering from Jawaharlal Nehru Technological University, Telangana, India, in 2014. He then joined the Jawaharlal Nehru Technological University Hyderabad, Telangana, India and received his M.Tech in Infrastructural Engineering in 2016. After his M.Tech, he worked as Assistant Professor at CMR College of Engineering and Techonology, Hyderabad, before joining as a research scholar in 2018 at the Department of Civil Engineering, Birla Institute of Technology and Science-Pilani, Hyderabad Campus. Overall his research interests include Ground Improvement, Slope stabilization using bio engineering methods. During his PhD, he has published his works in several journals of international repute and presented his works at different national and international conferences, including Indian Geotechnical Society, the American Society of Civil Engineers, and many others.

Gunde Sachin Chakravarthy

Research Scholar

Department of Civil Engineering

BITS Pilani, Hyderabad Campus

Hyderabad-500078, India

Email: sachinchakravarthy973@gmail.com

Biography of Supervisor

Prof. Anasua GuhaRay is presently an Associate Professor in Geotechnical Engineering Division of Department of Civil Engineering, BITS-Pilani Hyderabad Campus and a Cross-Appointed faculty of the Department of Civil and Environmental Engineering in Hiroshima University, Japan. She is a university gold medalist in B.E. Civil Engineering from Jadavpur University, Kolkata. She has completed her M.Tech. and Ph.D. in Geotechnical Engineering from IIT Kharagpur. Her major research areas include reliability application in geotechnical engineering, utilisation of waste materials for ground improvement and stabilisation of expansive soil with activated binders. She has published a number of papers in peer reviewed journals and conferences. 3 Ph.D. students have graduated under her supervision till date and presently, she is the supervisor of 4 more Ph.D. students. She has received a number of sponsored research grants including Early Career Research grant and SERB Power Grant from DST, Indo-Austria and Indo-Japan bilateral project grant from DST, Asian Smart Cities Research and Innovation Network. She is the recipient of “Outstanding Reviewer Recognition” from International Journal of Geomechanics, ASCE in the year 2015, 2017 and 2018. She is a life member of Indian Geotechnical Society and an Associate Member of American Society of Civil Engineers.

Prof. Anasua GuhaRay

Associate Professor

Department of Civil Engineering

Birla Institute of Technology and Science, Pilani, Hyderabad Campus

500078, India

Email: guharay@hyderabad.bits-pilani.ac.in

Biography of Co-Supervisor

Prof. Arkamitra Kar is currently working as an Associate Professor in the Department of Civil Engineering, at BITS-Pilani, Hyderabad Campus, India since July 2015. His research interests are the characterizations of alternative construction materials and durability studies of concrete prepared with such materials. Prof. Kar is an alumnus of West Virginia University (WVU), from where he obtained both his MS (2010) and Ph.D. (2013) in Civil Engineering with a perfect GPA of 4.0. Prof. Kar also obtained his license as an “Engineer-In-Training” from the West Virginia State Board of Registration for Professional Engineers in 2010. Prof. Kar is a senior member of the RILEM Technical Committee for “Mechanical Properties of Alkali-activated concrete” [TC MPA]. He is the leader of the round robin tests on fiber-reinforced alkali-activated concrete (AAC). For his work with AAC, Prof. Kar was awarded the 2012 ASCE Freeman Fellowship, the 2013 WVU Dissertation Fellowship, and the 2015 BITS Outstanding Potential for Excellence in Research and Academics (OPERA) grant. Prof. Kar is presently the faculty-in-charge of the Concrete Technology Laboratory and the Advanced Materials Characterization Laboratory at BITS-Pilani, Hyderabad, graduating 2 doctoral scholars as supervisor, 1 doctoral scholar as co-supervisor, and 6 Master’s Degree Thesis students. His lab currently has 5 doctoral research scholars, 2 Master’s students working on several projects. Prof. Kar’s research has resulted in him acquiring 1 government-sponsored and 1 industry-funded projects as the PI, and 2 other projects as the co-PI. His research publications have more than 500 citations on Google Scholar with an h-index of 16 and i-10 index of 18. Prof. Kar has various collaborations at international and national level with reputed institutions including Curtin University, University of Pittsburgh, Portland State University, Politecnico di Milano, University of Antwerp, Indian Institute of Technology Ropar, and National Institute of Technology Meghalaya. Prof. Kar also has industrial collaborations with Kingspan Ltd. in Ireland and M/s. Aliens Developers in India.

Prof. Arkamitra Kar

Associate Professor

Department of Civil Engineering

Birla Institute of Technology and Science, Pilani, Hyderabad Campus 500078, India

Email: arkamitra.kar@hyderabad.bits-pilani.ac.in